1990

Kinetic and equilibrium study of the 2,3-furan ortho-quinodimethane - 4,5-dihydrocyclobuta[b]furan and 9,10-phenanthrene ortho-quinodimethane - 1,2-dihydrocyclobuta[l]phenanthrene interconversions and related studies

Craig Wilson Montgomery
Iowa State University

Order Number 9110537

Kinetic and equilibrium study of the 2,3-furan *ortho*-quinodimethane - 4,5-dihydrocyclobuta[*b*]furan and 9,10-phenanthrene *ortho*-quinodimethane - 1,2-dihydrocyclobuta[*l*]phenanthrene interconversions and related studies

Montgomery, Craig Wilson, Ph.D.

Iowa State University, 1990

U·M·I
300 N. Zeeb Rd.
Ann Arbor, MI 48106

Kinetic and equilibrium study of the 2,3-furan *ortho*-quinodimethane - 4,5-dihydrocyclobuta[*b*]furan and 9,10-phenanthrene *ortho*-quinodimethane - 1,2-dihydrocyclobuta-[*l*]phenanthrene interconversions and related studies

by

Craig Wilson Montgomery

A Dissertation Submitted to the

Graduate Faculty in Partial Fulfillment of the

Requirements for the Degree of

DOCTOR OF PHILOSOPHY

Department: Chemistry
Major: Organic Chemistry

Approved:

Signature was redacted for privacy.

In Charge of Major Work

Signature was redacted for privacy.

For the Major Department

Signature was redacted for privacy.

For the Graduate College

Iowa State University
Ames, Iowa

1990

TABLE OF CONTENTS

GENERAL INTRODUCTION

The challenge and the rewards derived from the study of reactive molecules has brought considerable attention to this area of chemistry. An important class of reactive molecules, the *o*-quinodimethanes, have been the subject of intensive investigation in the Trahanovsky group. A current research effort in the Trahanovsky group and the primary subject of this dissertation is the study of the interconversion between selected *o*-quinodimethanes and their cyclized isomers.

This dissertation is divided into three sections. Section I describes the preparation, characterization, and kinetic analysis of the electrocyclic ring opening of 4-*tert*-butyl-4,5-dihydrocyclobuta[*b*]furan (**1**) and 4,5-dihydrocyclobuta[*b*]furan (**2**). In addition a minimum enthalpy difference was determined for **1** and **2** and their respective *o*-quinodimethane isomers. Section II describes the preparation, characterization and kinetic analysis of the electrocyclic ring opening of 1,2-dihydrocyclobuta[*l*]phenanthrene (**3**). Furthermore, an approximate K_{eq} has been determined for the interconversion between **3** and its *o*-quinodimethane isomer. Section III presents results for the attempted photochemical generation of a furan *o*-quinodimethane and an unusual dimerization product.

Explanation of Dissertation Format

Each section of this dissertation is presented in the form of a full paper suitable for publication in a journal of the American Chemical Society. Therefore, each section has an independent numbering system with references following the experimental of each section. Research presented in the results and experimental of each section was performed by the author unless otherwise noted.

SECTION I. KINETIC AND EQUILIBRIUM STUDY OF THE 2,3-FURAN *ortho*-QUINODIMETHANE-4,5-DIHYDROCYCLOBUTA[*b*]FURAN INTERCONVERSION

INTRODUCTION

o-Quinodimethanes constitute a class of reactive molecules which have received considerable interest in the last 30 years as indicated by recent reviews.[1-3] 2,3-Furan *o*-quinodimethane (**2**), also known as 2,3-dimethylene-2,3-dihydrofuran, has been the subject of much attention in the Trahanovsky group.[4-6] Compound **2** was first proposed by Winberg in 1960 as an intermediate formed in the pyrolysis of 2-methyl-3-furylmethyltrimethylammonium hydroxide (**1**).[7] The dimeric product arising from **2** was not elucidated but believed to be one of two [4 + 4] dimers, **3** or **4**. Subsequently, several

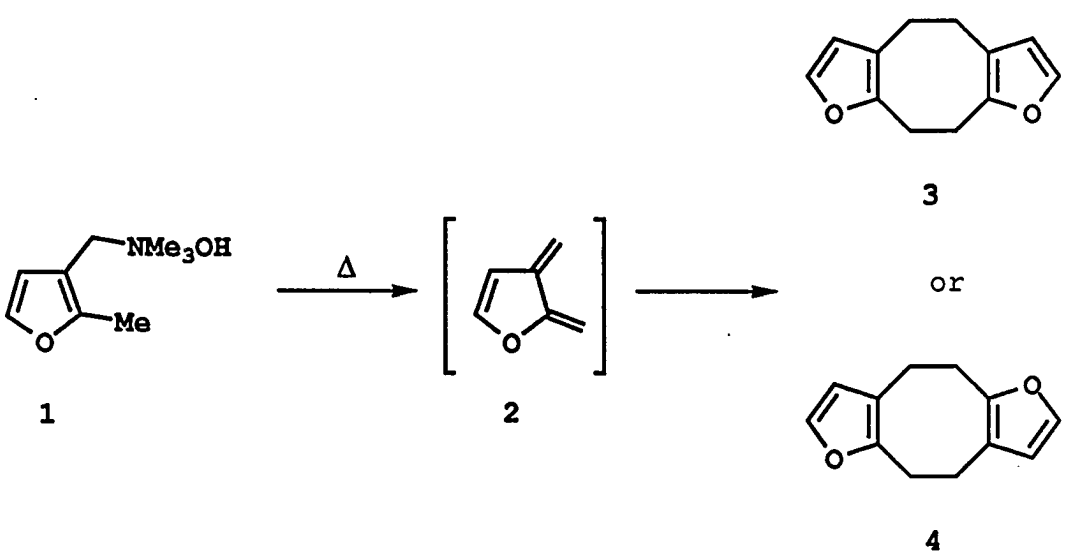

1 **2** **3** or **4**

other routes to **2** have been developed, each involving a 1,4 elimination.[2]

In 1981 Trahanovsky et al. reported the generation of 2,3-dimethylene-2,3-dihydrofuran (**2**) from the flash vacuum pyrolysis of 2-methyl-3-furylmethyl benzoate (**5**), the identification of **2** by ^{1}H NMR at -60 °C and the quantitative [4 + 4] dimerization of **2** to **3**.[4] Since this initial

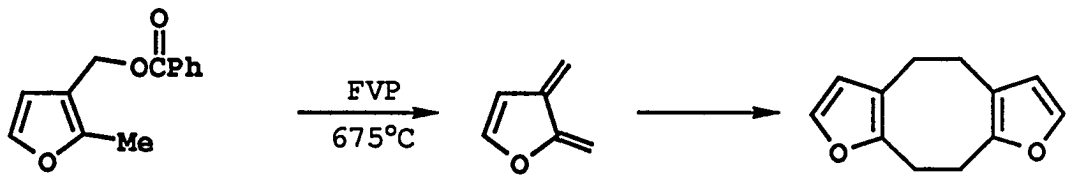

5 **2** **3**

observation, significant progress has been made in the Trahanovsky group to fully understand the chemistry of this molecule.[5,6]

2,3-Dimethylene-2,3-dihydrofuran (**2**) is now known to dimerize rapidly to **3** via a diradical intermediate (**6**).[5] Secondary deuterium kinetic isotope effect studies showed that the [4 + 4] cycloaddition proceeds via a stepwise mechanism and that the rate-determining step involves initial bond formation at the 3-methylene position to form **6**. The possibility of a

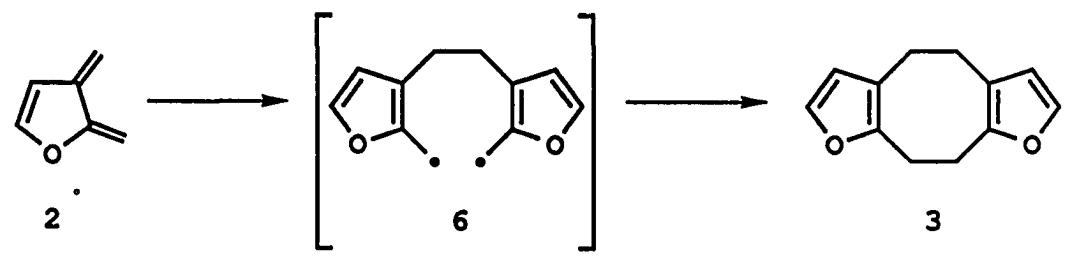

2 **6** **3**

zwitterionic intermediate instead of a diradical intermediate was ruled out based on insensitivity of dimerization rate to solvent polarity.

In light of these experimental data *o*-quinodimethanes **7** and **8** were synthesized to obtain further support for the two-step

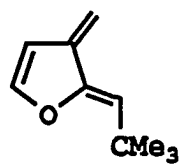

7

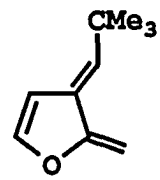

8

diradical mechanism.[6] As expected, **7** dimerizes at a rate similar to that recorded for the parent system, but compound **8** is much less reactive, forming little, if any dimer. These results provided additional evidence that bonding occurs at the 3-methylene position in the rate-determining step.[6]

The present study extends the investigation of 2,3-dimethylene-2,3-dihydrofuran (**2**) to include the energetics of the equilibrium between 4,5-dihydrocyclobuta[*b*]furan (**9**) and **2**. The significance of this work is highlighted by two previous

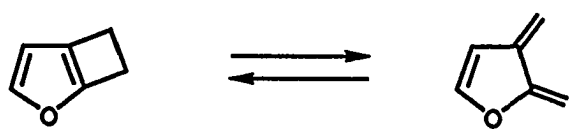

9 **2**

studies. First, the study of the *o*-xylylene (**10**) - benzocyclobutene (**11**) equilibrium published by Roth in 1981 demonstrated that benzocyclobutene (**11**) is 13 kcal/mol more stable than *o*-xylylene (**10**) with an enthalpy of activation for ring opening of 26 kcal/mol.[8-10] Second, MNDO calculations published in 1987 suggested **9** was 18 kcal/mol less stable than **2**, and it was predicted that **9** would be unstable at room temperature.[11]

Noting that the Dewar Resonance Energy for furan is approximately 2 kcal/mol compared to 21 kcal/mol for benzene, we predicted that **2** would be more stable than **9**.[12] It was also predicted that a significant energy barrier would exist between the two isomers such that both could be observed at room temperature. These predictions were not in agreement with those based on the MNDO calculations but were supported by the energy barrier determined for the *o*-xylylene (**10**) - benzocyclobutene (**11**) equilibrium. The results of our study correspond with our predictions. These results will be compared with Roth's work as well as with the reported MNDO calculations.

Our investigation began with **8** as it had been shown to be stable at room temperature; therefore, it was easier to handle. Compound **2** was subsequently investigated. Electrocyclization of **2** in an argon matrix by Munzel and Schweig in 1987 indicated potential success for our approach.[11] Our study is reported herein.

RESULTS

2-Methyl-3-furyl(*tert*-butyl)methyl benzoate (**12**) was prepared using previously reported procedures.[4,6] Incorporation of rigorous techniques for handling air and water sensitive compounds resulted in improved yields for the Grignard and benzoylation steps.[13] 2-Methyl-3-furylmethyl benzoate (**5**) was also prepared as reported previously.[4]

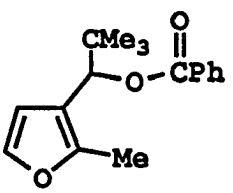

12

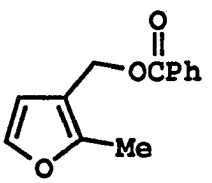

5

2-Methylene-3-*tert*-butylmethylene-2,3-dihydrofuran (**8**) was generated by the flash vacuum pyrolysis of 2-methyl-3-furyl(*tert*-butyl)methyl benzoate (**12**) with isomers **13** and **14** forming as undesirable side products.[6] Through yield

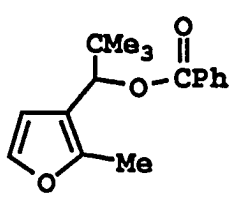

12

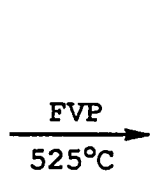

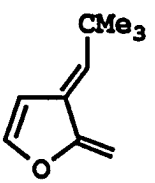

8

+

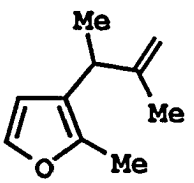

13

+

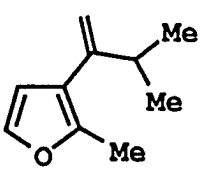

14

optimization experiments the yield of **8** was improved to 56% and was obtained at an oven temperature of 525 °C and a condenser temperature of -5 °C. Under the conditions developed approximately 2% benzoic acid relative to **8** was permitted to enter the trap; however, shaking the pyrolysate with pulverized Na_2CO_3 removed the trace amounts of benzoic acid. Compound **8** was stable at -78 °C and could be stored for weeks without significant degradation. Further analysis indicated that, although not isolable, **8** was stable in solution in the presence of oxygen, nitrogen, water and light but decomposed upon exposure to acid.

2,3-Dimethylene-2,3-dihydrofuran (**2**) was prepared by the flash vacuum pyrolysis of 2-methyl-3-furylmethyl benzoate (**5**) at 675 °C using a condenser temperature of -20 °C.[4] The yield of **2** was optimized by collecting in diethyl ether which was

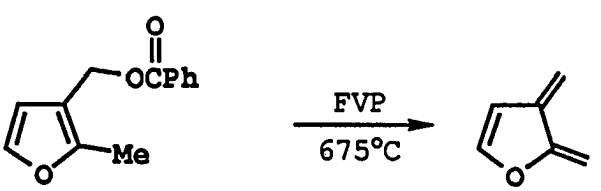

5 **2**

added to the trap through a side-arm. The optimized yield was 89% and was determined indirectly by measuring the quantity of dimer (**3**) formed. Previously reported dimer yields were in excess of 97% making this a reasonable method.[4,5]

4-*tert*-Butyl-4,5-dihydrocyclobuta[*b*]furan (**15**) was prepared by photolysis of 2-methylene-3-*tert*-butylmethylene-2,3-dihydrofuran (**8**) in pentane under nitrogen. The photolysis was

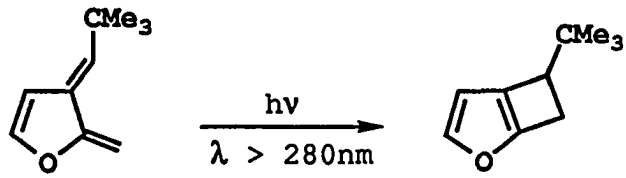

8 **15**

performed using a Conrad-Hanovia medium pressure mercury-vapor lamp with a pyrex filter. The disappearance of starting material was monitored by UV spectroscopy using aliquots taken from the reaction vessel at two-hour intervals. The reaction was determined complete when UV data indicated starting material, with a λ_{max} of 314 nm, had disappeared. The photolysis solvent was removed followed by immediate addition of the appropriate NMR solvent: $CDCl_3$ for NMR product and yield analyses and benzene-d_6 for the kinetic runs and preparing standards of **15** used in pyrolysate analyses. The use of benzene-d_6 was necessary to avoid complications caused by the acidity of $CDCl_3$.

^1H NMR data of starting material (**8**) and photolysis product (**15**) corroborated the UV data and indicated the presence of a new compound (Appendix, Figures A-5, A-7 and A-8 on pages 106, 110 and 112). The vinylic proton signals of **8** were the

predominate downfield signals in the ^{1}H NMR spectrum of the starting material. In striking contrast to this spectrum was that of the photolysate: the proton signals of **8** disappeared and signals expected for **15** were present. Aside from the aromatic proton signals of **15** in the ^{1}H NMR spectrum, a multiplet appeared centered at 3.1 ppm. In addition, long-range coupling was evident between one set of methylene hydrogens and the upfield furan hydrogen. Analysis of the second order coupling in the multiplet at 3.1 ppm was performed using the Nicolet NT-300 NMR simulation software (Appendix, Figures A-1 and A-2 on page 99). Coupling constants and chemical shifts indicated an electrocyclic closure had occurred. Further evidence for **15** was provided by ^{13}C NMR data (Appendix, Figures A-11, A-12 and A-13 on pages 118, 120 and 122). FT-IR analysis of **15** was also performed; however, the presence of side products from the pyrolysis step obscured a significant portion of the IR spectrum.

To analyze the IR spectrum of **15** it was necessary to collect a spectrum of **15** followed by warming in a sealed tube to destroy most of **15**. Subsequent collection of a second spectrum and comparison of the two spectra made possible the identification of IR signals due to **15**. These signals were similar in frequency to those reported by Schweig for 4,5-dihydrocyclobuta[*b*]furan (**9**).

The stability of **15** in the presence of oxygen, acid and $AgNO_3$ was studied. Although oxygen was passed through a solution of **15** in hexanes for 6 h, no decomposition was observed; however, considerable decomposition did occur when a solution of **15** in hexanes was washed with 2 M $HNO_{3(aq)}$. When exposed to a saturated solution of $AgNO_{3(aq)}$ the photolysis product rearranged to a new compound which has not been identified.[14] In addition to this stability study it was learned through experimental work that **15** decomposed when exposed to silica gel, alumina, sodium carbonate and GC conditions.

4,5-Dihydrocyclobuta[*b*]furan (**9**) was prepared by low temperature photolysis of 2,3-dimethylene-2,3-dihydrofuran (**2**) in pentane Dimer **3** was a side product of the photochemical

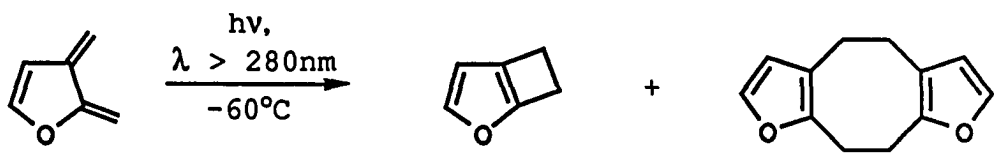

2 **9** **3**

electrocyclization of **2**. The photolysis was performed using a vacuum-jacketed low-temperature immersion well with a pyrex filter, a Conrad-Hanovia medium-pressure mercury-vapor lamp and argon for degassing (Appendix, Figure A-15 on page 126). The temperature of the reactor was maintained between -50 and

-70 °C by immersion in a dry ice-isopropanol bath. The disappearance of starting material was monitored by adding aliquots from the reactor solution to a 50-fold excess of methyl acrylate under argon at half-hour intervals and analyzing the solution for adduct **16** by GC. When adduct was

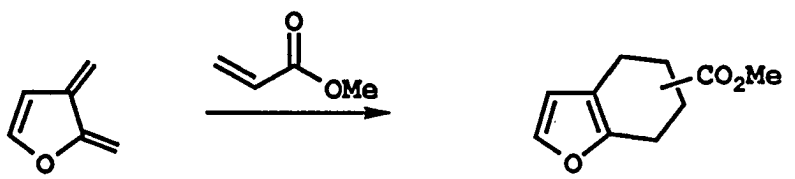

2 **16**

no longer present the photolysis was considered complete. A check on this method was provided by low temperature ^1H NMR analysis of the reactor solution after a typical photolysis. The ^1H NMR spectrum showed only **9** and **3** were present with **9** the major product. The predominance of **9** relative to **3** was possible only by photolyzing **2** at low concentrations, preferably less than 80 mg per liter. After photolyzing the volume of pentane was reduced by distillation to 0.15 ml and then the appropriate solvent was added: acetone-d_6 for NMR product analysis, $CDCl_3$ for yield analysis and benzene-d_6 for kinetic runs and preparing standards of **9** used in pyrolysate analyses.

Unlike the *tert*-butyl system, low temperature ^1H NMR analysis of the reactor solution before and after photolysis of

2,3-dimethylene-2,3-dihydrofuran (**2**) indicated that the [4 + 4] dimer (**3**) formed during the photolysis in addition to the expected major product, 4,5-dihydrocyclobuta[*b*]furan (**9**). Spectra of starting material **2** and products **3** and **9** may be found in the Appendix (Appendix, Figures A-6, A-9 and A-10 on pages 108, 114 and 116). Compound **9** exhibited two two-proton upfield triplets with long-range coupling between the methylene hydrogens forming one of the triplets and the upfield furan ring signal. Additional evidence for **9** was provided by ^{13}C NMR and FT-IR data.

Difficulty was encountered in identifying the ^{13}C NMR and IR signals of **9** due to contamination with the [4 + 4] dimer (**3**) and other minor impurities. Therefore, the following method was employed: samples of compound **9** were prepared for ^{13}C NMR and IR analysis and the spectra collected. The samples were subsequently warmed in sealed tubes to destroy a significant quantity of **9**. Oxygen was removed from the tubes prior to sealing by the freeze-thaw technique. Collection of subsequent ^{13}C and IR spectra made it possible to determine the position of ^{13}C NMR and IR signals of **9**. For the ^{13}C NMR analysis only the four furan ring carbons could be clearly identified (Appendix, Figure A-14 on page 124), whereas in the IR analysis all signals reported by Schweig were observed (Figure 7 on page 36).[11]

The pyrolysis product mixture from 2-methyl-3-furyl(*tert*-butyl)methyl benzoate (**12**) was analyzed by ^{1}H NMR for the presence of 4-*tert*-butyl-4,5-dihydrocyclobuta[*b*]furan (**15**). The data processor of the Nicolet NT-300 was switched to the double precision mode for the ^{1}H NMR analysis as it enabled us to obtain a greater signal to noise ratio and higher dynamic range thereby enhancing the sensitivity of the spectrometer. No signals for **15** were observed. By adding small quantities of **15** to the pyrolysis product solution it was determined that if **15** were present it was so in a concentration of less than 0.5% of that recorded for 2-methylene-3-*tert*-butylmethylene-2,3-dihydrofuran (**8**) (Figure 8 on page 39).

In a similar manner the pyrolysis product mixture from 2-methyl-3-furylmethyl benzoate (**5**) was also analyzed by ^{1}H NMR using the double precision mode of the Nicolet NT-300 data processor. However, unlike 2-methylene-3-*tert*-butylmethylene-2,3-dihydrofuran (**8**), 2,3-dimethylene-2,3-dihydrofuran (**2**) was unstable at room temperature making direct observation of the pyrolysis product mixture a cumbersome task. Therefore, **2** was allowed to dimerize by slowly warming the pyrolysate to room temperature in CS_2 under nitrogen. After ^{1}H NMR analysis in the double precision mode the sample was warmed at 68.3 °C for one half-life of 4,5-dihydrocyclobuta[*b*]furan (**9**). Subsequent ^{1}H NMR scanning in the double precision mode revealed several of the peaks initially observed were of thermally labile

compounds of which one might have been due to **9** based on chemical shift data (Figure 9 on page 41). Though confirmation could not be made it was evident from this analysis that **9** could not be present in the pyrolysis product mixture in a concentration greater than 2.6% of the concentration determined for **2**.

Kinetic data for the electrocyclic ring opening of both 4,5-dihydrocyclobuta[*b*]furan (**9**) and 4-*tert*-butyl-4,5-dihydrocyclobuta[*b*]furan (**15**) were collected by ^{1}H NMR spectroscopy. In Table 1 are listed the time-dependent integration data for a typical run involving **15**, and Figure 1 shows several ^{1}H NMR spectra from this run arranged chronologically. It should be apparent from Figure 1 that the cleavage product, 2-methylene-3-*tert*-butylmethylene-2,3-dihydrofuran (**8**), does not persist but decays to several products with time. The data from Table 1 were subsequently plotted in Figure 2 using a first order rate equation. Integration data for **15** is shown as a function of time with $k = 2.18 \pm 0.01 \times 10^{-4}$ s^{-1}.

Representative data are also included for the electrocyclic opening of 4,5-dihydrocyclobuta[*b*]furan (**9**). In general, the data collected for **9** resulted in first order plots more scattered than those obtained for **15**. In Table 2 are presented the time-dependent integration data for a typical run involving **9**, and Figure 3 shows several ^{1}H NMR spectra from this run arranged chronologically. Figure 4 is a plot of the data in

Table 1. Rate of disappearance of 4-*tert*-butyl-4,5-dihydrocyclobuta[*b*]furan (**15**) at 85.25 °C in benzene-d_6[a]

Time x 10^{-3}, s	Integration[b,c] A	Integration[b,c] B
0.000	321.1	671.7
1.228	248.7	530.3
2.451	198.3	414.0
3.613	159.8	331.2
4.830	128.4	263.5
6.008	107.0	215.8
7.189	91.3	170.7
8.374	75.8	150.4
9.115	72.5	128.9
10.923	59.6	102.2
59.002	31.6	45.1

[a]Rate constant: $k = 2.18 \pm 0.01 \times 10^{-4}$ s^{-1}.

[b]The range for integration A is approximately 4.70-4.60 ppm, and the signal followed arises from one proton of **15**. The range for integration B is approximately 2.95-2.85 ppm, and the signal followed arises from two protons of **15**. Though these ranges vary slightly between runs, they were held constant in each run.

[c]The standard was diphenylmethane, and its concentration was 2.5×10^{-2} M. The tabulated integrations are relative to the methylene singlet which was set at 200.

Figure 1. Chronologically ordered spectra of 4-*tert*-butyl-4,5-dihydrocyclobuta[*b*]furan (**25**) for kinetic run at 85 °C: a) time = 0.0 min, b) time = 41 min, c) time = 100 min, d) time = 152 min, e) time = 62 h. The solvent was benzene-d_6 and the standard was diphenylmethane (• indicates methylene peak)

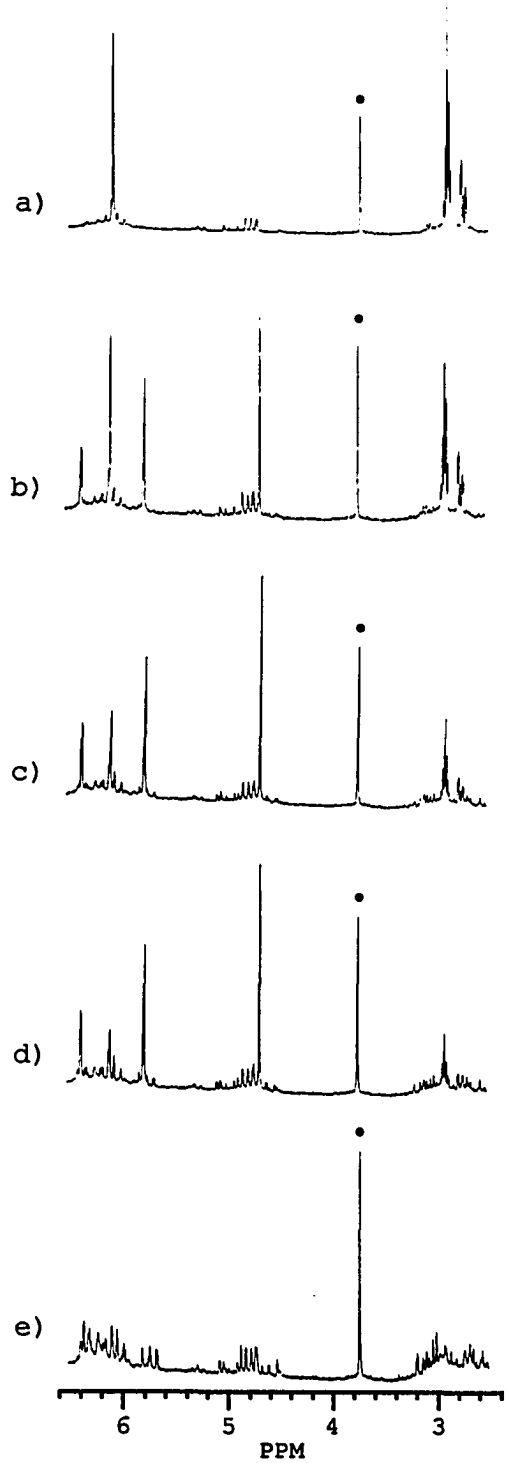
a)
b)
c)
d)
e)
6
5
4
3
PPM

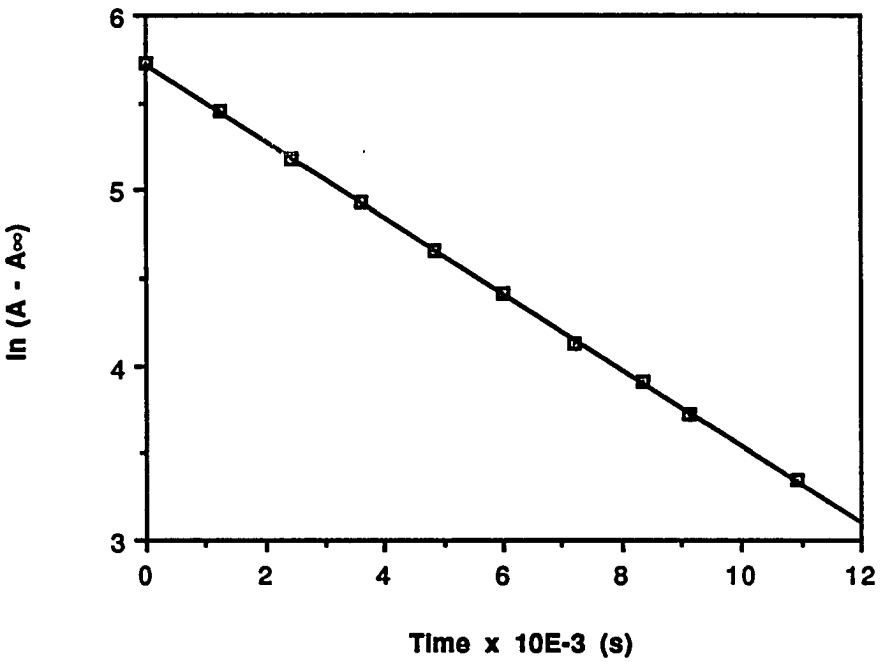

Figure 2. Plot of ln (A - A_∞) vs. time at 85.25°C. Data were obtained from Table 1 and represent the disappearance of 4-*tert*-butyl-4,5-dihydrocyclobuta[*b*]furan (**15**). The rate constant derived from the line is k = 2.18 ± 0.01 x 10^{-4} s^{-1}

Table 2. Rate of disappearance of 4,5-dihydrocyclobuta-[*b*]furan (**9**) at 83.25 °C in benzene-d_6[a]

Time x 10^{-4}, s	Integration[b,c]
0.0000	176.9
1.4324	149.5
5.0789	101.3
5.8137	95.5
6.9001	87.3
8.1747	86.7
9.0987	84.7
12.5257	79.7
13.4417	71.2
14.1826	68.7
15.7964	69.3
16.8894	63.0
75.5691	56.8

[a]Rate constant: $k = 1.51 \pm 0.10 \times 10^{-5}$ s^{-1}.

[b]The range for integration is approximately 6.05-5.95 ppm, and the signal followed arises from one proton of **9**. Though the range varies slightly between runs, it was held constant in each run.

[c]The standard was diphenylmethane, and its concentration was 3.6×10^{-2} M. The tabulated integrations are relative to the methylene singlet which was set at 200.

Figure 3. Chronologically ordered spectra of 4,5-dihydrocyclobuta[*b*]furan (**9**) for kinetic run at 83 °C: a) time = 0.00 h, b) time = 4.0 h, c) time = 16.1 h, d) time = 22.7 h, e) time = 210 h. The solvent was benzene-d_6 and the standard was diphenylmethane (• indicates methylene peak)

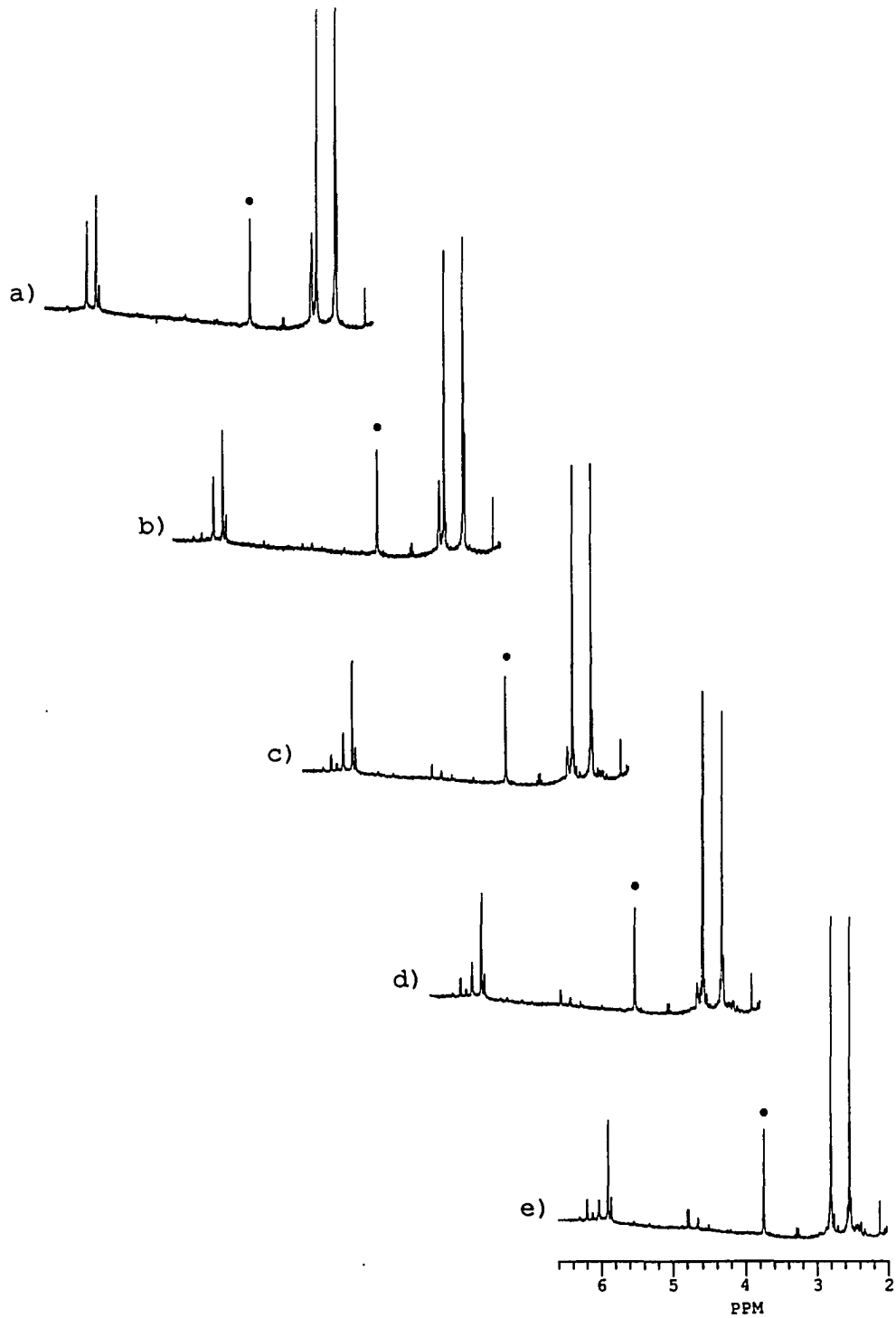
a)
b)
c)
d)
e)
6
5
4
3
2
PPM

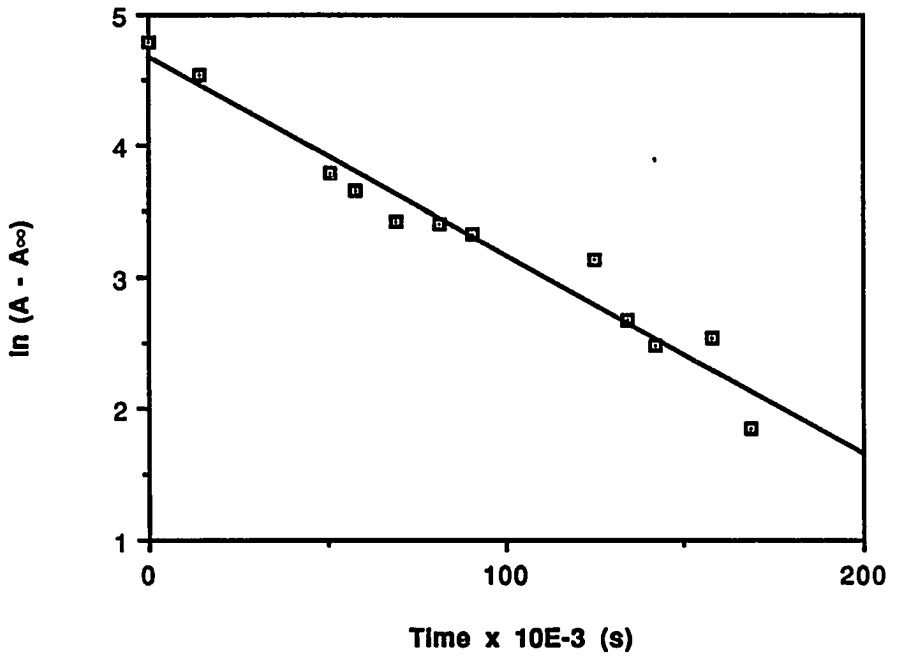

Figure 4. Plot of ln ($A - A_{\infty}$) vs. time at 83.25 °C. Data were obtained from Table 2 and represent the disappearance of 4,5-dihydrocyclobuta[*b*]furan (**9**). The rate constant derived from the line is $k = 1.51 \pm 0.10 \times 10^{-5}\ s^{-1}$

Table 2 using a first order rate equation with integration data for **9** shown as a function of time.

Comparison of Figure 4 with Figure 2 reveals an increased scatter of data points for the plot in Figure 4. A plausible explanation for increased variance of plotted data is that baseline distortion caused by the proton signals of pentane reduced the accuracy of the integrations. Due to the volatility of 4,5-dihydrocyclobuta[*b*]furan (**9**) it was impossible to remove all the pentane from the photolysis solvent. Thus the kinetics sample consisted of 80% benzene-d_6 and 20% pentane, resulting in a huge NMR signal for pentane and considerable baseline distortion.

A first-order rate expression was used to obtain rate constants for the kinetic data collected for the electrocyclic ring opening of both **9** and **15**.[15] All integration data were corrected by subtracting the infinity point integration prior to least squares analysis. The activation parameters and preexponential factors were calculated on a microcomputer using software designed to perform least squares analysis of kinetic data.[16] Brief summaries of kinetic data collected for **9** and **15** are presented in Table 3 and Table 4 and activation parameters are presented in Table 5.[16,17] The Arrhenius plot, with Log k as a function of 1000/K, for **15** is shown in Figure 5 and for **9** in Figure 6.

Table 3. First-order rate constants for the electrocyclic ring opening of 4-*tert*-butyl-4,5-dihydrocyclobuta[*b*]furan (**15**)

Temp, °C	k, s^{-1}
55.10 ± 0.10	$5.69 \pm 0.66 \times 10^{-6}$
70.15 ± 0.05	$4.07 \pm 0.29 \times 10^{-5}$
85.25 ± 0.10	$2.10 \pm 0.07 \times 10^{-4}$

Table 4. First-order rate constants for the electrocyclic ring opening of 4,5-dihydrocyclobuta[*b*]furan (**9**)

Temp, °C	k, s^{-1}
68.25 ± 0.15	$3.32 \pm 0.32 \times 10^{-6}$
83.25 ± 0.15	$1.59 \pm 0.12 \times 10^{-5}$
98.10 ± 0.20	$5.95 \pm 0.87 \times 10^{-5}$

Table 5. Activation parameters for the electrocyclic ring opening of 4,5-dihydrocyclobuta[*b*]furan (**9**) and 4-*tert*-butyl-4,5-dihydrocyclobuta[*b*]furan (**15**)

Cmpd	Ea, kcal/mol	Log A, s^{-1}	$\Delta H^{\ddagger}$ at 25 °C, kcal/mol	$\Delta S^{\ddagger}$ at 25 °C, cal/K mol
9	24.4 ± 0.5	10.1 ± 0.3	23.8 ± 0.5	-14.2 ± 1.5
15	28.0 ± 0.8	13.4 ± 0.5	27.4 ± 0.8	0.8 ± 2.3

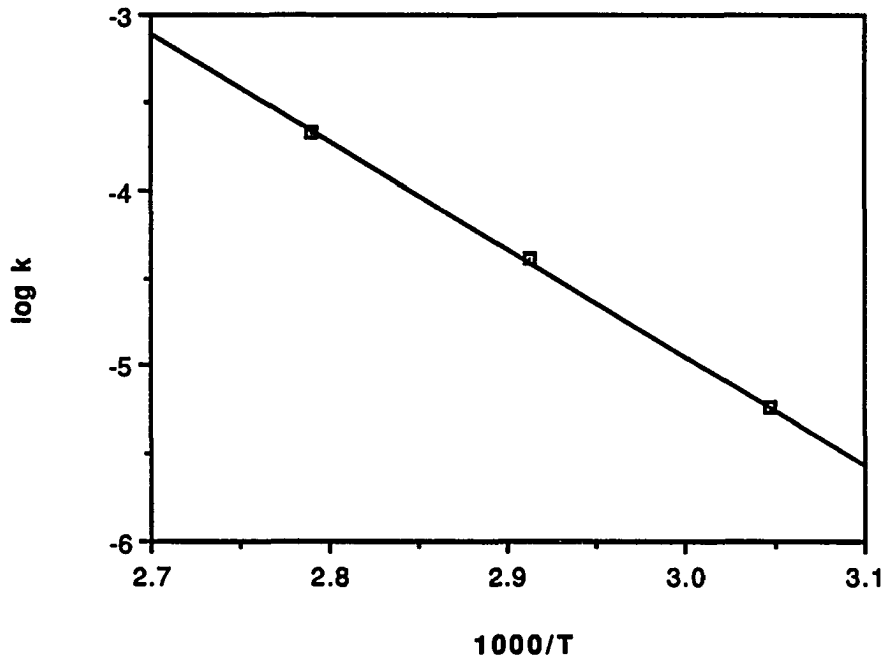

Figure 5. Plot of log k vs. 1000/T for the electrocyclic ring opening of 4-*tert*-butyl-4,5-dihydrocyclobuta[*b*]furan (**15**). Data were obtained from Table 3. The slope of the line is -6.12 and the y-intercept is 13.4

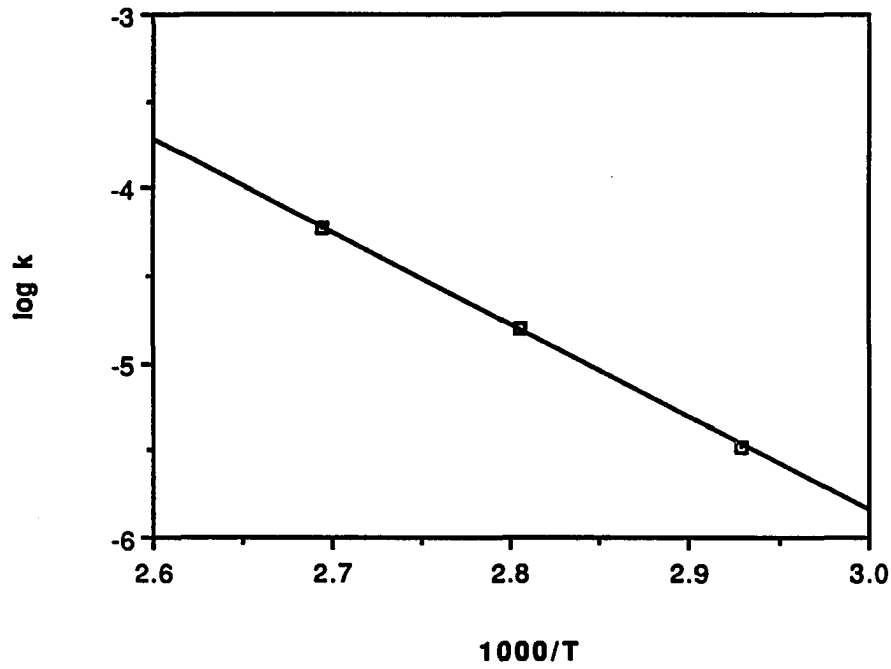

Figure 6. Plot of log k vs. 1000/T for the electrocyclic ring opening of 4,5-dihydrocyclobuta[*b*]furan (**9**). Data were obtained from Table 4. The slope of the line is -5.33 and the y-intercept is 10.1

The significant scatter of the kinetic data for ring opening of 4,5-dihydrocyclobuta[*b*]furan (**9**) and the large infinity point values led to reevaluation of the data. The infinity point values and rate constants were redetermined using a nonlinear least squares program capable of performing curve fitting tasks. From the recalculated rate constants given in Table 6 the activation parameters in Table 7 were determined. The rate constants are somewhat larger than those calculated using the linear least squares method with experimental infinity point values. However, the effect on activation parameters is insignificant.

It is noteworthy that the value for $\Delta S^{\ddagger}$ determined by both methods of evaluation is more negative than those presented in this dissertation and the literature for the ring opening of other cyclobutene ring systems. Typically, $\Delta S^{\ddagger} = 0$ eu for ring opening of a cyclobutene ring system. However, Rickborn has observed a $\Delta S^{\ddagger} = -4.5$ eu for the ring opening of 7,7-dimethoxybenzocyclobutene in *tert*-butylbenzene.

Though our research has not led to a definite explanation for the large negative value for $\Delta S^{\ddagger}$, two possibilities are suggested: first, the large negative values may arise from error in the kinetic data. As mentioned earlier, the significant scatter of the kinetic data is attributed to the presence of pentane in the kinetic samples. This quantity of pentane was sufficient to cause baseline distortions in the ^{1}H

Table 6. Recalculated first-order rate constants for the electrocyclic ring opening of 4,5-dihydrocyclobuta[*b*]furan (**9**)

Temp, °C	k, s^{-1}
68.25 ± 0.15	$5.44 \pm 0.98 \times 10^{-6}$
83.25 ± 0.15	$2.22 \pm 0.36 \times 10^{-5}$
98.10 ± 0.20	$8.92 \pm 0.98 \times 10^{-5}$

Table 7. Activation parameters for the electrocyclic ring opening of 4,5-dihydrocyclobuta[*b*]furan (**9**)

Cmpd	Ea, kcal/mol	Log A, s^{-1}	$\Delta H^{\ddagger}$ at 25°C, kcal/mol	$\Delta S^{\ddagger}$ at 25°C, cal/K mol
9	23.6 ± 0.6	9.8 ± 0.3	23.0 ± 0.6	-15.6 ± 1.6

NMR spectra which may have led to increased error in the integrations. It has been determined that variation of the largest and smallest rate constants by ± 20% can result in a $\Delta S^{\ddagger}$ = -5 eu in the most extreme case. That is, if one increases the smallest rate constant by 20% and decreases the largest rate constant by 20% a $\Delta S^{\ddagger}$ of -5 eu is obtained.

Therefore, it is suggested that the large negative value, $\Delta S^{\ddagger}$ = -15 eu, may be a consequence of experimental error

A second possible explanation for the $\Delta S^{\ddagger}$ value is that the transition state of (9) is stabilized by the benzene solvent thus reducing $\Delta H^{\ddagger}$. The more ordered transition state would also lead to a more negative $\Delta S^{\ddagger}$.

DISCUSSION

The synthesis of the 4,5-dihydrocyclobuta[*b*]furan system has been reported twice. The first report in 1969 involved conversion of 1,2-bis(trimethylsiloxy)cyclobutene (**16**) to the corresponding acyloin **17** which cyclized with the malononitrile anion to give a 4,5-dihydrocyclobuta[*b*]furan derivative **18**.[20] Identification of **18** was based on elemental analysis. In 1987

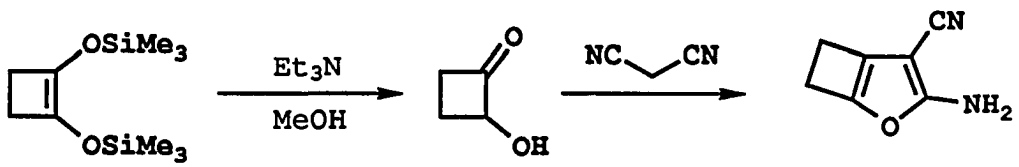

16 **17** **18**

parent 4,5-dihydrocyclobuta[*b*]furan (**9**) was prepared photochemically in an argon matrix at 16 K, and identification

9

of **9** was made by UV/VIS and IR spectroscopy.[11] The stability of **9** was estimated on the basis of MNDO calculations in conjunction with experimental data for the *o*-xylylene (**10**) - benzocyclobutene (**11**) equilibrium. However, the predicted instability of **9** is not in agreement with our data.

Our solution-phase photochemical synthesis of 4-*tert*-butyl-4,5-dihydrocyclobuta[*b*]furan (**15**) and 4,5-dihydrocyclobuta[*b*]furan (**9**) and subsequent kinetic analyses indicated the 4,5-dihydrocyclobuta[*b*]furan system was stable at room temperature when in solution. Our identification of **15** and **9** included IR analysis, and all the absorptions reported by Schweig as diagnostic for **9** were observed as indicated in the spectra shown in Figures 7a and 7b. Further support for the identity of **15** was available in the published ^{1}H NMR data of 1-*tert*-butylacenaphthene (**19**) and 1-*tert*-butylbenzocyclobutene (**20**).[21] The three hydrogen substituents on the ethano moiety

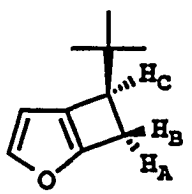

15

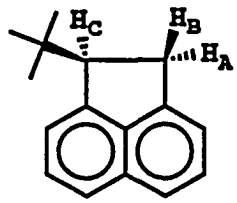

19

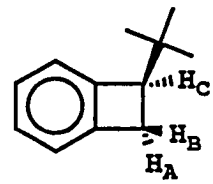

20

of **19** and **20** resulted in chemical shift and coupling values similar to those for **15**. It should be noted that the chemical shift order for **15** was $H_A > H_C > H_B$ and for **19** and **20** it was $H_C > H_A > H_B$. This difference may be due to the electron withdrawing nature of the oxygen in **15**. The most significant information in Table 6 is contained in the coupling constants,

Figure 7. IR spectra. a) **9** in heptane after photolysis of **2** (background subtracted). The five diagnostic hands observed by Schweig are present (• indicates diagnostic peak): IR (liquid cell, 0.10 mm path length) 1624 (m), 1231 (s), 1111 (s), 1032 (s), 912 (s) cm^{-1} [lit.[11] IR (argon matrix) 1608.8 (s) 1234.2 (s), 1115.4 (m), 1034.6 (s), 912.4 (s) cm^{-1}]. b) The sample used for Figure 7a after warming in a sealed tube. All diagnostic bands have disappeared

a)

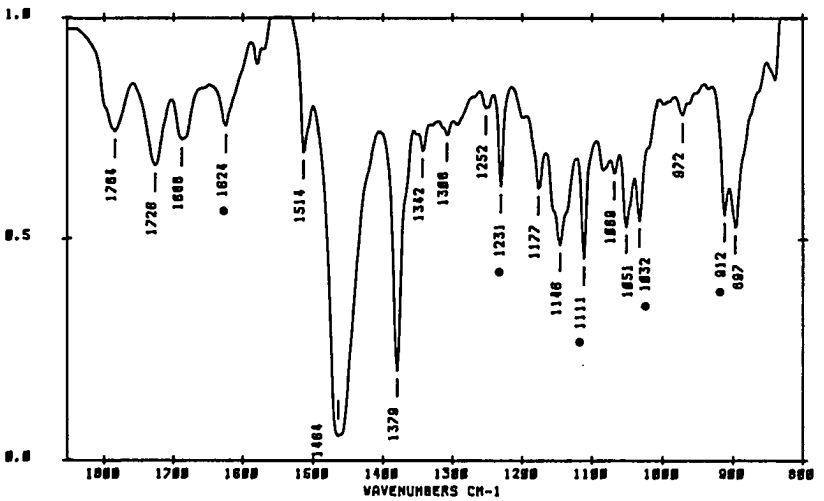
1.0
0.5
0.0
1784
1728
1666
1624
1514
1484
1379
1342
1306
1252
1231
1177
1148
1111
1068
1051
1032
972
912
887
1800
1700
1600
1500
1400
1300
1200
1100
1000
900
800
WAVENUMBERS CM-1

b)

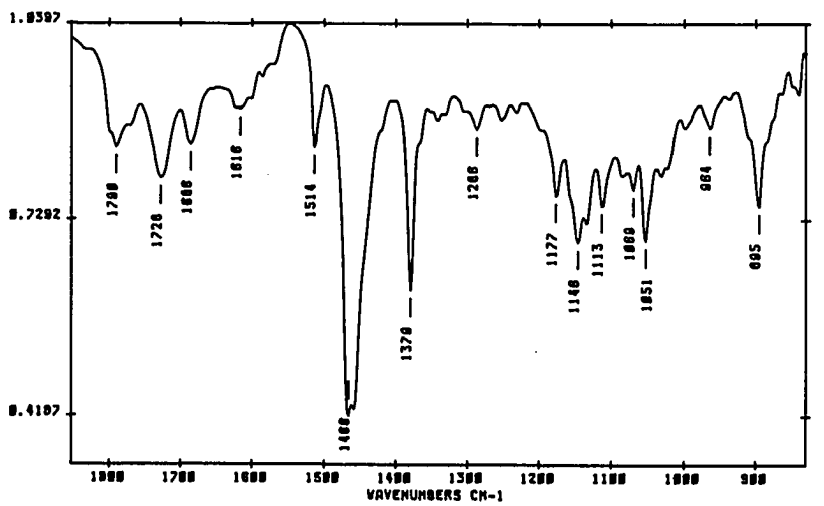
1.0397
0.7292
0.4187
1780
1726
1666
1616
1514
1488
1378
1268
1177
1148
1113
1068
1051
984
885
1800
1700
1600
1500
1400
1300
1200
1100
1000
900
WAVENUMBERS CM-1

Table 6. ^1H NMR data for the ethano moiety of compounds **15**, **19**, and **20**

Cmpd	H_A	H_B	H_C	J_{AB}	J_{AC}	J_{BC}	Solvent
15	3.21	3.01	3.12	-12.6	3.90	<2.0	$CDCl_3$
19	3.40	3.03	3.53	-17.88	8.25	3.28	$CDCl_3$
20	3.03	2.84	3.29	-14.15	5.59	2.83	CCl_4

as their similarity give support for the structure proposed for **15**.

With ^1H NMR data for 4,5-dihydrocyclobuta[*b*]furans **9** and **15** in hand, we were in a position to check for trace amounts of **9** and **15** in the pyrolysis product mixtures of 2-methyl-3-furylmethyl benzoate (**5**) and 2-methyl-3-furyl(*tert*-butyl)methyl benzoate (**12**), respectively. From ^1H NMR spectra of the pyrolysate of **20** it was apparent the closed form was not present in a concentration greater than 0.5% of the product 2-methylene-3-*tert*-butylmethylene-2,3-dihydrofuran (**8**) (see Figures 8a, 8b). From ^1H NMR spectra of the pyrolysate of **5** prior to and after warming for one half-life of **9** it was apparent the concentration of **9** could not exceed 2.6% of the concentration of the major pyrolysis product of **5** (see Figures 9a and 9b).

Figure 8. ^1H NMR spectrum segment of the pyrolysis products from 2-methyl-3-furyl(*tert*-butyl)methyl benzoate (**12**) in benzene-d_6. a) This spectral segment is the region in which protons A-C of compound **15** are known to appear. b) This spectrum segment is of the same solution after addition of 1.5% of **15** relative to **8**. Note the indicated doublet which arises from **15**

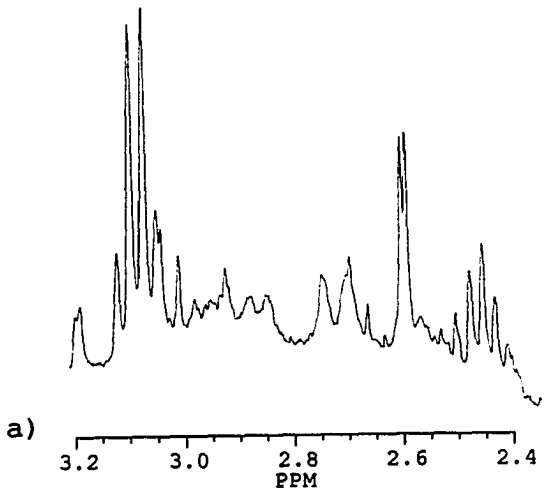
a)
3.2
3.0
2.8
2.6
2.4
PPM

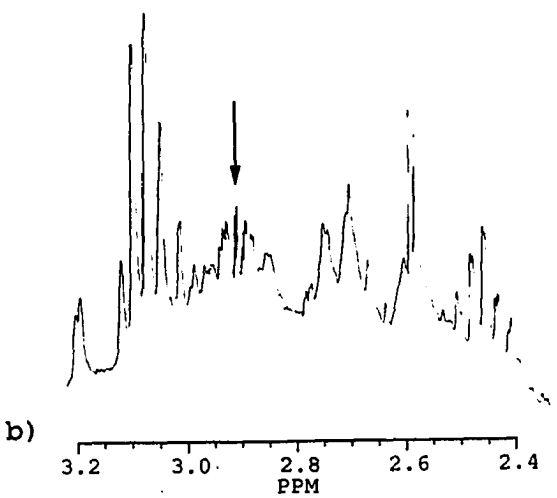
b)
3.2
3.0
2.8
2.6
2.4
PPM

Figure 9. ^{1}H NMR spectrum of the dimerized pyrolysis product of **5**. a) Spectrum segment prior to sample warming. The peak which has been cut-off is of the dimer **(3)**. b) Spectrum segment following warming

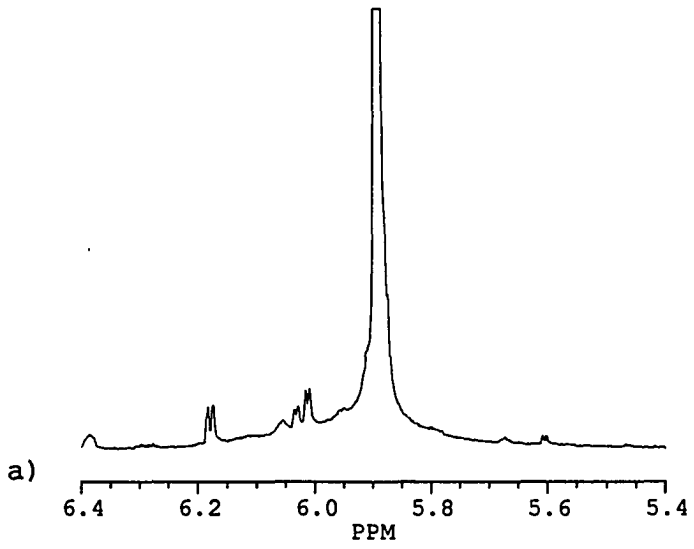
a)
6.4
6.2
6.0
5.8
5.6
5.4
PPM

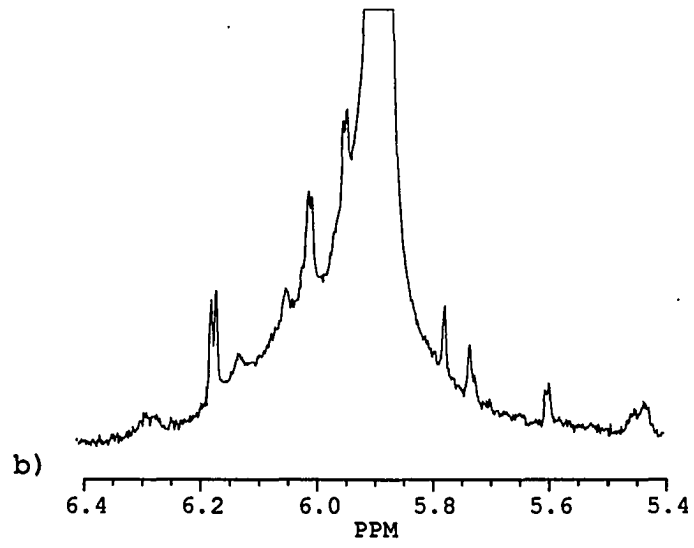
b)
6.4
6.2
6.0
5.8
5.6
5.4
PPM

If **9** were present in Figure 9b a proton signal arising from **9** would appear in the region between 6.2 and 6.0 ppm. Two doublets in this region were affected by sample warming; therefore, one of the doublets may arise from **9**. The integration of the larger doublet relative to the dimer signal is 2.6:100. Thus, **9** was not present in a concentration greater than 2.6% of the pyrolysis product of **5**.

Successful synthesis of the 4,5-dihydrocyclobuta[*b*]furans **9** and **15** allowed us to analyze the kinetics of the electrocyclic ring opening of **9** and **15**. Relevant to our kinetic study are

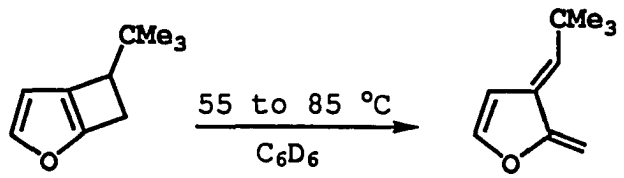

15 **8**

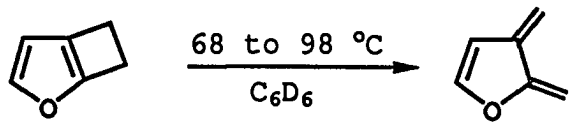

9 **2**

recently published studies on the *o*-quinodimethane (**10**) - benzocyclobutene (**11**) equilibrium and the recent MNDO calculations of the relative thermodynamic stability of 2,3-

dimethylene-2,3-dihydrofuran (**2**) and 4,5-dihydrocyclobuta[*b*]furan (**9**).[8-11] In addition, the energetics for the interconversion of cyclobutene (**21**) and cisoid butadiene (**22**) have been reported as well as the effects of substituents on the ring cleavage of both benzocyclobutene (**11**) and cyclobutene (**21**).[19,22-34] These studies will be discussed and related to our data.

Over the last decade the activation parameters for the *o*-quinodimethane (**10**) - benzocyclobutene (**11**) equilibrium have been determined by various methods.[8-10] The results and the methods employed are listed in Table 7, and the data refer to the equilibrium as shown below. Comparing the average $\Delta H^{\ddagger}$ determined for the electrocyclic ring opening of **11** with the values determined for the two dihydrocyclobuta[*b*]furans, **9** and **15**, it is evident that electrocyclic ring opening of the furan system is considerably more rapid. The difference in rate is likely due to the substantially greater aromatic stabilization of benzocyclobutene (**11**) relative to either of the 4,5-dihydrocyclobuta[*b*]furans studied.

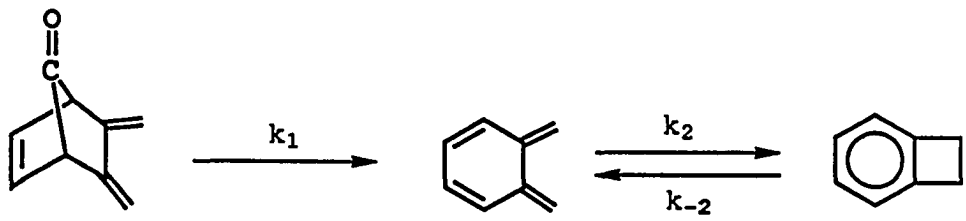

23 **10** **11**

Table 7. Activation parameters obtained by Roth for *o*-xylylene (**10**)-benzocyclobutene (**11**) equilibrium

$\Delta H^{\ddagger}$ **11,10** kcal mol^{-1}	$\Delta S^{\ddagger}$ **11,10** cal K^{-1} mol^{-1}	$\Delta H^{\ddagger}$ **10,11** kcal mol^{-1}	$\Delta S^{\ddagger}$ **10,11** cal K^{-1} mol^{-1}	Method
38.9	–	25.6	-5.8	shock-tube measurements in gas phase[a]
38.9	4.66	28.4	0.39	solution flash photolysis to general *o*-quinodimethane followed by trapping with dienophile[b]
37.4	1.06	26.3	-6.1	*o*-quinodimethane generations from benzocyclobutene followed by trapping with O_2 in gas phase[c,d]

[a]Ref. 9.

[b]Ref. 8.

[c]Ref. 10.

[d]This method required the K_{eq} determined from shock-tube measurements.

The effect of the aromatic stabilization in the benzocyclobutene system and the two dihydrocyclobuta[*b*]furan systems is represented in Figure 10. The energy diagrams are based on literature data and results presented in this dissertation.[9,22,35] To provide a common point of reference for each of the diagrams the *o*-quinodimethanes, best interpreted as polyenes, were set at the same enthalpy level as *cisoid* 1,3-butadiene.[5,36]

Comparing the first two diagrams in Figure 10 one observes a 22 kcal/mol resonance stabilization of benzocyclobutene (**11**) relative to cyclobutene (**21**). To determine whether this value is reasonable analysis of the two diagrams is made using the Dewar Resonance Energy of 21 kcal/mol and using the methodology developed by Dewar et al. and Baird.[12c,37,12a] Accordingly, fusion of an ethylene unit to a 1,3-butadiene to form the illustrated "classical structure with 'localized' bonds" results in 10 kcal/mol of pi-bond stabilization. Delocalization of the pi electrons of this hypothetical structure results in resonance stabilization of 21 kcal/mol. However, the resonance energy of benzocyclobutene is approximately 4 kcal/mol less than that for benzene.[38] The determination of resonance energy differences was performed by Doering et al. and involved study of heats of hydrogenation. Therefore, this correction is applied to obtain a value of 27 kcal/mol which is similar to the experimental value.

Figure 10. Energy diagrams for the interconversion of cyclobutene (**21**) with cisoid-butadiene (**22**), benzocyclobutene (**11**) with *o*-xylylene (**10**), 4,5-dihydrocyclobuta[*b*]furan (**9**) with 2,3-dimethylene-2,3-dihydrofuran (**2**) and 4-*tert*-butyl-4,5-dihydrocyclobuta[*b*]furan (**15**) with 2-methylene-3-*tert*-butylmethylene-2,3-dihydrofuran (**8**). All *o*-quinodimethanes as well as **22** are set at the same energy level

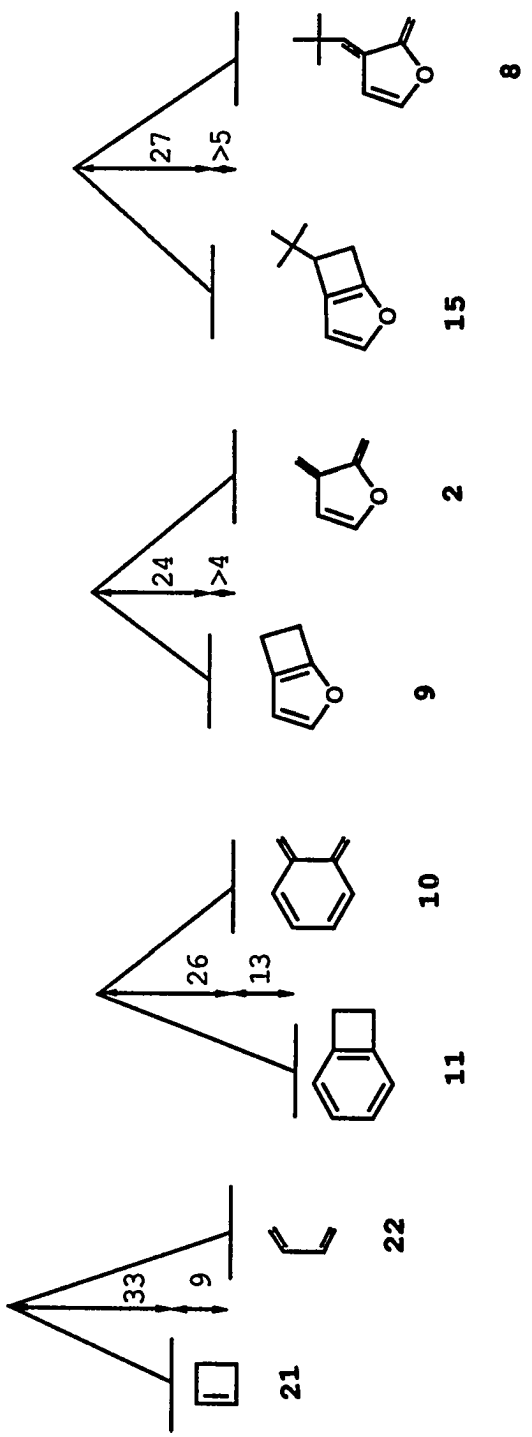
33
9
21
22
26
13
11
10
24
>4
9
2
27
>5
15
8

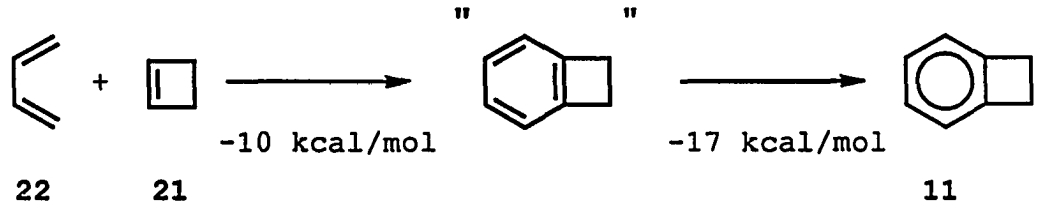

22 21 11

Related to the resonance stabilization of benzocyclobutene (**11**) is the resonance stabilization of the transition state for ring opening. If this resonance stabilization were not present in the transition state one would expect $\Delta H^{\ddagger}$ for ring closure of approximately 42 kcal/mol and a $\Delta H^{\ddagger}$ for ring opening of 55 kcal/mol. These values are based on the activation enthalpies for the cyclobutene system and were determined using the following reasoning: if resonance stabilization of the transition state were not present the rate of ring closure for *o*-xylylene (**10**) would be similar to that of *cisoid* 1,3-butadiene (**22**) as neither compound is resonance stabilized. The $\Delta H^{\ddagger}$ for ring opening of **11** would be 22 kcal/mol greater than cyclobutene (**21**), reflecting 22 kcal/mol of resonance stabilization of **11** relative to **21**.

The interconversion of 4,5-dihydrocyclobuta[*b*]furan (**9**) and 2,3-furan *o*-quinodimethane (**2**) is represented in the third diagram of Figure 10. When compared with the benzocyclobutene diagram it is evident the resonance stabilization of **9** is significantly less than that for benzocyclobutene (**11**). This is expected as calculations by Dewar and calculations by Hess

and Schaad indicate furan has a resonance stabilization of approximately 2 kcal/mol.[12c,12d]

Comparing the interconversion of **9** and **2** with that for the cyclobutene system one observes the transition state for ring opening of **9** is 10 kcal/mol less than that for **21**. This lower transition state cannot be attributed to a resonance effect which would be insignificant as furan has only 2 kcal/mol of resonance stabilization. Therefore, bond formation must be greater than bond breaking in the transition state for the parent furan system relative to the cyclobutene system.

The preceding discussion of the parent furan system also applies to the *tert*-butyl substituted furan system. However, comparison of the energy diagrams for the two furan systems reveals the $\Delta H^{\ddagger}$ for ring opening of 4,5-dihydrocyclobuta[*b*]-furan (**9**) is 4 kcal/mol less than that recorded for 4-*tert*-butyl-4,5-dihydrocyclobuta[*b*]furan (**15**). This difference in $\Delta H^{\ddagger}$ may be attributed to the steric interaction between the *tert*-butyl substituent and the hydrogen in the 4-position of 2-methylene-3-*tert*-butylmethylene-2,3-dihydrofuran (**8**). This interaction would be expected to increase as **15** underwent electrocyclic ring opening and the methylene groups rotated to form the exocyclic pi bonds of **8**. Hence, the transition state energy for the electrocyclic ring opening of **15** is expected to be greater than that for **9**.

The energy barriers for ring opening of 4-*tert*-butyl-4,5-dihydrocyclobuta[*b*]furan (**15**) and 4,5-dihydrocyclobuta[*b*]furan (**9**) were determined through kinetic analysis. The minimum difference in enthalpy between **15** and 2-methylene-3-*tert*-butylmethylene-2,3-dihydrofuran (**8**) and between **9** and 2,3-dimethylene-2,3-dihydrofuran (**2**) was calculated using the following expression. To solve this expression for ΔH° it was

$$K_{eq} = \exp(\Delta S^\circ/R)\exp(-\Delta H^\circ/RT)$$

necessary to supply values for the unknown K_{eq} and ΔS°. The ΔS° value was based on the average value for the entropy difference for benzocyclobutene (**11**) going to *o*-xylylene (**10**), ΔS° = 7.3 cal/mol K.[10] An upper limit of the value for K_{eq} was determined by NMR spectroscopic analysis of the pyrolysis product from the appropriate benzoate.

By pyrolyzing 2-methyl-3-furyl(*tert*-butyl)methyl benzoate (**12**) a thermal equilibrium was established between **8** and **15**. In the subsequent ^1H NMR analysis of the pyrolysate an upper limit for the quantity of **15** present was placed at less than 0.5% of **8**. Compound **15** was not actually observed but this value reflects the detection limit determined for **15**. This enabled calculation of a $K_{eq(\mathbf{8},\mathbf{15})} < 0.005$. In a similar manner it was determined that the detection limit for **9** was 2.6% of **2** leading to the estimation $K_{eq(\mathbf{9},\mathbf{2})} < 0.026$. Finally,

it should be noted that these maximum values for K_{eq} were determined at elevated temperatures. As the temperature decreases K_{eq} will decrease. Therefore, the values for K_{eq} are overestimated, and the values for ΔH° are underestimated.

As noted earlier a substituent effect was observed in the electrocyclic ring opening of the 4,5-dihydrocyclobuta[*b*]furans studied. Further consideration of this effect is warranted given the numerous studies of such effects appearing in the literature and their relevance to understanding the chemistry of such ring openings.[19,23-32] Ring opening of cyclobutene (**21**), itself, and the effect of substituents have received close scrutiny in the recent literature.[23-30] This work has been related to benzocyclobutene (**11**) and its derivatives substituted in the 1-position, and both the cyclobutene (**21**) and benzocyclobutene (**11**) studies relate to our work. Results show that cyclobutenes with a single electron-donating substituent in the 3-position prefer an outward rotation during thermally induced conrotatory ring opening.[23-27,30] Donor substituents have also been shown to reduce the transition state energy (see Table 8).[23,24] These effects of donor substituents have been explained theoretically.[24-29]

Studies regarding substituent effects on 1-substituted benzocyclobutenes are sparse and have been reported in a predominantly qualitative manner.[19,31-34] However, Sammes has reported an energy of activation for ring opening of

Table 8. Electron donor substituent effects on the activation energy for ring opening of cyclobutene[a]

Substituent	ΔE_a kcal/mol
$-CH_3$	-0.8
-Cl	-3.1
-OEt	-9.0
-OAc	-4.7

[a]Ref. 21 and 22.

Table 9. Activation energies for electrocyclic ring opening[a]

	E_a, kcal/mol		E_a, kcal/mol
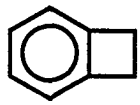	39.9		32.9
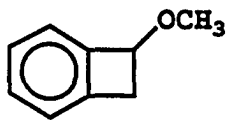	31.3	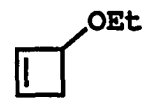	23.5
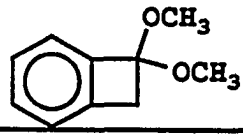	33.6	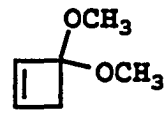	32.8

[a]Ref. 31, 3.

1-methoxybenzocyclobutene (**24**) and Rickborn has provided the value for 1,1-dimethoxybenzocyclobutene (**25**) and compared these results with the cyclobutene analogues.[19,30-32] A summary appears in Table 9.[19] In the monosubstituted case one notices an almost equivalent reduction in activation energy for the cyclobutene and benzocyclobutene derivatives. The parallel behavior is not apparent for the disubstituted compounds, and the reason for this difference is unknown. Assuming there is a parallel between the donor substituent effects on the monosubstituted benzocyclobutenes and cyclobutenes, it is reasonable to infer a similar effect on the 4-substituted 4,5-dihydrocyclobuta[*b*]furan analogue. Specifically, based on previous work one would expect an alkyl substituent to reduce the energy of activation to ring opening by roughly 1 kcal/mol. However, a reduction in energy of activation to ring opening of the substituted furan was not observed. As mentioned earlier this was likely due to steric interaction between the *tert*-butyl substituent and the hydrogen in the 4-position resulting in an elevated transition state. Hence, we observed that the stabilizing effect, which one might expect to see enhanced by a larger alkyl group, was offset by the increased steric interaction which occurred with ring opening.

EXPERIMENTAL

Methods and Materials

Pyrolyses were carried out in a standard flash vacuum pyrolysis apparatus which has been described, and a liquid-nitrogen-cooled trap was employed to collect the reactive furan species.[39] Following each pyrolysis the apparatus was filled with nitrogen and the trap transferred to a dry-ice isopropanol bath. Photolyses were performed using a water-cooled 450 W medium pressure Conrad-Hanovia immersion lamp, and a vacuum-jacketed immersion well suitable for low temperature photolyses was used in conjunction with a pyrex filter. ^{1}H and ^{13}C NMR data were collected with both Nicolet NT-300 and Bruker WM-300 spectrometers, UV data with a Perkin-Elmer 320 spectrophotometer, IR data with an IBM IR/98 spectrometer, and GC data with a Hewlett-Packard 5840 gas chromatograph. GC/MS data were collected using a Finnigan 4000 with an INCOS data system. Kinetic results were obtained using a stirred oil bath incorporating a 125 W blade heater, an adjustable thermoregulator (H-R and Co.) and a precision thermometer (0.1 °C graduations, F.H. Sargent and Co.). The photolysis solvent was spectral grade (Aldrich Gold Label). Benzene-d_6, used for kinetics and pyrolysis product studies, was purchased from Cambridge Isotope Laboratories. All solvents, except for those

used in the benzoate syntheses, were deaerated. Nitrogen was used for deaeration unless otherwise noted.

2-Methyl-3-furyl(*tert*-butyl)methyl benzoate (12)

Ethyl 2-methyl-3-furoate was prepared using the procedure described by Trahanovsky, Cassady and Woods.[4] The ethyl ester was subsequently converted to **12** in five steps using the procedure developed by Huang.[6] The final step required benzoylation of 2-methyl-3-furylmethyl(*tert*-butyl) alcohol. A 4.4-g (0.026-mol) quantity of the alcohol was converted to **12** and chromatographed on silica gel to provide 5.6 g (0.021 mol, 81%) of the purified compound (**12**). ^{1}H NMR ($CDCl_3$) (Appendix, Figure A-3): δ8.07-8.04 (m, 2H), 7.57-7.41 (m, 3H), 7.20 (d, J = 1.9 Hz, 1H), 6.33 (d, J = 1.9 Hz, 1H), 5.67 (s, 1H), 2.35 (s, 3H), 1.04 (s, 9H) [lit. ^{1}H NMR ($CDCl_3$) δ8.12-7.90 (m, 2H), 7.57-7.35 (m, 3H), 7.21 (d, J = 2 Hz, 1H), 6.32 (d, J = 2 Hz, 1H), 5.76 (s, 1H), 2.37 (s, 3H) 1.08 (s, 9H)].

2-Methyl-3-furylmethyl benzoate (5)

Compound **5** was prepared in three steps following the procedure developed by Trahanovsky, Cassady and Woods.[4] The final step required benzoylation of 2-methyl-3-furylmethyl alcohol. A 22.6-g (0.202-mol) quantity of the alcohol was converted to **5** and vacuum distilled using a vigreux column (126-128 °C, 0.30 torr) to provide 28.1 g (0.130 mol, 64%) of the purified compound (**5**). ^{1}H NMR ($CDCl_3$) (Appendix, Figure

A-4): δ8.04-8.01 (m, 2H), 7.55-7.41 (m, 3H), 7.26 (d, J = 1.9 Hz, 1H), 6.41 (d, J = 1.9 Hz, 1H), 5.15 (s, 2H), 2.35 (s, 3H) [lit.[4] ^{1}H NMR ($CDCl_3$) δ8.2-7.9 (m, 2H), 7.7-7.3 (m, 3H), 7.25 (d, J = 2 Hz, 1H), 6.41 (d, J = 2 Hz, 1H), 5.16 (s, 2H), 2.35 (s, 3H)].

Pyrolysis of 2-methyl-3-furyl(*tert*-butyl)methyl benzoate (12)

A 0.750-g (2.76-mmol) quantity of **12** was placed in the sample chamber followed by evacuation of the apparatus to 2 x 10^{-4} torr. The oven temperature was 525 °C during the pyrolysis which lasted 7 h. The sample chamber temperature was 60 °C, and the condenser temperature range was -4 to -8 °C. Prior to pyrolysis of the benzoate a 10 ml aliquot of pentane was distilled into the pyrolysis trap. At approximately the half-way point in the pyrolysis the sample-head was cooled and an additional 10 ml of pentane was distilled into the pyrolysis trap. Following the pyrolysis the final 10 ml of pentane was distilled over. The pyrolysate was diluted with 45 ml of pentane and warmed to near room temperature. Subsequently, the solution was shaken under nitrogen for 15 min with pulverized Na_2CO_3 and filtered under nitrogen. The sample was stored under nitrogen at -78 °C in preparation for photolyzing.

In determination of the pyrolysis yield a 0.100-g (0.368-mmol) quantity of benzoate was pyrolyzed, and collected in $CDCl_3$ which was added directly to the trap by pipet. Anisole

served as the internal standard. The yield of 2-methylene-3-*tert*-butylmethylene-2,3-dihydrofuran (**8**) was 30.9 mg (0.206 mmol, 56%). ^{1}H NMR ($CDCl_3$) (Appendix, Figure A-5): δ6.78 (m, 1H), 6.08 (m, 1H), 5.82 (s, 1H), 4.70 (d, J = 2.7, 1H), 4.54 (m, 1H), 1.16 (s, 9H) [lit.[6] ^{1}H NMR ($CDCl_3$): δ6.77 (m, 1H), 6.06 (d, J = 2.7 Hz, 1H), 5.81 (s, 1H), 4.68 (d, J = 2 Hz, 1H), 4.52 (d, J = 2 Hz, 1H), 1.16 (s, 9H).

Pyrolysis of 2-methyl-3-furylmethyl benzoate (5)

A 0.315-g (1.46-mmol) quantity of **5** was placed in the sample chamber followed by evacuation of the apparatus to 5 x 10^{-5} torr. The oven temperature was 675 °C during the pyrolysis which lasted 2 h. The sample chamber temperature was 60 °C and the condenser temperature was -20 °C. Following the pyrolysis 30 ml of diethyl ether was distilled into the pyrolysis trap in such a manner that it deposited above the pyrolysate. The pyrolysis solution was subsequently stored under nitrogen at -78 °C in preparation for photolysis.

In determination of the pyrolysis yield a 0.205-g (0.949-mmol) quantity of benzoate was pyrolyzed and collected in 10 ml diethyl ether. The yield was determined indirectly by slowly warming the solution to room temperature allowing the monomer to dimerize, removing the solvent, and determining the quantity of dimer by ^{1}H NMR using anisole as an internal standard. As the dimerization yield is known to be in excess of 97% the

yield of 2,3-dimethylene-2,3-dihydrofuran (**2**) was calculated based on the quantity of dimer present. The yield of **2** was 8.98 mg (0.845 mmol, 89%). A ^{1}H NMR of 2,3-dimethylene-2,3-dihydrofuran (**2**) was collected of an aliquot from the photolysis reactor prior to irradiation. ^{1}H NMR (4:3 $CDCl_3$/pentane) (Appendix, Figure A-6): δ6.77 (s, 1H), 5.78 (s, 1H), 5.25 (s, 1H), 4.96 (s, 1H), 4.87 (s, 1H), 4.70 (s, 1H) [lit.[5] ^{1}H NMR (1:1 $CS_2/CDCl_3$) δ6.76 (m, 1H), 5.78 (m, 1H), 5.23 (m, 1H), 4.94 (s, 1H), 4.84 (m, 1H), 4.65 (m, 1H)].

Photolysis of 2-methylene-3-*tert*-butylmethylene-2,3-dihydrofuran (8)

The photoreactor was charged with 600 ml of spectrophotometric grade pentane (Aldrich Gold Label) and the reactor was deaerated for 1/2 h. A 0.10-g (0.67 mmol) quantity of **8** was added to the reactor (higher concentrations may be used) and the solution was deaerated for another 2 h followed by irradiation with the mercury-vapor lamp. Photolyses typically lasted 7 h, and the disappearance of starting material (λ_{max} = 314 nm) was monitored by collecting UV spectra of aliquots from the photolysis solution. Following the reaction the product solution was concentrated to ca. 50 ml by distillation and stored over molecular sieves under nitrogen at -78 °C.

The yield of 4-*tert*-butyl-4,5-dihydrocyclobuta[*b*]furan (**15**) was determined by ^{1}H NMR spectroscopy as described below. An aliquot was removed from the reactor solution prior to photolyzing to determine the amount of **8** present by ^{1}H NMR spectroscopy. After conversion to **15** a second aliquot was similarly analyzed to determine the amount of **15** present which in turn allowed calculation of the yield of **15**.

The aliquots taken from the photochemical reactor were diluted with $CDCl_3$ such that the final solution of $CDCl_3$/pentane was 3:1 (v:v). Gated decoupling of the pentane signals sufficiently increased the dynamic range of the NMR spectrometer to allow collection of ^{1}H NMR data for the dilute sample and enabled accurate integration of the data. Samples were maintained at -60 °C during scanning, eliminating sample degradation. Durene served as the internal standard, and the reaction yield was 0.47 mmol (70%) of **15**. ^{1}H NMR ($CDCl_3$) (see Appendix, Figures A-7 and A-8): δ7.36 (m, H), 6.26 (d, J_{CD} = 1.79 Hz, H_D), 3.21 (octet, J_{AC} = 3.90 Hz, J_{AB} = 12.60 Hz, H_A), 3.12 (q, J_{CD} = 1.79 Hz, J_{AC} = 3.90 Hz, H_C), 3.01 (doublet of multiplets, J_{AB} = 12.6 Hz, H_B), 1.97 (s, integration obscured by pentane); ^{13}C NMR ($CDCl_3$) (Appendix, Figures A-11, A-12 and A-13) δ152.64, 144.78, 124.62, 108.16, 51.10, 35.31, 31.83, 26.87.

IR analysis of 4-*tert*-butyl-4,5-dihydrocyclobuta[*b*]furan (15)

To analyze **15** by FT-IR spectroscopy solvent was removed from the sample at reduced pressure, and the sample was dissolved in CCl_4 followed by collection of FT-IR data. The solution was subsequently added to a tube modified for sealing and taken through two freeze-thaw cycles using a dry ice-isopropanol bath. The tube was sealed and heated for 71 h at 70.5 °C which was sufficient to destroy 99.9% of **15** and an FT-IR spectrum was collected. By comparing the two spectra partial IR analysis of **15** was possible: IR (liquid cell, 0.10 mm path length) 1111 (s), 989 (m), 939 (m) cm^{-1}.

Photolysis of 2,3-dimethylene-2,3-dihydrofuran (2)

The photoreactor was charged with 600 ml of spectrophotometric grade pentane (Aldrich Gold Label) and the reactor was immersed in a dry ice-isopropanol bath while deaerating the solvent with argon. After deaerating 1/2 h a 0.042-g (0.44-mmol) quantity of **2** was added to the reactor and the solution was deaerated for another hour. Irradiation of the reactor solution was interrupted at 30 min intervals to add dry ice to the coolant bath. The duration of the photolysis was typically 3.25 h, and a low concentration of starting material was necessary to suppress photochemically induced intermolecular reactions.

Progress of the photolyses was monitored by withdrawing aliquots periodically and adding to an excess of deaerated methyl acrylate under nitrogen. The solution was subsequently analyzed by GC for the Diels Alder adduct, and the photolysis was considered complete when adduct no longer appeared in the GC trace. Following the photolysis the product solution was stored over molecular sieves at -78 °C under argon.

The yield of **2** was determined by ^{1}H NMR spectroscopy in a manner similar to that for **15**. It should be noted the photolysis procedure was modified slightly as deaeration time after addition of **2** was extended to 5 h. An aliquot was removed from the reactor before and after the photolysis for ^{1}H NMR analysis. The mass of each aliquot removed from the photoreactor was determined indirectly and each aliquot was diluted with a known mass of standard solution consisting of $CDCl_3$ as solvent and durene as standard. Gated decoupling was used to enable accurate integration of standard and downfield proton signals. Instrument parameters were the same as those used to determine the yield of 4-*tert*-butyl-4,5-dihydrocyclobuta[*b*]furan (**15**), and samples were maintained at -60 °C during scanning. The yield of **9** was 8.6 x 10^{-2} mmol (18%): ^{1}H NMR (Acetone-d_6) (see Appendix, Figures A-9 and A-10): δ7.40 (doublet of triplets, J_{AB} = 1.5 Hz, J_{AC} = 0.9 Hz, H_A), 6.23 (d, J_{AB} = 1.5 Hz, H_B), 3.25 (doublet of triplets, J_{AC} = 0.9 Hz, J_{CD} = 2.8 Hz, H_C), 2.83 (t, J_{CD} = 2.8 Hz, H_D). The

yield of dimer **3** was 9.88 x 10^{-2} g (5.3 x 10^{-2} mmol; 11%): ^{1}H NMR (Acetone-d_6) δ7.22 (d, J_{AB} = 1.7 Hz, H_A), 6.12 (d, J_{AB} = 1.7 Hz, H_B), 3.04 (s, 4H), 2.80 (s, 4H) [lit.[5] ^{1}H NMR ($CDCl_3$): δ 7.12 (d, J = 2 Hz, 2H), 6.05 (d, J = 2 Hz, 2H), 3.00 (s, 4H), 2.74 (s, 4H).

^{13}C and IR analysis of 4,5-dihydrocyclobuta[*b*]furan (9)

To analyze **9** by ^{13}C NMR a sample was prepared in acetone-d_6, added to a modified NMR tube, taken through three freeze-thaw cycles using a dry ice-isopropanol bath and sealed under vacuum. A decoupled ^{13}C spectrum was collected followed by warming at 74 °C for 72 h which was sufficient to destroy 75% of **9**. A second decoupled ^{13}C NMR made possible the identification of the four furan ring carbons while the two methylene carbons were unidentifiable due to the presence of pentane: ^{13}C NMR (acetone-d_6) (Appendix, Figure A-14) δ152.90, 146.23, 123.11, 108.98.

To analyze **9** by FT-IR a sample was prepared and the volume of pentane solvent was reduced to 0.15 ml by fractional distillation, diluted with 0.2 ml of heptane and an FT-IR spectrum was collected. After collection of the FT-IR spectrum the solution was added to a tube modified for sealing and taken through two freeze-thaw cycles using a dry ice-isopropanol bath followed by sealing. The sealed tube was warmed at 70.5 °C for 78 h which was sufficient to destroy 70% of **9**, and an FT-IR

spectrum was collected. By comparing the two spectra the IR absorbances of **9** were determined: IR (liquid cell, 0.10 mm path length) 1624 (m), 1231 (s), 1111 (s), 1031 (s), 912 (s) cm^{-1} [lit.[11] IR (argon matrix) 1608.8 (s), 1234.2 (s), 1115.4 (m), 1034.6 (s), 912.4 (s) cm^{-1}].

Procedure for analyzing the pyrolysate of 2-methyl-3-furyl(*tert*-butyl)methyl benzoate (12) for the presence of 4-*tert*-butyl-4,5-dihydrocyclobuta[*b*]furan (15)

A 0.1015-g (0.373-mmol) quantity of **12** was pyrolyzed and 3 ml of CS_2 was added through a side-arm. The volume of solvent was reduced to 0.1 ml under vacuum and 1.0 ml of benzene-d_6 was added in addition to a known quantity of standard (diphenylmethane). An 11,000 scan ^1H NMR spectrum was subsequently collected on the Nicolet NT-300 in the double precision mode and compared with that of a sample of **15** in benzene-d_6.

A sample of **15** was prepared by reducing the pentane solvent to a minimum and dissolving in benzene-d_6 followed by addition of a known quantity of standard and diluting to 5 ml in a volumetric flask. A measured quantity of this standard solution was added to the sample of **12** such that the ratio of **12:15** was 100:1.25 and a 10,000 ^1H NMR spectrum was collected on the Nicolet NT-300 in the double precision mode. By comparing the spectra of **12** with and without the standard of 15

it was determined that the detection limit for **15** in the original spectrum was below 0.5% relative to **12**.

Procedure for analyzing the pyrolysate of 2-methyl-3-furylmethyl benzoate (5) for the presence of 4,5-dihydrocyclobuta[*b*]furan (9)

A 0.2020-g (0.935-mmol) quantity of **5** was pyrolyzed and 2 ml of CS_2 was added through a side-arm. The material in the trap was warmed slowly to room temperature and maintained at room temperature for 2.5 h which allowed 2,3-dimethylene-2,3-dihydrofuran (**2**) to dimerize. Subsequently, 2 ml of benzene-d_6 was added and a quantity of this solution was added to a modified NMR tube, taken through three freeze-thaw cycles and sealed. Following acquisition of a 1600 scan ^1H NMR spectrum on the Nicolet NT-300 in the double precision mode the sample was warmed for 45.5 h at 68.25 °C. A second 1600 scan ^1H NMR spectrum was collected on the Nicolet NT-300 in the double precision mode, and the two spectra were analyzed in the region between 6.00 and 6.20 ppm for the presence of a dihydrocyclobuta[*b*]furan proton signal. As warming was sufficient to destroy 44% of **9** if present the region between 6.00 and 6.20 ppm was analyzed for a signal of a thermally labile compound. Though it was not possible to assign a specific signal to **9** it was ascertained that if **9** were formed

in the pyrolysis of **5** it would not be present in a concentration greater than 2.6% of the concentration of **2**.

Procedure for measuring rate constants for the electrocyclic ring opening of 4-*tert*-butyl-4,5-dihydrocyclobuta[*b*]furan (15)

In preparation for the kinetic run the volume of the photolysis solution containing **15** was reduced to 25 ml by fractionally distilling the pentane. A 6-ml aliquot of the photolysis solution was added to a flask flushed with nitrogen. The solvent volume was reduced under vacuum until the ratio of **15**:pentane was approximately 1:1. The sample was added to a modified NMR tube in addition to 0.80 ml of benzene-d_6 and a weighed 40-ul aliquot of a diphenylmethane standard solution. Following two freeze-thaw cycles the tube was evacuated to 10^{-2} torr while cooling at -78 °C. The tube was sealed and a ^{1}H NMR spectrum collected. The kinetics sample was submerged in the previously described oil bath, and the concentration of **15** was determined periodically by ^{1}H NMR after quenching the tube in ice water. All runs lasted approximately two and one-half half-lives, and rate constants were calculated as mentioned previously.

Procedure for measuring rate constants for the electrocyclic ring opening of 4,5-dihydrocyclobuta[*b*]furan (9)

In preparation for the kinetics run the volume of the photolysis solution containing **9** was reduced to 0.15 ml by

fractionally distilling the pentane. The concentrated solution was added to a modified NMR tube in addition to approximately 0.70 ml benzene-d_6 and a weighed aliquot of standard solution (approximately 30 ul) containing diphenylmethane as standard. The tube was sealed and kinetics were followed in the manner described for **15**.

REFERENCES

1. Charlton, J. L.; Alauddin M. M. *Tetrahedron*, **1987**, *43*, 2873.
2. Van den Berg, K. J. Ph.D. Dissertation, University of Groningen, The Netherlands, 1990.
3. (a) Fallis, A. G. *Can. J. Chem.* **1984**, *62*, 183. (b) McCullough, J. J. *Acc. Chem. Res.* **1980**, *13*, 270.
4. Trahanovsky, W. S.; Cassady, T. J.; Woods, T. L. *J. Am. Chem. Soc.* **1981**, *103*, 6691.
5. Chou, C. H.; Trahanovsky, W. S. *J. Am. Chem. Soc.* **1986**, *108*, 4138.
6. Huang, Y. C. Ph.D. Dissertation, Iowa State University, Ames, Iowa, 1987.
7. Winberg, H. E.; Fawcett, F. S.; Mochel, W. E.; Theobald, C. W. *J. Am Chem. Soc.* **1960**, *82*, 1428.
8. Roth, W. R.; Biermann, M.; Dekker, H.; Jochems, R.; Mosselman, C.; Hermann, H. *Chem. Ber.* **1978**, *111*, 3892.
9. Roth, W. R.; Scholz, P. *Chem Ber.* **1981**, *114*, 3741.
10. Roth, W. R.; Ebbrecht, T.; Beitat, A. *Chem. Ber.* **1988**, *121*, 1357.
11. Munzel, N.; Schweig, A. *Angew. Chem. Int. Ed. Engl.* **1987**, *26*, 471.
12. (a)Baird, N. C. *J. Chem. Educ.* **1971**, *48*, 509. (b) Lowry, T. H.; Richardson, K. S. *Mechanism and Theory in Organic*

Chemistry, Second Edition; Harper and Row: New York, 1981, p 111. (c) Dewar, M. J. S.; Harget, A. J.; Trinajstic, N. *J. Am. Chem. Soc.* **1969**, *91*, 6321. d) Hess, B. A.; Schaad, L. J.; Holyoke, C. W. *Tetrahedron* **1972**, *28*, 3657.

13. (a) Kramer, G. W.; Levy, A. B.; Midland, M. M. in Brown, H. C. *Organic Synthesis via Boranes*; Wiley: New York, 1975. (b) Shriver, D. F.; Drezdzon, M. A. *The Manipulation of Air-sensitive Compounds*, 2nd ed.; Wiley: New York, 1986; Chapter 1.
14. Paquette, L. A. *Acc. Chem. Res.* **1971**, *4*, 280.
15. Espenson, J. H. *Chemical Kinetics and Reaction Mechanisms*; McGraw-Hill: New York, 1981; Chapter 1.
16. Kinetics program provided by J. J. Gajewski and K. Gilbert, SERENA Software, Bloomington, Indiana.
17. Bevington, P. R. *Data Reduction and Error Analysis for the Physical Sciences*; McGraw-Hill: New York, 1969, p 18.
18. Nonlinear least squares software was provided by J. H. Espenson, Iowa State University, 1990.
19. Moss, R. J.; White, R. O.; Rickborn, B. *J. Org. Chem.* **1985**, *50*, 5132.
20. Ruhlman, V. K.; Kokkali, A.; Becker, H.; Seefluth, H.; Friedenberger, U. *J. fur Pracktische Chemie* **1969**, *311*, 844.
21. (a) Bubb, W. A.; Sternhell, S. *Aust. J. Chem.* **1976**, *29*, 1685. (b) Fay, C. K.; Grutzner, J. B.; Johnson, L. F.;

Sternhell, S.; Westerman, P. W. *J. Org. Chem.* **1973**, *38* 3122.

22. Wiberg, K. B.; Fenoglio, R. A. *J. Am. Chem. Soc.*, **1968**, *90*, 3395.

23. Houk, K. N. In *Strain and Its Implications in Organic Chemistry*; de Meijere A.; Blechert, S., Eds; NATO ASI Series 273; Kluwer: Boston, 1989; p 25.

24. Kirmse, W.; Rondan, N. G.; Houk K. N. *J. Am. Chem. Soc.* **1984**, *106*, 7989.

25. Rondan, N. G.; Houk, K. N. *J. Am. Chem. Soc.* **1985**, *107*, 2099.

26. Houk, K. N.; Spellmeyer, D. C.; Jefford, C..W.; Rimbault, C. G.; Ying Wang, Miller, R. D. *J. Org. Chem.* **1988**, *53*, 2125.

27. (a) Rudolf, K.; Spellmeyer, D. C.; Houk, K. N. *J. Org. Chem.* **1987**, *52*, 3708. (b) Buda, A. B.; Wang. Y.; Houk, K. N. *J. Am. Chem. Soc.* **1989**, *54*, 2264.

28. Dolbier, W. R., Jr.; Koroniak, H.; Burton, D. J.; Bailey, A. R.; Shaw, G. S.; Hansen, S. W. *J. Am. Chem. Soc.* **1984**, *106*, 1871.

29. Dolbier, W. R., Jr.; Koroniak, H.; Burton, D. J.; Heinze, P. L.; Bailey, A. R.; Shaw, G. S.; Hansen, S. W. *J. Am. Chem. Soc.* **1987**, *109*, 219.

30. Curry, M. J.; Stevens, I. D. R. *J. Chem. Soc., Perkin Trans. 2* **1980**, 1391.

31. Arnold, B. J.; Sammes, P. G.; Wallace, T. W. *J. Chem. Soc., Perkin Trans. 1* **1974**, 409.

32. Moss, R. J.; Rickborn, B. *J. Org. Chem.* **1984**, *49*, 3694.

33. Scheiss, P.; Rutschmann, S. *Chimia* **1985**, *39*, 213.

34. Oppolzer, W. *Synthesis*, **1978**, 793.

35. (a) Carr, R. W., Jr.; Walters, W. D. *J. Phys. Chem.* **1965**, *69*, 1073. (b) Squillacote, M. E.; Sheridan, R. S.; Chapman, O. L.; Anet, F. A. L. *J. Am. Chem. Soc.* **1979**, *101*, 3657.

36. Trahanovsky, W. S.; Macias, J. R. *J. Am. Chem. Soc.* **1986**, *108*, 6820.

37. Dewar, M. J. S.; de Llano, C. *J. Am. Chem. Soc.* **1969**, *91*, 789.

38. Turner, R. B.; Goebel, P.; Mallon, B. J.; Doering, W. von E.; Coburn, J. F., Jr.; Pomerantz, M. *J. Am. Chem. Soc.* **1968**, *90*, 4315.

39. Trahanovsky, W. S.; Ong, C. C.; Pataky, J. G.; Weitl, F. L.; Mullen, P. W.; Clardy, J. C.; Hansen, R. S. *J. Org. Chem.* **1971**, *36*, 3575.

APPENDIX

Detailed Description of the Preparation of 2-Methyl-3-furyl(*tert*-butyl)methyl Benzoate

Ethyl 2-methyl-3-furoate[1]

Chloroacetaldehyde (50 g, 310 mmol) in a 50% aqueous solution was added to a stirred solution of pyridine (67 ml) and ethyl acetoacetate (35 g, 270 mmol) over a 10 min period. The solution was stirred for 4 h then allowed to stand overnight. The layers were separated followed by extraction of the aqueous layer with ether (4 x 15 ml). The organic layers were combined and washed successively with water (4 x 15 ml) and brine (3 x 15 ml). After drying ($MgSO_4$) and solvent removal the crude product was purified by vacuum distillation to yield 21.2 g (138 mmol, 52%) of ethyl 2-methy-3-furoate.

2-methyl-3-furoic acid[2]

A mixture of ethyl 2-methyl-3-furoate (17.2 g, 112 mmol) in 20% aqueous NaOH (80 ml) was refluxed for 2 h. After the mixture cooled to room temperature 55 ml concentrated HCl was added with stirring. The white solid which formed was collected by suction filtration and washed twice with cold water. Drying overnight yielded 13.0 g (103 mmol, 92%) of 2-methyl-3-furoic acid.

2-Methyl-3-furoyl chloride[2]

A solution of 2-methyl-3-furoic acid (7.16 g, 56.8 mmol) was stirred in 20 ml of thionyl chloride at 40 °C overnight. Thionyl chloride was removed from the product solution followed by distillation at reduced pressure to yield 6.52 g (45.4 mmol, 80%) of 2-methyl-3-furoyl chloride: bp 75 °C, 25 torr.

2-Methyl-3-furyl *t*-butyl ketone[2]

A flask was charged with copper iodide (9.6 g, 50.5 mmol) and flushed with nitrogen. A 50 ml quantity of dry ether (Na) was added by cannula followed by 2-methyl-3-furoyl chloride (4.9 g, 34 mmol). After the stirred mixture was cooled to -78 °C and 18.7 ml of a 2 M solution of *tert*-butylmagnesium chloride was slowly added by cannula. The stirred mixture was allowed to reach room temperature overnight. The reaction mixture was poured into a mixture of 2 N HCl (50 ml) and ice (50 g). The aqueous layer was washed with ether (2 x 50 ml), and the combined ether layers were washed successively with 2 N HCl (4 x 50 ml), saturated $NaHCO_3$ (2 x 50 ml) and brine (1 x 50 ml). After drying ($MgSO_4$) the solvent was removed to yield 5.0 g (30 mmol, 88%) of the ketone.

2-Methyl-3-furylmethyl(*tert*-butyl) alcohol[2]

2-Methyl-3-furyl *tert*-butyl ketone (5.0 g, 30 mmol) was added dropwise to a stirred mixture of $LiAlH_4$ (1.3 g, 31 mmol) in 25 ml of dry ether (Na) at 0 °C under nitrogen. The mixture

was allowed to stir overnight then cooled to 0 °C. A 1.3 ml quantity of water was added dropwise to the solution followed 1.3 ml of a 10% aqueous NaOH solution and 4.0 ml of water. The aluminum salt was removed by suction filtration. The solution was dried ($MgSO_4$) followed by solvent removal to yield 4.4 g (26 mmol, 87%) of 2-methyl-3-furylmethyl(*tert*-butyl) alcohol.

2-Methyl-3-furyl(*tert*-butyl)methyl benzoate[2]

2-Methyl-3-furylmethyl(*tert*-butyl) alcohol was stirred in 100 ml of THF under nitrogen at 0 °C while approximately 10.8 ml of n-butyl lithium (2 M in hexane) was added by syringe. The addition was complete when the solution turned light yellow which indicated the presence of a dianion. Care was taken to avoid adding excess n-butyl lithium as the dianion was an undesirable reactive species. After stirring 10 min freshly distilled benzoyl chloride (2.6 g, 18.7 mmol) was added dropwise by syringe over 5 min. The solution was stirred overnight at room temperature. After addition of water (15 ml) the layers were separated and the aqueous layer was washed with ether (2 x 15 ml). The combined organic layers were washed successively with water (1 x 15 ml), saturated $NaHCO_3$ (2 x 15 ml) and brine (2 x 15 ml). Following drying ($MgSO_4$) the solvent was removed. The crude product was chromatographed on silica gel (5% ether in hexanes) to yield 5.56 g (20.4 mmol, 78%) of 2-methyl-3-furyl(*tert*-butyl)methyl benzoate.

Detailed Description of the Preparation of 2-Methyl-3-furylmethyl Benzoate

2-Methyl-3-furylmethyl alcohol[1]

Methyl 2-methyl-3-furoate (31.3 g, 223 mmol) in 125 ml of dry ether (Na) was slowly added dropwise to a stirred mixture of $LiAlH_4$ (15.5 g, 401 mmol) in 145 ml of dry ether at 0 °C under nitrogen. The mixture was stirred for 5 h followed by cooling to 0 °C and dropwise addition of 15.5 ml of water. Subsequently, a 15.5 ml quantity of a 15% aqueous NaOH solution was added dropwise followed by 46.4 ml of water. The resulting aluminum salt was removed by suction filtration. The solution was dried ($MgSO_4$) and the solvent removed to yield 22.63 g (202 mmol, 91%) of the alcohol.

2-Methyl-3-furylmethyl benzoate[1]

Benzoyl chloride (28.7 g, 204 mmol) in 125 ml dry ether (Na) was added dropwise to a stirred solution of 2-methyl-3-furylmethyl alcohol (22.6 g, 202 mmol) and triethylamine (24.5 g, 242 mmol) in 250 ml dry ether. The solution was stirred for 11 h. After addition of water (250 ml) the layers were separated, and the aqueous layer was extracted twice with 35 ml of ether. The ether layers were combined and washed successively with 1 M hydrochloric acid (3 x 70 ml), saturated $NaHCO_3$ (2 x 70 ml) and saturated sodium chloride (3 x 70 ml). After drying ($MgSO_4$) and solvent removal, vacuum distillation

using a vigreux column gave 28.11 g (130 mmol, 64%) of the pure benzoate: bp 128 °C, 0.30 torr. During the distillation care was taken to separate the benzoate from low boiling compounds resulting in loss of some benzoate. The product contained no triethyl amine or benzoyl chloride as shown by GC.

Detailed Description of the Preparation for Low Temperature Photolyses

A vacuum jacketed quartz immersion well (Ace Glass 7858-08) was inserted into a 500 ml reactor vessel (Ace Glass 7841-04) supported by a photochemical reactor stand (Ace Glass 7837). The reactor was charged with 550 ml of spectrophotometric grade pentane (Aldrich) and fitted with an adapter connected to a bubbler, low temperature thermometer and an 18 ga teflon sparger tube. Argon was passed through the sparger tube. The immersion well was fitted with a pyrex filter supported by a number 9 neoprene stopper and cushioned by two o-rings. The filter was inserted into the immersion well in conjunction with the water inlet tube which supplied water for cooling the lamp.

The water inlet tube was connected to the water inlet port of the immersion well with a modified septum. A filter and flow sensor were connected to the free end of the coolant line prior to attachment to a water faucet. The flow sensor was connected the Water-Flow Power Cut-Off (Ace Glass 12160-15).

The water exit port of the immersion well was attached to a 1/4" ID section of Tygon tubing. The water flow was carefully adjusted such that the water was siphoned from the immersion well by the Tygon tubing attached to the exit port and new Tygon tubing provided the best siphoning effect. This passive flow setup was necessary to avoid problems which might arise with a pressurized cooling system.

The quartz glass of the 450 W medium-pressure mercury-vapor lamp (Ace Glass 7825-34) was cleaned with reagent grade isopropanol prior to lowering into the pyrex filter. The apparatus was clamped to a lattice rack with the lower portion in a dewar partially filled with isopropanol. Subsequently, the dewar was filled with crushed dry ice and additional isopropanol such that the level of pentane in the reactor was below that of the surrounding coolant bath. As the vacuum jacketed immersion well was not an exceptional insulator, it was necessary to maintain a constant flow of water through the cooling jacket to avoid having water freeze in the lamp cooling system.

After degassing the solution 0.5 h, 2,3-dimethylene-2,3-dihydrofuran was added to the vessel by cannula followed with an additional 1 h of degassing. The actual photolysis was performed as described in the experimental. The power supply was Ace Glass model 7830-34.

Addendum to: "Procedure for Measuring Rate Constants for the Electrocyclic Ring Opening of 4-*tert*-Butyl-4,5-dihydrocyclobuta[*b*]furan (15)" of The Experimental

In addition to the typical kinetic runs the possibility of ring opening catalysis by side-products in the photolysis solution was investigated. The sample of **15** for this investigation was prepared in a manner similar to that by which previous samples were prepared. However, the solvent used was that obtained from a spent kinetics sample. Therefore, the concentration of all side-products in the photolysis product solution was doubled. The run was conducted in the usual manner, and no catalysis was observed.

APPENDIX REFERENCES

1. Trahanovsky, W. S.; Cassady, T. J.; Woods, T. L. *J. Am. Chem. Soc.* **1981**, *103*, 6691.

2. Huang, Y. C. Ph.D. Dissertation, Iowa State University, Ames, Iowa, 1987.

Table A-1. Rate of disappearance of 4-*tert*-butyl-4,5-dihydrocyclobuta[*b*]furan (**15**) at 70.15 °C in benzene-d_6. First run[a]

Time x 10^{-4}, s	Integration[b,c] A	Integration[b,c] B
0.0000	187.6	401.5
0.7578	147.4	323.3
1.4993	108.6	241.8
2.1565	87.0	183.1
2.8097	72.7	153.0
3.5997	52.0	110.6
4.3137	44.5	94.9
5.2007	35.9	72.5
17.2235	13.8	20.5

[a]Rate constant: $k = 3.94 \pm 0.08 \times 10^{-5}$ s^{-1}.

[b]The range for integration A is approximately 4.70-4.60 ppm, and the signal followed arises from one proton of **15**. The range for integration B is approximately 2.95-2.85 ppm, and the signal followed arises from two protons of **15**. Though these ranges vary slightly between runs, they were held constant in each run.

[c]The standard was diphenylmethane, and its concentration was 2.1×10^{-2} M. The tabulated integrations are relative to the methylene singlet which was set at 200.

Table A-2. Rate of disappearance of 4-*tert*-butyl-4,5-dihydrocyclobuta[*b*]furan (**15**) at 70.15 °C in benzene-d_6. Second run[a]

Time x 10^{-4}, s	Integration[b,c] A	Integration[b,c] B
0.0000	199.4	421.5
0.7990	127.3	272.5
1.5401	98.2	206.1
2.1285	79.2	169.6
2.8665	59.3	121.7
3.5878	46.2	99.4
4.3603	36.3	78.3
5.1758	31.5	62.8
21.7355	14.2	21.6

[a]Rate constant: $k = 4.40 \pm 0.11 \times 10^{-5}$ s^{-1}.

[b]The range for integration A is approximately 4.70-4.60 ppm, and the signal followed arises from one proton of **15**. The range for integration B is approximately 2.95-2.85 ppm, and the signal followed arises from two protons of **15**. Though these ranges vary slightly between runs, they were held constant in each run.

[c]The standard was diphenylmethane, and its concentration was 2.1×10^{-2} M. The tabulated integrations are relative to the methylene singlet which was set at 200.

Table A-3. Rate of disappearance of 4-*tert*-butyl-4,5-dihydrocyclobuta[*b*]furan (**15**) at 70.15 °C in benzene-d_6. Third run[a]

Time x 10^{-4}, s	Integration[b,c] A	Integration[b,c] B
0.0000	339.0	707.9
0.7203	275.0	562.8
1.4021	209.9	421.1
2.0616	178.8	340.4
3.0096	132.7	262.5
3.7783	109.9	211.7
4.4743	97.9	176.4
5.3433	85.6	158.2
20.0328	43.9	74.8

[a]Rate constant: $k = 3.86 \pm 0.10 \times 10^{-5}$ s^{-1}.

[b]The range for integration A is approximately 4.70-4.60 ppm, and the signal followed arises from one proton of **15**. The range for integration B is approximately 2.95-2.85 ppm, and the signal followed arises from two protons of **15**. Though these ranges vary slightly between runs, they were held constant in each run.

[c]The standard was diphenylmethane, and its concentration was 2.1×10^{-2} M. The tabulated integrations are relative to the methylene singlet which was set at 200.

Table A-4. Rate of disappearance of 4-*tert*-butyl-4,5-dihydrocyclobuta[*b*]furan (**15**) at 85.25 °C in benzene-d_6. First run[a]

Time x 10^{-3}, s	Integration[b,c] A	Integration[b,c] B
0.000	349.5	733.6
1.164	280.1	585.4
1.927	238.7	505.5
2.696	208.5	435.2
3.705	168.8	347.5
5.056	135.6	275.8
5.952	117.0	238.3
6.930	99.8	198.6
8.726	79.5	144.1
43.809	21.8	36.5

[a]Rate constant: $k = 2.09 \pm 0.01 \times 10^{-4}$ s^{-1}.

[b]The range for integration **A** is approximately 4.70-4.60 ppm, and the signal followed arises from one proton of **15**. The range for integration B is approximately 2.95-2.85 ppm, and the signal followed arises from two protons of **15**. Though these ranges vary slightly between runs, they were held constant in each run.

[c]The standard was diphenylmethane, and its concentration was 2.3×10^{-2} M. The tabulated integrations are relative to the methylene singlet which was set at 200.

Table A-5. Rate of disappearance of 4-*tert*-butyl-4,5-dihydrocyclobuta[*b*]furan (**15**) at 85.25 °C in benzene-d_6. Second run[a]

Time x 10^{-3}, s	Integration[b,c] A	Integration[b,c] B
0.000	321.1	671.7
1.228	248.7	530.3
2.451	198.3	414.0
3.613	159.8	331.2
4.830	128.4	263.5
6.008	107.0	215.8
7.189	91.3	170.7
8.374	75.8	150.4
9.115	72.5	128.9
10.923	59.6	102.2
59.002	31.6	45.1

[a]Rate constant: $k = 2.18 \pm 0.01 \times 10^{-4}$ s^{-1}.

[b]The range for integration A is approximately 4.70-4.60 ppm, and the signal followed arises from one proton of **15**. The range for integration B is approximately 2.95-2.85 ppm, and the signal followed arises from two protons of **15**. Though these ranges vary slightly between runs, they were held constant in each run.

[c]The standard was diphenylmethane, and its concentration was 2.5×10^{-2} M. The tabulated integrations are relative to the methylene singlet which was set at 200.

Table A-6. Rate of disappearance of 4-*tert*-butyl-4,5-dihydrocyclobuta[*b*]furan (**15**) at 85.25 °C in benzene-d_6. Third run[a]

Time x 10^{-3}, s	Integration[b,c] A	Integration[b,c] B
0.000	300.6	632.2
1.265	231.7	483.5
2.569	178.7	384.0
3.839	141.9	294.3
5.055	114.6	240.8
6.295	91.8	188.6
7.698	74.7	148.5
8.739	71.3	131.5
9.708	64.3	112.4
81.700	24.5	29.7

[a]Rate constant: $k = 2.04 \pm 0.04 \times 10^{-4}$ s^{-1}.

[b]The range for integration A is approximately 4.70-4.60 ppm, and the signal followed arises from one proton of **15**. The range for integration B is approximately 2.95-2.85 ppm, and the signal followed arises from two protons of **15**. Though these ranges vary slightly between runs, they were held constant in each run.

[c]The standard was diphenylmethane, and its concentration was 2.6×10^{-2} M. The tabulated integrations are relative to the methylene singlet which was set at 200.

Table A-7. Rate of disappearance of 4-*tert*-butyl-4,5-dihydrocyclobuta[*b*]furan (**15**) at 55.10 °C in benzene-d_6. First run[a]

Time x 10^{-5}, s	Integration[b,c] A	Integration[b,c] B
0.00000	300.2	628.6
0.32587	252.9	535.7
0.65006	209.9	447.8
0.97430	179.7	371.7
1.29835	150.2	308.7
1.62240	127.5	260.4
1.94655	112.3	227.2
2.27040	95.8	193.3
2.59460	85.3	165.8
2.93480	73.1	142.2
3.24125	60.5	123.4
13.26285	25.0	45.8

[a]Rate constant: $k = 6.16 \pm 0.06 \times 10^{-6}$ s^{-1}.

[b]The range for integration A is approximately 4.70-4.60 ppm, and the signal followed arises from one proton of **15**. The range for integration B is approximately 2.95-2.85 ppm, and the signal followed arises from two protons of **15**. Though these ranges vary slightly between runs, they were held constant in each run.

[c]The standard was diphenylmethane, and its concentration was 2.7×10^{-2} M. The tabulated integrations are relative to the methylene singlet which was set at 200.

Table A-8. Rate of disappearance of 4-*tert*-butyl-4,5-dihydrocyclobuta[*b*]furan (**15**) at 55.10 °C in benzene-d_6. Second run[a]

Time x 10^{-5}, s	Integration[b,c] A	Integration[b,c] B
0.00000	34.1	58.3
0.32475	28.5	54.2
0.65107	24.3	46.4
0.97749	21.3	39.7
1.30147	17.7	33.9
1.60557	15.5	29.9
1.92985	14.0	26.5
2.26465	10.8	21.7
2.55390	10.2	19.1
2.71732	9.2	17.4
3.08962	8.2	15.6
11.23322	1.1	2.4

[a]Rate constant: $k = 4.94 \pm 0.08 \times 10^{-6}$ s^{-1}.

[b]The range for integration A is approximately 4.70-4.60 ppm, and the signal followed arises from one proton of **15**. The range for integration B is approximately 2.95-2.85 ppm, and the signal followed arises from two protons of **15**. Though these ranges vary slightly between runs, they were held constant in each run.

[c]The standard was diphenylmethane, and its concentration was 2.6×10^{-2} M. The tabulated integrations are relative to the methylene singlet which was set at 200.

Table A-9. Rate of disappearance of 4-*tert*-butyl-4,5-dihydrocyclobuta[*b*]furan (**15**) at 55.10 °C in benzene-d_6. Third run[a]

Time x 10^{-5}, s	Integration[b,c] A	Integration[b,c] B
0.00000	108.5	235.0
0.33940	96.8	196.8
0.67085	83.0	169.6
0.86505	72.2	155.8
1.20868	62.6	131.9
1.55356	61.7	114.5
1.94216	52.5	98.9
2.19469	51.0	97.7
2.42479	46.3	88.5
2.74249	40.1	78.6
12.15281	20.5	47.9

[a]Rate constant: $k = 5.96 \pm 0.16 \times 10^{-6}$ s^{-1}.

[b]The range for integration A is approximately 4.70-4.60 ppm, and the signal followed arises from one proton of **15**. The range for integration B is approximately 2.95-2.85 ppm, and the signal followed arises from two protons of **15**. Though these ranges vary slightly between runs, they were held constant in each run.

[c]The standard was diphenylmethane, and its concentration was 2.6×10^{-2} M. The tabulated integrations are relative to the methylene singlet which was set at 200.

Table A-10. Rate of disappearance of 4,5-dihydrocyclobuta-[*b*]furan (**9**) at 98.10 °C in benzene-d_6. First run[a]

Time x 10^{-4}, s	Integration[b,c]
0.0000	129.9
0.3038	104.3
0.6062	90.8
0.9087	82.0
1.2121	71.4
1.5140	78.7
1.8180	67.4
2.1190	61.1
2.6658	59.4
3.2656	54.9
3.8679	48.1
4.4861	45.1
5.0873	43.9
10.9140	37.8

[a]Rate constant: $k = 5.07 \pm 0.22 \times 10^{-5}$ s^{-1}.

[b]The range for integration is approximately 6.05-5.95 ppm, and the signal followed arises from one proton of **9**. Though the range varies slightly between runs, it was held constant in each run.

[c]The standard was diphenylmethane, and its concentration was 1.7×10^{-2} M. The tabulated integrations are relative to the methylene singlet which was set at 200.

Table A-11. Rate of disappearance of 4,5-dihydrocyclobuta-[*b*]furan (**9**) at 98.10 °C in benzene-d_6. Second run[a]

Time x 10^{-4}, s	Integration[b,c]
0.0000	163.0
0.4662	122.5
0.9831	102.5
1.6352	80.2
2.1256	74.6
2.4567	70.7
2.7187	68.1
3.2059	61.9
3.7010	64.4
16.5366	50.1

[a]Rate constant: $k = 5.98 \pm 0.48 \times 10^{-5}\ s^{-1}$.

[b]The range for integration is approximately 6.05-5.95 ppm, and the signal followed arises from one proton of **9**. Though the range varies slightly between runs, it was held constant in each run.

[c]The standard was diphenylmethane, and its concentration was 1.4×10^{-2} M. The tabulated integrations are relative to the methylene singlet which was set at 200.

Table A-12. Rate of disappearance of 4,5-dihydrocyclobuta-[*b*]furan (**9**) at 98.10 °C in benzene-d_6. Third run[a]

Time x 10^{-4}, s	Integration[b,c]
0.0000	85.8
0.3987	66.9
0.6617	62.2
1.0725	52.5
1.4933	44.6
2.0408	41.2
2.4025	39.0
2.8242	37.3
3.2465	34.9
3.6679	33.9
15.8571	29.5

[a]Rate constant: $k = 6.80 \pm 0.24 \times 10^{-5}\ s^{-1}$.

[b]The range for integration is approximately 6.05-5.95 ppm, and the signal followed arises from one proton of **9**. Though the range varies slightly between runs, it was held constant in each run.

[c]The standard was diphenylmethane, and its concentration was 3.4×10^{-2} M. The tabulated integrations are relative to the methylene singlet which was set at 200.

Table A-13. Rate of disappearance of 4,5-dihydrocyclobuta-[*b*]furan (**9**) at 83.25 °C in benzene-d_6. First run[a]

Time x 10^{-4}, s	Integration[b,c]
0.0000	176.9
1.4324	149.5
5.0789	101.3
5.8137	95.5
6.9001	87.3
8.1747	86.7
9.0987	84.7
12.5257	79.7
13.4417	71.2
14.1826	68.7
15.7964	69.3
16.8894	63.0
75.5691	56.8

[a]Rate constant: $k = 1.51 \pm 0.10 \times 10^{-5}$ s^{-1}.

[b]The range for integration is approximately 6.05-5.95 ppm, and the signal followed arises from one proton of **9**. Though the range varies slightly between runs, it was held constant in each run.

[c]The standard was diphenylmethane, and its concentration was 3.6×10^{-2} M. The tabulated integrations are relative to the methylene singlet which was set at 200.

Table A-14. Rate of disappearance of 4,5-dihydrocyclobuta-[*b*]furan (**9**) at 83.25 °C in benzene-d_6.
Second run[a]

Time x 10^{-4}, s	Integration[b,c]
0.0000	238.0
0.7680	216.4
2.5077	178.9
3.9522	163.1
4.7050	150.5
5.7241	142.2
8.3606	122.2
9.9473	115.4
11.5583	109.7
12.4888	106.3
62.4201	84.1

[a]Rate constant: $k = 1.53 \pm 0.03 \times 10^{-5}\ s^{-1}$.

[b]The range for integration is approximately 6.05-5.95 ppm, and the signal followed arises from one proton of **9**. Though the range varies slightly between runs, it was held constant in each run.

[c]The standard was diphenylmethane, and its concentration was 2.8×10^{-2} M. The tabulated integrations are relative to the methylene singlet which was set at 200.

Table A-15. Rate of disappearance of 4,5-dihydrocyclobuta-[*b*]furan (**9**) at 83.25 °C in benzene-d_6. Third run[a]

Time x 10^{-4}, s	Integration[b,c]
0.0000	265.2
0.6477	241.5
2.2160	193.1
3.8973	158.0
5.0656	149.9
5.6460	147.3
8.4602	129.5
9.9231	121.5
11.6969	117.0
12.7801	108.7
62.4307	93.5

[a]Rate constant: $k = 1.73 \pm 0.09 \times 10^{-5}$ s^{-1}.

[b]The range for integration is approximately 6.05-5.95 ppm, and the signal followed arises from one proton of **9**. Though the range varies slightly between runs, it was held constant in each run.

[c]The standard was diphenylmethane, and its concentration was 2.8×10^{-2} M. The tabulated integrations are relative to the methylene singlet which was set at 200.

Table A-16. Rate of disappearance of 4,5-dihydrocyclobuta-[*b*]furan (**9**) at 68.25 °C in benzene-d_6. First run[a]

Time x 10^{-4}, s	Integration[b,c]
0.0000	214.5
4.0083	177.0
11.5680	140.7
19.9634	113.2
25.1207	100.4
29.0147	96.3
36.9761	90.9
42.8235	83.5
45.6681	83.3
49.8921	78.9
53.8836	77.2
174.1521	54.6

[a]Rate constant: $k = 3.50 \pm 0.20 \times 10^{-6}$ s^{-1}.

[b]The range for integration is approximately 6.05-5.95 ppm, and the signal followed arises from one proton of **9**. Though the range varies slightly between runs, it was held constant in each run.

[c]The standard was diphenylmethane, and its concentration was 2.4×10^{-2} M. The tabulated integrations are relative to the methylene singlet which was set at 200.

Table A-17. Rate of disappearance of 4,5-dihydrocyclobuta-[*b*]furan (**9**) at 68.25 °C in benzene-d_6. Second run[a]

Time x 10^{-4}, s	Integration[b,c]
0.0000	161.7
5.3894	141.4
8.3108	134.1
13.6019	116.0
16.7605	107.0
20.8649	104.1
24.3072	94.7
29.5094	86.4
33.7596	85.8
41.5555	77.8
46.2918	75.6
205.7543	53.5

[a]Rate constant: $k = 3.51 \pm 0.13 \times 10^{-6}$ s^{-1}.

[b]The range for integration is approximately 6.05-5.95 ppm, and the signal followed arises from one proton of **9**. Though the range varies slightly between runs, it was held constant in each run.

[c]The standard was diphenylmethane, and its concentration was 2.4×10^{-2} M. The tabulated integrations are relative to the methylene singlet which was set at 200.

Table A-18. Rate of disappearance of 4,5-dihydrocyclobuta-[*b*]furan (**9**) at 68.25 °C in benzene-d_6. Third run[a]

Time x 10^{-4}, s	Integration[b,c]
0.0000	149.2
8.6069	117.6
12.9803	102.7
21.5691	95.1
25.2118	83.2
29.4421	78.5
38.9532	76.3
45.8015	70.2
58.7109	65.0
201.2179	47.8

[a]Rate constant: $k = 2.95 \pm 0.22 \times 10^{-6}$ s^{-1}.

[b]The range for integration is approximately 6.05-5.95 ppm, and the signal followed arises from one proton of **9**. Though the range varies slightly between runs, it was held constant in each run.

[c]The standard was diphenylmethane, and its concentration was 2.6×10^{-2} M. The tabulated integrations are relative to the methylene singlet which was set at 200.

Figure A-1. Upfield multiplet in the ^{1}H NMR spectrum of 4-*tert*-butyl-4,5-dihydrocyclobuta[*b*]furan (**15**)

Figure A-2. Computer simulation of the upfield multiplet found in the ^{1}H NMR spectrum of (**15**)

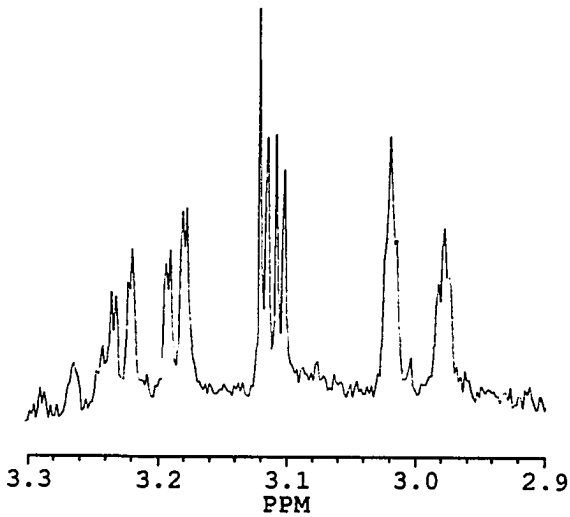

Figure A-1.

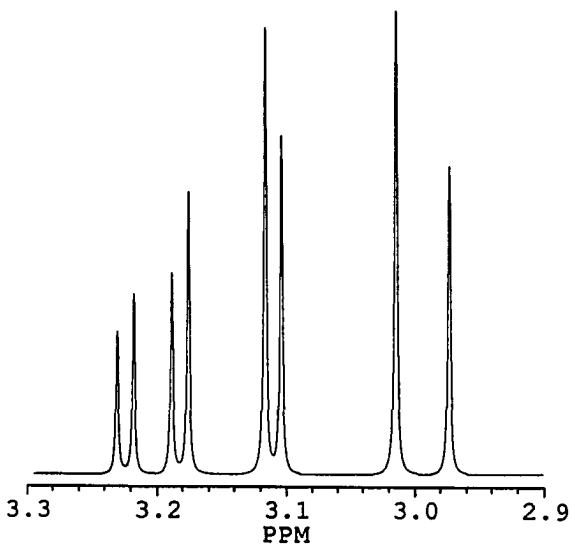

Figure A-2.

Figure A-3. ^{1}H NMR spectrum of 2-methyl-3-furyl(*tert*-butyl)methyl benzoate (**12**) in $CDCl_3$

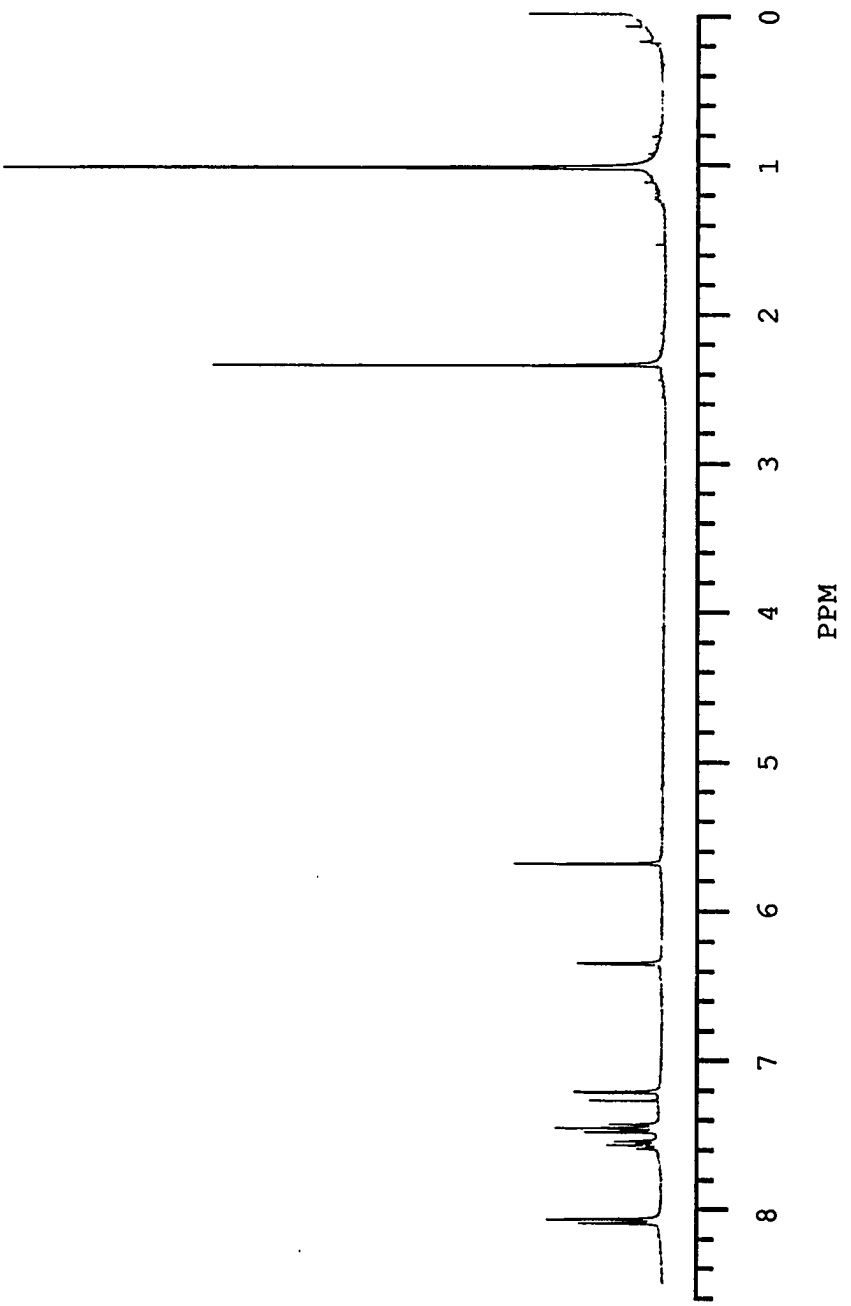
0
1
2
3
4
5
6
7
8
PPM

Figure A-4. ^{1}H NMR spectrum of 2-methyl-3-furyl methyl benzoate (5) in $CDCl_3$

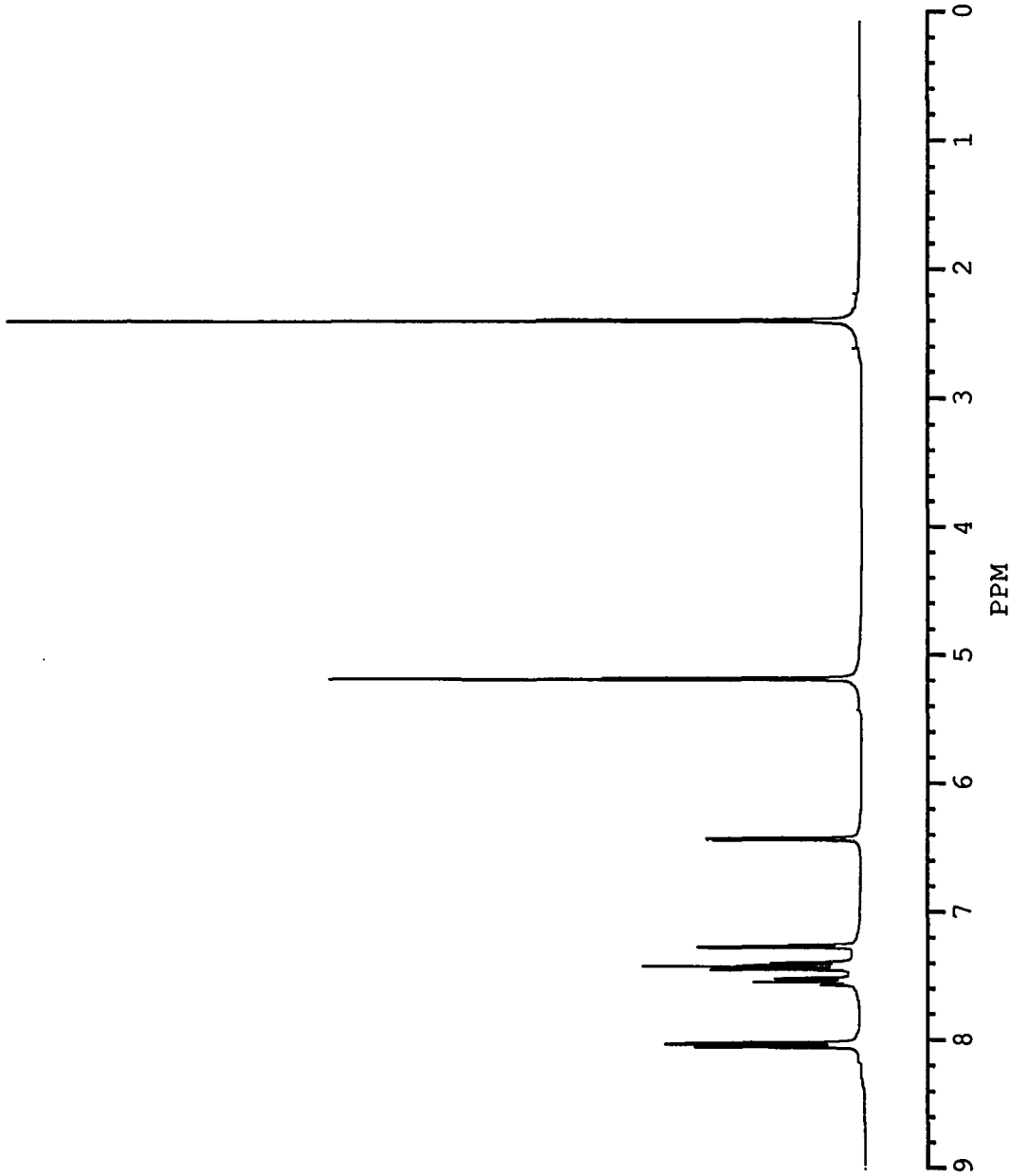
0
1
2
3
4
5
6
7
8
9
PPM

Figure A-5. ^{1}H NMR spectrum of 2-methylene-3-*tert*-butylmethylene-2,3-dihydrofuran (**8**) in $CDCl_3$

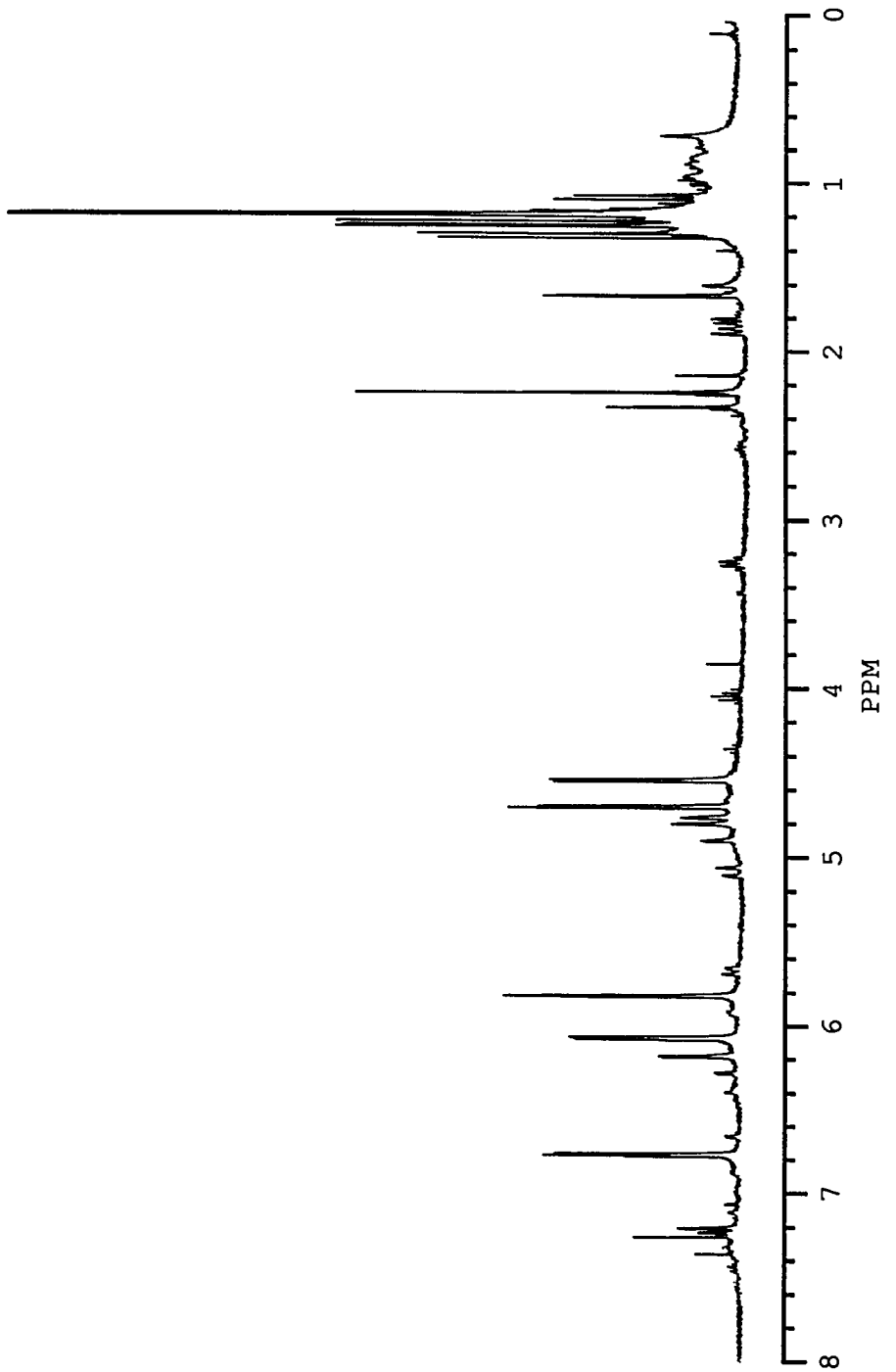
0
1
2
3
4
5
6
7
8
PPM

Figure A-6. ^{1}H NMR spectrum of 2,3-dimethylene-2,3-dihydrofuran (**2**) pentane/$CDCl_3$, v:v (3:4). The peaks of **2** are indicated

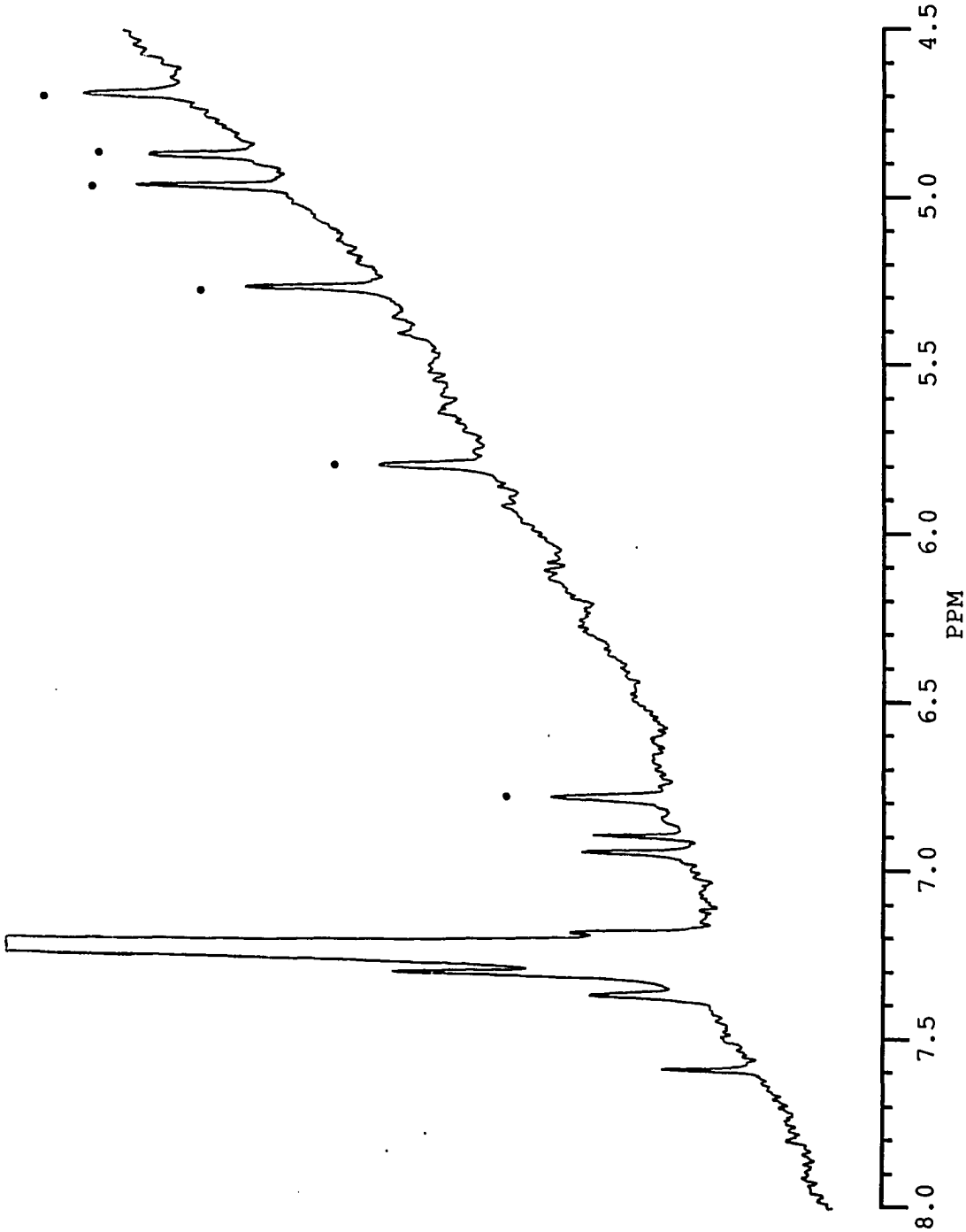
4.5
5.0
5.5
6.0
6.5
7.0
7.5
8.0
PPM

Figure A-7. ^{1}H NMR spectrum of 4-*tert*-butyl-4,5-dihydrocyclobuta[*b*]furan (**15**) in $CDCl_3$

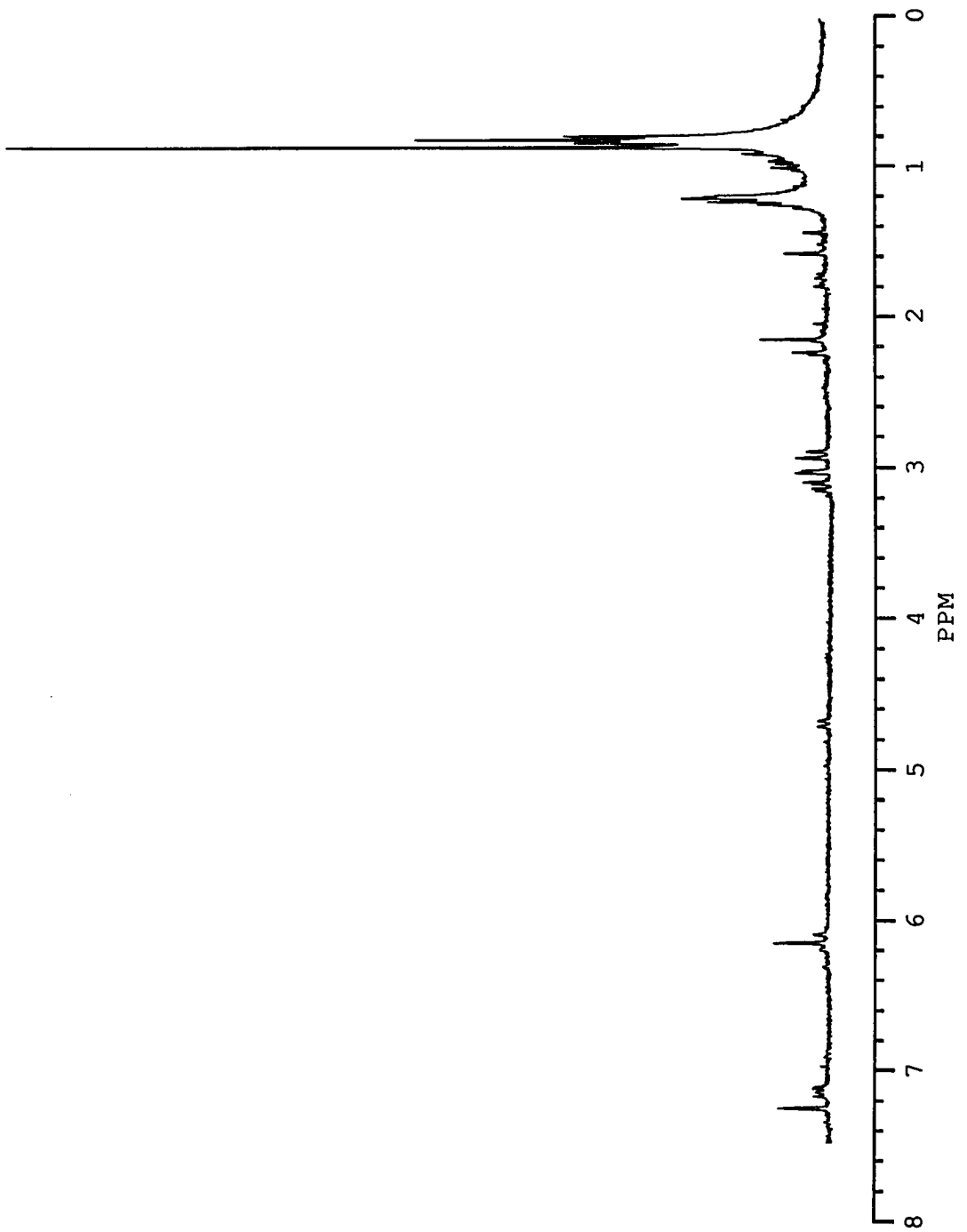
0
1
2
3
4
5
6
7
8
PPM

Figure A-8. A magnified segment of the spectrum in Figure A-7

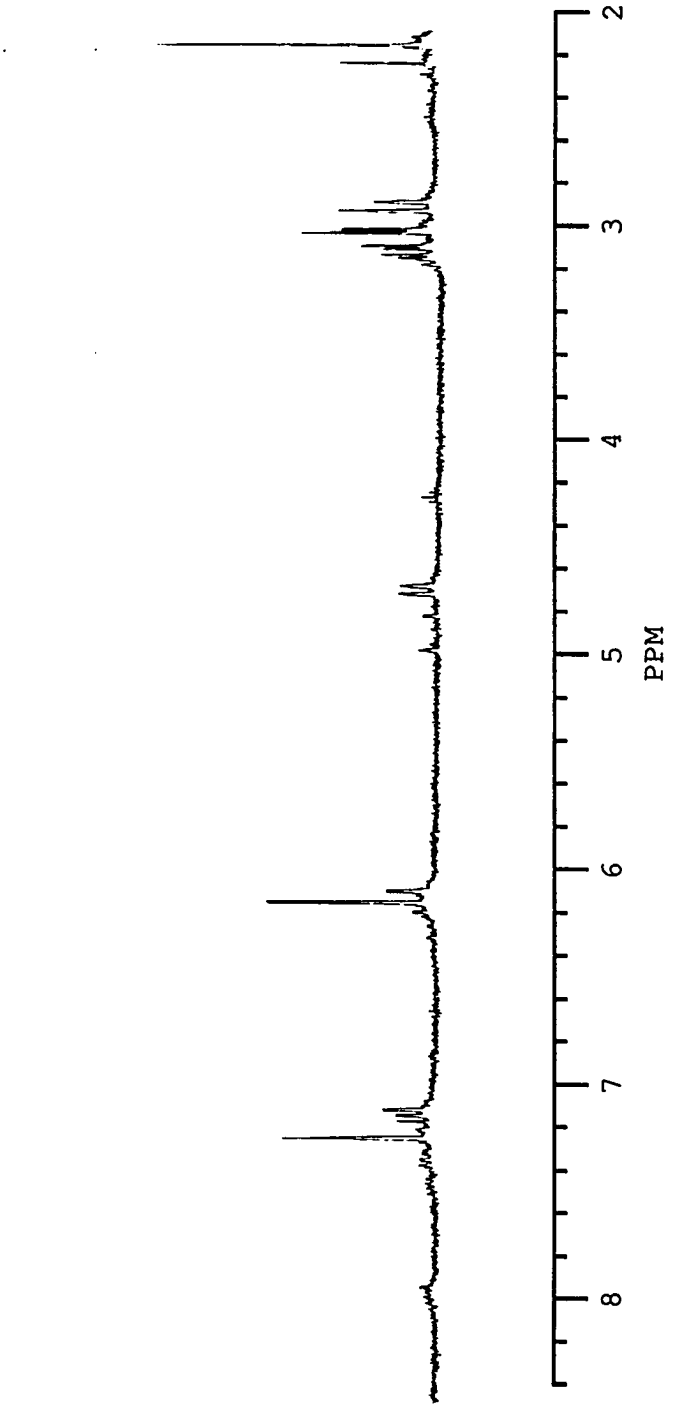
2
3
4
5
6
7
8
PPM

Figure A-9. ^{1}H NMR spectrum of 4,5-dihydrocyclobuta[*b*]furan (**9**) in acetone-d_6 with pentane as a contaminant

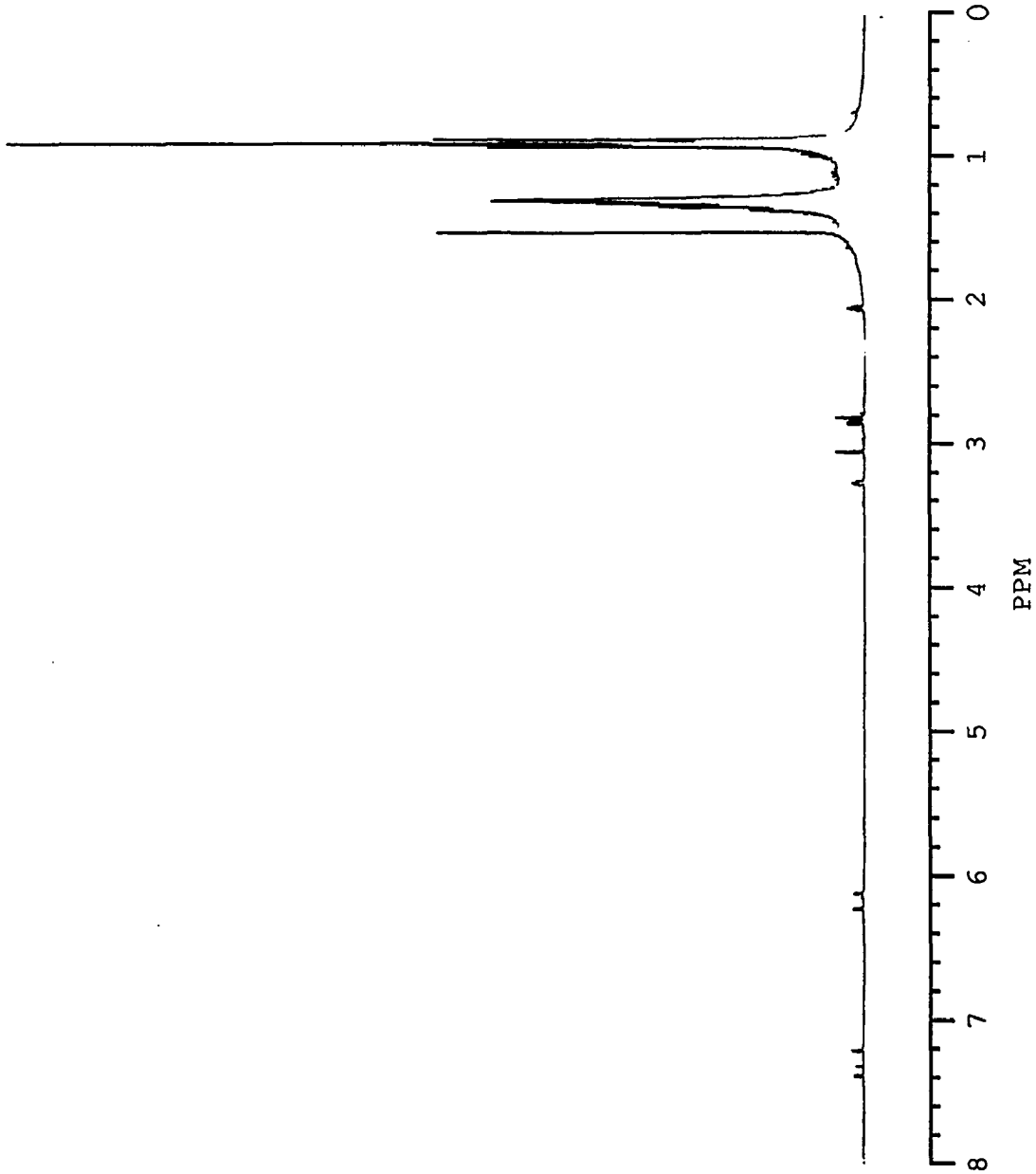
0
1
2
3
4
5
6
7
8
PPM

Figure A-10. An expanded segment of the spectrum from Figure A-9

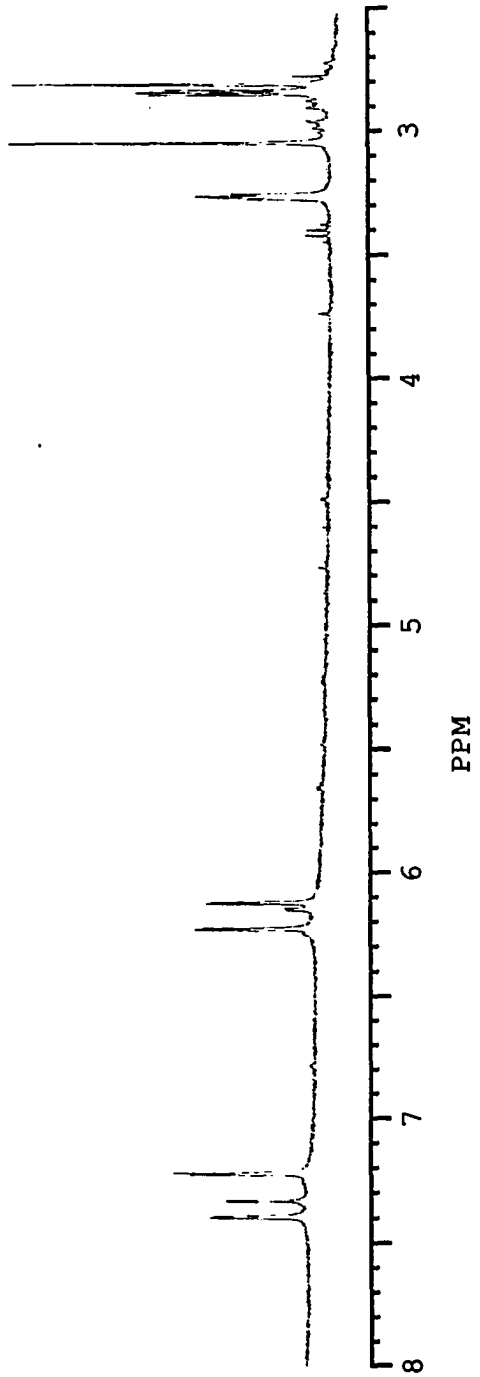
3
4
5
6
7
8
PPM

Figure A-11. Decoupled ^{13}C NMR spectrum of 4-*tert*-butyl-4,5-dihydrocyclobuta[*b*]furan (**15**) in the presence of isomers. The solvent is $CDCl_3$

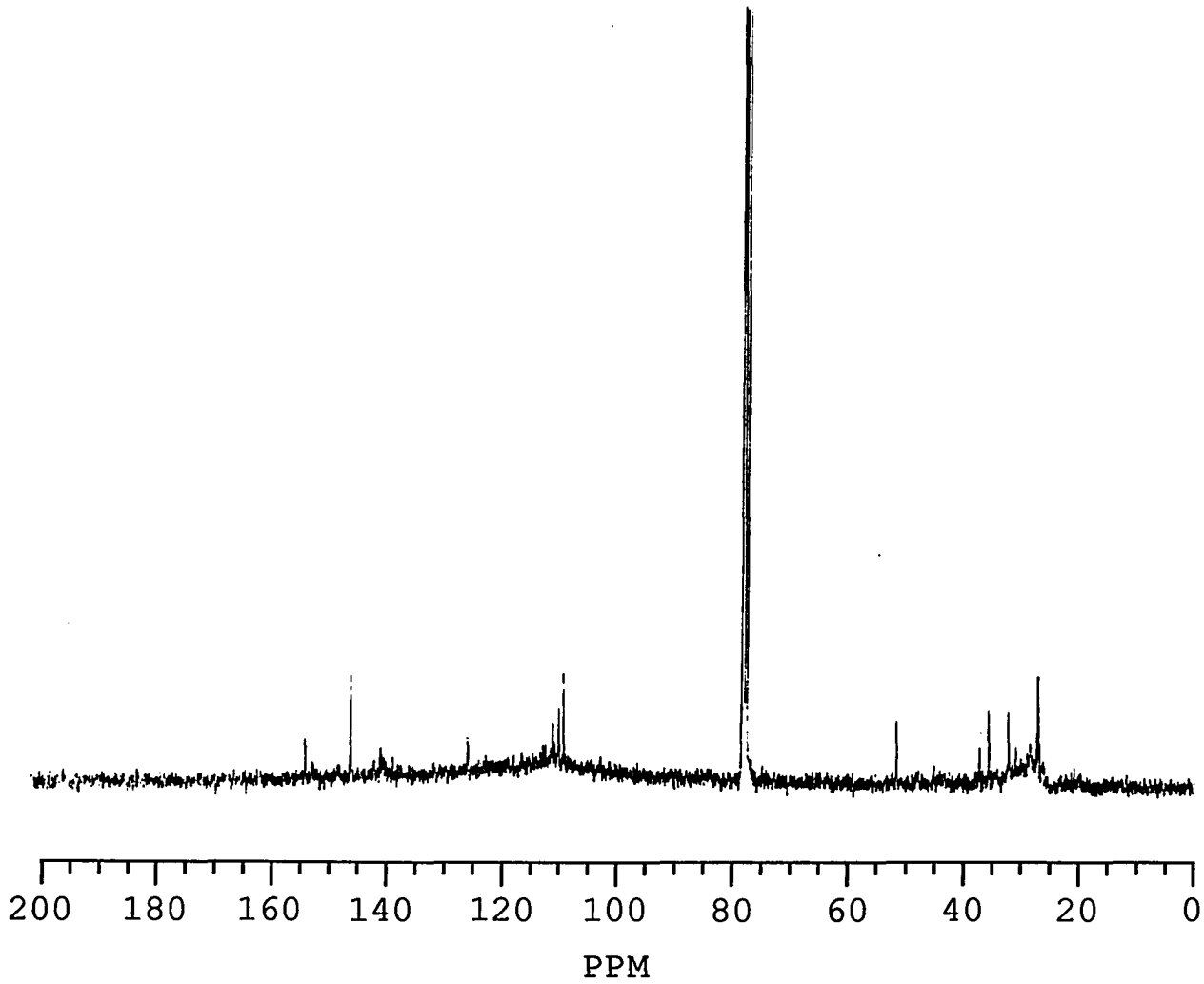
200
180
160
140
120
100
80
60
40
20
0
PPM

Figure A-12. Nondecoupled ^{13}C NMR spectrum of 4-*tert*-butyl-4,5-dihydrocyclobuta[*b*]furan (**15**) in the presence of isomers **13** and **14**. The solvent is $CDCl_3$

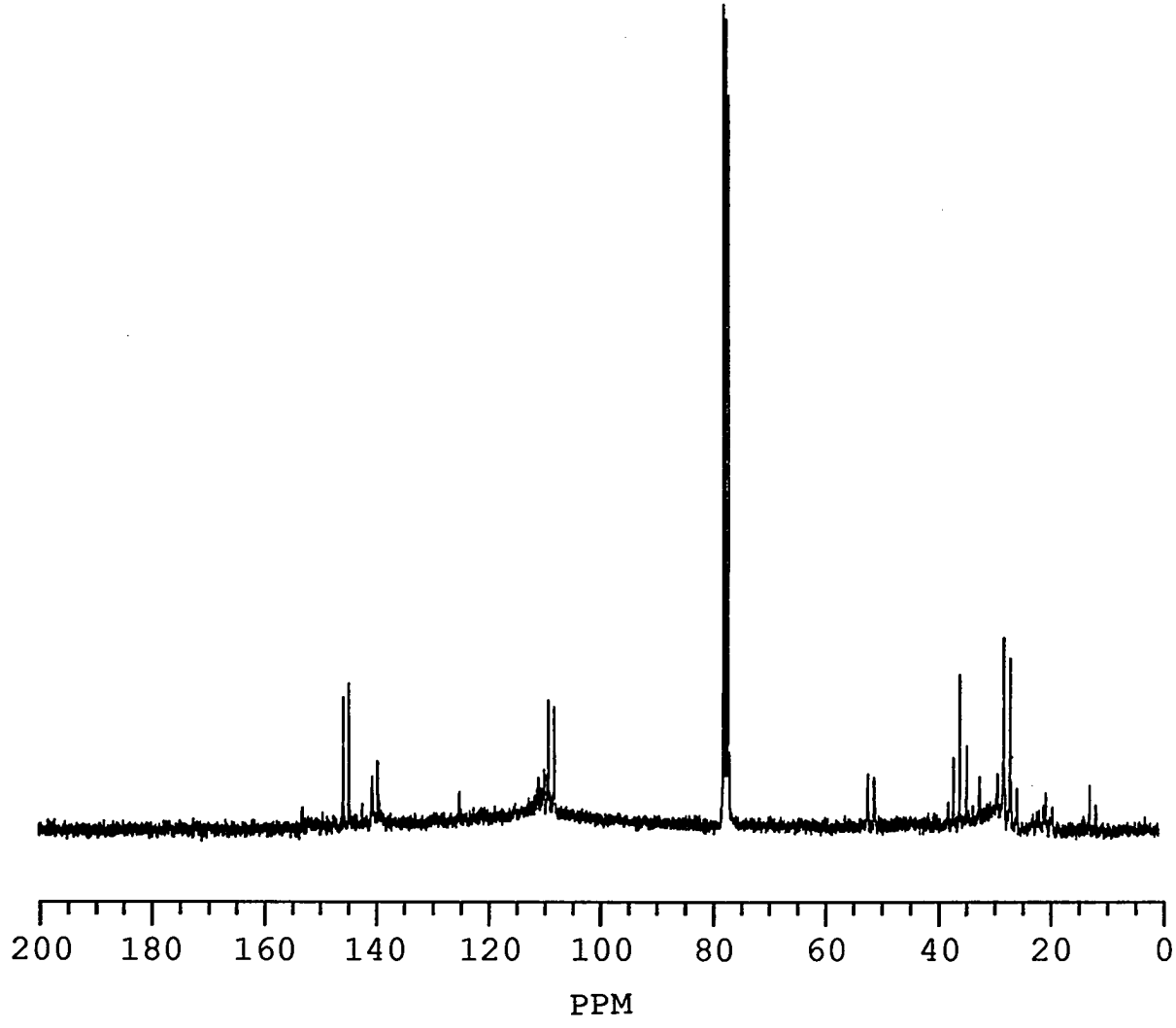
200
180
160
140
120
100
80
60
40
20
0
PPM

Figure A-13. Decoupled ^{13}C NMR spectrum of 2-methylene-3-*tert*-butylmethylene-2,3-dihydrofuran (**8**) in the presence of isomers **13** and **14**. The solvent is $CDCl_3$ (spectrum courtesy of Yih-chuan Jason Huang)

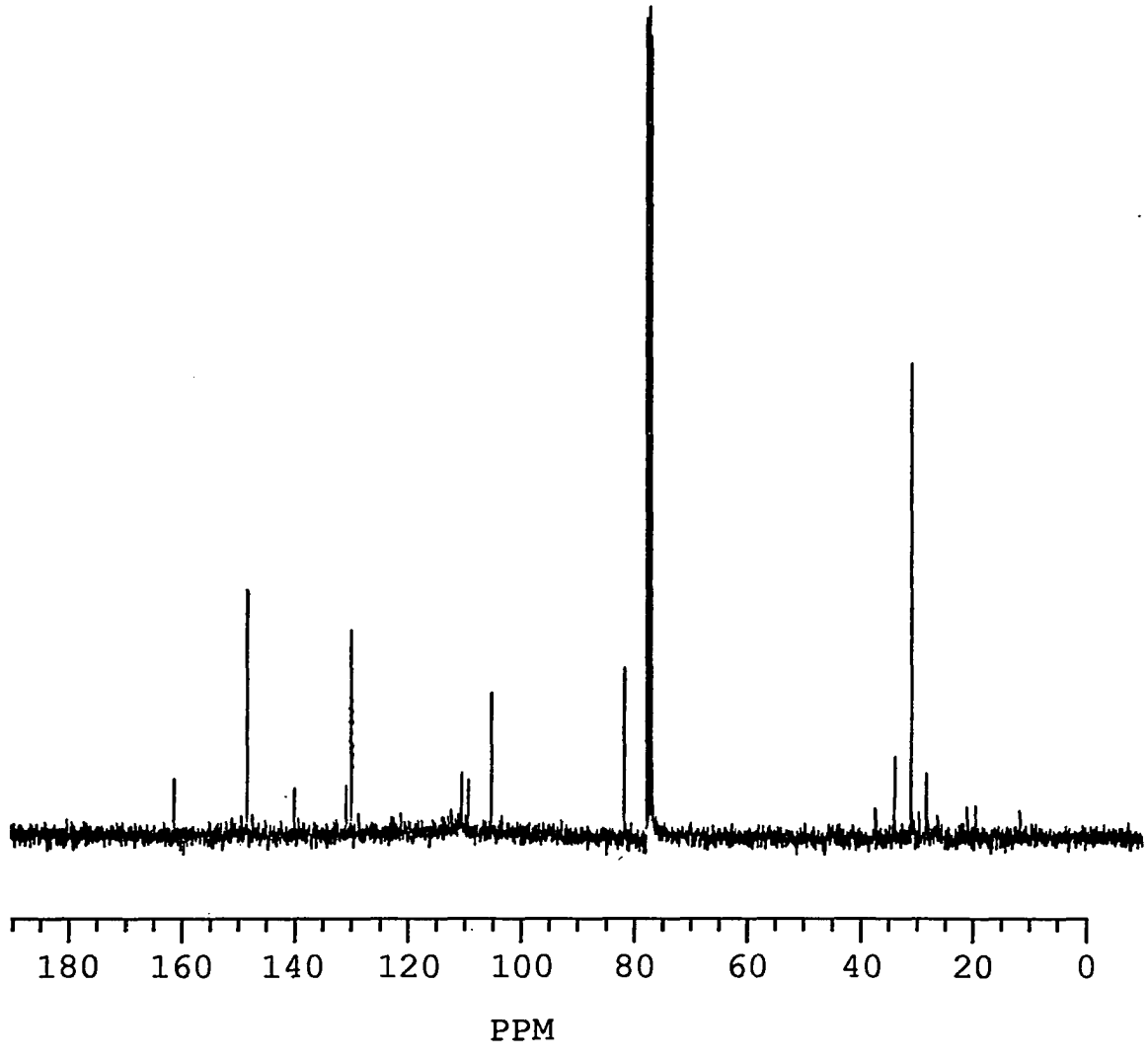
180
160
140
120
100
80
60
40
20
0
PPM

Figure A-14. Decoupled ^{13}C NMR spectrum of 4,5-dihydrocyclobuta[*b*]furan (**9**). The solvent is $CDCl_3$

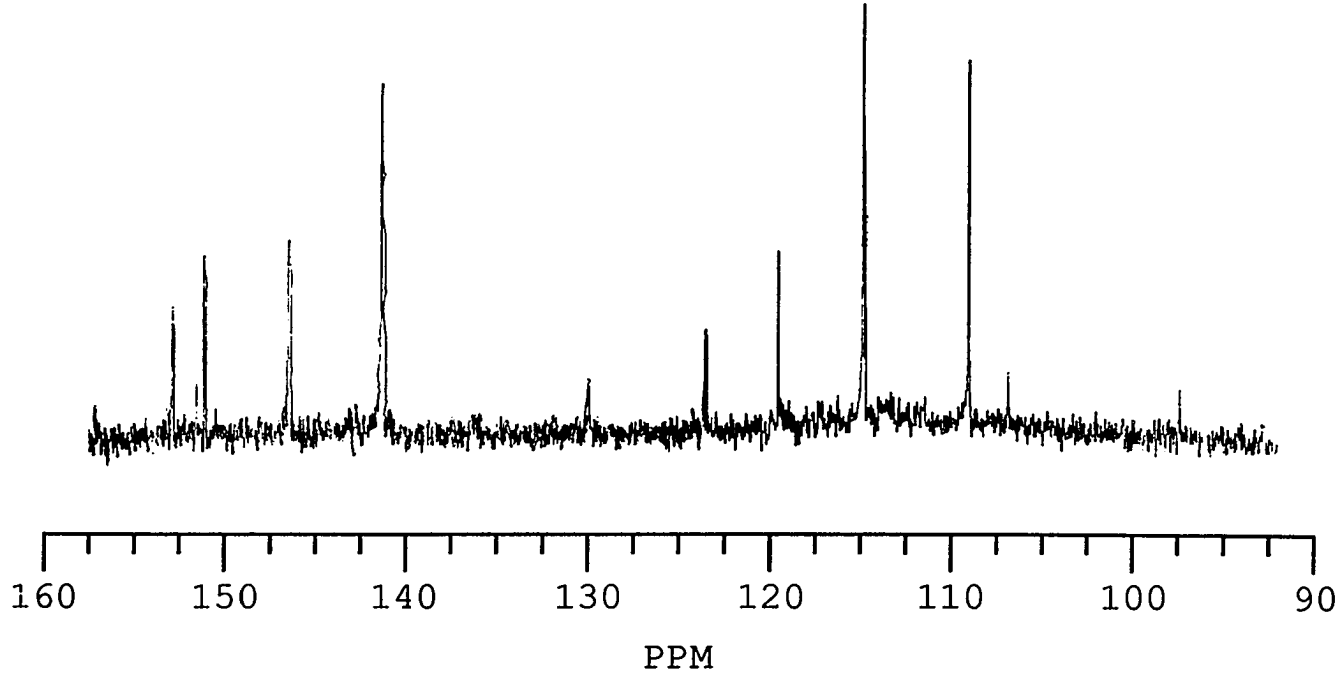
160
150
140
130
120
110
100
90
PPM

Figure A-15. Decoupled ^{13}C NMR spectrum of the solution used to obtain the spectrum in Figure A-14 after destroying 70% of the 4,5-dihydrocyclobuta[*b*]furan (**9**) originally present

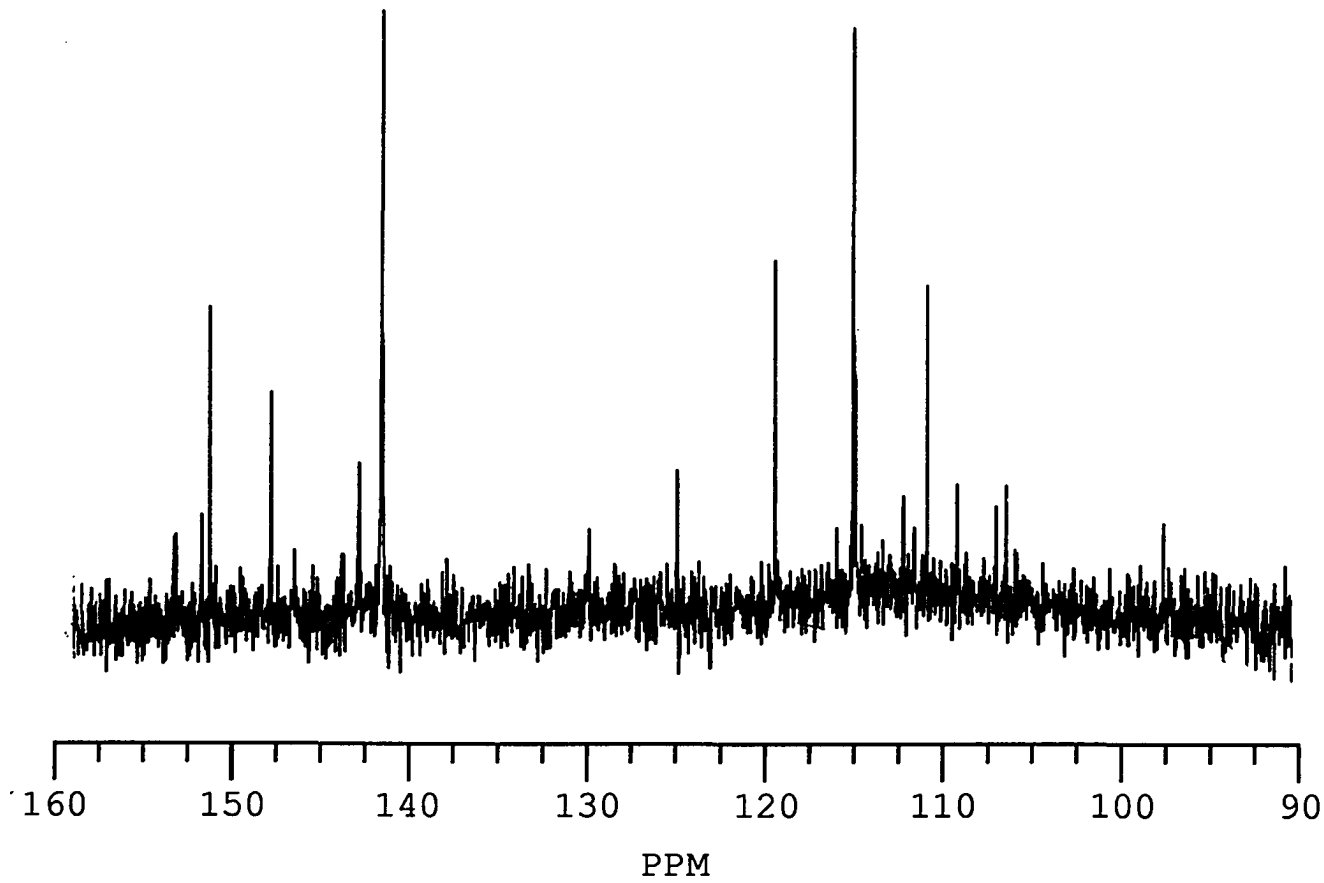
160
150
140
130
120
110
100
90
PPM

Figure A-16. Low-temperature photolysis apparatus: A) vacuum jacketed immersion well, B) reactor vessel, C) solution to be photolyzed, D) lamp cooling water, E) filter sleeve and support for light source

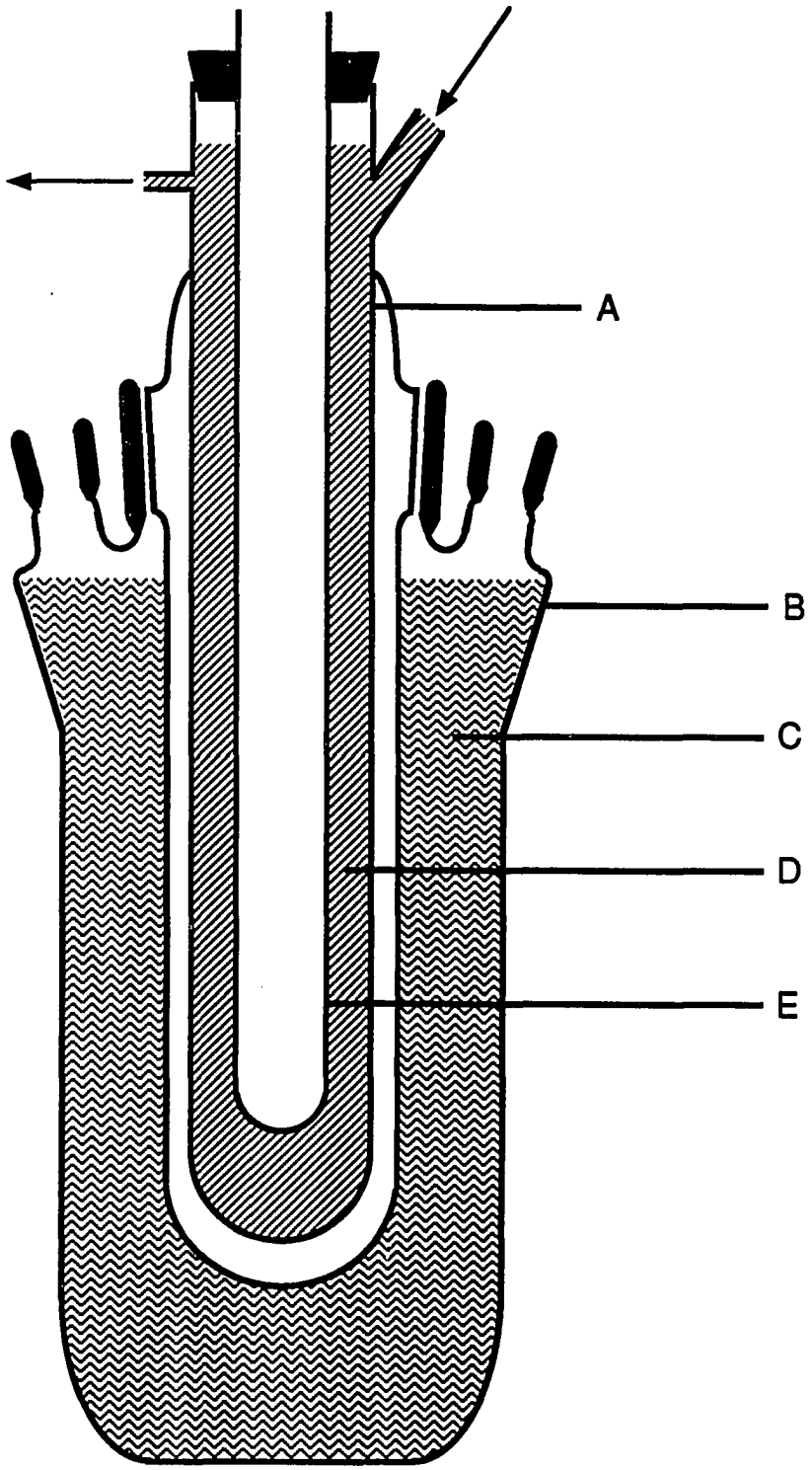
A
B
C
D
E

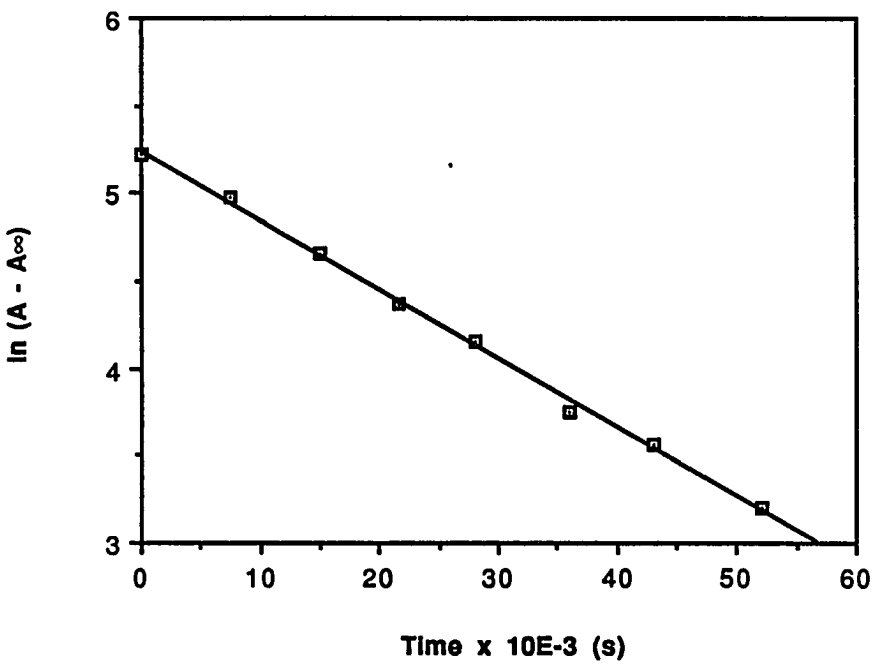

Figure A-17. Plot of ln ($A - A_\infty$) vs. time at 70.15 °C. Data were obtained from Table A-1 and represent the disappearance of 4-*tert*-butyl-4,5-dihydrocyclobuta[*b*]furan (**15**). The rate constant derived from the line is $k = 3.94 \pm 0.08 \times 10^{-5}\ s^{-1}$

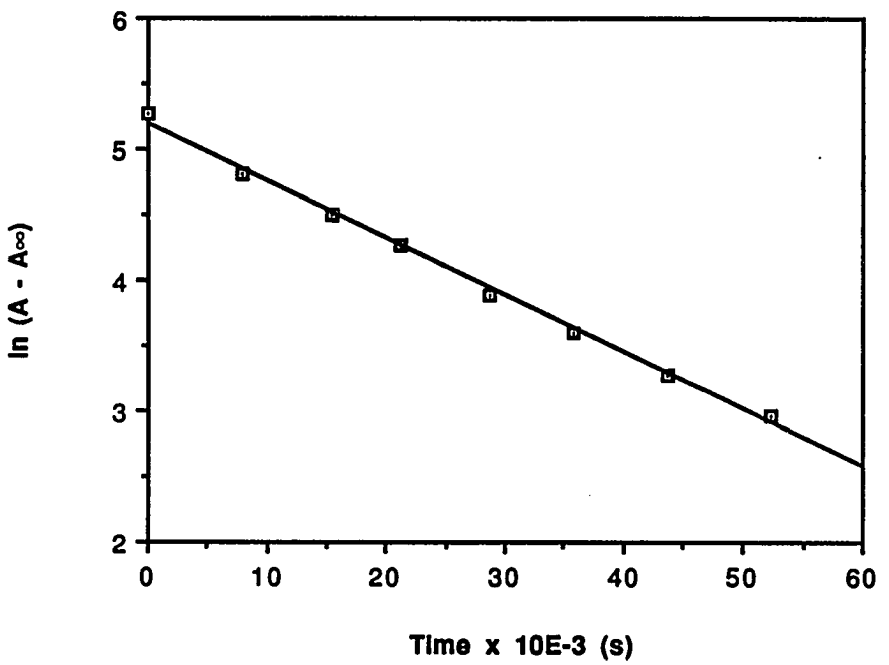

Figure A-18. Plot of ln ($A - A_\infty$) vs. time at 70.15 °C. Data were obtained from Table A-2 and represent the disappearance of 4-*tert*-butyl-4,5-dihydrocyclobuta[*b*]furan (**15**). The rate constant derived from the line is $k = 4.40 \pm 0.11 \times 10^{-5}\ s^{-1}$

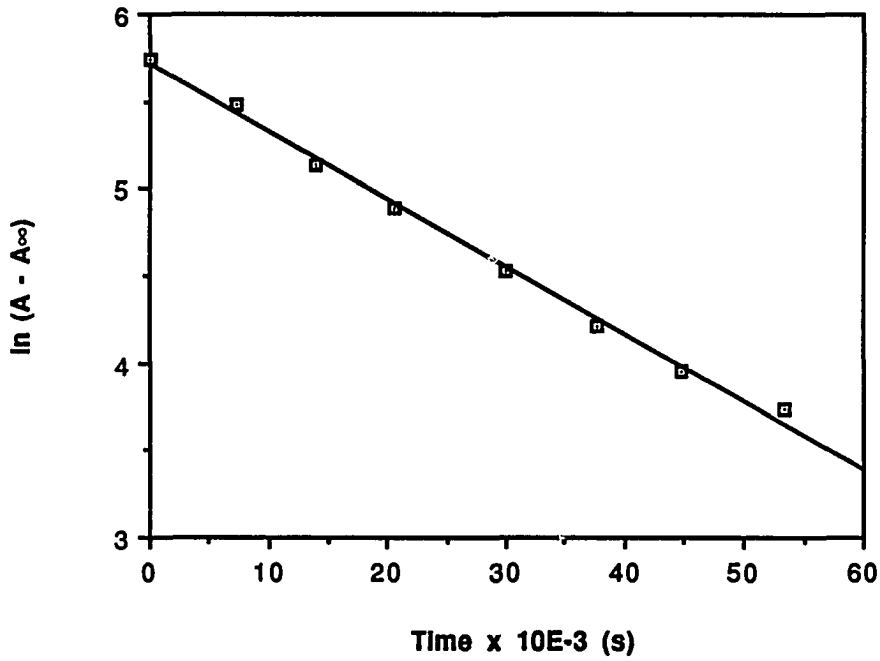

Figure A-19. Plot of ln ($A - A_\infty$) vs. time at 70.15 °C. Data were obtained from Table A-3 and represent the disappearance of 4-*tert*-butyl-4,5-dihydrocyclobuta[*b*]furan (**15**). The rate constant derived from the line is $k = 3.86 \pm 0.10 \times 10^{-5}\ s^{-1}$

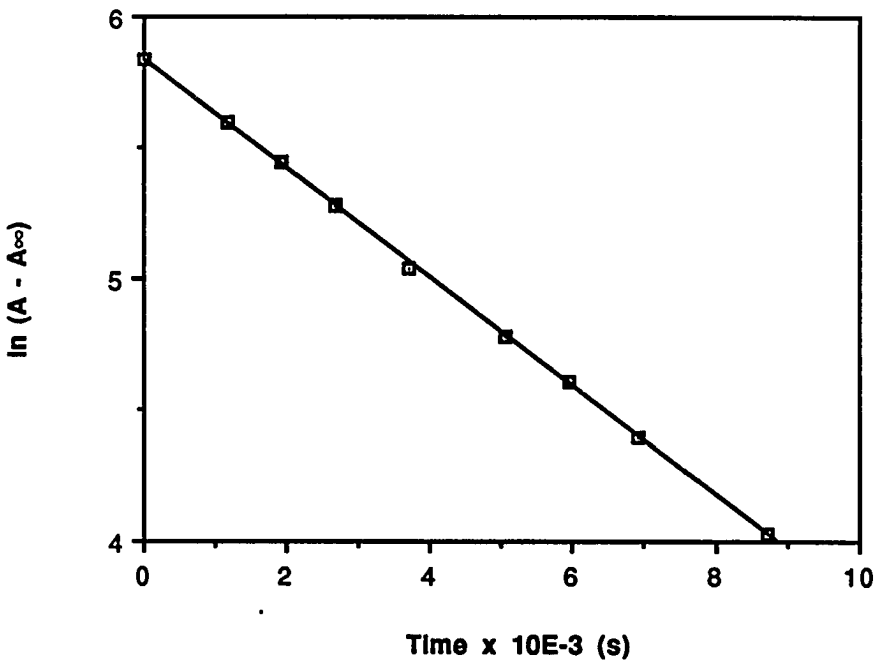

Figure A-20. Plot of ln ($A - A_\infty$) vs. time at 85.25 °C. Data were obtained from Table A-4 and represent the disappearance of 4-*tert*-butyl-4,5-dihydrocyclobuta[*b*]furan (**15**). The rate constant derived from the line is $k = 2.09 \pm 0.01 \times 10^{-4}\ s^{-1}$

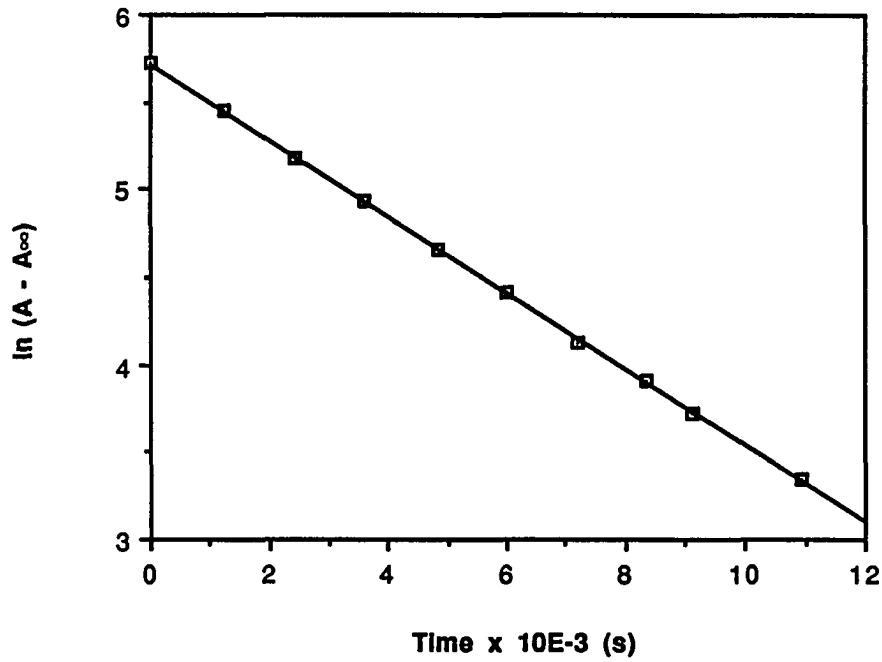

Figure A-21. Plot of ln (A - A_∞) vs. time at 85.25 °C. Data were obtained from Table A-5 and represent the disappearance of 4-*tert*-butyl-4,5-dihydrocyclobuta[*b*]furan (**15**). The rate constant derived from the line is k = 2.18 ± 0.01 x 10^{-4} s^{-1}

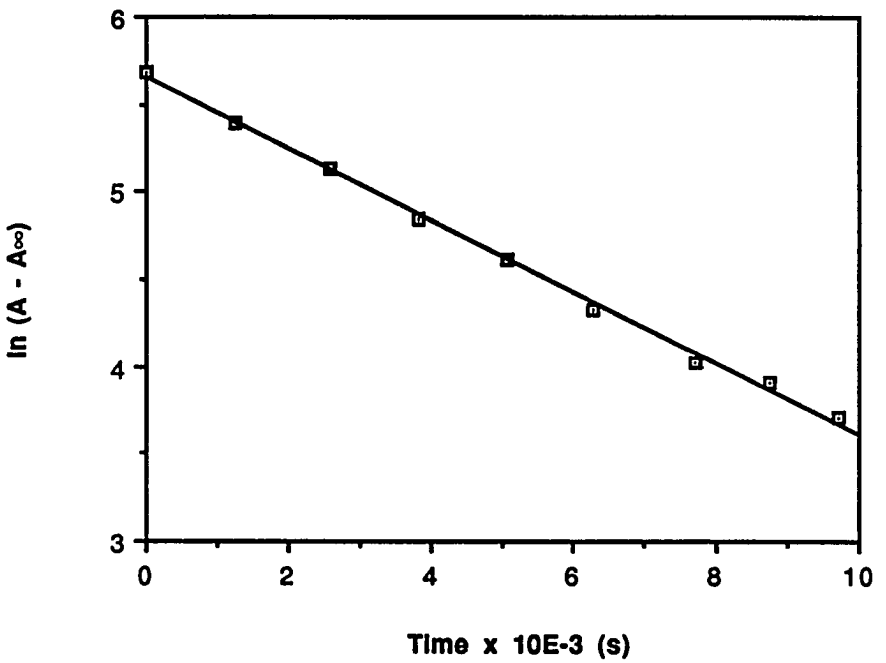

Figure A-22. Plot of ln ($A - A_\infty$) vs. time at 85.25 °C. Data were obtained from Table A-6 and represent the disappearance of 4-*tert*-butyl-4,5-dihydrocyclobuta[*b*]furan (**15**). The rate constant derived from the line is $k = 2.04 \pm 0.04 \times 10^{-4}\ s^{-1}$

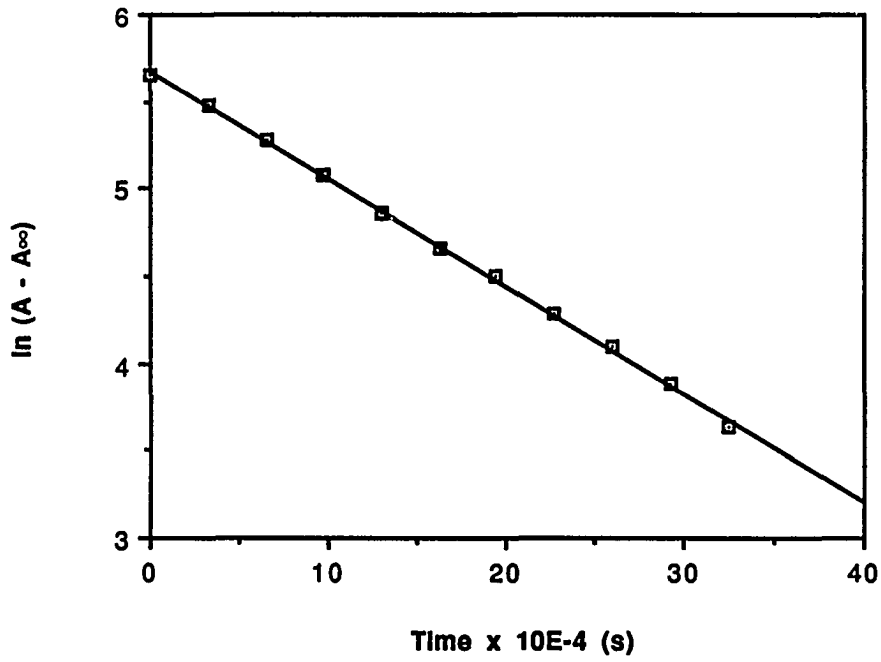

Figure A-23. Plot of ln ($A - A_\infty$) vs. time at 55.10 °C. Data were obtained from Table A-7 and represent the disappearance of 4-*tert*-butyl-4,5-dihydrocyclobuta[*b*]furan (**15**). The rate constant derived from the line is $k = 6.16 \pm 0.06 \times 10^{-6}\ s^{-1}$

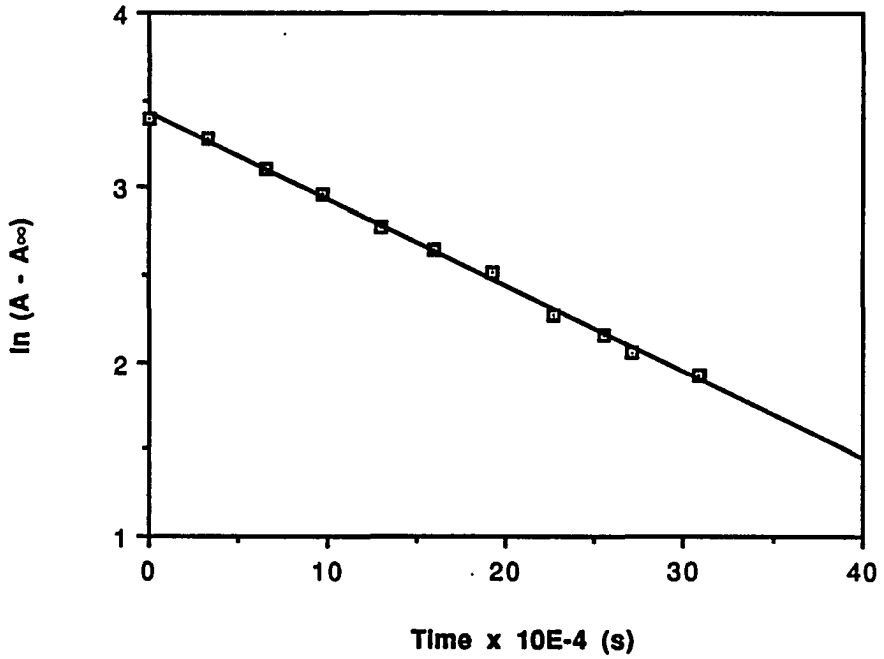

Figure A-24. Plot of ln ($A - A_\infty$) vs. time at 55.10 °C. Data were obtained from Table A-8 and represent the disappearance of 4-*tert*-butyl-4,5-dihydrocyclobuta[*b*]furan (**15**). The rate constant derived from the line is $k = 4.94 \pm 0.08 \times 10^{-6}\ s^{-1}$

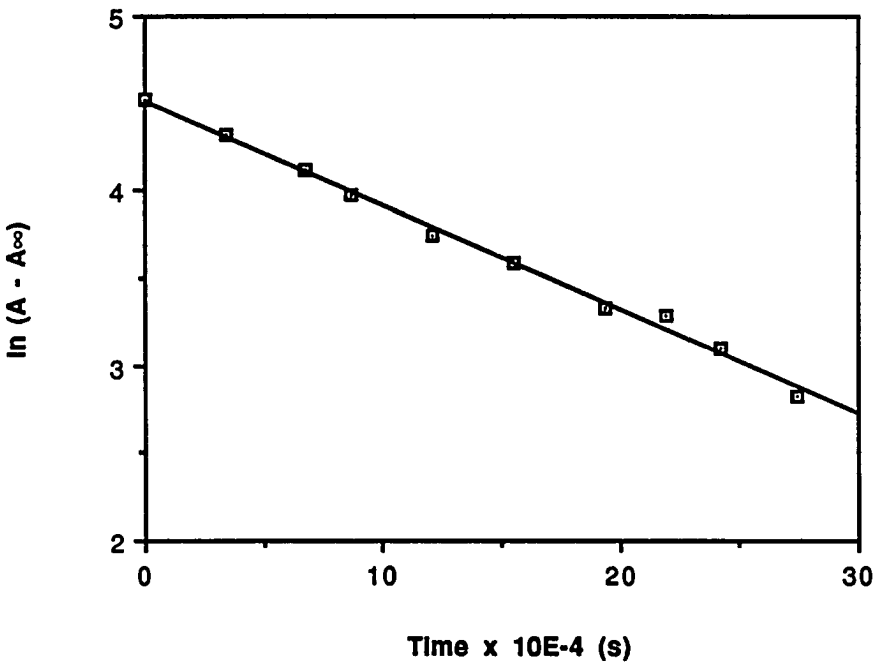

Figure A-25. Plot of ln ($A - A_\infty$) vs. time at 55.10 °C. Data were obtained from Table A-9 and represent the disappearance of 4-*tert*-butyl-4,5-dihydrocyclobuta[*b*]furan (**15**). The rate constant derived from the line is $k = 5.96 \pm 0.16 \times 10^{-6}\ s^{-1}$

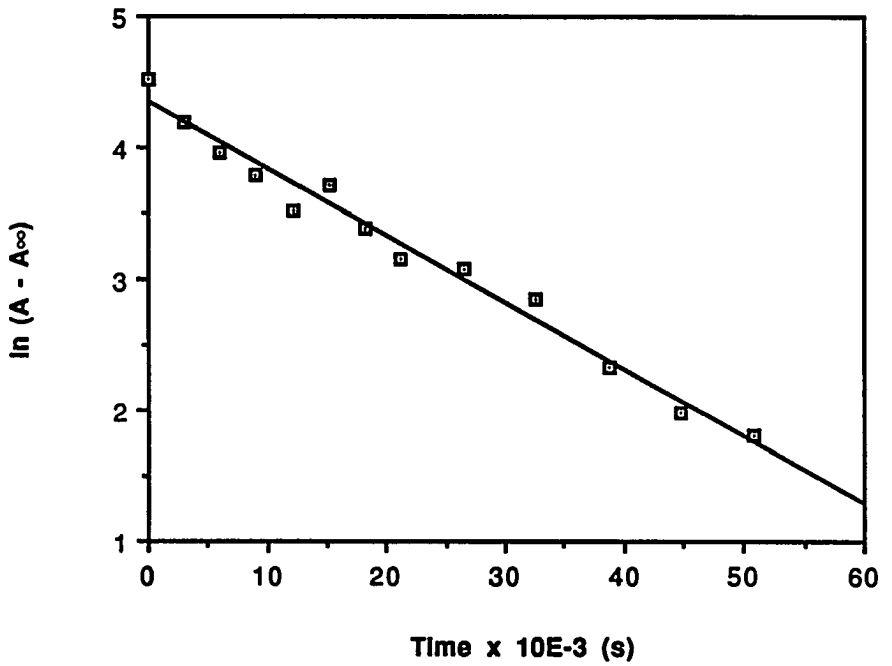

Figure A-26. Plot of ln (A - A_∞) vs. time at 98.10 °C. Data were obtained from Table A-10 and represent the disappearance of 4,5-dihydrocyclobuta[*b*]furan (**9**). The rate constant derived from the line is k = 5.07 ± 0.22 x 10^{-5} s^{-1}

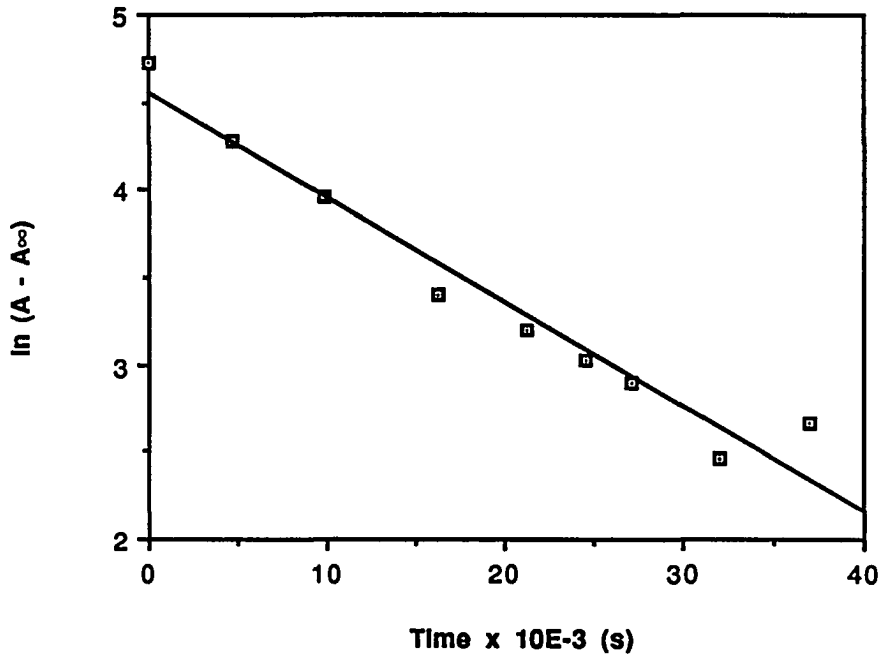

Figure A-27. Plot of ln ($A - A_\infty$) vs. time at 98.10 °C. Data were obtained from Table A-11 and represent the disappearance of 4,5-dihydrocyclobuta[*b*]furan (**9**). The rate constant derived from the line is $k = 5.98 \pm 0.48 \times 10^{-5}\ s^{-1}$

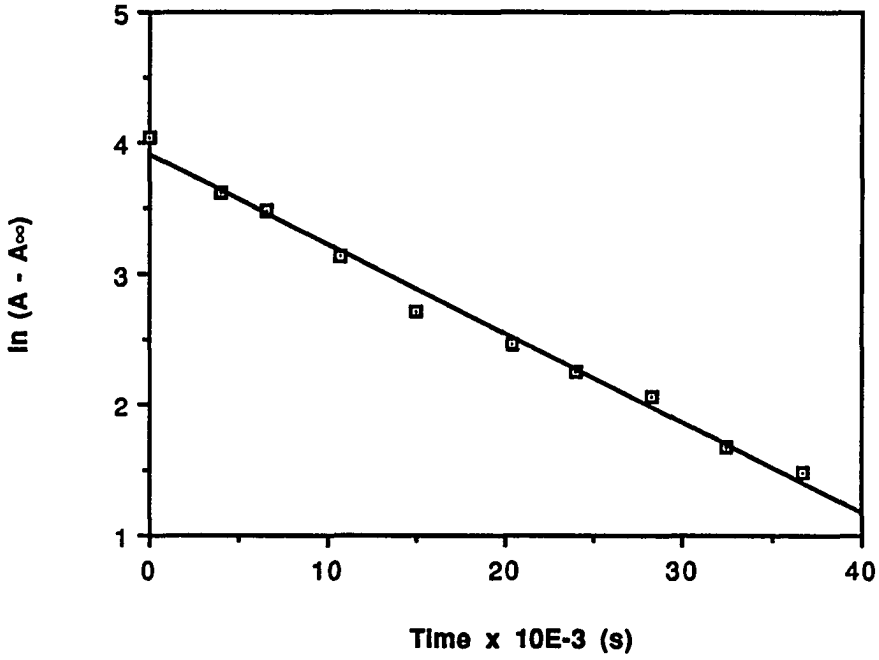

Figure A-28. Plot of ln ($A - A_{\infty}$) vs. time at 98.10 °C. Data were obtained from Table A-12 and represent the disappearance of 4,5-dihydrocyclobuta[*b*]furan (**9**). The rate constant derived from the line is $k = 6.80 \pm 0.24 \times 10^{-5}\ s^{-1}$

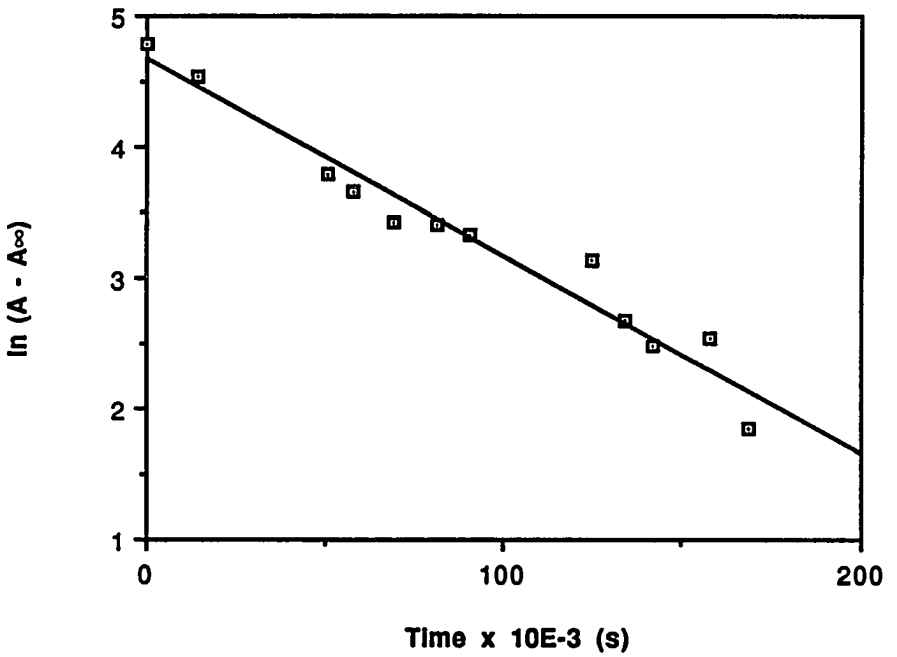

Figure A-29. Plot of ln (A - A_∞) vs. time at 83.25 °C. Data were obtained from Table A-13 and represent the disappearance of 4,5-dihydrocyclobuta[*b*]furan (**9**). The rate constant derived from the line is k = 1.51 ± 0.10 x 10^{-5} s^{-1}

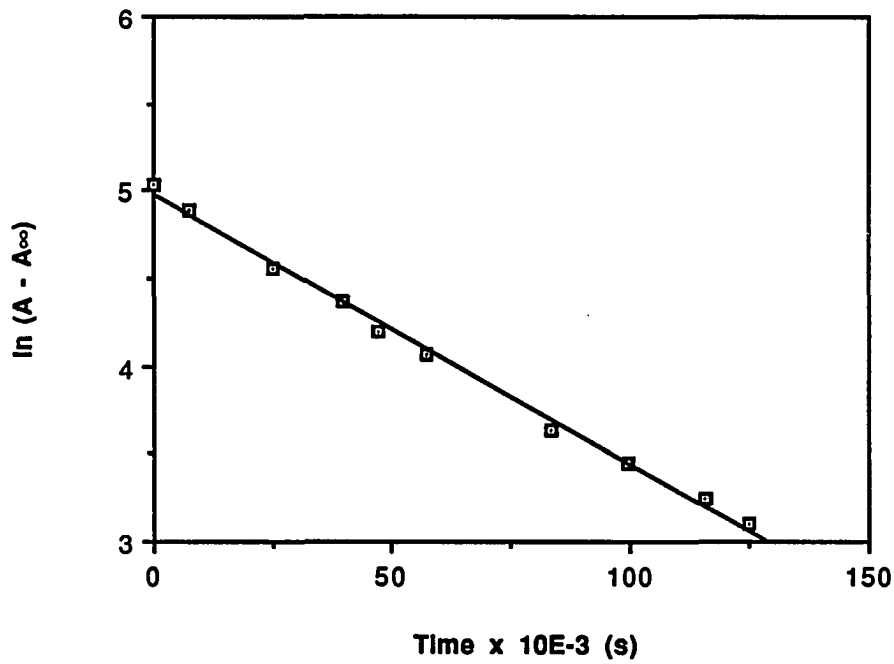

Figure A-30. Plot of ln ($A - A_\infty$) vs. time at 83.25 °C. Data were obtained from Table A-14 and represent the disappearance of 4,5-dihydrocyclobuta[*b*]furan (**9**). The rate constant derived from the line is $k = 1.53 \pm 0.03 \times 10^{-5}\ s^{-1}$

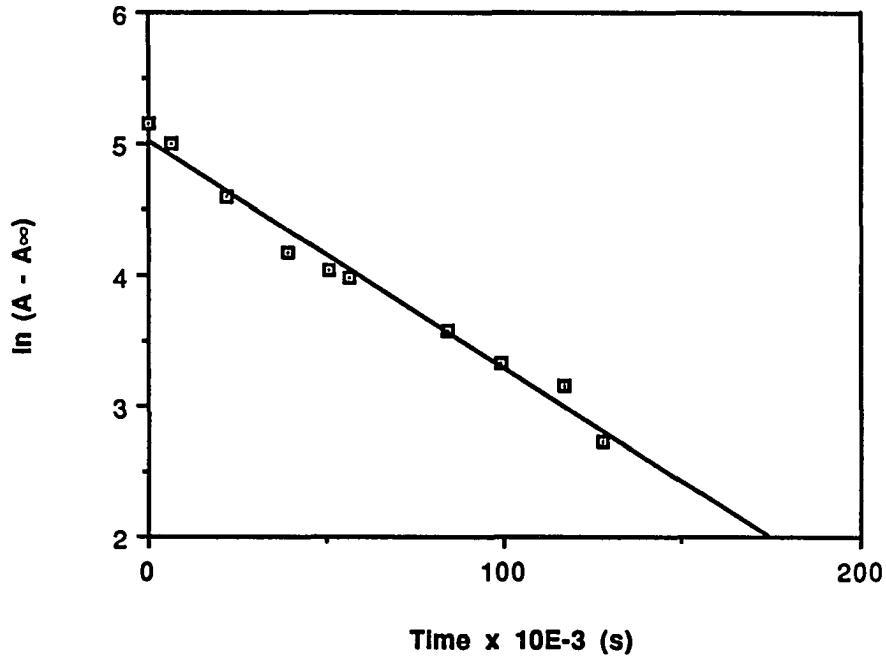

Figure A-31. Plot of ln (A - A_∞) vs. time at 83.25 °C. Data were obtained from Table A-15 and represent the disappearance of 4,5-dihydrocyclobuta[*b*]furan (**9**). The rate constant derived from the line is k = 1.73 ± 0.09 x 10^{-5} s^{-1}

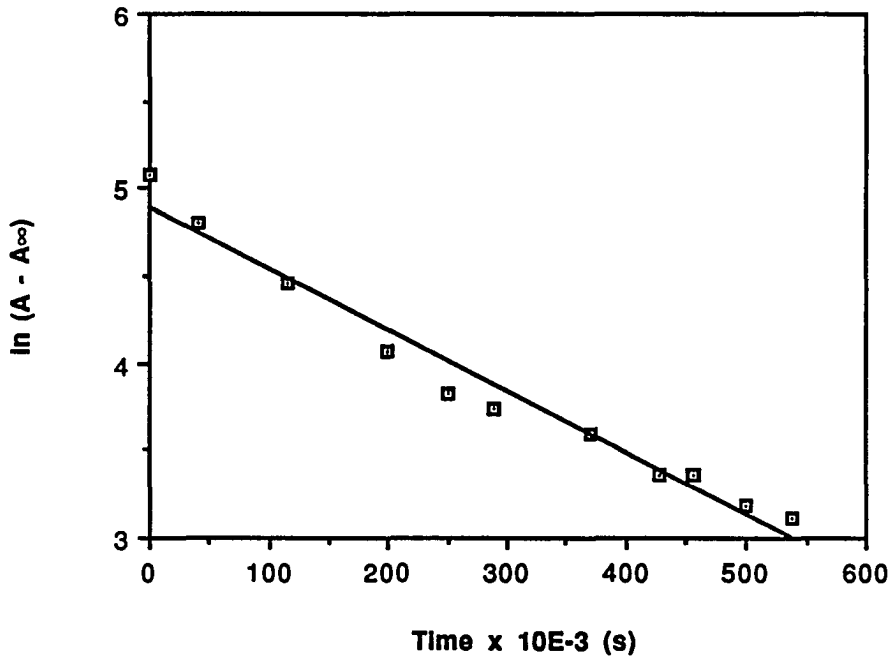

Figure A-32. Plot of ln ($A - A_\infty$) vs. time at 68.25 °C. Data were obtained from Table A-16 and represent the disappearance of 4,5-dihydrocyclobuta[*b*]furan (**9**). The rate constant derived from the line is $k = 3.50 \pm 0.20 \times 10^{-6}\ s^{-1}$

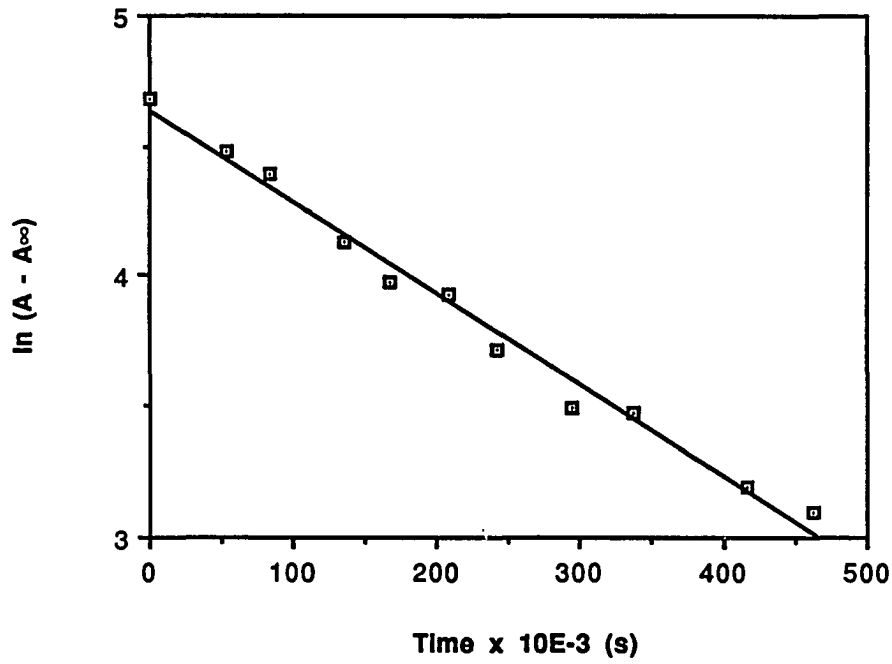

Figure A-33. Plot of ln ($A - A_{\infty}$) vs. time at 68.25 °C. Data were obtained from Table A-17 and represent the disappearance of 4,5-dihydrocyclobuta[*b*]furan (**9**). The rate constant derived from the line is $k = 3.51 \pm 0.13 \times 10^{-6}\ s^{-1}$

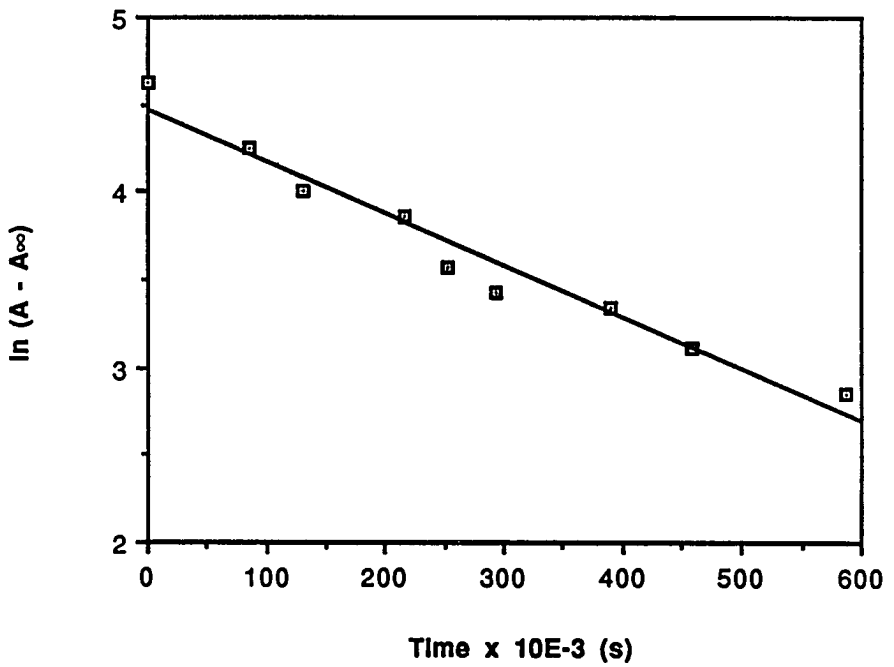

Figure A-34. Plot of ln ($A - A_\infty$) vs. time at 68.25 °C. Data were obtained from Table A-18 and represent the disappearance of 4,5-dihydrocyclobuta[*b*]furan (**9**). The rate constant derived from the line is $k = 2.95 \pm 0.22 \times 10^{-6}$ s^{-1}

SECTION II. KINETIC AND EQUILIBRIUM STUDY OF THE 9,10-PHENANTHRENE *ortho*-QUINODIMETHANE-1,2-DIHYDROCYCLOBUTA[*l*]PHENANTHRENE INTERCONVERSIONS

INTRODUCTION

o-Quinodimethanes, an important class of reactive molecules, have been the subject of intensive investigation during the last 30 years.[1-4] The first evidence for an *o*-quinodimethane was reported in 1957 by Cava when he suggested the intermediacy of the dibromo *o*-xylylene **1** in the formation of α,α'-dibromobenzocyclobutene (**2**).[5] Since this initial

1 **2**

report the study of *o*-xylylenes has led to their characterization, an understanding of their physical properties, and considerable development of their synthetic utility.[1-4,6-14]

In 1981 Roth reported the energy profile for the *o*-xylylene (**3**) - benzocyclobutene (**4**) interconversion shown (enthalpy units are in kcal/mol). The shock-tube technique

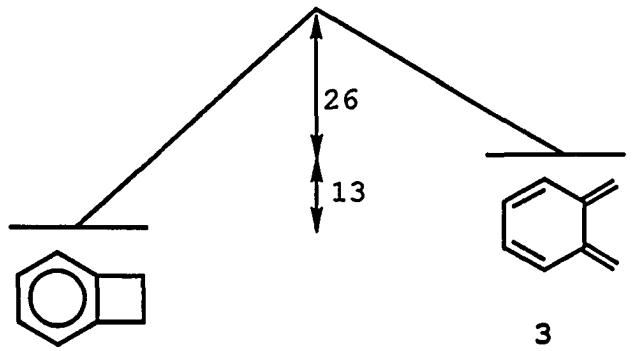

4 3

was used to generate an equilibrium between **3** and **4**, and thermodynamic and activation constants were indirectly determined by measuring the UV absorbance of **3**. A similar energy profile for the phenanthrene system had not been established. In addition to broadening the knowledge of *o*-quinodimethanes, study of the phenanthrene system might show what effect aromatic stabilization has on the equilibrium between an *o*-quinodimethane and its cyclized isomer.[15] Thus we undertook study of the equilibrium illustrated below.

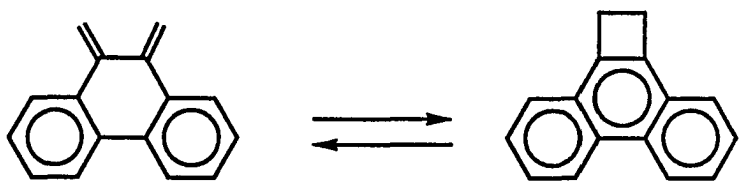

5 6

It is noteworthy that 9,10-phenanthrene *o*-quinodimethane (**5**) may be viewed as an *o*-xylylene annulated to two benzene

rings. The benzannulation would be expected to lead to a considerably more stable *o*-quinodimethane. Indeed, it will be shown that *o*-quinodimethane **5** equilibrated with its cyclized isomer **6** at 200 °C with a K_{eq} near unity. By "freezing" the equilibrium at 9 °C subsequent ^1H NMR analysis led to observation of both **5** and **6**. This is the first example of an equilibrated sample of an *o*-quinodimethane and cyclized isomer in which both have been observed.

Initial syntheses of 9,10-phenanthrene *o*-quinodimethane (**5**) and 1,2-dihydrocyclobuta[*l*]phenanthrene (**6**) appeared independently in the literature.[16-21] 9,10-Phenanthrene *o*-quinodimethane (**5**), the first isomer reported, was initially generated by various 1,4 pyrolytic eliminations. Evidence for **5** was obtained from trapping experiments and isolation of the [4 + 2] dimer. Later, characterization by UV and ^1H NMR analysis confirmed the existence of **5**, and kinetic studies by Trahanovsky and Macias demonstrated its reactivity.[8]

The unsubstituted 1,2-dihydrocyclobuta[*l*]phenanthrene (**6**) was first observed and characterized in 1965.[16-18] Emil White later established a synthetic route to 9,10-phenanthrene *o*-quinodimethane which led to 1,2-dihydrocyclobuta[*l*]-phenanthrene (**6**) in quantity.[22]

Derivatives of 1,2-dihydrocyclobuta[*l*]phenanthrene (**6**) have received considerable attention in the literature. In 1964 Cava reported the photochemical decarbonylation of

dihydrophencyclone to give 1,2-diphenyl-1,2-dihydrocyclobuta-[*l*]phenanthrene.[23] Since this synthesis, routes to derivatized 1,2-dihydrocyclobuta[*l*]phenanthrene have been reported in the literature which involve [2 + 2] cycloaddition to phenanthrene, ring fusion of 1,2-diphenyl derivatives, ring closure of *o*-quinodimethane derivatives and enolate additions to 9,10-phenanthryne.[24-35] Variations of these routes have also been used in addition to less direct methods.[36-39] The synthetic and electrochemistry of the 9,10-dihydrocyclobuta[*l*]-phenanthrene derivatives has also been explored.[40-47]

In addition to the synthetic routes reviewed above, ring opening studies of 1,2-dihydrocyclobuta[*l*]phenanthrene derivatives have also been reported.[23] Ring opening of 1,2-diphenyl-1,2-dihydrocyclobuta[*l*]phenanthrene was indirectly shown to occur by Cava by trapping the resulting *o*-quinodimethane with SO_2.[23] Hacker and Turro have studied the photochemical ring opening of 9-phenanthrocyclobutenone and its subsequent thermal electrocyclic reversion.[48] Bauld has

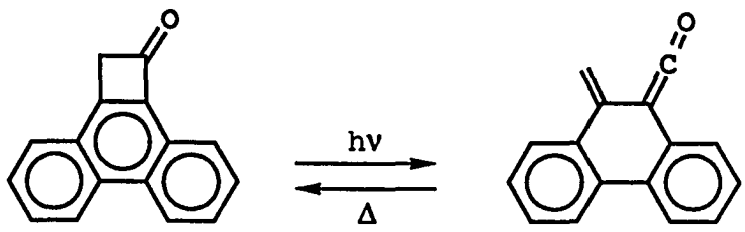

studied the ring opening of a derivatized anion.[41,42] Our study of the 9,10-phenanthrene *o*-quinodimethane (**5**) ring opening kinetics as well as the interconversion between **5** and **6** is reported herein.

RESULTS

Synthesis and Kinetic Analysis of 1,2-Dihydrocyclobuta[*l*]phenanthrene (6)

Trimethyl(10-trimethylsilylmethyl-9-phenanthrylmethyl)-ammonium iodide (**7**) was prepared in six steps using a modification of the procedure developed by Macias.[8] Compound **7**

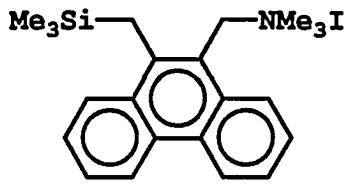

7

was converted to 9,10-phenanthrene *o*-quinodimethane (**5**) in solution as reported followed by solution-phase photochemical conversion to 1,2-dihydrocyclobuta[*l*]phenanthrene (**6**) in 55%

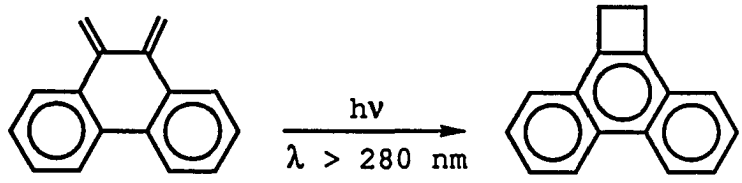

5 **6**

yield. The photolysis was performed using a Conrad-Hanovia medium-pressure immersion lamp with a pyrex filter. The melting point and ^{1}H NMR data obtained for **6** corresponded with

the literature data (Appendix, Figure A-4 on page 216).[22] ^{13}C NMR data were also collected as they had not been previously reported (Appendix, Figure A-11 on page 230).

The characterization data collected for the pyrolysis product did not provide conclusive evidence that the compound synthesized was **6**. Some ambiguity existed because our data and the literature data may also be ascribed to the [4 + 4] dimer (**8**) which could arise from **5**.[22] Therefore, to provide

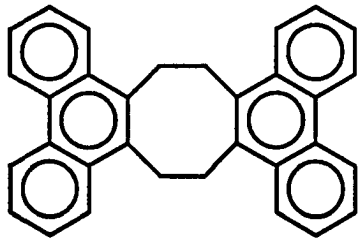

8

further evidence that the compound isolated was **6** the ^{13}C satellites of the ethano bridge proton signal in the ^{1}H NMR of **6** were analyzed.

It has been shown qualitatively that $^{1}J_{CH}$ values, i.e., coupling constants which give rise to ^{13}C satellites, are dependent on the hybridization of the carbon atom.[49] Thus, an increase in ring strain of a carbocycle will lead to greater s orbital character in the carbon-hydrogen bonds and an increase in the $^{1}J_{CH}$ value. Some examples which are relevant to the structural identification of **6** are shown in Table 1.

Table 1. $^{1}J_{CH}$ values in Hz for some benzocycloalkenes and cycloalkanes

		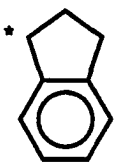	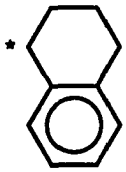	
170	138	127	126	
		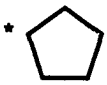	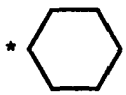	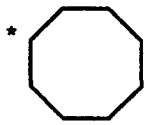
160	134	128.5	125	124.5

The ^{13}C satellites observed in our analysis arose from the isotopomer **6a** present in natural abundance, and the couplings observed resulted from the five-spin heteronuclear system shown. It was assumed that long range couplings with the

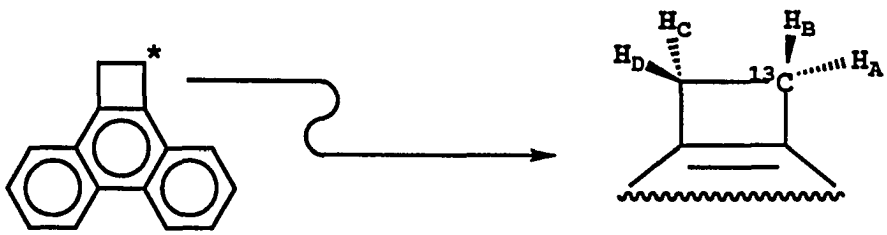

6a

aromatic protons were unimportant. Using coupling constants based on those for ^{13}C satellites published for cyclobutene, the spectrum was simulated with Nicolet NT-300 NMR simulation software.[50] The $^{1}J_{CH}$ value was estimated to be 138.4 ± 0.1Hz (Appendix, Figure A-1 on page 218). The data in Table 1 indicate this $^{1}J_{CH}$ value is in the range expected for a four-membered ring fused to an aromatic system.

Further evidence for our proposed structure of the photolysis product was provided by the $^{1}J_{CH}$ values determined for the eight-membered ring of 4H,5H,9H,10H-cyclocta[1,2-*b*:6,5-*b'*]-difuran (**9**).[51] Comparing these values with coupling

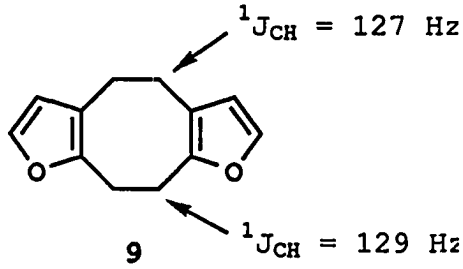

9

constants in Table 1 it is apparent the coupling constants for **9** are somewhat larger than expected for an eight-membered ring fused to an aromatic system. However, the variation is slight and may be attributed to the electron-withdrawing nature of the furan ring. These couplings are not in the range expected for a four-membered ring and offer convincing evidence that our photolysis product is **6** and not the [4 + 4] dimer **8**.

Kinetic data for the electrocyclic ring opening of 1,2-dihydrocyclobuta[*l*]phenanthrene **6** were collected by ^1H NMR spectroscopy. In Table 2 are listed the time-dependent integration data for a typical run involving **6**, and Figure 1 shows several ^1H NMR spectra for this run arranged chronologically. It should be apparent from Figure 1 that the ring opening product, 9,10-phenanthrene *o*-quinodimethane (**5**), did not accumulate in measurable quantity. The data from Table 2 are plotted in Figure 2 using a first order rate equation and give $k_{obs} = 2.77 \times 10^{-6}\ s^{-1}$.

A first-order rate expression was used to obtain rate constants for all the kinetic data collected for the electrocyclic ring opening of **6**.[52] The infinity point integration was consistently zero. The temperature range for the kinetic study was 30 °C. A brief summary of kinetic data collected for the ring opening of **6** is presented in Table 3.

The possibility that the ring-opening product **5** reverted back to **6** during the kinetic runs was subsequently investigated. Three kinetic runs were performed at a single

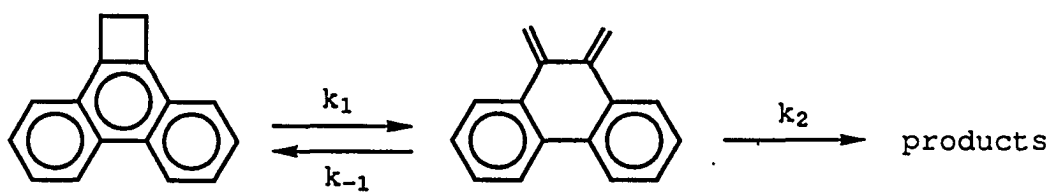

6 **5**

Table 2. Rate of disappearance of 1,2-dihydrocyclobuta-[*l*]phenanthrene (**6**) at 131.95 °C in benzene-d_6. first run[a]

Time x 10^{-4}, s	Integration[b,c]
0.0000	274.4
4.2387	245.5
12.5977	196.4
15.9315	183.4
24.3420	128.0
28.7306	120.3
41.0036	87.8
47.7966	72.6
54.3182	62.8
254.0342	0.0

[a]Rate constant: $k = 2.77 \pm 0.07 \times 10^{-6}$ s^{-1}.

[b]The range for integration is approximately 3.15-3.00 ppm, and the signal followed arises from four protons of **6**. Though the range varies slightly between runs, it was held constant in each run.

[c]The standard was mesitylene, and its concentration was 7.2×10^{-2} M. The tabulated integrations are relative to the signal arising from the protons of the three methyl groups on mesitylene which was set at 300.

Figure 1. Chronologically ordered spectra of 1,2-dihydrocyclobuta[*l*]phenanthrene (**6**) for kinetic run at 131.95 °C: a) time = 0.0 min, b) time = 67.6 h, c) time = 115.4 h, d) time = 706.2 h. The solvent was benzene-d_6 and the standard was mesitylene (• indicates mesityleme peak)

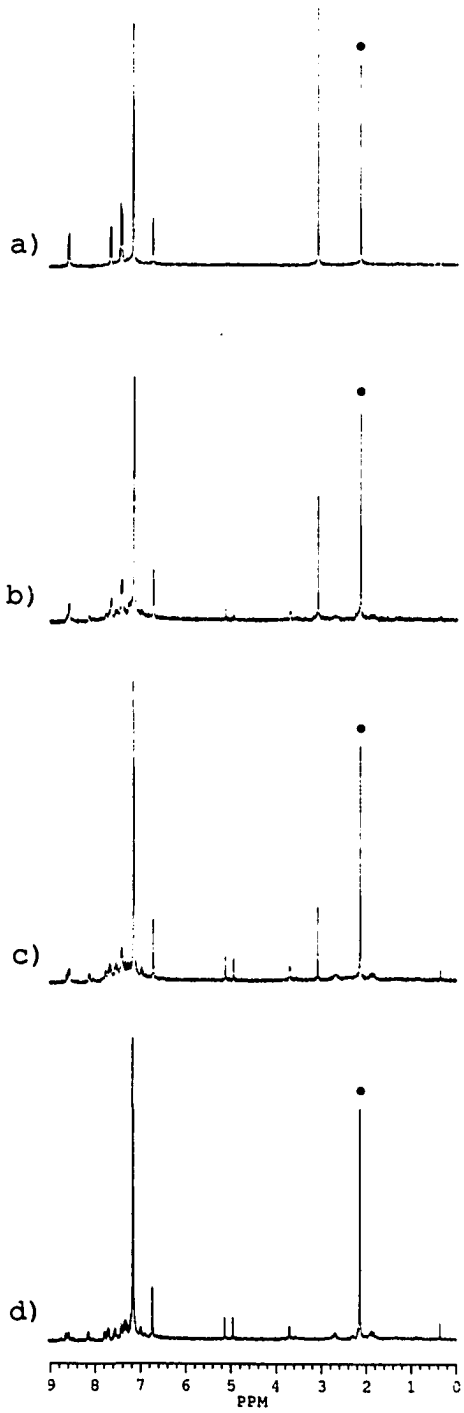
a)
b)
c)
d)
9 8 7 6 5 4 3 2 1 0
PPM

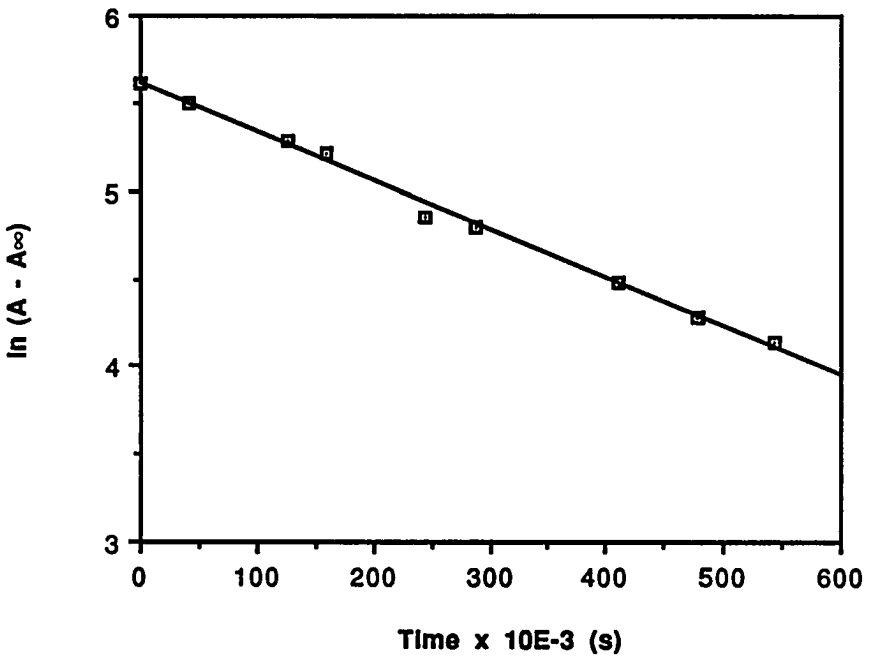

Figure 2. Plot of ln (integration) vs. time at 131.95 °C. Data were obtained from Table A-12 and represent the disappearance of 1,2-dihydrocyclobuta[*l*]phenanthrene (**6**). The rate constant derived from the line is $k = 2.77 \pm 0.07 \times 10^{-6}\ s^{-1}$

Table 3. First-order rate constants for the electrocyclic ring opening of 1,2-dihydrocyclobuta[*l*]phenanthrene (**6**)

Temp, °C	k, s^{-1}
162.15	$5.62 \pm 0.13 \times 10^{-5}$
146.95	$1.30 \pm 0.03 \times 10^{-5}$
131.95	$2.82 \pm 0.06 \times 10^{-6}$

temperature using an excess of N-phenylmaleimide (**10**) to trap **5**. The yield of the Diels-Alder adduct was greater than 95%, and k_{obs} did not vary with the concentration of N-phenylmaleimide indicating $k_{obs} = k_1$. These data are presented in Table 4.

With the establishment of k_1 it was possible to determine activation parameters and the preexponential factor for the electrocyclic ring opening. Activation parameters are presented in Table 5. The Arrhenius plot for **6**, with log k as a function of 1000/T, is shown in Figure 3.

Table 4. First-order rate constants for the electrocyclic ring opening of 1,2-dihydrocyclobuta[*l*]-phenanthrene (**6**) in the presence and absence of N-phenylmaleimide (**10**). The temperature was 147.0 °C and the solvent was benzene-d_6

$k \times 10^6$, s^{-1}	Quantity of **10** relative to starting material
12.9	0
12.8	3.8-fold excess
13.0	4.8-fold excess
12.9	7.0-fold excess

Table 5. Activation parameters for the electrocyclic ring opening of 1,2-dihydrocyclobuta[*l*]-phenanthrene (**6**)

Ea, kcal/mol	Log A, s^{-1}	$\Delta H^{\ddagger}$ at 25 °C, kcal/mol	$\Delta S^{\ddagger}$ at 25 °C, cal/K mol
34.7 ± 0.2	13.2± 0.1	34.1 ± 0.2	-0.2 ± 0.4

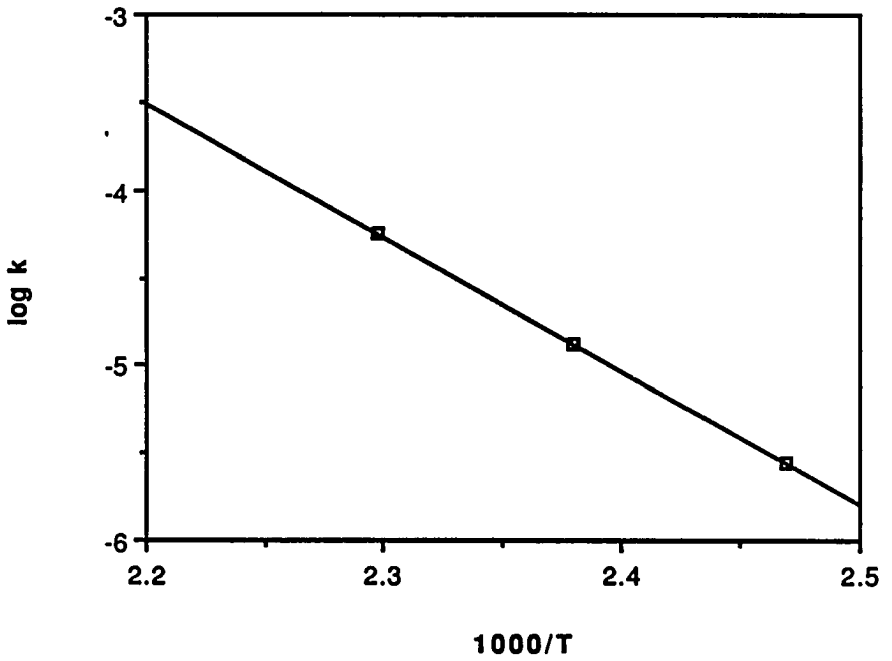

Figure 3. Plot of log k vs. 1000/T for the electrocyclic reaction of 1,2-dihydrocyclobuta[*l*]phenanthrene (**6**). Data were obtained from Table 2. The slope of the line is -7.58 and the y-intercept is 13.2.

Study of the 1,2-Dihydrocyclobuta[*l*]phenanthrene (6)- 9,10-Phenanthrene *o*-Quinodimethane (5) Interconversion.

Three distinct approaches were employed to investigate the equilibrium between **5** and **6**. The equilibrium was initially studied in solution using sealed NMR tube methodology developed for studying kinetics. By preparing ampuls of **6**, heating each ampul at 200 °C for a predetermined length of time and analyzing by ^{1}H NMR, an equilibrium constant was determined for the interconversion of **5** and **6**. Mesitylene served as the internal standard, and benzene-d_6 was the solvent.

The presence of **5** in this initial study was based on the appearance of two transient singlets between 5 and 6 ppm. These singlets were shown to arise from **5** by comparing a sample from the equilibrium study with an authentic sample of **5** generated from trimethyl(10-trimethylsilylmethyl-9-phenanthrylmethyl)ammonium iodide (**7**) using the Ito-Nakatsuka-Saegusa method.[8,53] Both samples were prepared for ^{1}H NMR analysis using the same solvent system. In each case the ^{1}H NMR signals appeared at 5.38 and 5.31 ppm and were present in a ratio of 1:1. The transiency of the signals observed in the equilibrium study gave further evidence for the presence of **5**.

A second approach to the equilibrium involved the pyrolysis of **6** at 700 °C and at 900 °C. The pyrolysate in each experiment was collected in a solution of CS_2/benzene-d_6 1:1 (v:v), and the dilute solutions were analyzed by ^{1}H NMR

(Appendix, Figure A-6 on page 226). The ratio of **6**:5 was 1:1 at 700 °C while **5** was not observed in the pyrolysate from the 900 °C run. It is presumed that the higher temperature run led to destruction of the *o*-quinodimethane.

The identification of **5** in the pyrolysate was based on the chemical shifts of the singlets at 5.37 ppm and 5.34 ppm. These values are similar to those observed for the solution phase equilibrium study which was performed in a similar solvent system. The identification of **6** in the pyrolysis sample was supported by a ^{1}H NMR of an authentic sample of **6** in the same solvent system. Though two multiplets observed in the ^{1}H NMR of **6** in the pyrolysate were somewhat obscured, all signals were visible and matched those of the authentic sample.

In an effort to approach the equilibrium from the *o*-quinodimethane side of **6**, 9-acetoxymethyl-10-methylphenanthrene (**11**) was prepared according to the procedure published by Adcock.[54] The acetate ester was pyrolyzed at 700 °C and the pyrolysate was collected in $CDCl_3/CS_2$ 1:1 (v:v). Three pyrolyses were sufficient to establish ^{1}H NMR evidence for the presence of **6** (Appendix, Figure A-8 on page 230). Spectroscopic evidence for **6** consisted of the methylene singlet at 3.45 ppm as well as downfield multiplets at 7.55, 7.72 and 8.66 ppm. These signals were shown to arise from **6** by comparing a ^{1}H NMR spectrum of the pyrolysate with an authentic sample of **6** in the same solvent system. The thermal lability

of the compound identified as **6** was also established, and its rate of disappearance was in the range expected for **6**.

9-Methyl-10-phenanthrylmethyl benzoate (**12**) was prepared from the acetate to obtain a better behaved ester pyrolysis. Trahanovsky has noted that benzoates typically undergo thermal rearrangement to eliminate the corresponding acid much more readily than acetates.[55] Synthesis of the benzoate required hydrolysis of the acetate followed by benzoylation with benzoyl chloride.[51] The two-step yield was 70%.

The benzoate was pyrolyzed at 670 °C, and the pyrolysate was collected in $CDCl_3/CS_2$ 1:1 (v:v). ^1H NMR product analysis gave evidence for **6** consisting of the methylene singlet at 3.45 ppm as well as downfield multiplets at 7.55, 7.72 and 8.66 ppm (Appendix, Figure A-9 on page 232). As noted earlier, these chemical shifts correspond to those of an authentic sample in the same solvent system. Further evidence for **6** was provided by following its rate of disappearance at 147 °C. The first-order plot of the data led to a rate constant $k = 1.35 \times 10^{-5}$ s^{-1} for the kinetic run which lasted 2.4 half-lives, and this value is comparable to that determined for an authentic sample of **6**. Spectroscopic evidence for the presence of **5** in the pyrolysate was also obtained. Singlets at 5.53 and 5.47 ppm were initially observed and gradually gave way to peaks for the [4 + 2] dimer **13**. The upfield peaks were easily identified and consisted of one-proton singlets at 5.29 and 5.08 ppm, a two-

proton AB quartet at 3.88 ppm , a two-proton multiplet at 2.91 ppm and a two-proton triplet at 2.01 ppm. The product ratio of 1:0.67 for **6:5** was recorded.

DISCUSSION

Evidence for 1,2-dihydrocyclobuta[*l*]phenanthrene (**6**) was first provided by Masamune in 1965 following an attempted synthesis of diphenyltetrahedrane.[16-18] Emil White later established a synthetic route which led to **6** in quantity, and he characterized **6** by IR, UV, ^{1}H NMR, fluorescence and mass spectroscopy.[22] The route chosen by White required a 1,4 elimination of trimethyl(10-methyl-9-phenanthrylmethyl)-ammonium chloride (**14**) to generate 9,10-phenanthrene *o*-quinodimethane (**5**) followed by photolysis at 254 nm to give 1,2-dihydrocyclobuta[*l*]phenanthrene (**6**) in 15% isolated yield. The low yield of **6** probably resulted from the harsh reaction conditions used to produce **5**.

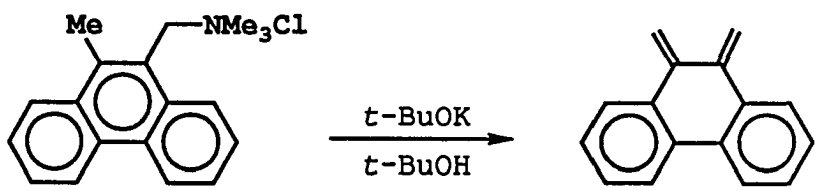

13 **5**

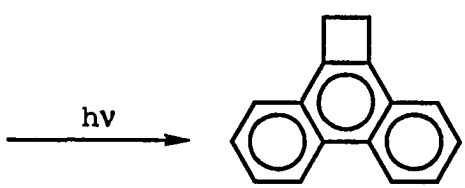

6

Our synthetic route also required photolysis of 9,10-phenanthrene *o*-quinodimethane (**5**), but our preparation of **5** used the milder conditions of the Ito-Nakatsuka-Saegusa method which was adapted to the phenanthrene system by Macias.[53,8] After 1,4 elimination promoted by TBAF the volume of the reaction solution was increased 500-fold by addition to pentane. The change in solvent polarity of the reaction solution precipitated the ammonium salts and lowered the concentration of **5** thus reducing intermolecular reactions. The yield of **6** was 55%.

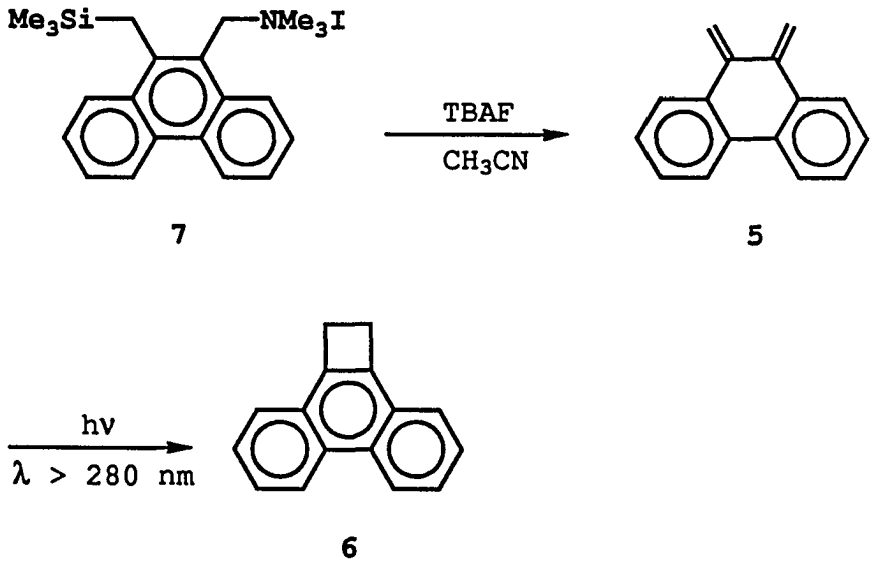

7 **5** **6**

Kinetic study of the electrocyclic ring opening of **6** led to rate constants for the disappearance of **6** at three temperatures over a 30 °C temperature range. The following reaction scheme indicates it was incumbent upon us to show that

$k_{obs} = k_1$ if activation parameters were to be determined for ring opening (Scheme 1). This reaction scheme allows one to

Scheme 1

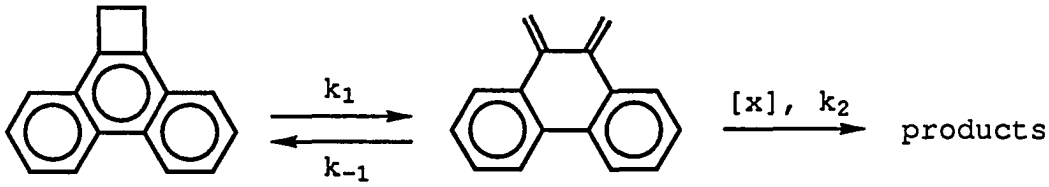

6 **5**

arrive at the following conclusion: if $k_2[x][5] >> k_{-1}[5]$ then k_1 is rate determining. In this expression x is any compound in solution which reacts with **5**. Thus, the expression may be more complicated if more than one species in solution reacts with **5** (eg. if there two reactive species reacting with **5** then $k_2[5]([x_1] + [x_2]) >> k_{-1}[5]$).

To simplify the reaction scheme and determine whether $k_{obs} = k_1$ we trapped intermediate **5** with an excess of N-phenylmaleimide (**10**) as indicated to give adduct **15**.[56] As **10** trapped more than 95% of **5** the previous inequality can be

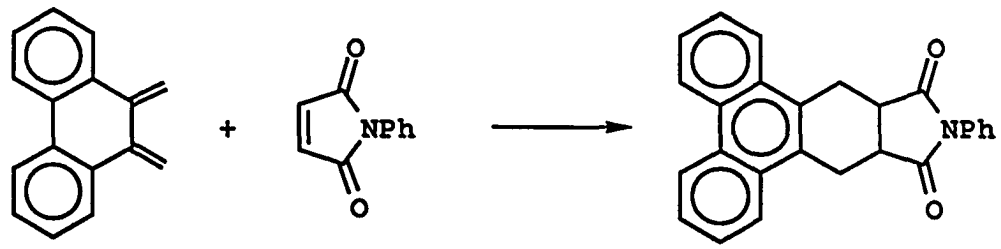

5 **10** **15**

rewritten to describe this trapping experiment. If $k_2[10][5] >> k_{-1}[5]$ then k_1 is rate determining. The rate of disappearance of **5** did not change with the addition of varying quantities of **10** indicating $k_{obs} = k_1$.

In the equilibrium study between **5** and **6** we approached the equilibrium from both sides. Methods included: 1) FVP of acetate and benzoate esters, **11** and **12**, 2) solution phase thermolysis of **6**, and 3) FVP of **6**. The routes with the relevant temperatures are displayed in Scheme 2.

The inability to obtain a well behaved pyrolysis with the acetate (**11**) led to study of the benzoate (**12**). Pyrolysis of the benzoate is thought to lead initially to 9,10-phenanthrene o-quinodimethane either by direct δ-elimination of benzoic acid or via a [3,3] sigmatropic shift followed by β-elimination.[51] Precedent for this mechanistic proposal is provided by the

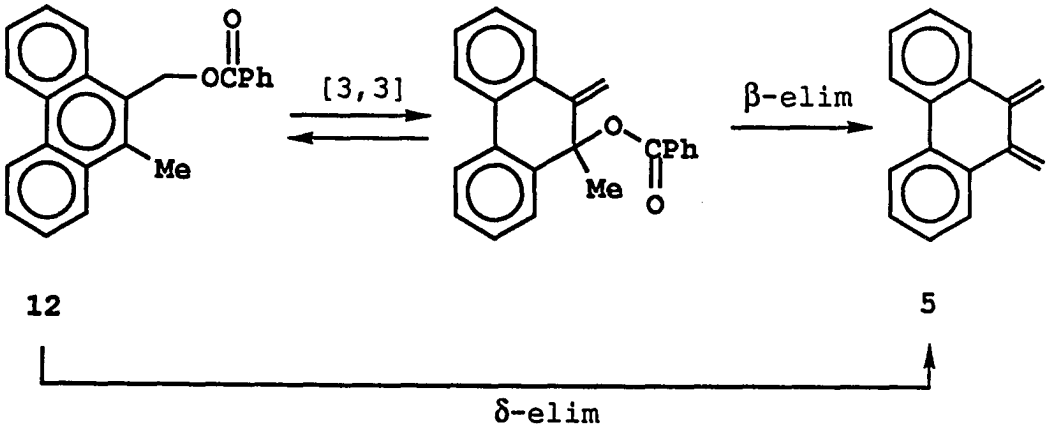

Scheme 2

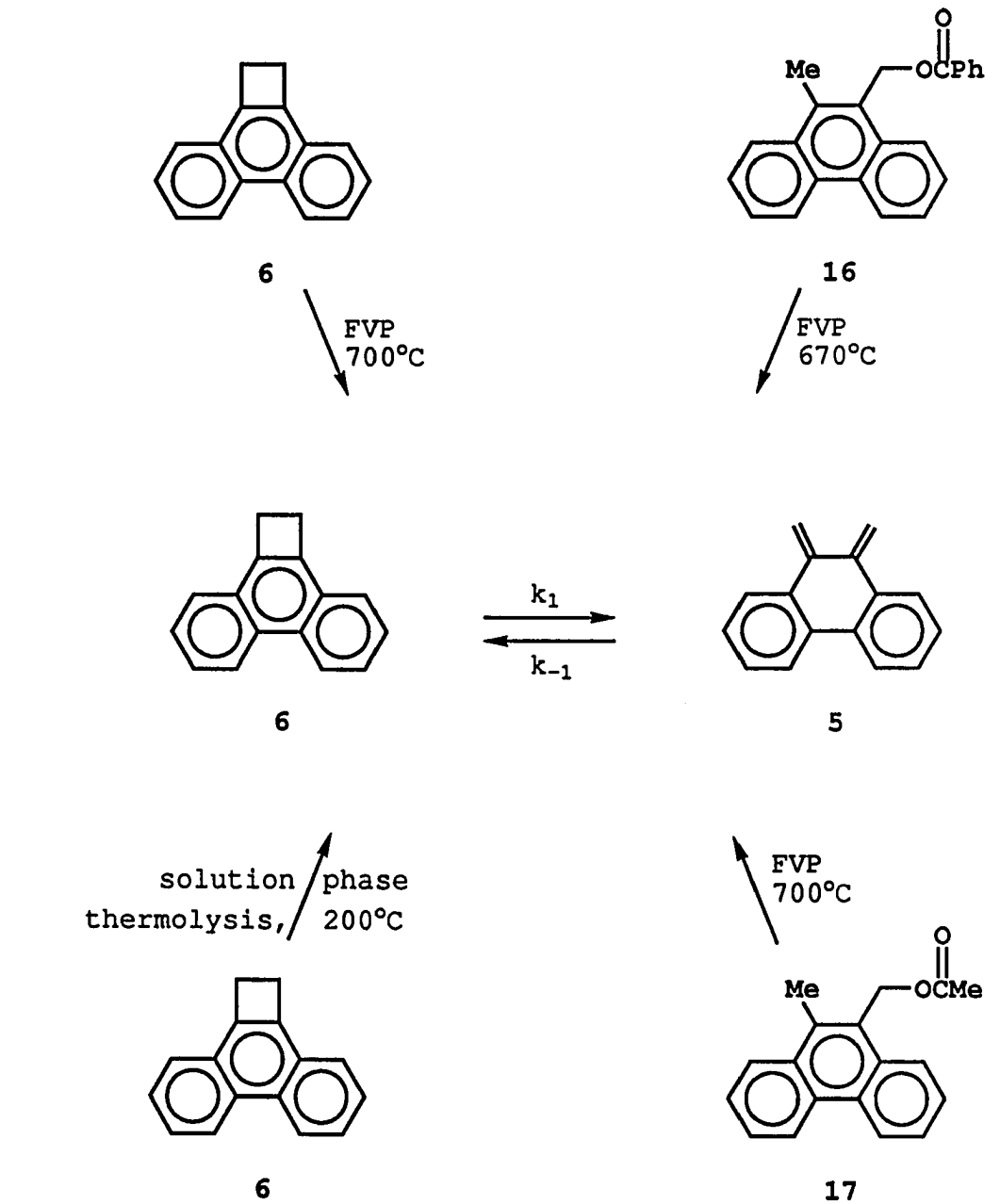
Me
OCPh
O
6
16
FVP
700°C
FVP
670°C
k_1
k_{-1}
6
5
solution phase
thermolysis, 200°C
FVP
700°C
Me
OCMe
O
6
17

formation of 2,3-dimethylene-2,3-dihydrofuran (**17**) from 2-methyl-3-furylmethyl benzoate (**16**) for which an analogous mechanistic scheme was presented.[51] Further evidence that the

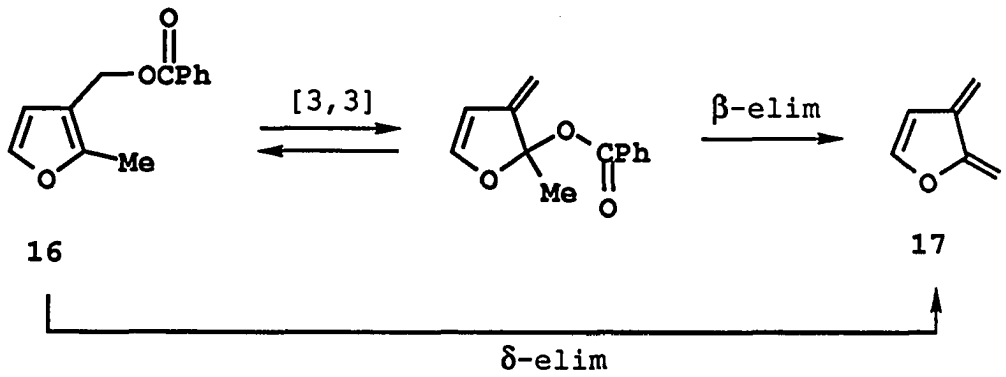

o-quinodimethane (**5**) was formed initially may be found in trapping experiments performed by Gardner and Sarrafizadeh, Stille et al., and Miller et al.[19-21] A 1,4 elimination leading directly to **5** was proposed for the pyrolysis of the acetate (**11**), the sulfone (**18**), and the ammonium salt (**14**) based on trapping products and isolation of [4 + 2] and [4 + 4] dimers, **13** and **8**. Additional support for the stepwise formation of **6** is found in the pyrolysis of

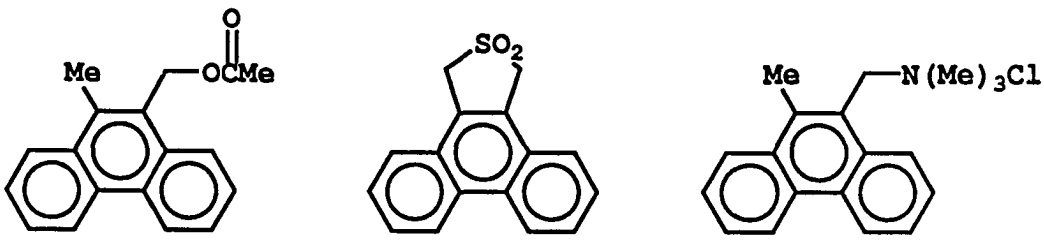

11 **18** **14**

1,3-dihydroisothianaphthene 2,2-dioxide (**19**) which was shown to lead to benzocyclobutene (**4**) via *o*-xylylene (**3**) using a dienophile to trap **3**.[57]

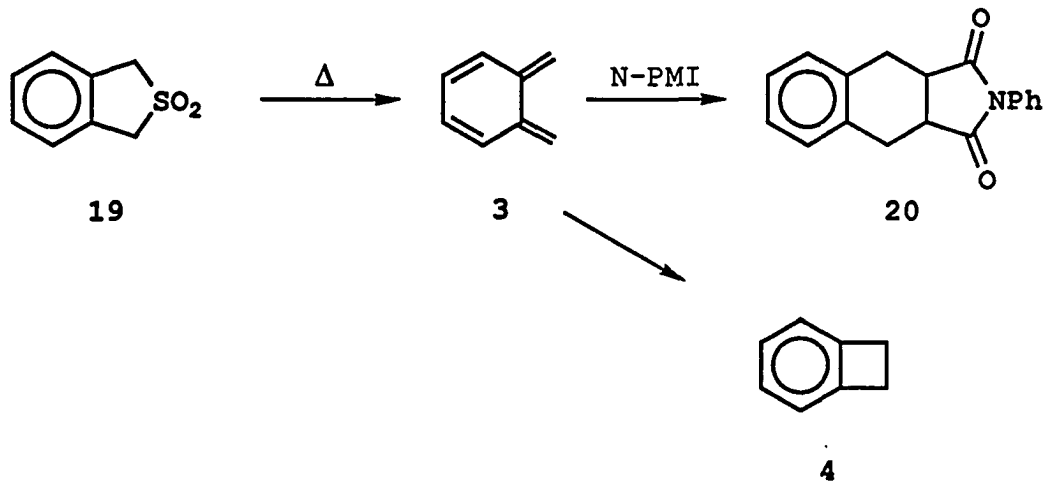

19 **3** **20**

4

Due to the nature of FVP it was difficult to determine the precise temperature at which equilibrium occurred in the pyrolysis of the 9-methyl-10-phenanthrylmethyl benzoate (**12**). However, pyrolysis of the benzoate led to one very important result: **6** formed in the gas phase via **5**. By itself this result indicates **6** is at least of comparable stability to **5** if not more stable at the pyrolysis temperature. The FVP of **6** at the same pyrolysis temperature indicated the corollary was also true: one may start with **6** and form **5** in the gas phase. Therefore, it is concluded that **5** and **6** must be of comparable stability under the pyrolysis conditions employed.

The solution phase determination of K_{eq} for the equilibrium between **5** and **6** was considered more reliable by virtue of the method: an exact temperature was known, and it was possible to determine whether an equilibrium had been reached. Ampuls of **6** were prepared, warmed for a predetermined length of time and analyzed by ^1H NMR. Some loss of **5** may have occurred during scanning but is considered minimal based on the low concentration of **5**, the reduced temperature of the probe, and the half-life of **5** for the dimerization pathway which was in excess of 400 h at the temperature employed. It is noteworthy that the concentration of **5** in this equilibrium was one to two orders of magnitude less than that used for the kinetic studies thereby effectively shunting any dimerization of **5**. Additionally, starting material had been purified by column chromatography and each ampul had been subjected to three freeze-thaw cycles prior to sealing to remove oxygen. The plot of the ratio **5:6** with respect to time enabled calculation of K_{eq} at 200 °C (Appendix, Figures A-2 and A-3, Table A-1). $K_{eq} = \frac{[5]}{[6]} = 1.5$ for the equilibrium. One may also estimate $\Delta H°$ for the equilibrium using the following equation.[52]

$$K_{eq} = \exp\left(\frac{\Delta S°}{R}\right) \exp\left(-\frac{\Delta H°}{RT}\right)$$

From Roth's data ΔS° is ca. 7.3 eu for the benzocyclobutene system.[12-14] Assuming similarity between the benzocyclobutene and 1,2-dihydrocyclobuta[*l*]phenanthrene systems one may estimate a ΔS° for the phenanthrene system and calculate an approximate ΔH°. This value is ΔH° = 3 kcal/mol.

In summary, the interconversion between **5** and **6** was approached from two directions. If the interconversion between **5** and **6** had not been observed the bidirectional approach would have demonstrated this fact. Additionally, a K_{eq} at 200 °C has been determined. The equilibrium is the first example of an equilibration between an *o*-quinodimethane and its cyclized isomer which can be observed. Previous work on the benzocyclobutene system depended on observation of *o*-xylylene (**3**) as the activity of benzocyclobutene (**4**) in the ultraviolet region was insufficient for observation.

In 1981 Roth established the following energy profile for the *o*-xylylene (**3**) - benzocyclobutene (**4**) equilibrium (Figure 3) from which two relevant observations are made: 1) benzocyclobutene (**4**) is 13 kcal/mol more stable than the corresponding *o*-quinodimethane isomer (**3**), and 2) the enthalpy of activation for ring opening is 39 kcal/mol.[13]

Adjacent to the energy profile for the benzene system is our profile for the phenanthrene system. The resonance stabilization of the central phenanthrene ring is 14 kcal/mol less than that for benzene based on Dewar Resonance Energies.

Therefore, one would expect 1,2-dihydrocyclobuta[*b*]phenanthrene (**6**) to be slightly less stable than its isomer 9,10-phenanthrene *o*-quinodimethane (**5**). Experimental results are in excellent agreement with predictions based on Dewar resonance

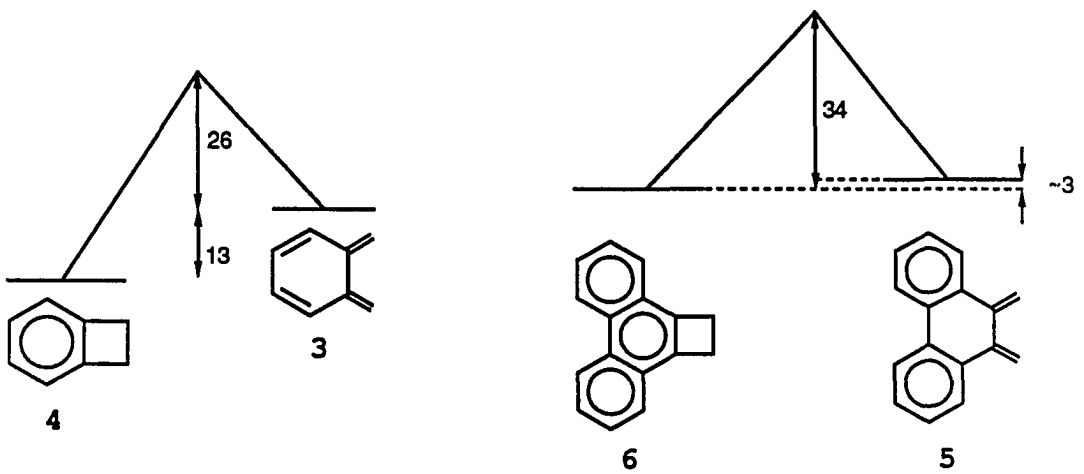

Figure 4. Energy profiles for the benzocyclobutene (**4**) - o-xylylene (**3**) and the 1,2-dihydrocyclobuta-[*1*]-phenanthrene (**6**) - 9,10-phenanthrene o-quinodimethane interconversions

energies.[58] The energy barrier for ring closure of **5** is higher than that for **3** which is likely due to less resonance stabilization in the transition state for the ring closure of **5**. The lower energy barrier for ring opening of **6** relative to **4** is probably the result of two interrelated factors: first, is the resonance stabilization of the transition state which is presumably greatest in **4**. This factor should lower the transition state for ring opening of **4** relative to **6**. Second,

resonance stabilization of the ground state is greater in **4** than in **6** and would be expected to increase the transition state for ring opening of **4** relative to **6**. It is evident this second factor predominates as the ring opening barrier for **4** is greater than that for **6**.

The difference in resonance stabilization of benzocyclobutene (**4**) and 1,2-cyclobuta[*l*]phenanthrene (**6**) is evident in the stabilities of these two compounds relative to their respective *o*-quinodimethane isomers. Hence, one observes a K_{eq} = ~1.5 for **5** and **6** at 200 °C while $K_{eq} = 3.4 \times 10^{-4}$ for **3** and **4** at the same temperature.[14]

In conclusion, rate constants, activation parameters and a K_{eq} at 200 °C have been obtained. The data have been related to the benzocyclobutene (**4**) - *o*-xylylene (**3**) energy profile and the data have been interpreted on the basis of resonance energies and steric interactions.

EXPERIMENTAL

Methods and Materials

Pyrolyses were carried out in a standard flash vacuum pyrolysis apparatus which has been described.[59] Photolyses were performed using a water cooled 450 W medium pressure Conrad-Hanovia immersion lamp and a standard pyrex immersion well. ^{1}H and ^{13}C NMR data were collected on the Nicolet NT-300, the Varian VXR-300 and the Bruker WM-200 spectrometers. UV data were collected with a Perkin-Elmer 320 spectrophotometer, GC/MS data with a Finnigan 4000 incorporating an INCOS data system and GC data with the Hewlett-Packard 5840A and the 5890 Series II gas chromatographs. Melting points were obtained with a Thomas Hoover melting point apparatus. Kinetic results were obtained using a stirred oil bath incorporating a 125 W blade heater, an adjustable thermoregulator (H-R and Co.) and a precision thermometer (0.2 °C graduations, Cole Parmer Instrument Company).

N-phenylmaleimide was kindly provided by Dr. M.G. Ranasinghe and recrystallized twice from cyclohexane prior to use [mp 86-87 °C (lit.[60] 89-89.8 °C)].

Synthesis of 1,2-Dihydrocyclobuta[*l*]phenanthrene (6)

All solvents listed below were deaerated with argon. Diethyl ether was distilled from sodium and acetonitrile was dried over molecular sieves.

Trimethyl(10-trimethylsilylmethyl-9-phenanthrylmethyl)-ammonium iodide (**7**) was prepared and recrystalized using a modification of the Macias procedure.[8] A 25.0-mg (5.35×10^{-2} mmol) quantity of **7** was added to 0.95 ml of acetonitrile followed by addition of a solution of 70 mg of tetra-*n*-butylammonium fluoride (prepared according to Fischer's procedure) in 0.95 ml of acetonitrile.[9] The mixture was stirred until the phenanthrene salt (**7**) disappeared. Within 45 s of the TBAF addition 30 ml of 50% ether in pentane was added to the reaction flask via syringe. Use of the syringe allowed vigorous mixing, a necessary step to extract 9,10-phenanthrene *o*-quinodimethane (**5**) from the salt solution. The two phases were allowed to partially separate over 5 min followed by transfer of the pentane-ether phase by cannula to the photoreactor charged with 600 ml of spectrophotometric grade pentane. Prior to transfer the reactor solvent had been deaerated for 2 h, and deaeration continued for an additional 3.5 h following the transfer. The photolysis was followed by removing samples periodically for UV analysis, and it was assumed the photolysis was complete when the UV absorbance of starting material (**5**) was no longer observed. The product was

purified by cooling the photolysis solution to -78 °C to precipitate trace quantities of suspended salts followed with warming to near room temperature and decanting. The solvent volume was reduced by fractional distillation under argon using a vigreux column, and the remaining pentane was removed at reduced pressure to give 6.05 mg (0.0296 mmol, 55%) of **6** as determined by ^{1}H NMR. Diphenylmethane served as an internal standard. Compound **6**: mp 131-132 °C (lit. 135.5-136 °C, Kofler); ^{1}H NMR (benzene-d_6) (Appendix, Figure A-4) δ 8.59-8.50 (m, 2H), 7.66-7.58 (m, 2H), 7.46-7.35 (m, 4H), 3.09 (s, 4H) [lit. ^{1}H NMR (CCl_4) δ 8.60 (m, 2H), 7.65 (m, 2H), 7.45 (m, 4H), 3.35 (s, 4H)]; ^{1}H NMR ($CDCl_3$) (Appendix, Figure A-11) δ 139.80, 130.45, 128.86, 126.60, 125.49, 123.72, 122.45, 28.03. When very pure **6** was required, such as for equilibrium studies and for obtaining a melting point, the sample was purified by flash column chromatography on silica gel (hexanes).

Synthesis of 10-Methyl-9-phenanthrylmethyl Benzoate (12)

Synthesis of 10-methyl-9-phenanthrylmethyl acetate (**11**) was accomplished following a previously reported procedure.[54] A 200-mg (0.754-mmol) quantity of the acetate was stirred in a solution of water (0.9 ml), methanol (3.3 ml), THF (3.3 ml), and 38 mg (0.91 mmol) of LiOH. The reaction was followed by TLC and determined complete when starting material was no longer observed (several hours). The solution was acidified

with 2 N HCl, and the product was extracted with methylene chloride (3 x 5 ml). The organic layers were combined and washed with saturated $NaHCO_3$ (2 x 5 ml) and brine (5 ml). The solution was dried ($MgSO_4$), and removal of the solvent at reduced pressure followed by drying overnight gave 148 mg (0.663 mmol, 87%) of the alcohol **21**: mp 166-168 °C (lit.[54] 169-171); ^1H NMR ($CDCl_3$) δ 8.73-8.66 (m, 2H), 8.31-8.10 (m, 2H), 7.68-7.57 (m, 2H), 5.30-5.23 (m, 2H), 2.83 (s, 3H). A 148-mg quantity of the alcohol (**21**) in methylene chloride was stirred with 101 mg of benzoyl chloride (0.718 mmol) and 101 mg of triethylamine (1.00 mmol) for 11 h.[51] Subsequently, 5 ml of 5% Na_2CO_3 was added, and the layers were separated. The aqueous layer was extracted with methylene chloride (3 x 5 ml) and the combined methylene chloride solutions was washed successively with 1 N HCl (4 x 5 ml), saturated Na_2CO_3 (3 x 5 ml) and brine (3 x 5 ml). The methylene chloride solution was dried ($MgSO_4$), and solvent was removed at reduced pressure. The product was recrystalized from absolute ethanol and toluene to yield 173.9 mg (0.533 mmol, 81%) of compound **11**: mp 138-139 °C; ^1H NMR ($CDCl_3$) (Appendix Figure A-5) δ 8.75-8.68 (m, 2H), 8.23-8.15 (m, 2H), 8.01 (m, 2H), 7.72-7.56 (m, 4H), 7.50 (m, 1H), 7.36 (m, 2H), 5.99 (s, 2H), 2.89 (s, 3H); high-resolution mass spectrum, calculated for $C_{23}H_{18}O_2$ 326.13068, measured 326.13004.

Pyrolysis of 1,2-Dihydrocyclobuta[*l*]phenanthrene (6)

A 1.78-mg (8.73 x 10^{-3}-mmol) quantity of **6** was placed in the sample chamber followed by evacuation of the apparatus to 5 x 10^{-5} torr. The oven temperature was 700 °C during the pyrolysis which lasted 2 h. The sample chamber temperature was 60 °C, and the product was collected in a single-walled trap cooled with liquid nitrogen. At the end of the pyrolysis the level of liquid nitrogen was raised slightly followed by distillation of 4 ml of CS_2/benzene-d_6 1:1 (v:v) into the trap through a side-arm. The trap was warmed sufficiently to thaw the solvent, and the solution was transferred to an NMR tube. ^{1}H NMR analysis revealed the presence of both 9,10-phenanthrene *o*-quinodimethane (**5**) and 1,2-dihydrocyclobuta[*l*]phenanthrene (**6**). As the spectra were somewhat obscured verification was made with authentic samples. Compound **5**: ^{1}H NMR (1:1 CS_2/benzene-d_6) (Appendix, Figure A-6) δ 5.37 (s, 2H), 5.34 (s, 2H), remaining signals obscured. Compound **6**: ^{1}H NMR (1:1 CS_2/benzene-d_6) (Appendix, Figure A-6) δ 8.54-8.49 (m, 2H), 7.43-7.37 (m, integration obscured), 3.22 (s, 4H), remaining signals obscured. The authentic sample of compound **5** was prepared by treatment of **7** with TBAF, while the authentic sample of compound **6** was prepared photolytically as described earlier. Authentic compound **5**: (1:1 CD_3CN/benzene-d_6) (Appendix, Figure A-7) δ 7.70 (m, 2H), 7.51 (m, 2H), 5.38 (s, 2H), 5.31 (s, 2H). The remaining 4H multiplet of authentic **5**

was obscured. Authentic compound **6**: (1:1 CS_2/benzene-d_6) δ 8.54-8.49 (m, 2H), 7.62-7.57 (m, 2H), 7.43-7.38 (m, 4H), 3.23 (s, 2H).

Pyrolysis of 10-Methyl-9-phenanthrylmethyl Acetate (11)

A 20.0-mg (7.57 x 10^{-2}-mmol) quantity of **11** was placed in the sample chamber followed by evacuation of the pyrolysis apparatus to 2 x 10^{-5} torr. The oven temperature was 700 °C during the pyrolysis which lasted 5 h. The sample chamber temperature was 190 °C, and the product was collected in a single-walled trap cooled with liquid nitrogen. At the end of the pyrolysis the level of the liquid nitrogen was raised slightly followed by distillation of 2 ml of CS_2/$CDCl_3$ 1:1 (v:v) into the trap through a side-arm. The trap was warmed to -78 °C and the pyrolysate was transferred to a test tube at -78 °C, shaken with a small quantity of Na_2CO_3 and added to an NMR tube at -78 °C following filtration. The sample was quickly warmed to room temperature, and ^1H NMR analysis revealed the presence of 1,2-dihydrocyclobuta[*l*]phenanthrene (**6**): ^1H NMR (1:1 CS_2/$CDCl_3$) (Appenidx, Figure A-8) δ 8.72-8.63 (m), 7.74-7.70 (m), 7.60-7.52 (m), 3.45 (s). The multiplets were distorted by other products making integrations impossible. An authentic sample of **6** was prepared as described earlier. Authentic **6**: ^1H NMR (1:1 CS_2/$CDCl_3$). δ 8.70-8.63 (m, 2H), 7.77-7.69 (m, 2H), 7.60-7.53 (m, 4H), 3.44 (s, 4H).

Further evidence for **6** was obtained in the following manner. The pyrolysate was placed in a modified NMR tube and taken through three freeze-thaw cycles. The tube was sealed under vacuum and the sample warmed in an oil bath at 147°C. Periodically, the sample was removed, cooled in pentane and a ^1H NMR spectrum collected. The material identified as **6** disappeared at a rate comparable to that observed for an authentic sample of **6**.

Pyrolysis of 10-Methyl-9-phenanthrylmethyl Benzoate (12)

A 30.0-mg (9.220×10^{-2}-mmol) quantity of **12** was placed in the sample chamber followed by evacuation of the pyrolysis apparatus to 1×10^{-4} torr. The oven temperature was 670 °C during the pyrolysis which lasted 4 h. The sample-head temperature was maintained at 130 °C, and the product was collected in a single-walled trap cooled with liquid nitrogen. At the end of the pyrolysis the level of the liquid nitrogen was raised slightly followed by distillation of 2 ml of $CS_2/CDCl_3$ 1:1 (v:v) into the trap through a side-arm. The trap was warmed to -78 °C, and the pyrolysate was transferred to an NMR tube at -78 °C. The sample was rapidly warmed to room temperature and scanned by ^1H NMR which revealed the presence of 1,2-dihydrocyclobuta[*l*]phenanthrene (**6**) and 9,10-phenanthrene *o*-quinodimethane (**5**). Compound **6**: ^1H NMR (1:1 $CS_2/CDCl_3$) (Appendix, Figure A-9) δ 8.70-8.63 (m), 7.77-7.69

(m), 3.44 (s). One multiplet arising from **6** was obscured and integrations were inaccurate due to the presence of other products. Compound **5**: ^{1}H NMR (1:1 $CS_2/CDCl_3$) (Appendix, Figure A-9) δ 5.52 (s, 2H), 5.46 (s, 2H). The remaining signals arising from **5** were obscured by signals arising from other products. The NMR sample was subsequently allowed to stand at room temperature for 48 h after which ^{1}H NMR analysis revealed the presence of a [4 + 2] dimer **13**. The downfield peaks in the spectrum were obscured by solvent and other products. Compound **13**: ^{1}H NMR (1:1 $CS_2/CDCl_3$) δ 5.29 (s, 1H), 5.08 (s, 1H), 3.88 (AB quartet, 2H, J = 16 Hz), 2.93-2.89 (m, 2H), 2.01 (t, 2H, J = 6 Hz) [lit ^{1}H NMR (benzene-d_6) δ 8.60-8.47 (m, 2H), 8.15 (br d, 1H), 7.75-6.95 (m, 13H), 5.16 (s, 1H), 4.95 (s, 1H), 3.67 (AB quartet, 2H, J = 18.0 Hz), 2.81-2.60 (m, 2H), 1.78 (t, 2H, J = 7 Hz).

Further evidence for **6** was obtained in the following manner. The solvent was removed from the pyrolysate at reduced pressure and the sample was dissolved in benzene-d_6. Following transfer of the solution to a modified NMR tube, the sample was taken through three freeze-thaw cycles and sealed under vacuum. Subsequently, a ^{1}H NMR spectrum was collected, and the NMR tube was immersed in an oil bath maintained at 147 °C. The rate of disappearance of **6** was monitored by periodically quenching the tube in pentane and scanning by ^{1}H NMR. Mesitylene served as the internal standard. The rate constant, k, for the

disappearance of **6** was 1.34×10^{-5} s^{-1} which is similar to the rate noted for an authentic sample of **6**.

Study of the Interconversion between 9,10-Phenanthrene o-Quinodimethane (5) and 1,2-Dihydrocyclobuta[*l*]phenanthrene (6)

To 2 ml of a 2.4×10^{-3} M solution of **6** in benzene-d_6 was added 0.588 mg of mesitylene in 1.08×10^{-2} ml of benzene-d_6. The mesitylene served as an internal standard. The solution was equally partitioned between five modified NMR tubes, and an additional quantity of benzene-d_6 was added in equal portion to each tube. The NMR tubes were each taken through two freeze-thaw cycles followed by sealing under vacuum. Each tube was subsequently scanned using ^1H NMR to determine the sample quality and check the ratio of standard:**6**. Using a variation of the ampul technique four of the tubes were warmed individually for predetermined periods of time followed by collection of a ^1H NMR and determination of the ratio of 5:6. The length of time each ampul was warmed was increased successively such that the ratio of 5:6 could be plotted as a function of time. Also recorded was the percent of **5** and **6**, relative to the initial quantity of **6**, after each interval of warming.

To show that the singlets monitored to determine [**6**] were indeed those of **6** the following work was performed. A spent

sample from the equilibrium experiment containing **5** and **6** was diluted with CD_3CN such that the ratio of CD_3CN/benzene-d_6 was 1:1 (v:v), and a ^1H NMR was collected. Compound **5**: ^1H NMR (1:1 CD_3CN: benzene-d_6) δ 5.38 (s, 1H), 5.31 (s, 1H). These signals were compared with those arising from an authentic sample of **5** prepared from trimethyl(10-trimethylsilylmethyl-9-phenanthrylmethyl)ammonium iodide (**7**) using TBAF as reagent. See experimental section describing the pyrolysis of **6** to obtain ^1H NMR data for the authentic sample of **5**.

Procedure for Measuring Rate Constants for the Electrocyclic Opening of 1,2-Dihydrocyclobuta[*l*]phenanthrene (6)

In preparation for a kinetic run a modified NMR tube was charged with 0.74 ml of benzene-d_6 which contained 2.3 mg (1.2 x 10^{-2} mmol) of 1,2-dihydrocyclobuta[*l*]phenanthrene (**6**) and 0.65 mg (5.39 x 10^{-3} mmol) mesitylene as an internal standard. Following two freeze-thaw cycles the tube was evacuated to 10^{-2} torr while cooling at -78 °C and sealed with a torch. A ^1H NMR spectrum was collected after which the tube was immersed in the previously described oil bath. The temperatures used for following kinetics were 132, 147, and 162 °C. The quantity of **6** relative to the internal standard was determined periodically by ^1H NMR after quenching the tube in ice water. All runs

lasted approximately two and one-half 1/2-lives, and the rate constants were calculated as mentioned previously.

Procedure for Trapping 9,10-Phenanthrene o-Quinodimethane (5) with N-Phenylmaleimide (10) and Kinetic Analysis

In preparation for the trapping experiment a modified NMR tube was charged with 0.81 ml of benzene-d_6 which contained 2.55 mg (1.25×10^{-2} mmol) of 1,2-dihydrocyclobuta[*l*]-phenanthrene (**6**), 0.433 mg (3.60×10^{-3} mmol) of the internal standard mesitylene, and 8.18 mg (4.73×10^{-2} mmol) of the trapping agent N-phenylmaleimide (**10**). The N-phenylmaleimide (**10**) was in a 3.8-fold excess relative to **6**. Following two freeze-thaw cycles the modified NMR tube was evacuated to 10^{-2} torr while cooling to -40 °C, and the tube was sealed with a torch. Two more samples were subsequently prepared containing a 4.8- and 7-fold excess of **10** relative to **6**.

After ^{1}H NMR spectra were collected for each of the samples the tubes were immersed in the previously described oil bath at 147 °C. The quantity of **6** relative to the internal standard was determined periodically by ^{1}H NMR after quenching the tubes in pentane. The three runs lasted approximately two and one-half 1/2-lives, and the rate constants were calculated as mentioned previously.

Due to the sublimation of approximately 5% of the solvent during the freeze-thaw cycles, the quantity of standard in the NMR tube as well as the volume of solvent were redetermined at the end of the kinetics run. The quantities of **6** and **10** added to the tube were based on the redetermined quantity of mesitylene.

The yield of the [4 + 2] adduct (**15**) which formed between N-phenylmaleimide **10** and 9,10-phenanthrene *o*-quinodimethane (**5**) was in excess of 95% in each of the three samples as determined by ^{1}H NMR. The adduct was subsequently separated from the kinetics samples by flash column chromatography on silica gel (32% ethyl acetate in hexanes), and the following characterization data collected. Compound **15**: ^{1}H NMR ($CDCl_3$) (Appendix, Figure A-10) δ 8.75-8.66 (m, 2H), 8.25-8.17 (m, 2H), 7.67-7.58 (m, 4H), 7.22-7.16 (m, 3H), 6.76-6.68 (m, 2H), 4.04 (m, 2H), 3.72-3.56 (m, 2H), 3.15 (m, 2H); high-resolution mass spectrum calculated for $C_{26}H_{19}NO$ 377.14158, measured 377.14177.

Analysis of Selected ^{13}C Satellites of 1,2-Dihydrocyclobuta[*l*]phenanthrene (6)

A ^{1}H NMR spectrum of a sample of **6** in benzene-d_6 was collected on the Bruker WM-200. The spinning rate of the tube was adjusted so that the spinning side-bands of the aliphatic proton signal did not overlap with the ^{13}C satellites. The ^{13}C satellites flanking the aliphatic proton signal were the

satellites of interest in this experiment, and they were sufficiently resolved to obtain chemical shifts of each peak in each of the two satellite multiplets (Appendix, Figures 1a and 1b).

Subsequently, these ^{13}C satellites were simulated using Nicolet NT-300 NMR simulation software. The coupling constants of the heteronuclear five-spin system analyzed were based on those for cyclobutene reported in the literature. The chemical shift differences used to simulate the spectrum were also based on values given for the cyclobutene system. After numerous iterations a simulated spectra of the two ^{13}C satellites was obtained in addition to the $^{1}J_{CH}$ value (Appendix, Figure 1c).[50]

REFERENCES

1. Charlton, J. L.; Alauddin M. M. *Tetrahedron*, **1987**, *43*, 2873.
2. Van den Berg, K. J. Ph.D. Dissertation, University of Groningen, The Netherlands, 1990.
3. McCullough, J. J. *Acc. Chem. Res.* **1980**, *13*, 270.
4. Fallis, A. G. *Can. J. Chem.* **1984**, *62*, 183.
5. (a) Cava, M. P.; Napier, D. R. *J. Am. Chem. Soc.* **1957**, *79*, 1701. (b) Cava, M. P.; Deana, A. A.; Muth, K. *J. Am. Chem. Soc.* **1959**, *81*, 6458.
6. Trahanovsky, W. S.; Macias, J. R. *J. Am. Chem. Soc.* **1986**, *108*, 6820.
7. Trahanovsky, W. S.; Chou, C. H.; Fischer, D. R.; Gerstein, B. C. *J. Am. Chem. Soc.* **1988**, *110*, 6579.
8. Macias, J. R. Ph.D. Dissertation, Iowa State University, Ames, Iowa, 1987.
9. Fischer, D. R. Ph.D. Dissertation, Iowa State University, Ames, Iowa, 1990.
10. Dolbier, W. R., Jr.; Kazumasa, M.; Michl, J.; Horak, D. V. *J. Am. Chem. Soc.* **1977**, *99*, 3876.
11. Dolbier, W. R. Jr.; Dulcere, J. P.; Sellers, S. F.; Koroniak, H.; Shatkin, B. T.; Clark, T. L. *J. Org. Chem.* **1982**, *47*, 2298.

12. Roth, W. R.; Biermann, M.; Dekker, H.; Jochems, R.; Mosselman, C.; Hermann, H. *Chem. Ber.* **1978**, *111*, 3892.

13. Roth, W. R.; Scholz, P. *Chem Ber.* **1981**, *114*, 3741.

14. Roth, W. R.; Ebbrecht, T.; Beitat, A. *Chem. Ber.* **1988**, *121*, 1357.

15. Gleicher, G. J.; Newkirk, D. D.; Arnold, J. C. *J. Am. Chem. Soc.*, **1973**, *95*, 2526.

16. Masamune, S.; Kato, M. *J. Am. Chem. Soc.* **1965**, *87*, 4190.

17. Masamune, S.; Kato, M. *J. Am. Chem. Soc.* **1966**, *88*, 610.

18. White, E. H.; Maier, G. E. Graeve, R.; Zirngibl, U.; Friend, E. W. *J. Am. Chem. Soc.* **1966**, *88*, 611.

19. Gardner, P. D.; Sarrafizadeh, R. *J. Am. Chem. Soc.* **1960**, *82*, 4287.

20. Stille, J. K.; Foster, R. T. *J. Org. Chem. Soc.* **1963**, *28*, 2708.

21. Millar, I. T.; Wilson, K. V. *J. Chem. Soc.* **1964**, 2121.

22. Anhlt, J. P.; Friend, E. W.; White, E. H. *J. Org. Chem.* **1972**, *37*, 1015.

23. Cava, M. P.; Mangold, D. *Tetrahedron Lett.* **1964**, *26*, 1751.

24. Hacker, N. P.; McOmie, J. F. W. *Tetrahedron*, **1984**, *40*, 5249.

25. Miyamoto, T.; Tanaka, S.; Odaira, Y. *J. Chem. Soc. Perkin Trans. I*, **1973**, 138.

26. McCulloch, R. K.; Stringer, M. B.; Wege, D. *Aust. J. Chem.*, **1977**, *30*, 1275.

27. Kaupp, G.; Stark, M. *Chem. Ber.* **1977**, *110*, 3084.

28. Kaupp, G.; Stark, M. *Chem. Ber.* **1978**, *111*, 3608.

29. Kaupp, G.; Stark, M. *Chem. Ber.* **1981**, *114*, 2217.

30. Saito, I.; Shimozono, K.; Miyazaki, S.; Matsuura, T. *Tetrahedron Lett.* **1980**, *21*, 2317.

31. Kawamura, Y.; Thurnauer, M.; Schuster, G. B. *Tetrahedron* **1986**, *42*, 6195.

32. Penn, J. H.; Gan, L. X.; Chan, E. Y.; Loesel, P. D. *J. Org. Chem.* **1989**, *54*, 601.

33. Sullivan, W. W.; Ullman, D.; Schechter, H. *Tetrahedron Lett.* **1969**, *6*, 457.

34. Shepherd, M. K. *J. Chem. Soc. Perkin Trans. I*, **1985**, 2689.

35. Viriot, M. L. *J. Chem. Res., Synop.* **1979**, *10*, 324.

36. Moritani, I.; Toshima, N.; Nakagawa, S.; Yakushiji, M. *Bull. Chem. Soc. Jpn.* **1967**, *40*, 2129.

37. Ballester, M.; Castaner, J.; Riera, J.; Armet, O. *J. Org. Chem.* **1986**, *51*, 1100.

38. Laarhoven, W. H.; Cuppen, Th. J. H. M. *J. Chem. Soc. Perkin Trans. I* **1972**, 2074

39. Mueller, E.; Thomas, R.; Zountsas, G. *Liebigs Ann. Chem.* **1972**, *758*, 16.

40. Stringer, M. B.; Wege, D. *J. Am. Chem. Soc.* **1978**, *31*, 1607.

41. Bauld, N. L.; Cessac, J. *J. Am. Chem. Soc.* **1975**, *97*, 2284.

42. Bauld, N. L.; Cessac, J.; Chang, C. S.; Farr, F. R.; Holloway, R. *J. Am. Chem. Soc.* **1977**, *98*, 4561.

43. Miyamoto, T.; Odaira, Y. *Tetrahedron Lett.* **1973**, 43.

44. Rieke, R. D.; White, C. K.; Rhyne, L. D.; Gordon, M. S.; McOmie, J. F. W.; Hacker, N. P. *J. Am. Chem. Soc.* **1977**, *99*, 5387.

45. Abou-Tiem, O.; Hacker, N. P.; Jansen, R. B.; McOmie, J. F. W.; Perry, D. H. *J. Chem. Soc. Perkin Trans. I* **1981**, 988.

46. Hacker, N. P.; McOmie, J. F. W.; Meunier-Piret, J.; Van Meerssche, M. *J. Chem. Soc. Perkin Trans. I* **1982**, 19.

47. Buckland, P. R.; Hacker, N. P. McOmie, J. F. W. *J. Chem. Soc Perkin Trans I* **1983**, 1443.

48. Hacker, N. P.; Turro, N. J. *J. Photochem.* **1983**, *22*, 131.

49. (a) Kalinowski, H. O.; Berger, S. B.; Braun, S. *Carbon-13 NMR Spectroscopy;* John Wiley and Sons: New York, 1988; Chapter 4. (b) Gunther, H.; Jikeli, G.; Schmickler, H.; Prestien, J. *Angew. Chem., Int. Ed. Engl.* **1973**, 12, 762.

50. Hill, E. A.; Roberts, J. D. *J. Am. Chem. Soc.* **1967**, *89*, 2047.

51. Trahanovsky, W. S.; Cassady, T. J.; Woods, T. L. *J. Am. Chem. Soc.* **1981**, *103*, 6691.

52. (a) Espenson, J. H. *Chemical Kinetics and Reaction Mechanisms;* McGraw-Hill: New York, 1981; Chapter 1. (b) Kinetics program provided by J. J. Gajewski and K. Gilbert, SERENA Software, Bloomington, Indiana.

53. Ito, Y.; Nakatsuka, M.; Saegusa, T. J. *J. Am. Soc.*, **1982**, *104*, 7609.

54. Adcock, W. E. *J. Org. Chem.*, **1961**, *26*, 4141.

55. Trahanovsky, W. S., personal communication, Iowa State University, 1990.

56. For examples of N-phenylmaleimide used to effectively trap *o*-quinodimethanes see: (a) Reference 1 in this section. (b) Swenton, J. S. Jurcak, J. G. *J. Org. Chem.* **1988**, *53*, 1530.

57. Klundt, I. R. *Chem. Rev.*, **1970**, *70*, 471.

58. (a) Dewar, M. J. S.; DeLano, C. *J. Am. Chem. Soc.* **1969**, *91*, 789. (b) Baird, N. C. *J. Chem. Educ.*, ***1971***, *48*, 509.

59. Trahanovsky, W. S.; Ong, C. C.; Pataky, J. G.; Weitl, F. L.; Mullen, P. W.; Clardy, J. C.; Hansen, R. S. *J. Org. Chem.* **1971**, *36*, 3575.

60. Cava, M. P.; Deana, A. A.; Muth, K.; Mitchell, M. J. *Organic Synthesis*, J. Wiley and Sons: New York, 1973; Collective Vol. V, p. 944.

APPENDIX

Detailed Description of the Preparation of Trimethyl(10-trimethylsilylmethyl-9-phenanthrylmethyl)ammonium Iodide

N,N-Dimethyl-9-phenanthrenemethylamine

To a 25.0-g (140-mmol) quantity of phenanthrene and a 10.5-g quantity of paraformaldehyde was added glacial acetic acid (30.0 ml), concentrated HCl (40.0 ml), and concentrated H_3PO_4 (15.0 ml).[1,2] The reaction mixture was stirred at 85 °C for 20 h. The mixture was later cooled to room temperature, and the organic product was extracted with a 5:1 ether-pentane solution (3 x 25 ml). The organic phase was washed with water (3 x 25 ml) and saturated $NaHCO_3$ (25 ml) followed by drying ($MgSO_4$) and removal of solvent at reduced pressure to provide an isomeric mixture of chloromethylphenanthrenes. Without further purification the mixture of chloromethylphenanthrenes was combined with 120 ml of dimethylamine, (3 M in methanol), and stirred at 65 °C under nitrogen.[3] After 17.5 h the solution was cooled to room temperature, acidified with 2 N HCl and extracted with ether (3 x 50 ml). The aqueous phase was subsequently basified with 10% NaOH and extracted with toluene (2 x 50 ml) followed by washing the combined toluene extracts with water (50 ml) and brine (50 ml). Reduction of the volume of toluene at reduced pressure resulted in 18.5 g of an oily crystalline material. Recrystallization from ethanol/water

(65/22) gave 7.8 g (0.33 mmol, 24%) of N,N-dimethyl-9-phenanthrenemethylamine: ^{1}H NMR ($CDCl_3$) δ 8.74-8.62 (m, 2H), 8.36-8.30 (m, 1H), 7.88-7.83 (m, 1H), 7.68-7.53 (m, 5H), 3.86 (s, 2H), 2.34(s, 6H).

Trimethyl(10-trimethylsilylmethyl-9-phenanthryl-methyl)ammonium iodide

A 7.8-g (33-mmol) quantity of N,N-dimethyl-9-phenanthrenemethylamine was heated to reflux for 5 h with 4.7 ml (75 mmol) of methyl iodide in 65 ml of absolute ethanol. The iodide salt was subsequently precipitated by addition of a large volume of ether and collected by suction filtration. The product was dried in an evacuated desiccator to yield 12.07 g (32 mmol, 97% yield) of trimethyl(9-phenanthrylmethyl)ammonium iodide.

Trimethyl(9-phenanthrylmethyl)ammonium iodide was converted to 9-methyl-10-dimethylaminomethylphenanthrene through a Sommelet-Hauser rearrangement.[4] A flask was charged with 100 ml of liquid ammonia which was dried by the addition of sodium. A 10-mg (1 crystal) quantity of $FeNO_3$ was added followed by 1.1 g (48 mmol) of sodium in 25-mg portions, and the mixture was stirred for 15 min. Appearance of a black suspension indicated formation of sodium amide. The iodide salt was added gradually over a 10 min interval through a gooch tube and the mixture was stirred for 2 h. Additional liquid

ammonia was distilled into the reaction vessel during this time when necessary. Excess sodium amide was destroyed by the addition of 3.0 g of NH_4Cl, and the liquid ammonia was allowed to boil off while stirring. Following addition of 50 ml of water with a dropping funnel 30 ml of toluene was added, and the organic layer was separated. The water layer was extracted with toluene (2 x 30 ml), washed with brine (2 x 30 ml) and dried ($MgSO_4$). The yield of 9-methyl-10-dimethylaminomethyl-phenanthrene was estimated at 1.95 g (7.8 mmol, 24%) from ^1H NMR analysis of the crude product. Total mass of the crude product was 2.86 g. The yield might be improved by increasing the length of the reaction time. The crude product was subsequently stirred in 50 ml of dry ether (Na) at 0 °C, and 9.2 ml (22.95 mmol) of n-BuLi (2.5 M in hexanes) was added. The mixture was stirred for 18 h followed by cooling to 0 °C and addition of 3.78 ml (29.78 mmol) of chlorotrimethylsilane. The mixture was stirred at room temperature for 24 h followed by quenching with 5 % $NaHCO_3$. After washing with water and drying ($MgSO_4$) the solvent was removed at reduced pressure. The product was distilled by Kughelrohr at 165 °C and 0.03 torr. The yield of 9-trimethylaminomethyl-10-trimethylsilylmethyl-phenanthrene was estimated at 1.53 g (4.7 mmol, 60%) from a ^1H NMR spectrum of a crude product sample. The entire 1.53-g (4.7 mmol) quantity of 9-dimethylaminomethyl-10-trimethylsilylmethylphenanthrene and 1.01 ml (16 mmol)

methyl iodide were heated to reflux in 20 ml of acetonitrile for 6 h followed by addition of a large quantity of ether to precipitate the salt.[5] The product was recrystallized once from acetone and ethyl acetate. Hot filtration was required to remove undissolved polymer. It should be noted that the formation of a small quantity of suspended polymer may be mistaken for undissolved product leading to addition of an excess of solvent. The yield of recrystallized product was 0.26 g (0.56 mmol, 12%): ^{1}H NMR (CD_3CN) δ 8.87-8.81 (m, 2H), 8.35-8.26(m, 2H), 7.84-7.66 (m, 4H), 5.31 (d, J_{AB} = 15 Hz, H_A), 4.98 (d, J_{AB} = 15 Hz, H_B), 3.27 (d, J_{CD} = 15 Hz, H_C), 3.05 (s, 9H), 2.87 (d, J_{CD} = 15 Hz, H_D), -0.11 (s, 9H) [lit. ^{1}H NMR (CD_3CN) δ 8.90-8.71 (m, 2H), 8.49-8.26 (m, 2H), 7.80-7.57 (m, 4H), 5.35 (d, J = 13.3 Hz, 1H), 5.01 (d, J = 13.3 Hz, 1H), 3.25 (d, J = 12.8 Hz, 1H), 3.13 (s, 9H), 2.90 (d, J = 12.8 Hz, 1H), -0.11 (s, 9H)].

APPENDIX REFERENCES

1. Badger, G. M.; Carruthers, W.; Cook, J. W.; Schoental, R. *J. Chem. Soc.* **1949,** 169.
2. Grummitt, O.; Buck, A. *Organic Synthesis;* Wiley: New York, 1955; Collect. Vol. III, p 195.
3. Shah, D. O.; Trivedi, K. N. *Indian J. Chem., Sect. B* **1976,** *12,* 1009.
4. Hauser, C. R.; Brasen, W. R. *Organic Synthesis;* Wiley: New York, 1963; Collect. Vol. IV, p 585.
5. Ito, Y.; Nakatsuka, M.; Saegusa, T. *J. Am. Chem. Soc.* **1982,** *104,* 7609.

Table A-1. Integration data for the interconversion between 1,2-dihydrocyclobuta[*l*]phenanthrene (**6**) and 9,10-phenanthrene *o*-quinodimethane (**5**) at 200 °C, and the ratio of **5**:**6**

Time x 10^{-3}, s	Integration[a,b] **6**	Integration[a,b] **5**	**5**:**6**
0.000	2.12	0.00	0.00
1.085	0.69	0.54	0.78
3.780	0.14	0.19	1.4
5.400	0.10	0.15	1.5
7.110	0.074	0.12	1.6

[a]The range for integration of **5** is 5.372-5.347 ppm and the two signals followed in this range arise from four protons of **5**. The integration range of **6** is 3.076-3.085 ppm, and the signal followed in this range arises from four protons of **6**.

[b]The standard was mesitylene, and its concentration was 1.47 x 10^{-5} M. The tabulated integrations are relative to the signal arising from the protons of the three methyl groups on mesitylene which was set at 1.00.

Table A-2. Rate of disappearance of 1,2-dihydrocyclobuta-[*l*]phenanthrene (**6**) measured at 147 °C in benzene-d_6, to demonstrate the presence of **6** in the pyrolysis product of 10-methyl-9-phenanthryl-methyl benzoate (**11**)[a]

Time x 10^{-4}, s	Integration[b,c]
0.0000	5.30
4.1316	3.83
7.9361	2.27
12.2021	1.03

[a]Rate constant: $k = 1.35 \pm 0.18 \times 10^{-5}$ s^{-1}.

[b]The range for integration is 3.11-3.08 ppm and the signal followed arise from four protons of **6**.

[c]The standard was benzene-d_6, and it was present in a quantity of 0.4% of the total volume of solution,. The tabulated integrations are relative to the proton signal of the standard which was set at 100.

Table A-3. Rate of disappearance of 1,2-dihydrocyclobuta-[*l*]phenanthrene (**6**) in the presence of a 3.8-fold excess of N-phenylmaleimide (**14**). The temperature was 147.0 °C and the solvent was benzene-d_6[a]

Time x 10^{-4}, s	Integration[b,c]
0.0000	1384.3
2.1334	946.2
4.0279	724.9
7.3979	491.9
8.5671	420.1
10.3494	329.2
11.4506	304.0
14.6676	194.3
58.6818	0.0

[a]Rate constant: $k = 1.30 \pm 0.03 \times 10^{-5}$ s^{-1}.

[b]The range for integration is 3.11-3.07 ppm, and the signal followed arises from four protons of **6**.

[c]The standard was mesitylene, and its concentration was 4.4×10^{-3} M. The tabulated integrations are relative to the signal arising from the protons of the three methyl groups on mesitylene which was set at 900.

Table A-4. Rate of disappearance of 1,2-dihydrocyclobuta-[*l*]phenanthrene (**6**) in the presence of a 4.8-fold excess of N-phenylmaleimide (**14**). The temperature was 147.0 °C and the solvent was benzene-d_6[a]

Time x 10^{-4}, s	Integration[b,c]
0.0000	1459.9
2.1334	1165.9
4.0279	866.4
7.3979	595.0
8.5671	491.1
10.3494	369.9
11.4506	359.3
14.6676	207.0
58.6818	0.0

[a]Rate constant: $k = 1.32 \pm 0.04 \times 10^{-5}$ s^{-1}.

[b]The range for integration is 3.11-3.07 ppm, and the signal followed arises from four protons of **6**.

[c]The standard was mesitylene, and its concentration was 4.4×10^{-3} M. The tabulated integrations are relative to the signal arising from the protons of the three methyl groups on mesitylene which was set at 900.

Table A-5. Rate of disappearance of 1,2-dihydrocyclobuta-[*l*]phenanthrene (**6**) in the presence of a 7.0-fold excess of N-phenylmaleimide (**14**). The temperature was 147.0 °C and the solvent was benzene-d_6[a]

Time x 10^{-4}, s	Integration[b,c]
0.0000	1364.0
2.1334	995.6
4.0279	780.1
7.3979	528.3
8.5671	415.8
10.3494	382.6
11.4506	295.5
14.6676	188.9
58.6818	0.0

[a]Rate constant: $k = 1.32 \pm 0.04 \times 10^{-5}$ s^{-1}.

[b]The range for integration is 3.11-3.07 ppm, and the signal followed arises from four protons of **6**.

[c]The standard was mesitylene, and its concentration was 4.3×10^{-3} M. The tabulated integrations are relative to the signal arising from the protons of the three methyl groups on mesitylene which was set at 900.

Table A-6. Rate of disappearance of 1,2-dihydrocyclobuta-[*l*]phenanthrene (**6**) at 162.15 °C in benzene-d_6. First run[a]

Time x 10^{-4} s	Integration[b,c]
0.0000	192.2
0.3212	160.2
0.9967	110.6
1.3644	93.6
1.7382	75.4
2.1061	61.3
2.4406	47.7
2.7547	40.0
3.0754	34.5
45.5974	0.0

[a]Rate constant: $k = 5.64 \pm 0.09 \times 10^{-5}\ s^{-1}$.

[b]The range for integration is approximately 3.15-3.00 ppm, and the signal followed arises from four protons of **6**. Though the range varies slightly between runs, it was held constant in each run.

[c]The standard was diphenylmethane, and its concentration was 2.5×10^{-2} M. The tabulated integrations are relative to the methylene singlet which was set at 200.

Table A-7. Rate of disappearance of 1,2-dihydrocyclobuta-[*l*]phenanthrene (**6**) at 162.15 °C in benzene-d_6. Second run[a]

Time x 10^{-4}, s	Integration[b,c]
0.0000	196.6
0.3212	163.0
0.9967	111.3
1.3644	90.2
1.7382	73.4
2.1061	59.1
2.4406	48.7
2.7547	40.3
3.0754	33.5
45.5974	0.0

[a]Rate constant: $k = 5.74 \pm 0.02 \times 10^{-5}$ s^{-1}.

[b]The range for integration is approximately 3.15-3.00 ppm, and the signal followed arises from four protons of **6**. Though the range varies slightly between runs, it was held constant in each run.

[c]The standard was diphenylmethane, and its concentration was 2.9×10^{-2} M. The tabulated integrations are relative to the methylene singlet which was set at 200.

Table A-8. Rate of disappearance of 1,2-dihydrocyclobuta-[*l*]phenanthrene (**6**) at 162.15 °C in benzene-d_6. Third run[a]

Time x 10^{-4}, s	Integration[b,c]
0.0000	193.3
0.3212	163.9
0.9967	108.2
1.3644	91.7
1.7382	75.4
2.1061	56.5
2.4406	50.4
2.7547	42.2
3.0754	37.2
45.5974	0

[a]Rate constant: $k = 5.48 \pm 0.11 \times 10^{-5}$ s^{-1}.

[b]The range for integration is approximately 3.15-3.00 ppm, and the signal followed arises from four protons of **6**. Though the range varies slightly between runs, it was held constant in each run.

[c]The standard was diphenylmethane, and its concentration was 1.3×10^{-2} M. The tabulated integrations are relative to the methylene singlet which was set at 200.

Table A-9. Rate of disappearance of 1,2-dihydrocyclobuta-[*l*]phenanthrene (**6**) at 146.95 °C in benzene-d_6. First run[a]

Time x 10^{-4}, s	Integration[b,c]
0.0000	70.9
2.6639	50.3
3.7133	43.9
4.6418	38.2
6.4765	31.3
7.3051	28.7
8.9542	22.3
10.0122	19.0
11.0245	17.9
11.8091	15.3
13.5746	12.2
14.6698	11.4
67.1398	0.0

[a]Rate constant: $k = 1.27 \pm 0.02 \times 10^{-5}$ s^{-1}.

[b]The range for integration is approximately 3.15-3.00 ppm, and the signal followed arises from four protons of **6**. Though the range varies slightly between runs, it was held constant in each run.

[c]The standard was mesitylene, and its concentration was 2.8×10^{-2} M. The tabulated integrations are relative to the signal arising from the protons of the three methyl groups on mesitylene which was set at 300.

Table A-10. Rate of disappearance of 1,2-dihydrocyclobuta-[*l*]phenanthrene (**6**) at 146.95 °C in benzene-d_6. Second run[a]

Time x 10^{-4}, s	Integration[b,c]
0.0000	252.9
1.2690	220.0
2.5411	185.6
5.4409	127.5
6.9461	103.8
8.2509	87.9
9.0057	81.8
12.0248	55.2
14.5390	36.9
15.8061	33.3
68.2761	0.0

[a]Rate constant: $k = 1.30 \pm 0.01 \times 10^{-5}$ s^{-1}.

[b]The range for integration is approximately 3.15-3.00 ppm, and the signal followed arises from four protons of **6**. Though the range varies slightly between runs, it was held constant in each run.

[c]The standard was mesitylene, and its concentration was 7.3×10^{-2} M. The tabulated integrations are relative to the signal arising from the protons of the three methyl groups on mesitylene which was set at 300.

Table A-11. Rate of disappearance of 1,2-dihydrocyclobuta-[*l*]phenanthrene (**6**) at 146.95 °C in benzene-d_6. Third run[a]

Time x 10^{-4}, s	Integration[b,c]
0.0000	269.3
1.2690	221.2
2.5411	205.2
5.4409	133.4
6.9461	111.6
8.2509	90.3
9.0057	82.9
12.0248	54.0
14.5390	38.4
15.8061	33.8
68.2761	0.0

[a]Rate constant: $k = 1.33 \pm 0.02 \times 10^{-5}\ s^{-1}$.

[b]The range for integration is approximately 3.15-3.00 ppm, and the signal followed arises from four protons of **6**. Though the range varies slightly between runs, it was held constant in each run.

[c]The standard was mesitylene, and its concentration was 7.7×10^{-2} M. The tabulated integrations are relative to the signal arising from the protons of the three methyl groups on mesitylene which was set at 300.

Table A-12. Rate of disappearance of 1,2-dihydrocyclobuta-[*l*]phenanthrene (**6**) at 131.95 °C in benzene-d_6. First run[a]

Time x 10^{-4}, s	Integration[b,c]
0.0000	274.4
4.2387	245.5
12.5977	196.4
15.9315	183.4
24.3420	128.0
28.7306	120.3
41.0036	87.8
47.7966	72.6
54.3182	62.8
254.0342	0.0

[a]Rate constant: $k = 2.77 \pm 0.07 \times 10^{-6}$ s^{-1}.

[b]The range for integration is approximately 3.15-3.00 ppm, and the signal followed arises from four protons of **6**. Though the range varies slightly between runs, it was held constant in each run.

[c]The standard was mesitylene, and its concentration was 7.2×10^{-2} M. The tabulated integrations are relative to the signal arising from the protons of the three methyl groups on mesitylene which was set at 300.

Table A-13. Rate of disappearance of 1,2-dihydrocyclobuta-[*l*]phenanthrene (**6**) at 131.95 °C in benzene-d_6. Second run[a]

Time x 10^{-4}, s	Integration[b,c]
0.0000	256.7
4.2387	221.2
12.5977	174.3
15.9315	161.0
24.3420	113.8
28.7306	108.3
41.0036	81.1
47.7966	66.5
54.3182	54.4
254.0342	0.0

[a]Rate constant: $k = 2.80 \pm 0.08 \times 10^{-6}\ s^{-1}$.

[b]The range for integration is approximately 3.15-3.00 ppm, and the signal followed arises from four protons of **6**. Though the range varies slightly between runs, it was held constant in each run.

[c]The standard was mesitylene, and its concentration was 7.4×10^{-3} M. The tabulated integrations are relative to the signal arising from the protons of the three methyl groups on mesitylene which was set at 300.

Table A-14. Rate of disappearance of 1,2-dihydrocyclobuta-[*l*]phenanthrene (**6**) at 131.95 °C in benzene-d_6. Third run[a]

Time x 10^{-4}, s	Integration[b,c]
0.0000	332.6
4.2387	300.5
12.5977	240.3
15.9315	213.3
24.3420	154.0
28.7306	152.8
41.0036	98.9
47.7966	86.6
54.3182	71.3
254.0342	0.0

[a]Rate constant: $k = 2.88 \pm 0.07 \times 10^{-6}$ s^{-1}.

[b]The range for integration is approximately 3.15-3.00 ppm, and the signal followed arises from four protons of **6**. Though the range varies slightly between runs, it was held constant in each run.

[c]The standard was mesitylene, and its concentration was 5.7×10^{-3} M. The tabulated integrations are relative to the signal arising from the protons of the three methyl groups on mesitylene which was set at 300.

Figure A-1. ^{13}C satellite analysis of the aliphatic proton peak arising from 1,2-dihydrocyclobuta[*l*]-phenanthrene (**6**). a) 1H NMR of **6** in benzene-d_6. b) Expansion of (a) such that the ^{13}C satellites are visible. c) Simulation of the ^{13}C satellites obtained after several iterations using Nicolet NT-300 NMR simulation software

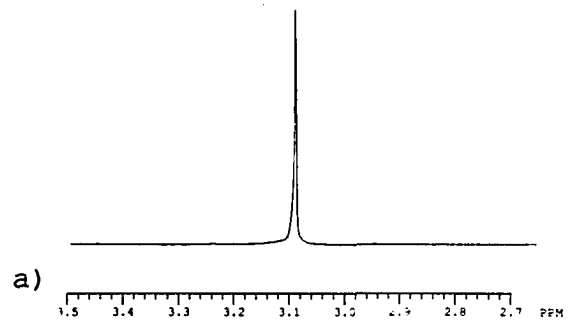
a)
3.5 3.4 3.3 3.2 3.1 3.0 2.9 2.8 2.7 PPM

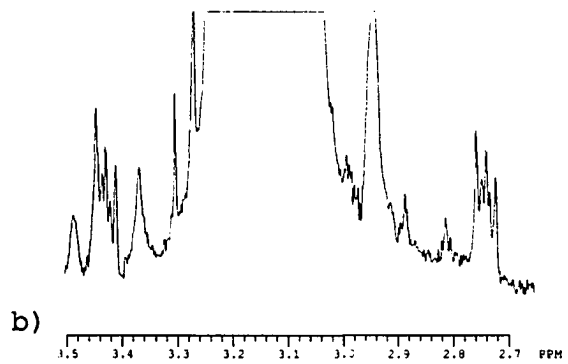
b)
3.5 3.4 3.3 3.2 3.1 3.0 2.9 2.8 2.7 PPM

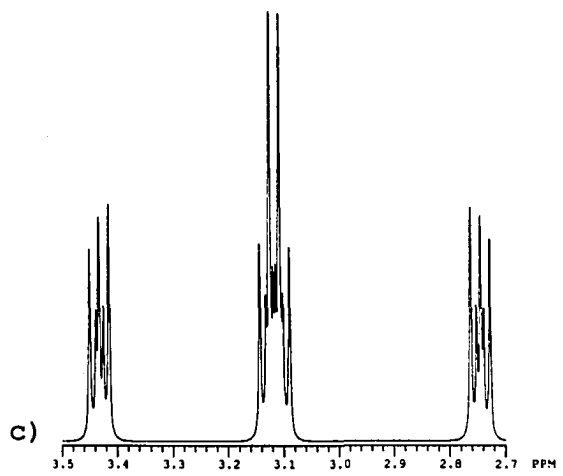
c)
3.5 3.4 3.3 3.2 3.1 3.0 2.9 2.8 2.7 PPM

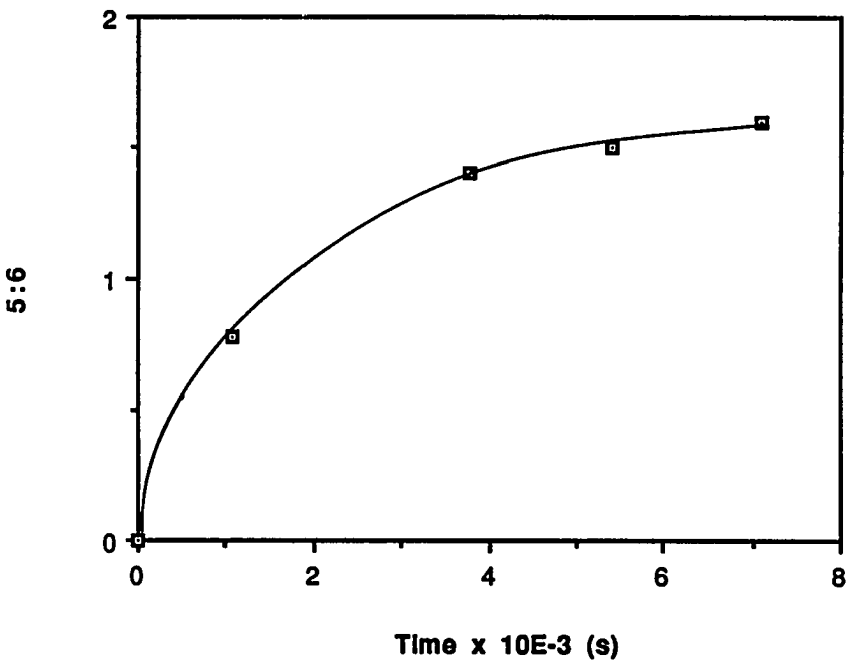

Figure A-2. Plot of the ratio of 9,10-phenanthrene *o*-quinodimethane (**5**): 1,2-dihydrocyclobuta-[*l*]phenanthrene (**6**) with respect to time. Data are from Table A-1

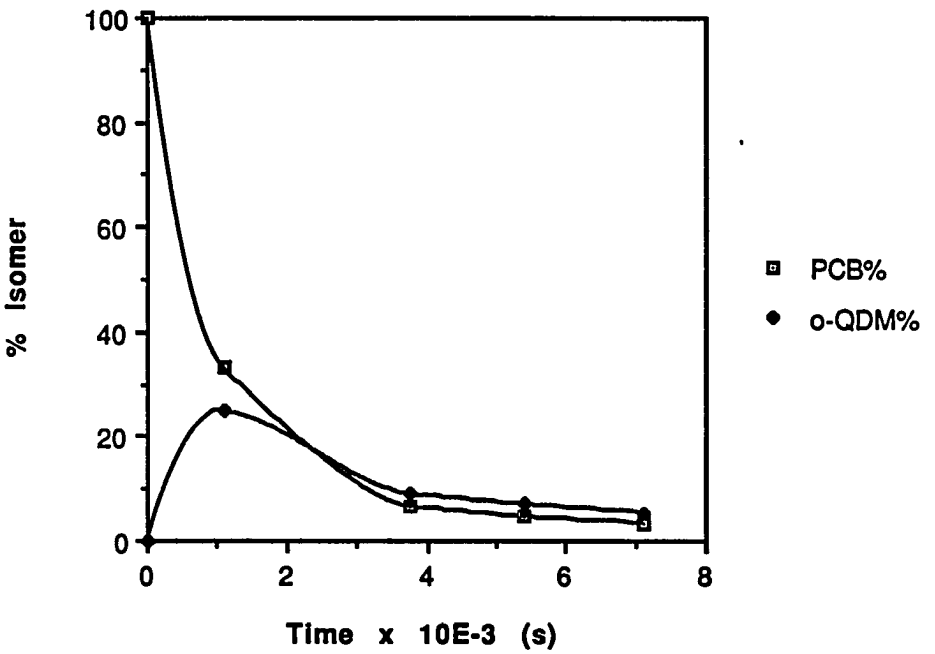

Figure A-3. Plot of the percent of 9,10-phenanthrene *o*-quinodimethane (**5**) and 1,2-dihydrocyclobuta-[*l*]phenanthrene (**6**), relative to the initial quantity of **6**, with respect to time (PCB = **6**, *o*-QDM = **5**). Data are from Table A-1

Figure A-4. ^{1}H NMR spectrum of 1,2-dihydrocyclobuta[*l*]phenanthrene (**6**) in benzene-d_6

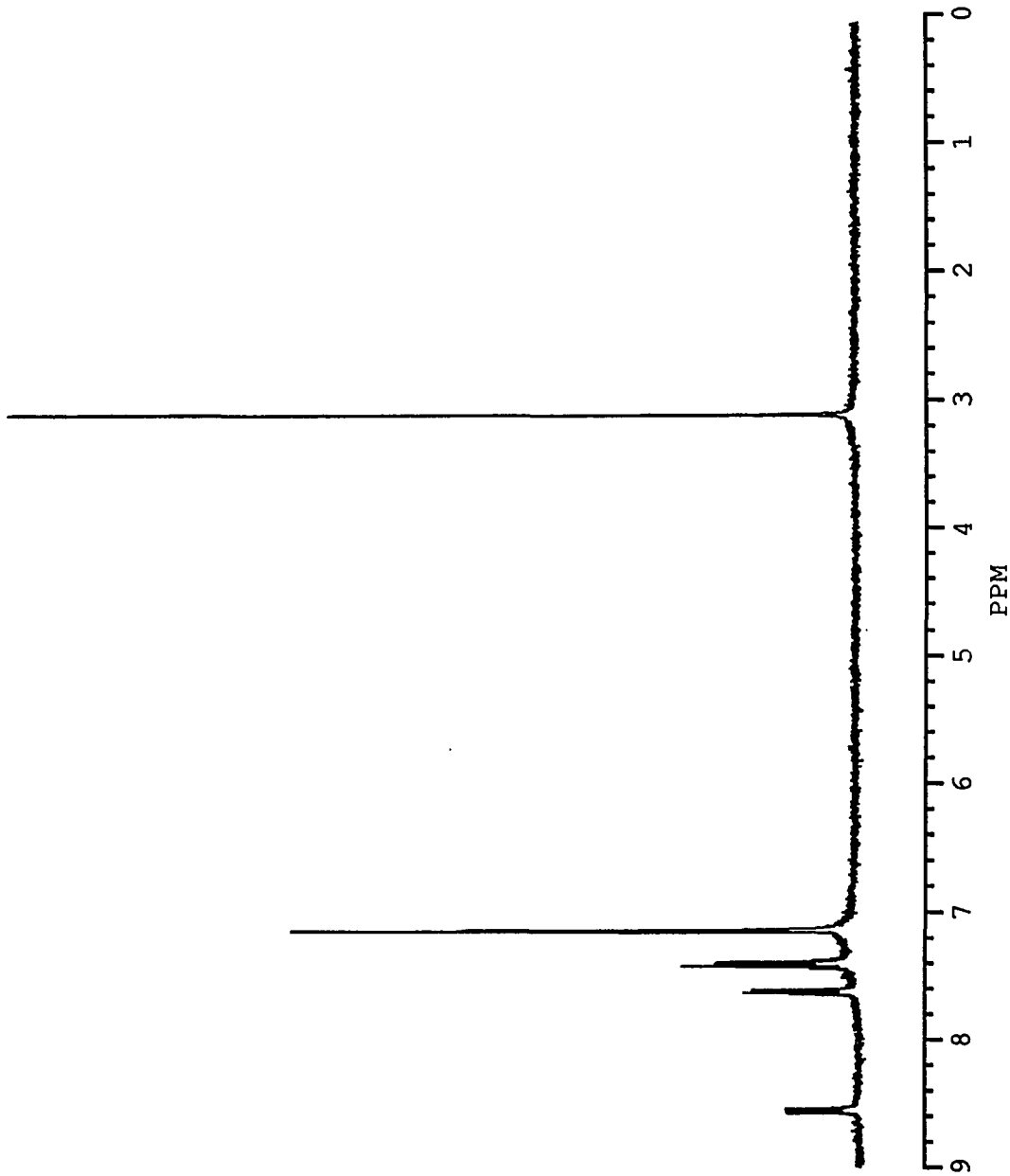
0
1
2
3
4
5
6
7
8
9
PPM

Figure A-5. ^{1}H NMR spectrum of 10-methyl-9-phenanthrylmethyl benzoate (**11**) in $CDCl_3$

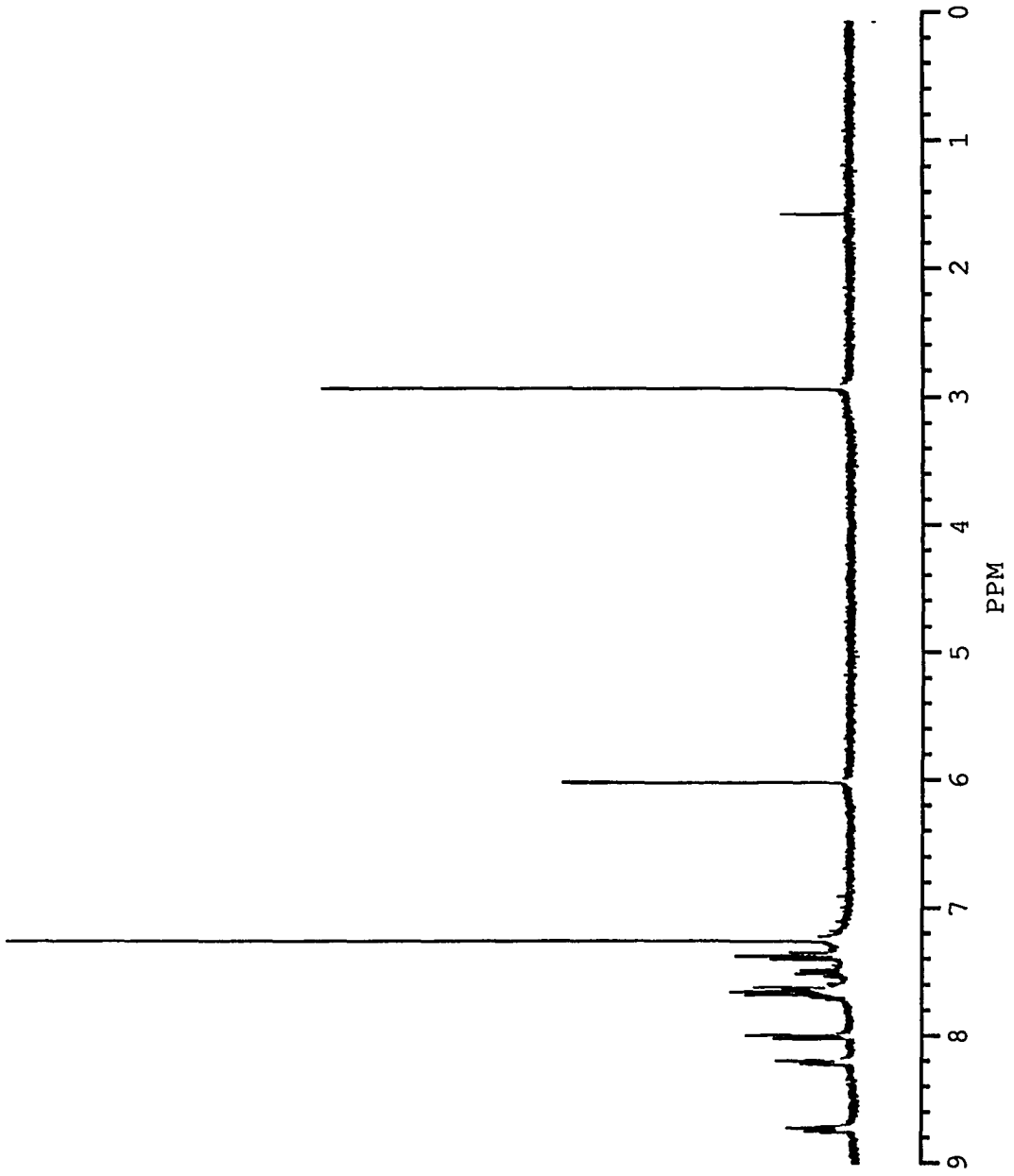
9
8
7
6
5
4
3
2
1
0
PPM

Figure A-6. ^{1}H NMR spectrum of the pyrolysate from 1,2-dihydrocyclobuta[*l*]phenanthrene (**6**) in 1:1 CS_2/C_6D_6

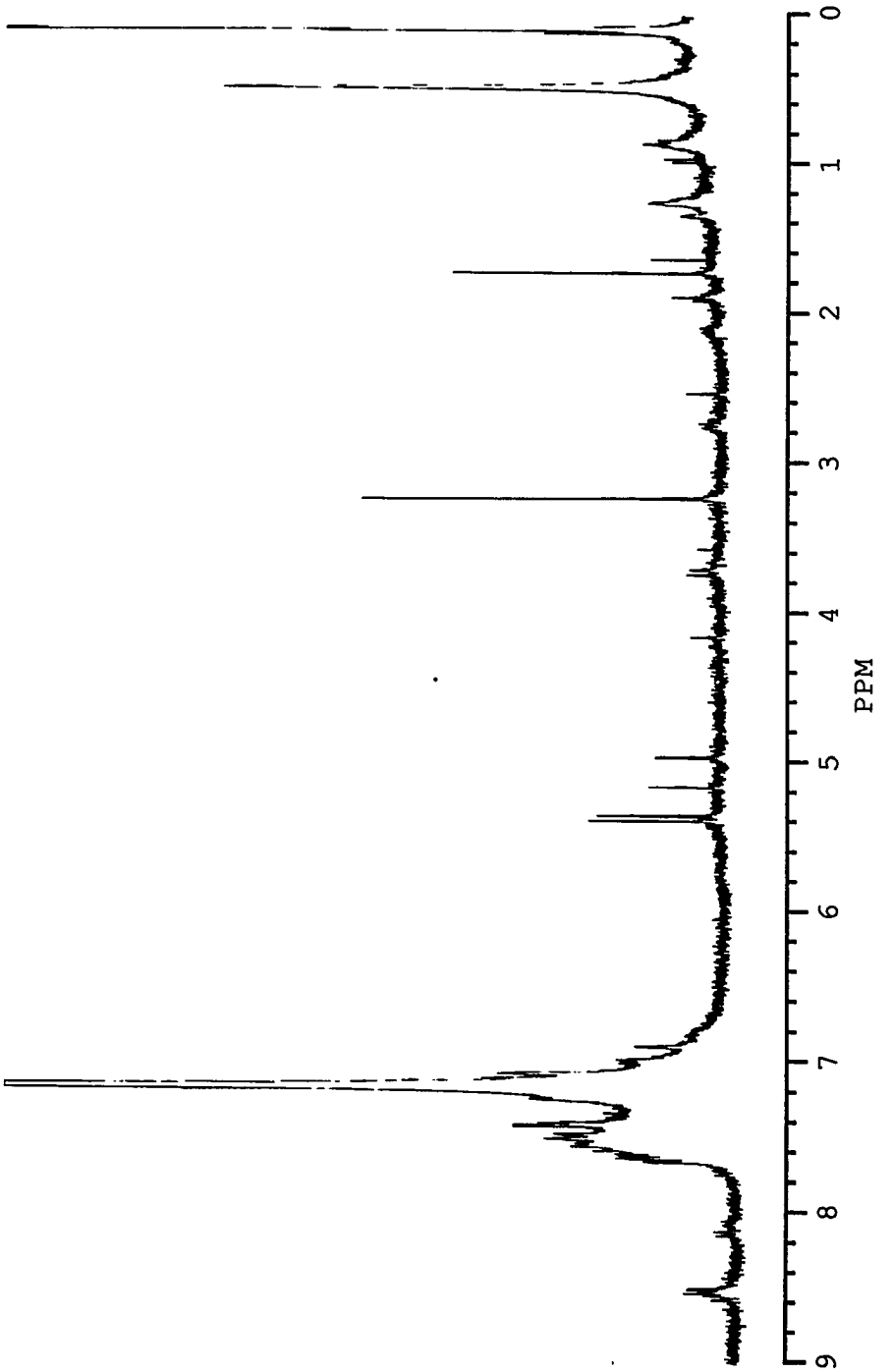
0
1
2
3
4
5
6
7
8
9
PPM

Figure A-7. ^{1}H NMR spectrum of 9,10-phenanthrene *o*-quinodimethane **(5)** in 1:1 CD_3CN/C_6D_6

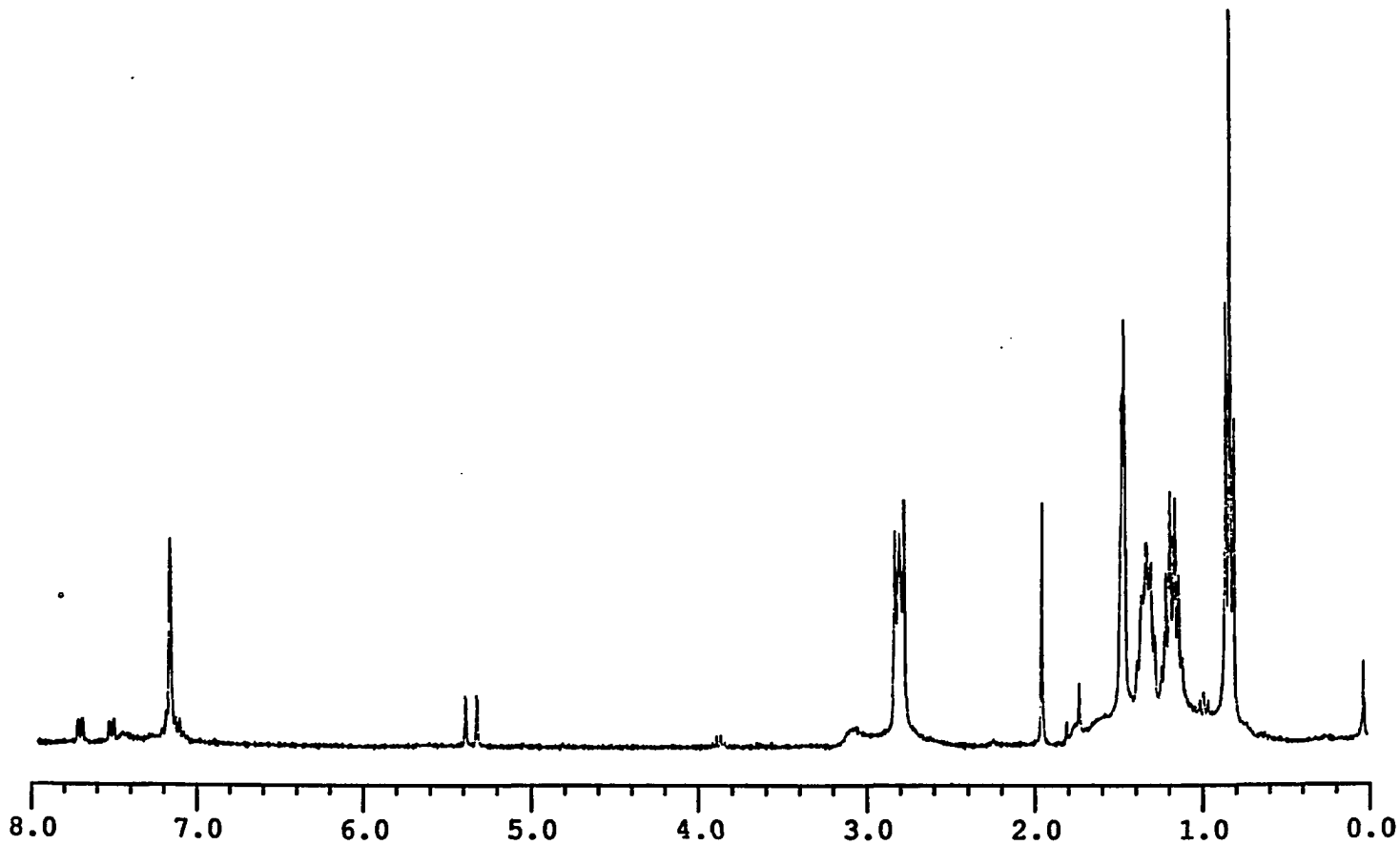
8.0
7.0
6.0
5.0
4.0
3.0
2.0
1.0
0.0

Figure A-8. ^{1}H NMR spectrum of the pyrolysate from 10-methyl-9-phenanthrylmethyl acetate **(10)** in 1:1 $CS_2/CDCl_3$

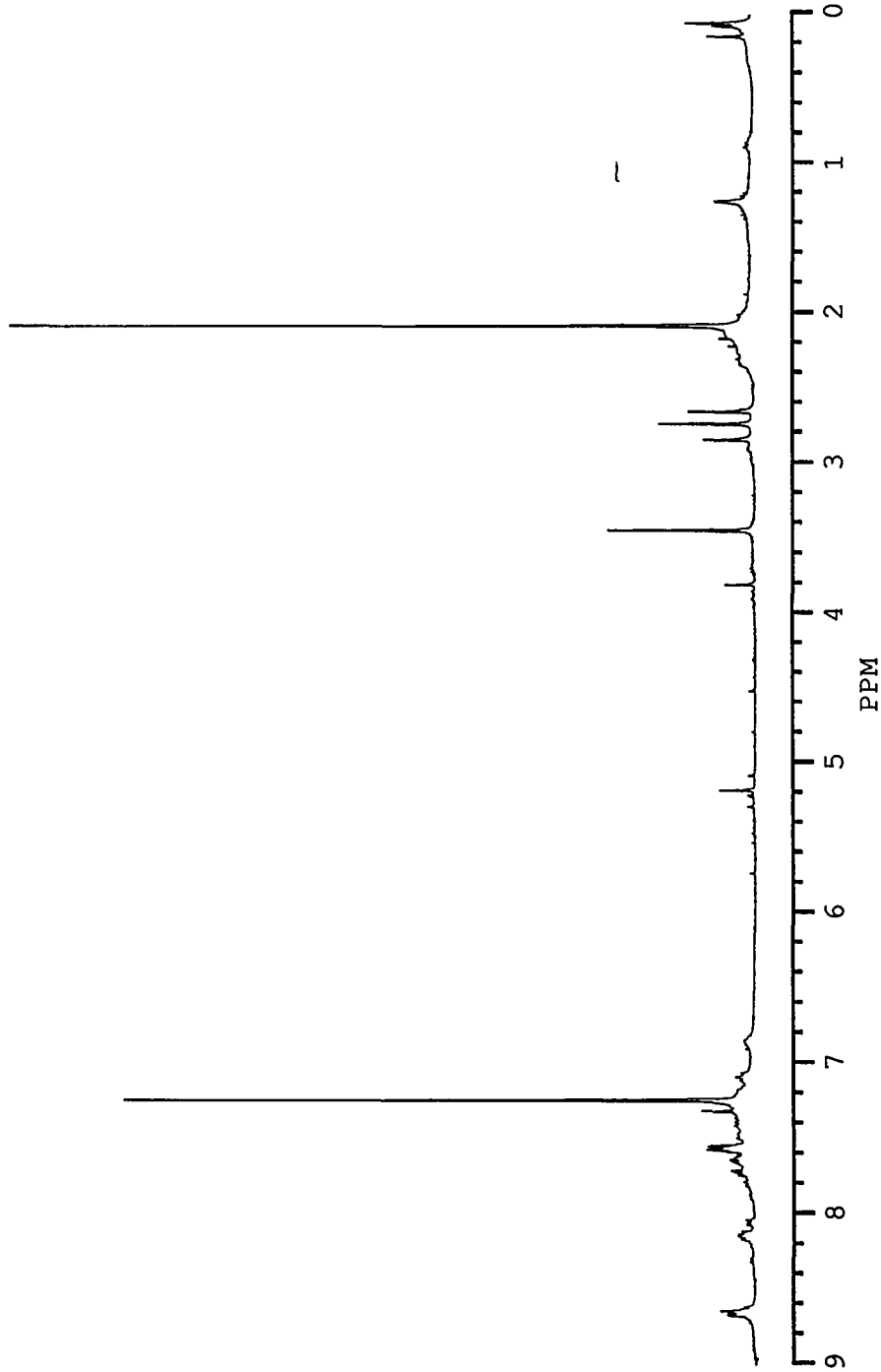
0
1
2
3
4
5
6
7
8
9
PPM

Figure A-9. ^{1}H NMR spectrum of the pyrolysate from 10-methyl-9-phenanthrylmethyl benzoate (**11**) in 1:1 $CS_2/CDCl_3$

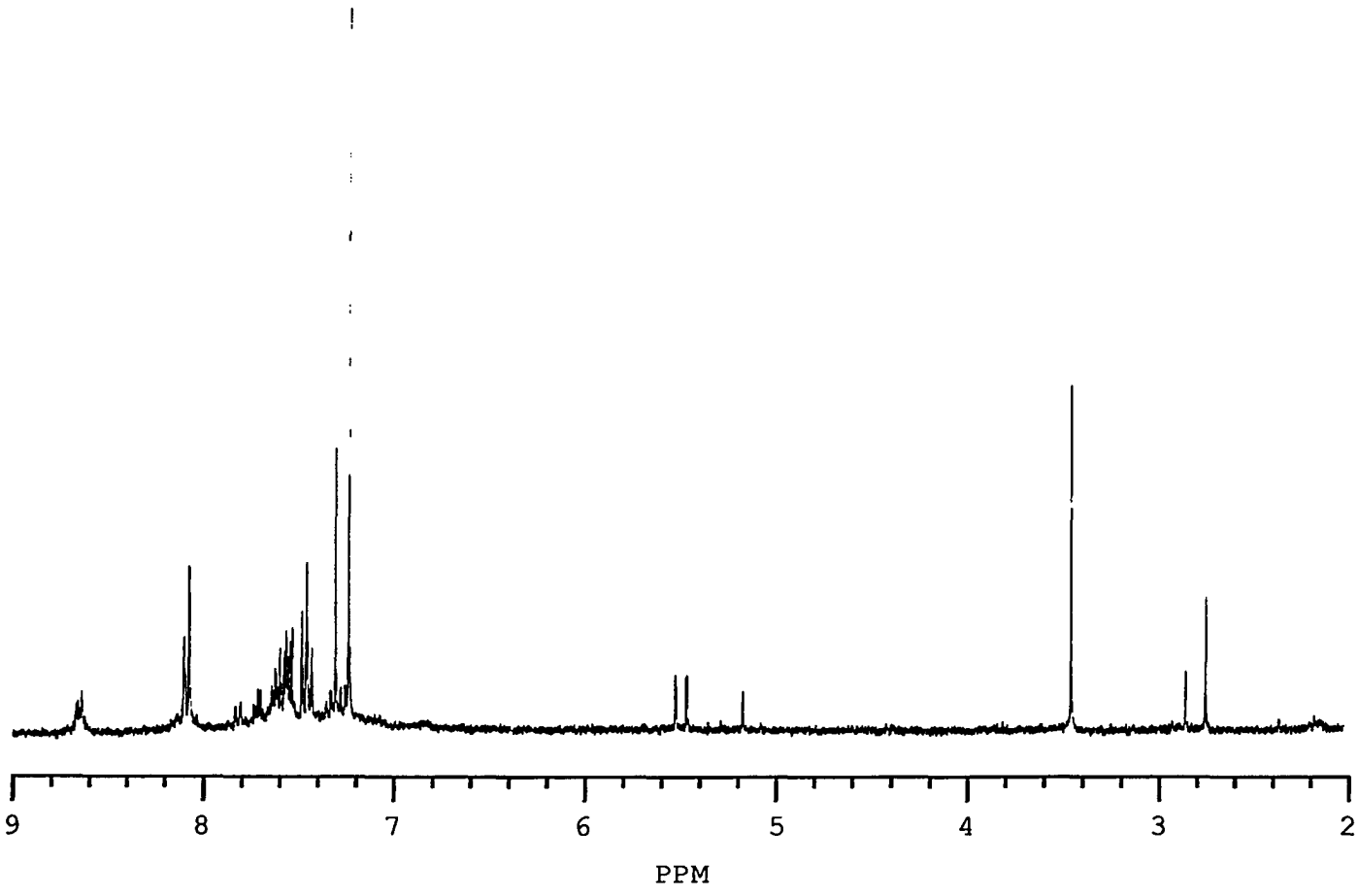
9
8
7
6
5
4
3
2
PPM

Figure A-10. ^{1}H NMR spectrum of the [4+2] adduct **(15)** arising from 9,10-phenanthrene *o*-quinodimethane **(5)** and N-phenylmaleimide **(14)** in $CDCl_3$

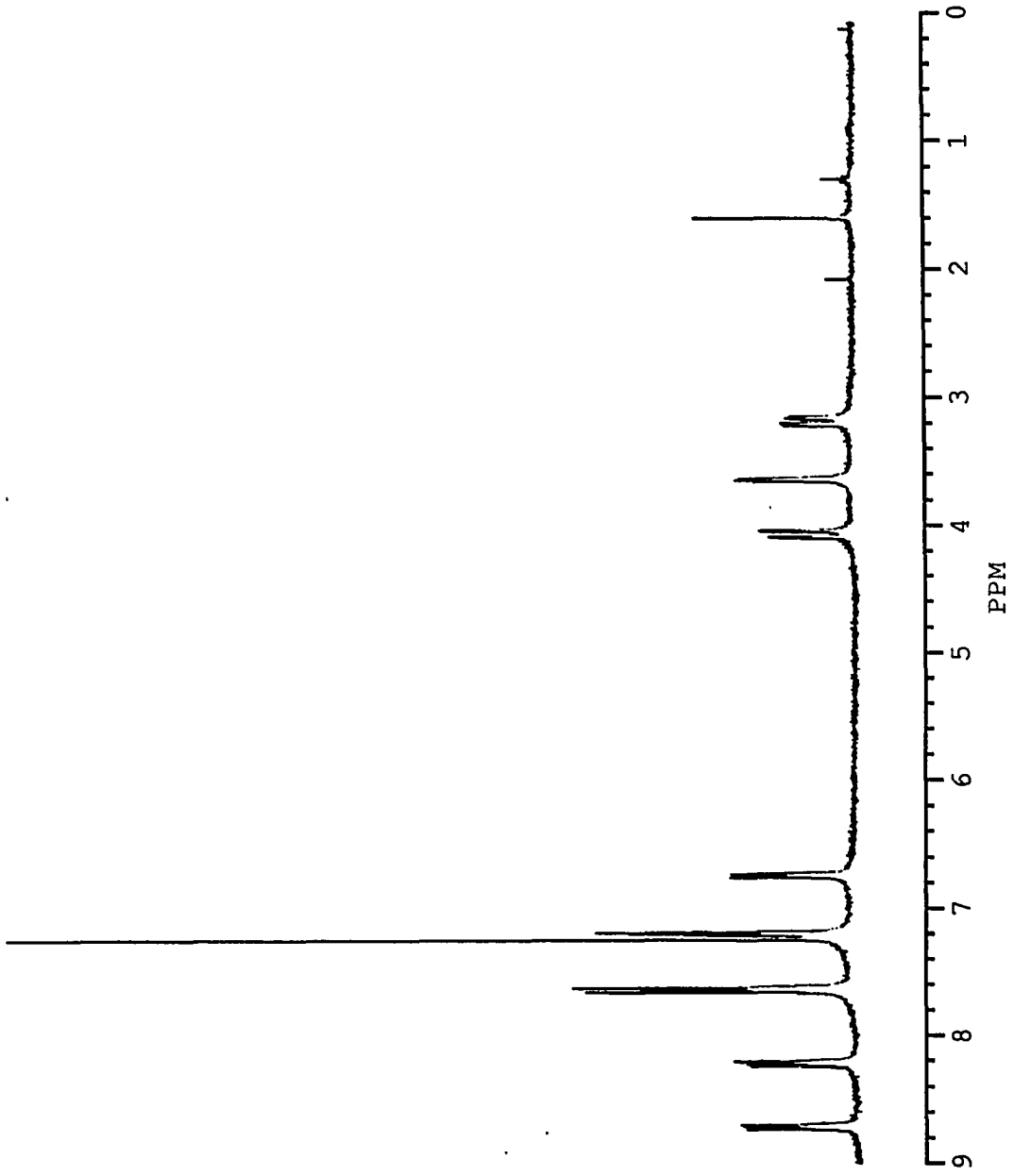
9
8
7
6
5
4
3
2
1
0
PPM

Figure A-11. Decoupled ^{13}C NMR spectrum of 1,2-dihydrocyclobuta[*l*]phenanthrene (**6**) in $CDCl_3$

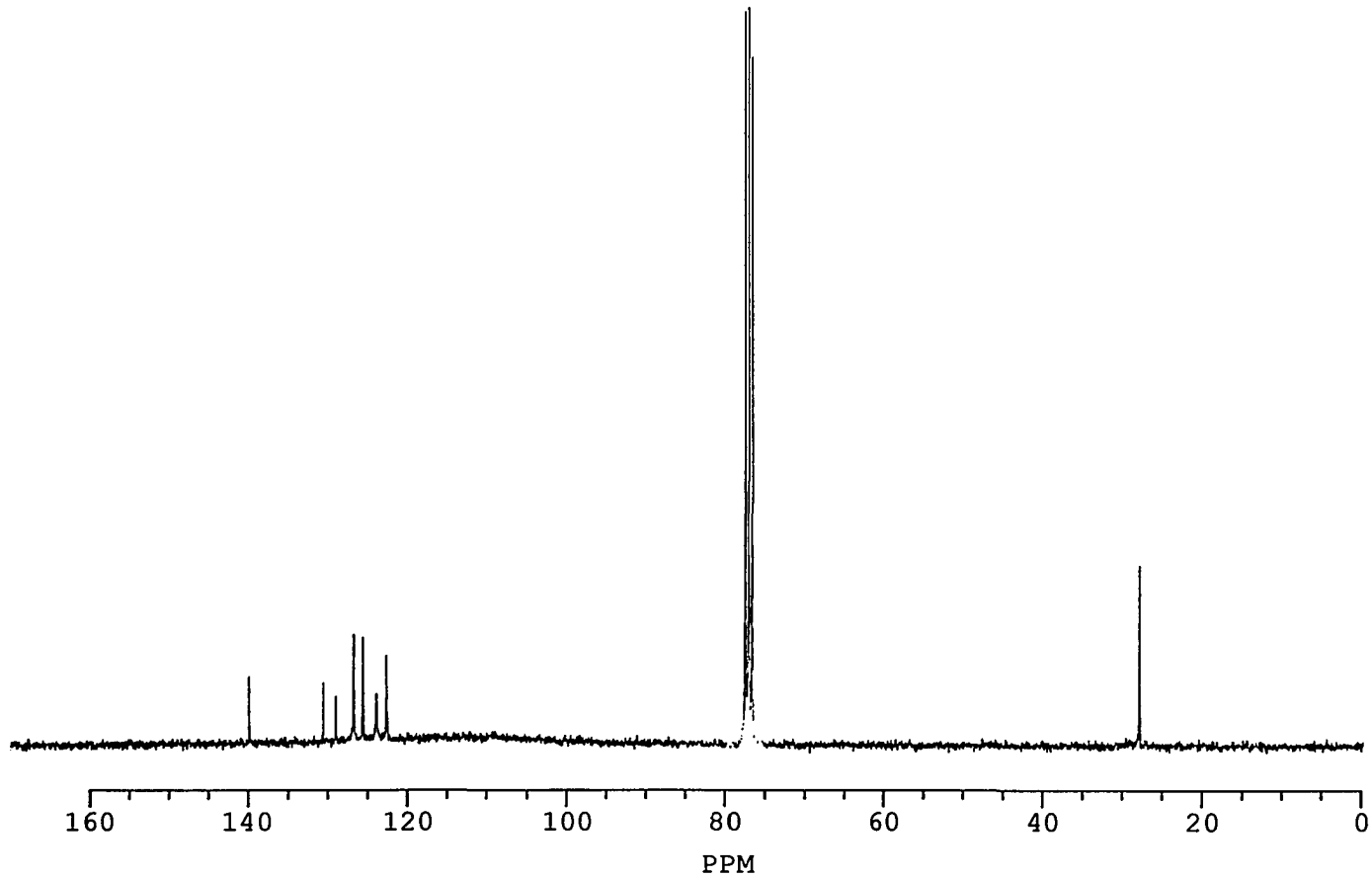
160
140
120
100
80
60
40
20
0
PPM

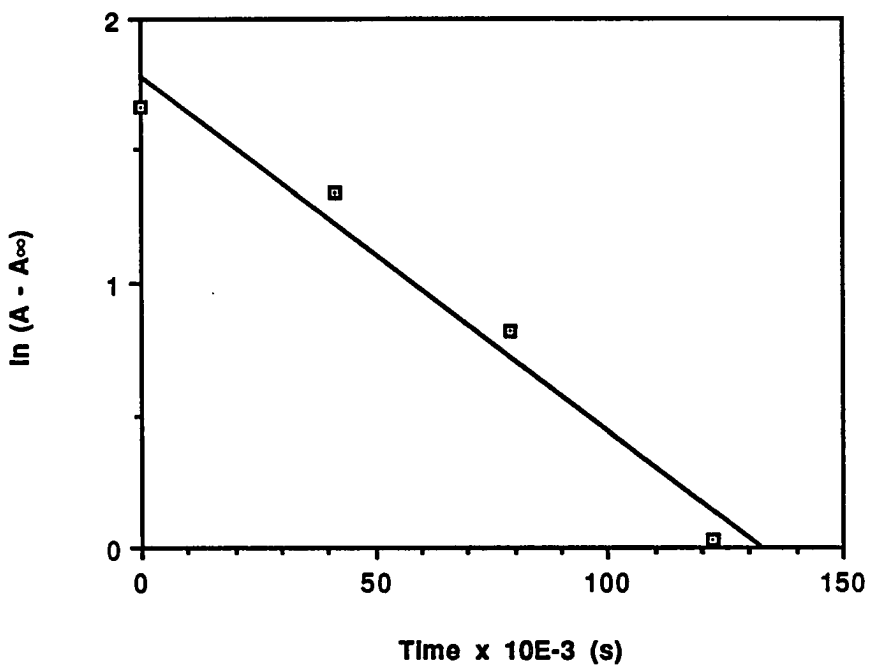

Figure A-12. Plot of the ratio of $(A - A_{\infty})$ vs. time at 147.0 °C. Data were obtained from Table A-2 and represent the disappearance of 1,2-dihydrocyclobuta[*l*]phenanthrene (**6**). The rate constant derived from the line is $k = 1.35 \pm 0.18 \times 10^{-5}\ s^{-1}$

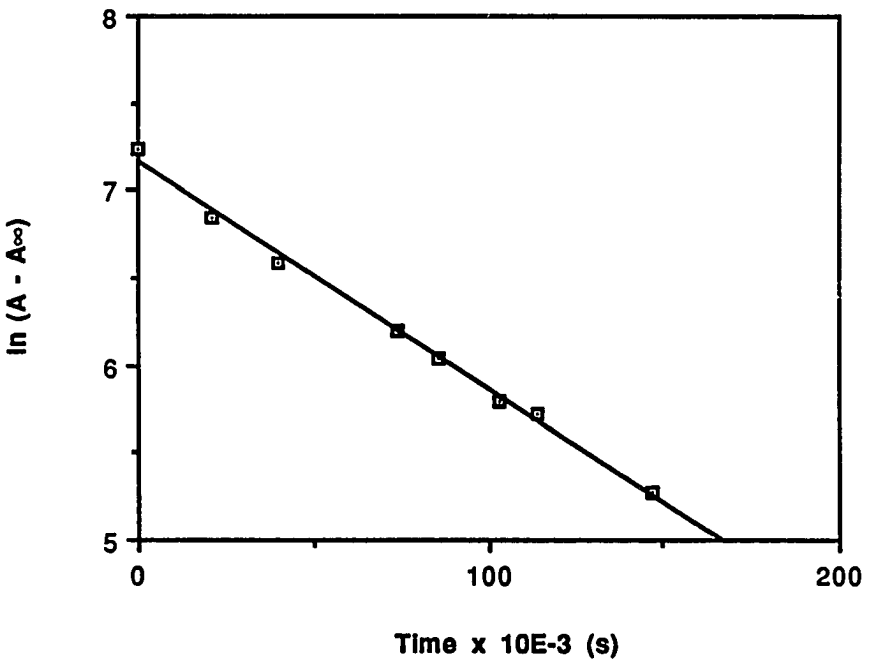

Figure A-13. Plot of ln (A - A_∞) vs. time at 147.0 °C. Data were obtained from Table A-3 and represent the disappearance of 1,2-dihydrocyclobuta[*l*]phenanthrene (**6**). The rate constant derived from the line is k = 1.30 ± 0.03 x 10^{-5} s^{-1}

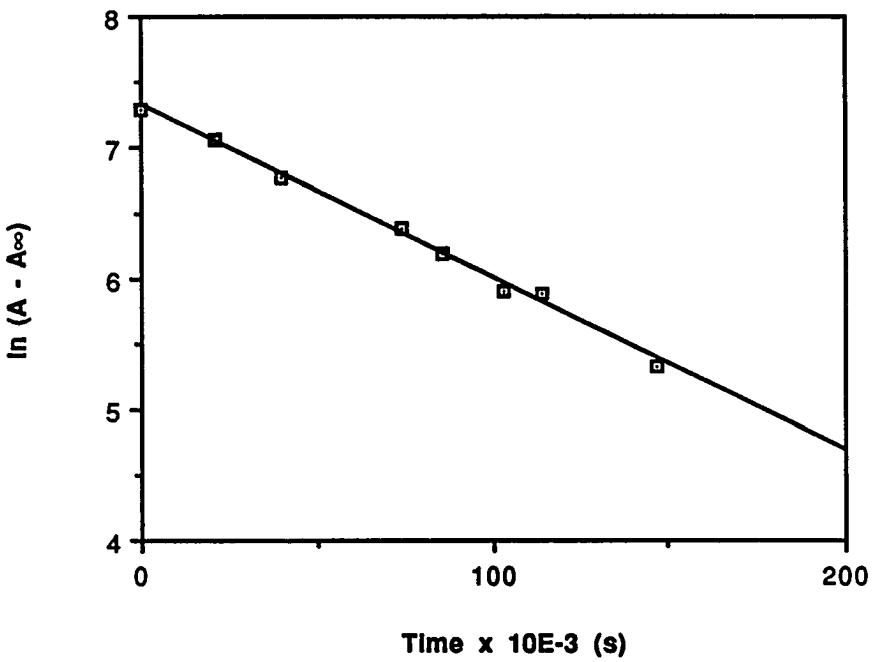

Figure A-14. Plot of ln ($A - A_\infty$) vs. time at 147.0 °C. Data were obtained from Table A-4 and represent the disappearance of 1,2-dihydrocyclobuta[*l*]phenanthrene (**6**). The rate constant derived from the line is $k = 1.32 \pm 0.04 \times 10^{-5}\ s^{-1}$

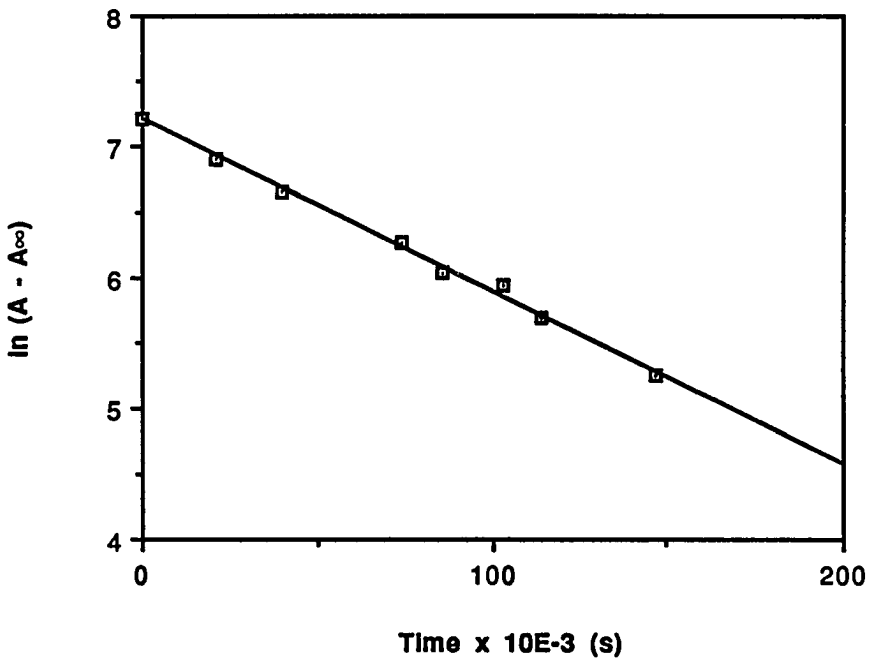

Figure A-15. Plot of ln (A - A_∞) vs. time at 147.0 °C. Data were obtained from Table A-5 and represent the disappearance of 1,2-dihydrocyclobuta[*l*]phenanthrene (**6**). The rate constant derived from the line is k = 1.32 ± 0.04 x 10^{-5} s^{-1}

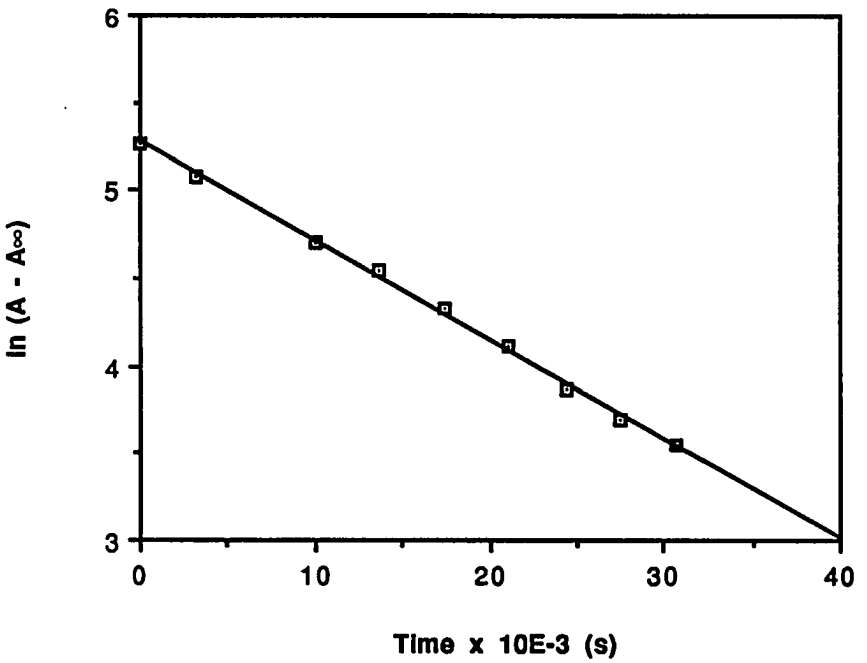

Figure A-16. Plot of ln ($A - A_\infty$) vs. time at 162.15 °C. Data were obtained from Table A-6 and represent the disappearance of 1,2-dihydrocyclobuta[*l*]phenanthrene (**6**). The rate constant derived from the line is $k = 5.64 \pm 0.09 \times 10^{-5}\ s^{-1}$

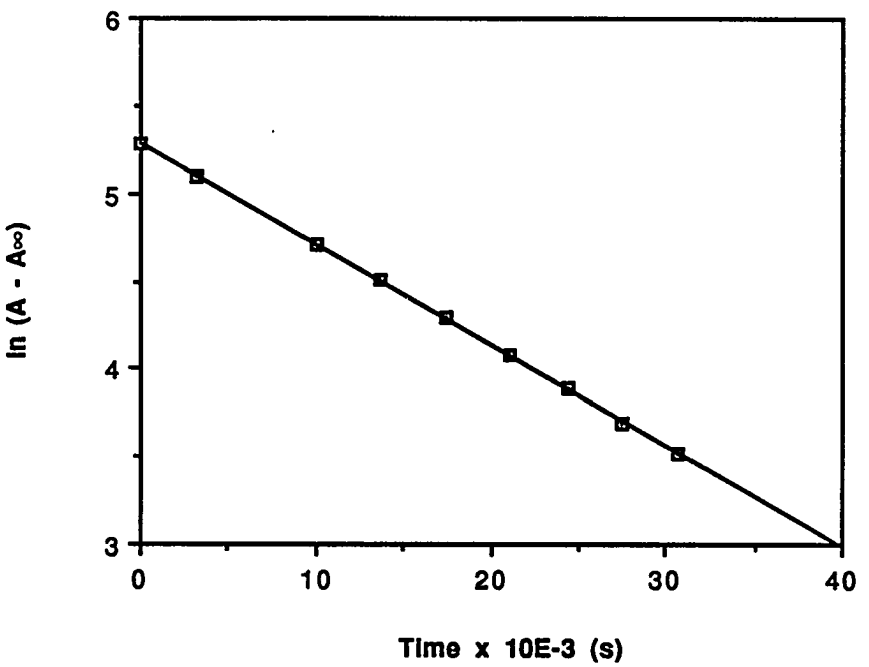

Figure A-17. Plot of ln ($A - A_\infty$) vs. time at 162.15 °C. Data were obtained from Table A-7 and represent the disappearance of 1,2-dihydrocyclobuta[*l*]phenanthrene (**6**). The rate constant derived from the line is $k = 5.74 \pm 0.02 \times 10^{-5}\ s^{-1}$

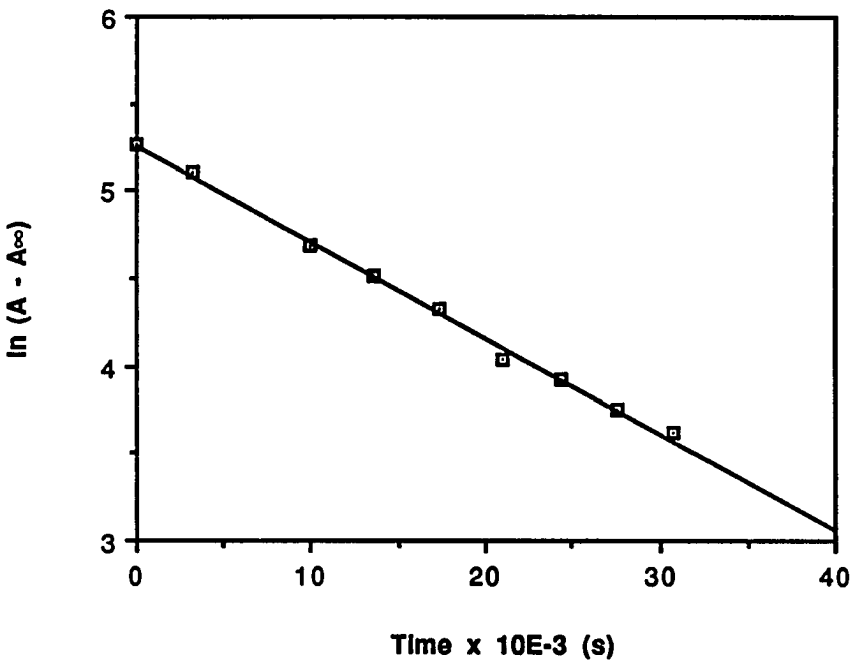

Figure A-18. Plot of ln (A - A_∞) vs. time at 162.15 °C. Data were obtained from Table A-8 and represent the disappearance of 1,2-dihydrocyclobuta[*l*]phenanthrene (**6**). The rate constant derived from the line is k = 5.48 ± 0.11 x 10^{-5} s^{-1}

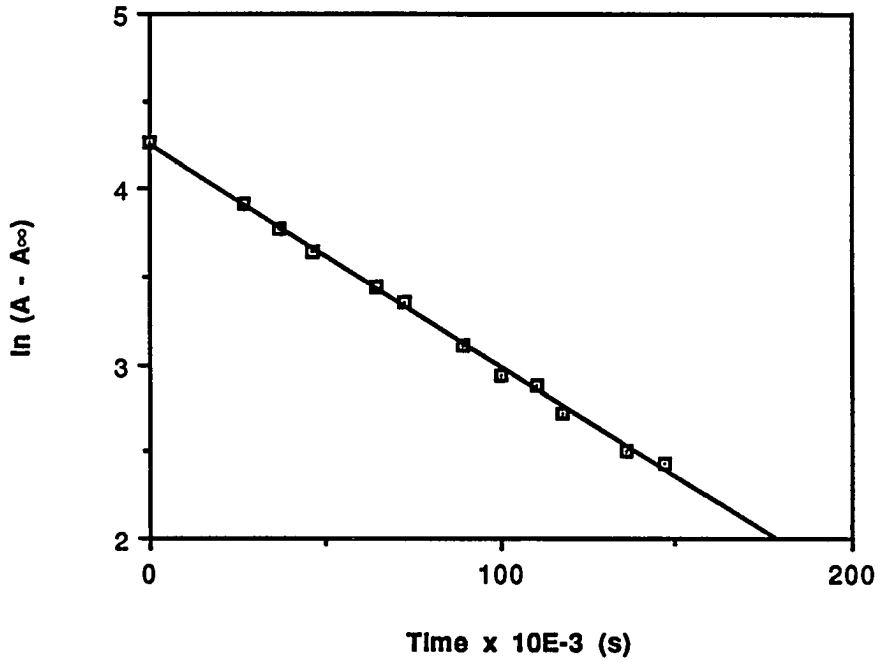

Figure A-19. Plot of ln (A - A_∞) vs. time at 146.95 °C. Data were obtained from Table A-9 and represent the disappearance of 1,2-dihydrocyclobuta[*l*]phenanthrene (**6**). The rate constant derived from the line is k = 1.27 ± 0.02 x 10^{-5} s^{-1}

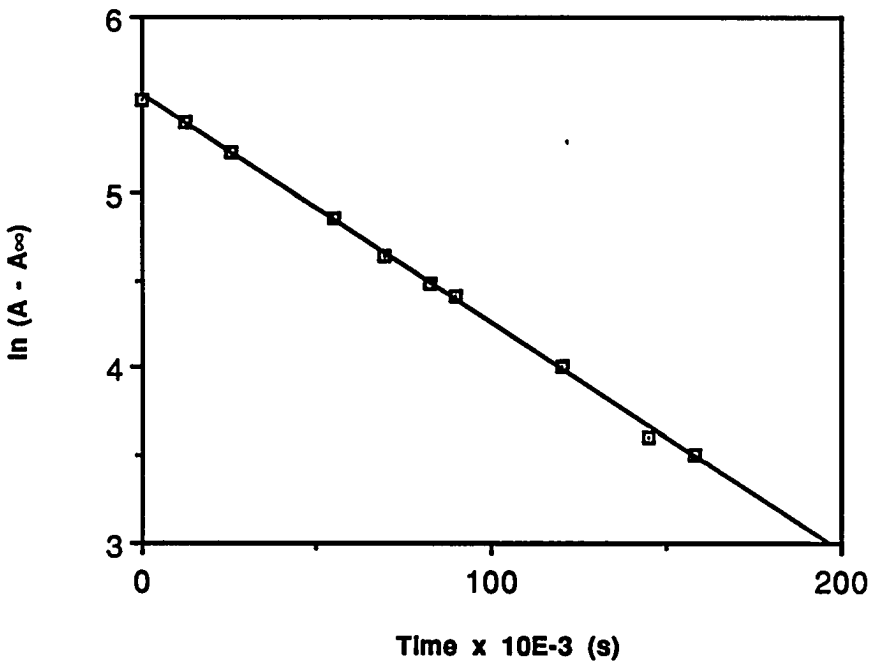

Figure A-20. Plot of ln ($A - A_\infty$) vs. time at 146.95 °C. Data were obtained from Table A-10 and represent the disappearance of 1,2-dihydrocyclobuta[*l*]phenanthrene (**6**). The rate constant derived from the line is $k = 1.30 \pm 0.01 \times 10^{-5}\ s^{-1}$

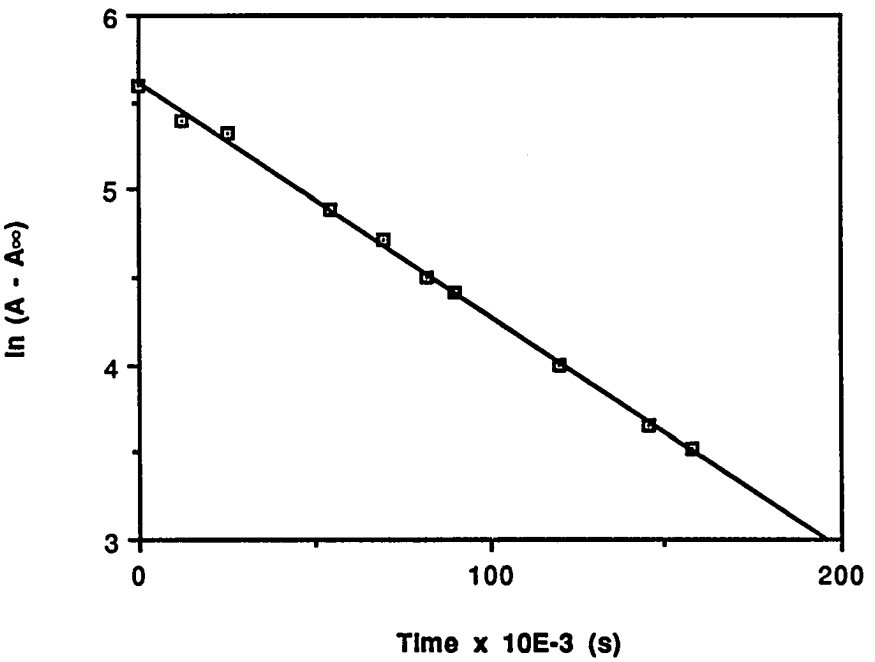

Figure A-21. Plot of ln ($A - A_\infty$) vs. time at 146.95 °C. Data were obtained from Table A-11 and represent the disappearance of 1,2-dihydrocyclobuta[*l*]phenanthrene (**6**). The rate constant derived from the line is $k = 1.33 \pm 0.02 \times 10^{-5}\ s^{-1}$

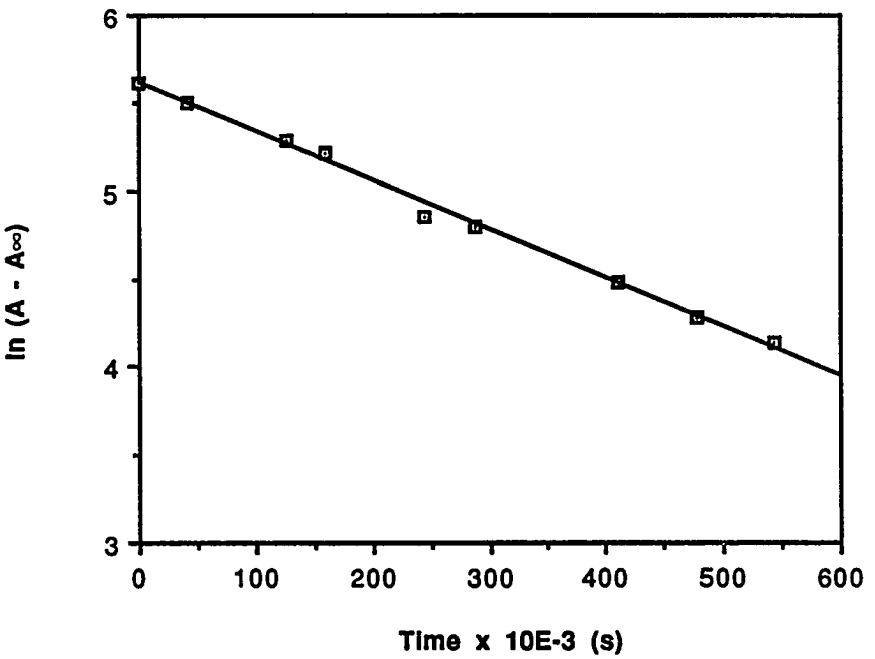

Figure A-22. Plot of ln (A - A_∞) vs. time at 131.95 °C. Data were obtained from Table A-12 and represent the disappearance of 1,2-dihydrocyclobuta[*l*]phenanthrene (**6**). The rate constant derived from the line is k = 2.77 ± 0.07 x 10^{-6} s^{-1}

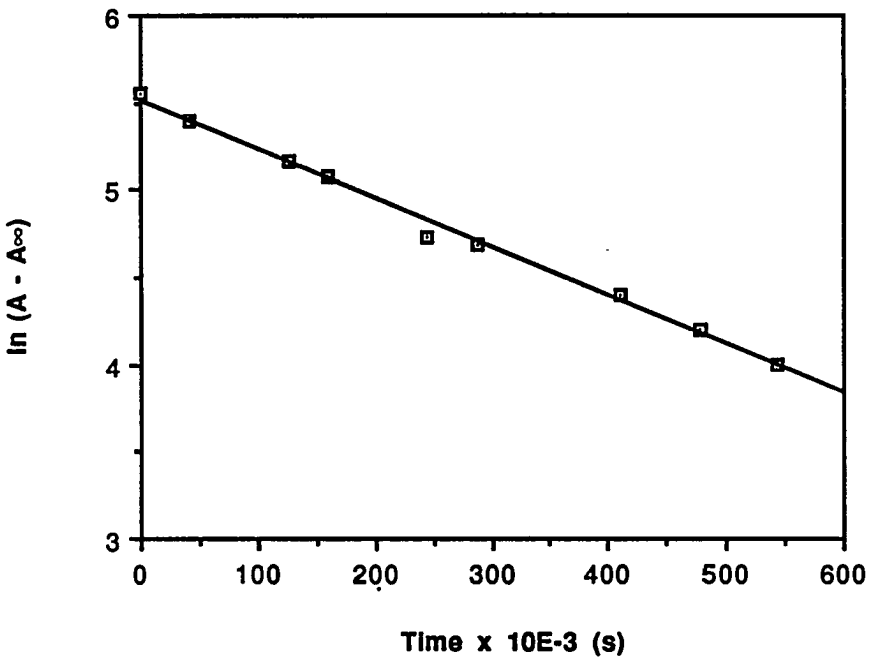

Figure A-23. Plot of ln ($A - A_\infty$) vs. time at 131.95 °C. Data were obtained from Table A-13 and represent the disappearance of 1,2-dihydrocyclobuta[*l*]phenanthrene (**6**). The rate constant derived from the line is $k = 2.80 \pm 0.08 \times 10^{-6}\ s^{-1}$

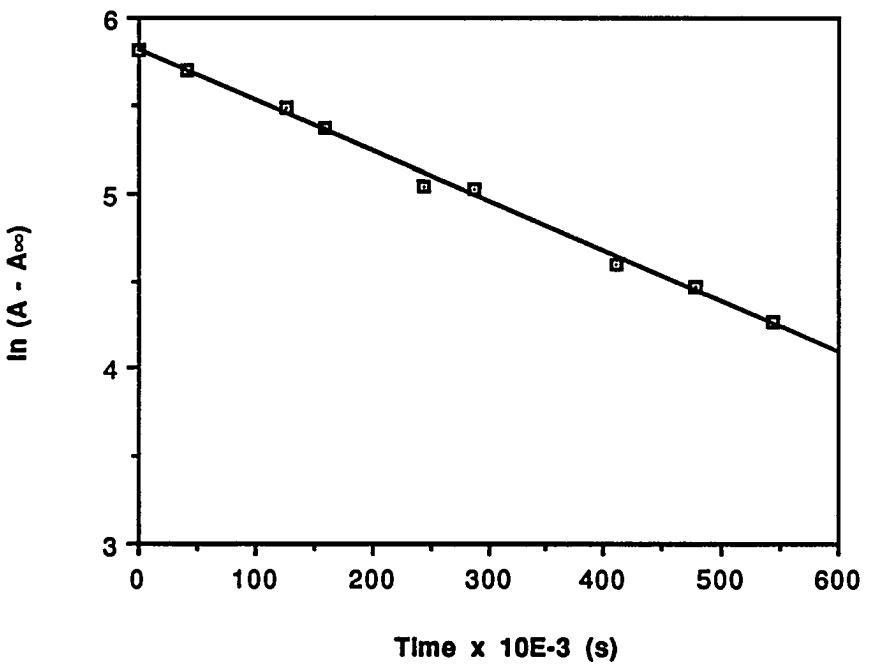

Figure A-24. Plot of ln ($A - A_\infty$) vs. time at 131.95 °C. Data were obtained from Table A-14 and represent the disappearance of 1,2-dihydrocyclobuta[*l*]phenanthrene (**6**). The rate constant derived from the line is $k = 2.88 \pm 0.07 \times 10^{-6}\ s^{-1}$

SECTION III. PHOTOCHEMICAL STUDY OF 2-METHYL-3-ETHENYLFURAN

INTRODUCTION

The 1,5 hydrogen transfer of *o*-alkylphenyl ketone is a well studied and understood photochemical rearrangement.[1,2] In a thorough review by Wagner the following mechanism was outlined in which all excited states result from n → π* transitions (Scheme 1).[2] It should be noted that proton

Scheme 1

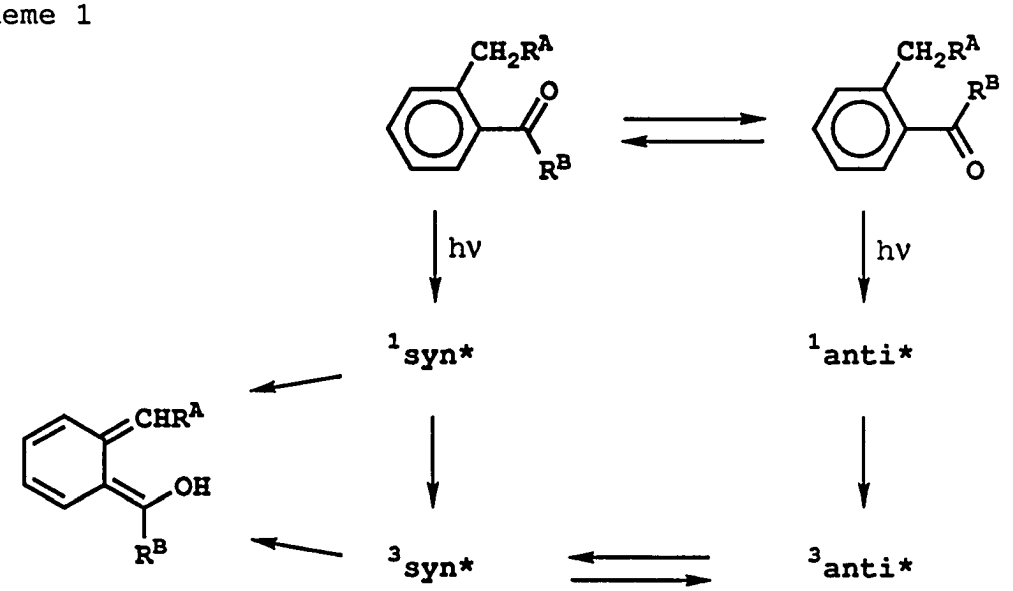

abstraction may occur from either the singlet or triplet state and that the resulting enol is an *o*-xylylene derivative. This photochemical intermediate (or the biradical precursor) has been trapped with a variety of dienophiles.[3,4]

Similar in reactivity to the *o*-alkylphenyl ketones are the *o*-alkylstyrenes. Through deuterium labelling studies by Scully

and Morrison the following mechanism was proposed for the observed photochemically induced deuterium scrambling (Scheme 2).[5] Later, to show that scrambling was indeed the result of

Scheme 2

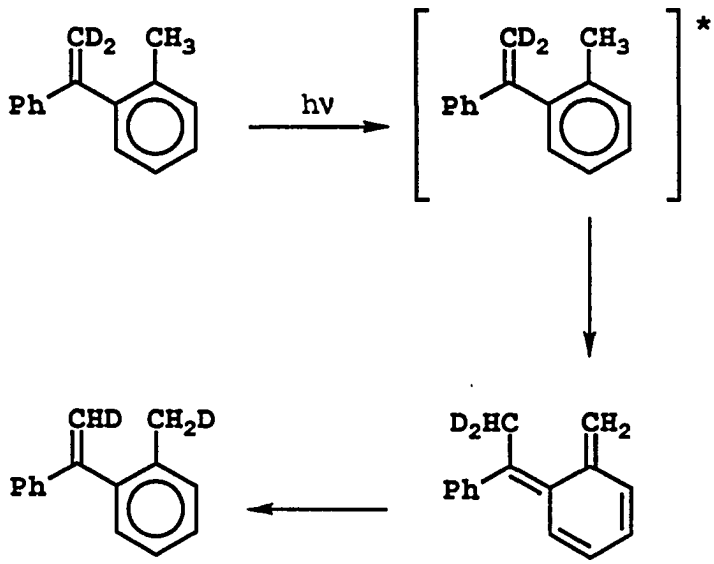

an intramolecular reaction, Pratt trapped the *o*-xylylene intermediate (**2**) with maleic anhydride to give the [4 + 2] adduct (**3**).[6]

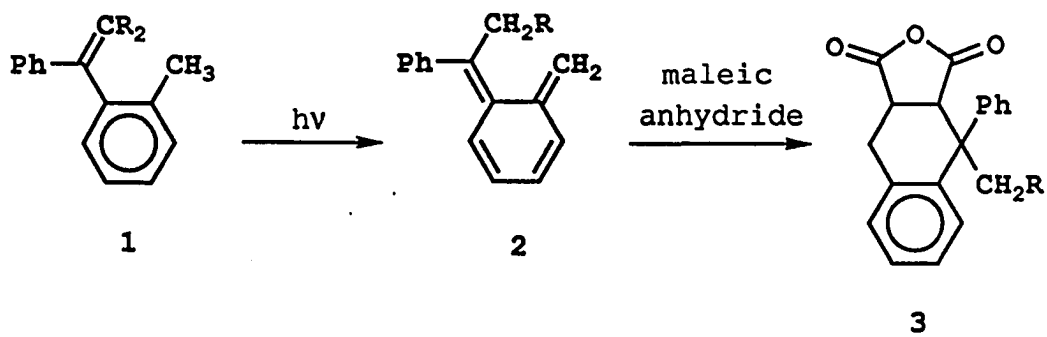

1 **2** **3**

Subsequently, a series of papers by Hornback further explored the chemistry of *o*-alkylstyrenes and showed that photochemically produced *o*-xylylenes could be trapped in an intramolecular Diels Alder reaction.[7-9] However, yields were

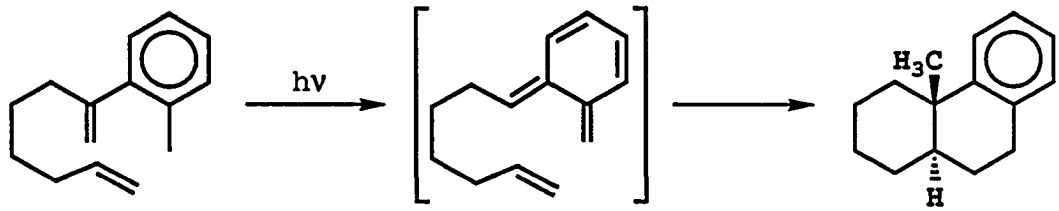

+ minor products

insufficient for developing this into a synthetically useful reaction.

Interest in our research group in the photochemical reactions reviewed stemmed from our study of thermally generated *o*-quinodimethanes. In an effort to extend the breadth of our work we undertook the investigation of the photochemistry of 2-methyl-3-ethenylfuran (**4**).

RESULTS

2-Methyl-3-ethenylfuran (**4**) was prepared in three steps from methyl 2-methyl-3-furoate (**5**). Compound **5** was reduced to 2-methyl-3-furfuryl alcohol (**6**) with $LiAlH_4$ followed by oxidation with CrO_3 in pyridine to give 2-methyl-3-furaldehyde (**7**).[10-14] Compound **7** was converted to **4** using the Wittig reaction (Scheme 3).[15]

Scheme 3

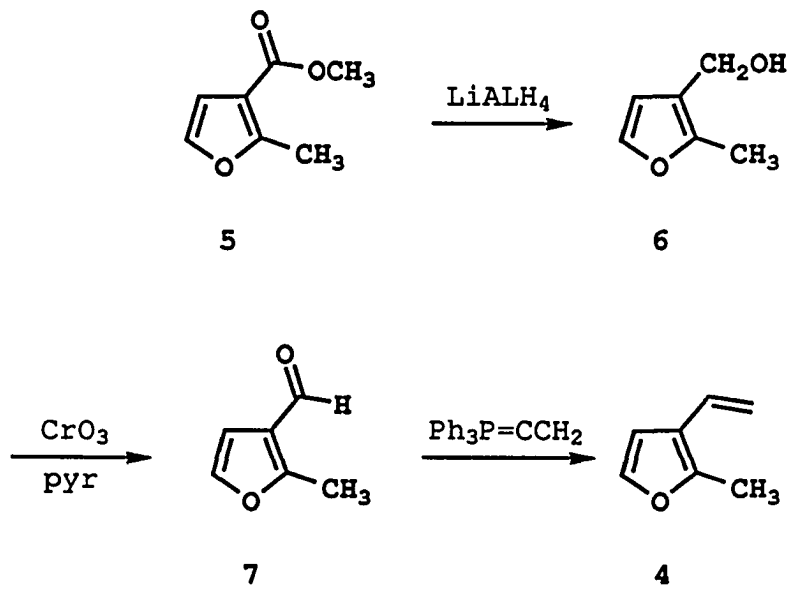

After purification by distillation 2-methyl-3-ethenylfuran (**4**) was photolyzed in pentane deaerated with argon. The photolysis was performed using a Conrad-Hanovia medium pressure mercury-vapor immersion lamp with a vycor filter. The photolysis was followed by removing aliquots at predetermined

intervals and analyzing by UV spectroscopy and gas chromatography. GC analysis indicated the formation of products from bimolecular reactions as their retention times were significantly longer than that of the starting material. The UV data collected did not give evidence for the formation of a 2-methylmethylene-3-methylene-2,3-dihydrofuran (**8**) as no absorption was observed in the range of 315 nm. The λ_{max} for 2,3-dimethylene-2,3-dihydrofuran is 313 nm and 314 nm for 2-methylene-3-*tert*-butylmethylene.[16,17]

Removal of the solvent by distillation followed by flash-column chromatography allowed isolation of a dimeric product (**9**). However, the apparent instability of **9** and the presence of other minor products of the same molecular weight made it difficult to obtain **9** in greater than 80% purity. Analysis by GC/MS indicated that **9** was a dimer of the starting material. Furthermore, the lack of a significant peak at 1/2 the mass of the parent ion suggested the dimer (**9**) was unsymmetrical, and the loss of $COCH_3$ suggested the presence of an acetyl group. These results were corroborated by ^1H NMR which contained two distinct methyl signals and ten distinct one-proton signals. The GC/FT-IR and solution-cell FT-IR data collected gave evidence for the presence of at least one if not two carbonyl functionalities in **9**. ^{13}C NMR data were not helpful due to the presence of impurities, and the COSY data, though helpful, did not make determination of the dimeric structure possible.

Though much is known about the structure of **9** it has not been completely elucidated at this time.

DISCUSSION

The photochemistry of furans has been reviewed in several recent publications.[18-21] Though not completely delineated there is indication that UV irradiation of the parent furan above 200 nm results in a $\pi \rightarrow \pi^*$ transition and that reactions occur from the triplet state.[18,22-25] The conclusion that a $\pi \rightarrow \pi^*$ transition occurs is based on the fact that an $n \rightarrow \pi^*$ transition has not been observed and on the absence of a theoretical n pure MO.[23] Additionally, for thiophene it was calculated the $n \rightarrow \pi^*$ transition occurs in the vacuum UV.

As the benzene system has been thoroughly studied, it may be possible to gain a better understanding of furan photochemistry by comparing studies of both.[21] Both systems are known to isomerize as illustrated.[21,26,27] However, it has

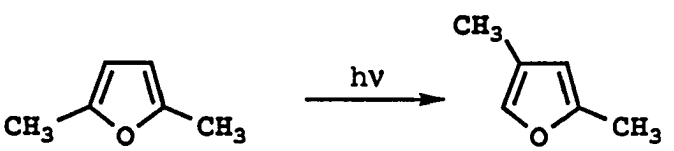

10 11

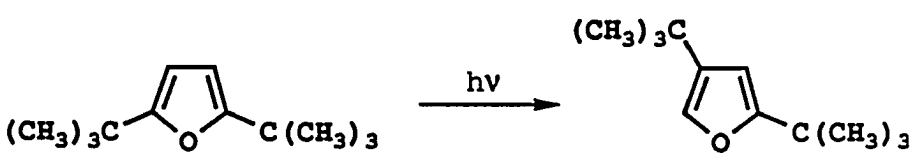

12 13

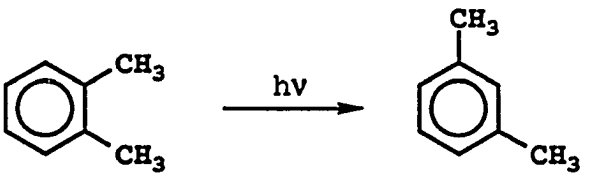

14 **15**

been shown in the case of the *tert*-butyl substituted furan, **12**, that isomerization may proceed through the ring contracted intermediate **16**, whereas the benzene isomerization likely proceeds through benzvalene (**17**).[21,27] Greater similarity between the two molecules is observed in the photochemically

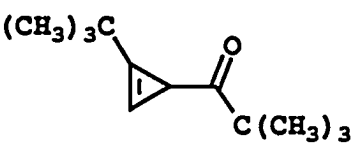

16

17

induced isomerization to their Dewar isomers **18** and **19**.[27-30] However, Dewar benzene (**19**) has a 1/2-life of two days at room

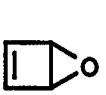

18

19

temperature whereas Dewar furan (**18**) was observed to decompose thermally at -65 °C and thought to have a room temperature 1/2-life of a few ms.[30]

The instability of furan photoproducts is made further evident by the decomposition which occurred when furan was photolyzed at 10 K in an argon matrix.[21] Nevertheless, it has

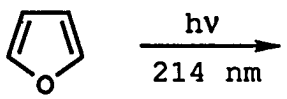

$CH_2CHCH{=}C{=}O$, $CH_3C{\equiv}CH$,

$CH_2C{=}CH_2$, $CH_2{=}C{=}CHCHO$

been possible to isolate cyclic products by careful photolysis of neat solutions.

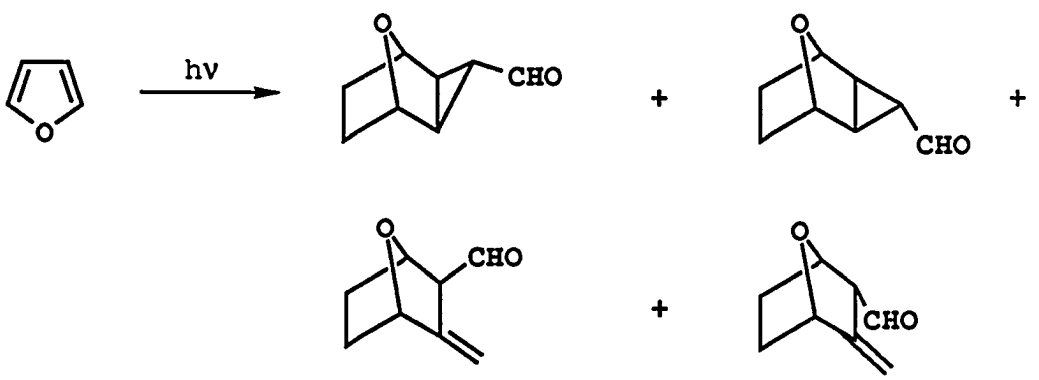

Photolysis of 2-methyl-3-ethenylfuran (**4**) was performed to further probe the similarities between the photochemistry of furan and benzene. Though the photochemistry of 2-ethenylfuran has been investigated, no work has been reported for either **4** or its isomer 2-ethenyl-3-methylfuran.[20] If one assumes similarity between the benzene and furan systems then one might

expect the formation of a 2,3-furan *o*-quinodimethane.[5-9,21] However, UV spectra collected during the photolysis did not

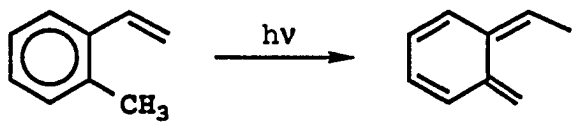

20 **21**

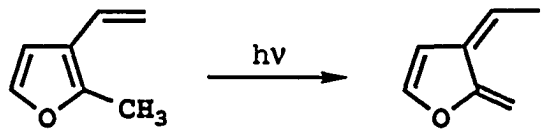

4 **8**

offer any evidence for the formation of an *o*-quinodimethane intermediate (λ_{max} = 315 nm). Furthermore, the mass spectra of dimeric products did not show any similarity to those obtained for the thermal dimerization of **8**. An additional method to test for the formation of **8** would be a Diels Alder trapping reaction. By adding a dienophile to the photolysis reactor prior to photolyzing, one might hope to trap the *o*-quinodimethane intermediate (**8**).[9]

Although the furan *o*-quinodimethane **8** was not observed we were pleased to discover a dimeric product (**9**) albeit in 5% yield based on a conversion of starting material. This

indicates that photofragmentation and bimolecular reactions with fragmentation products need not be the only reaction manifolds available to furan derivatives: photodimerization is an alternate reaction pathway when an aromatic furan derivative is photolyzed.[21] If further work were performed on this system it might be of interest to use a pyrex filter instead of a vycor filter in an attempt to reduce the degree of photofragmentation. Whether photochemical reactions would occur with UV radiation of this wavelength is unknown.

The identity of the furan dimer **9** is not presently known inspite of the extensive attempts to identify it. Its instability, low yield and impurity have been difficult problems to surmount. However, it is known that **9** is unsymmetrical and contains one or two carbonyl groups.

EXPERIMENTAL

Methods and Materials

Photolyses were performed using a water-cooled 450 W medium pressure Conrad-Hanovia immersion lamp in conjunction with a quartz immersion well and vycor filter. NMR data were collected with the Nicolet NT-300, the Varian VXR-300, and the Varian VXR-500 spectrometers. UV data were collected with a Perkin-Elmer 320 spectrophotometer, IR data with an IBM IR/98 spectrometer and GC data with a Hewlett-Packard 5890 Series II gas chromatograph. GC/MS data were collected using a Finnigan 4000 with an INCOS data system. The photolysis solvent was spectral grade (Aldrich Gold Label).

2-Methyl-3-furaldehyde (7)

2-Methyl-3-furfuryl alcohol (**6**) was prepared using a previously reported procedure.[10] 2-Methyl-3-furaldehyde (**7**) was prepared from the alcohol using Collin's reagent.[11-14] A flask was charged with 1.5 l of methylene chloride (distilled from CaH_2) and 94 ml of pyridine (distilled from BaO). The solution was stirred at 5 °C while 60.0 g (0.600 mol) of CrO_3 (dried in vacuo over PO_5) was slowly added. The solution was stirred for 1 h at room temperature followed by addition of 11.2 g (0.0999 mol) of **6**. After stirring an additional 15 min the organic phase was decanted and the tarry residue was washed with ether (3 x 500 ml). The combined organic phases was

washed successively with 5% NaOH (3 x 11), 5% HCl (11), $NaHCO_3$ (11) and brine (11). The solution was dried ($MgSO_4$), and the solvent was removed at reduced pressure to yield 3.73 g (0.0339 mol, 34%) of **7**: ^1H NMR ($CDCl_3$) δ 9.88 (s, 1 H), 7.25 (d, J = 2 Hz, 1 H), 6.63 (d, J = 2 Hz, 1 H), 2.54 (t, 3H) [lit. ^1H NMR ($CDCl_3$) δ 9.93 (s, 1 H), 7.30 (d, J = 2 Hz, 1 H), 6.65 (d, J = 2 Hz, 1 H), 2.60 (s, 3 H).

2-Methyl-3-ethenylfuran (4)[15]

A suspension of 13.2 g (0.0370 mol) methyltriphenylphosphonium bromide in 100 ml of THF at 0 °C was titrated with phenyllithium (1.8 M in cyclohexane/ether 70:30) to a yellow endpoint. Subsequently, an additional 19.7 ml of the phenyllithium solution was added, and the mixture was stirred at room temperature for 30 min. After cooling the Wittig reagent solution to 0 °C 3.73 g (0.0339 mol) of 2-methyl-3-furaldehyde (**7**) in THF (15 ml) was added followed by stirring for 2 h. A 1.0-ml quantity of methanol was added, and the supernatant was decanted. The remaining slurry was washed with hexanes/ether 4:1 (3 x 50 ml), and during each washing the mixture was warmed prior to decanting the solvent. The organic layers were combined and filtered through celite followed by removal of the solvent by distillation using a vigreux column. The product was subsequently distilled using a short-path distillation apparatus to yield 1.27 g (.0118 mol, 35%) of **4**:

^1H NMR ($CDCl_3$) (Appendix, Figure A-1) δ 7.21 (d, J_{AB} = 1.7 Hz, 1 H_A), 6.51 (d of d, J_{CD} = 17.9 Hz, J_{CE} = 10.8 Hz, H_C), 6.46 (d, J_{AB} = 1.7 Hz, 1 H_B), 5.34 (d, J_{CD} = 17.9 Hz, H_D), 5.07 (d, J_{CE} = 10.8 Hz, H_E), 2.29 (s, 3H); high resolution mass spectrum, calculated for C_7H_8O 108.05752, measured 108.05753.

Photolysis of 2-Methyl-3-ethenylfuran (4)

A photoreactor was equipped with a quartz immersion well, a vycor filter and a Conrad-Hanovia medium pressure mercury vapor lamp. The reactor was charged with 600 ml of spectrophotometric grade pentane (Aldrich Gold Label) and 0.21 g (1.9 mmol) of 2-methyl-3-ethenylfuran (**4**). The reactor solution was degassed for 3 h followed by photolyzing the solution for the following intervals 32 min, 21 min and 20 min. At this point 65% of the starting material had disappeared as determined by GC using mesitylene as an internal standard. The volume of the photolysis solution was reduced by distillation using a vigreux column and the distillate was purified by flash column chromatography on silica gel (hexanes) to yield an analytical quantity of an unidentified dimer **9**: ^1H NMR (C_6D_6) (Appendix, Figures A-2, A-3 and A-4) δ 6.26 (br t, J_{AB} = 4.6 Hz, H_A), 5.65 (s, 1 H), 5.44 (m, 1 H), 5.23 (m, 1 H), 5.05 (s, 1 H), 3.15 (m, 1 H), 2.51 (d of d, J_{AB} = 4.6 Hz, J_{BC} = 17.4 Hz, H_B), 2.42 (m, 1 H), remaining proton signal obscured but identified by COSY (Appendix, Figure A-6); GC-IR 1720, 1427,

1368, 1227 cm^{-1}; FT-IR 1701, 1678, 1421, 1358, 1240 cm^{-1}; GC-MS 216.1, 173.1, 131.1, 43.0.

REFERENCES

1. Sammes, P. G. *Tetrahedron* **1976**, *32*, 405.
2. Wagner, P. J. in "Rearrangements in Ground and Excited States"; DeMayo, P., Ed.; Academic Press: New York, 1980; Vol. 3, p 381.
3. Ogata, Y.; Takagi, K. *J. Org. Chem.* **1974**, *39*, 1385.
4. Hamer, N. K. *J. Chem. Soc., Perkin Trans. 1* **1979**, 508.
5. Scully F.; Morrison, H. A. *J. Chem. Soc., Chem. Commun.* **1973**, 529.
6. Pratt, A. C. *J. Chem Soc., Chem. Commun.* **1974**, 183.
7. Hornback, J. M.; Mawhorter, L. G.; Carlson, S. E.; Bedont, R. A. *J. Org. Chem.* **1979**, *44*, 3698.
8. Hornback, J. M.; Barrows, R. D. *J. Org. Chem.* **1982**, *47*, 4285.
9. Hornback, J. M.; Barrows, R. D. *J. Org. Chem.* **1983**, *48*, 90.
10. Trahanovsky, W. S.; Cassady, T. J.; Woods, T. L. *J. Am. Chem. Soc.* **1981**, *103*, 6691.
11. Ratcliffe, R. W. *Organic Synthesis*, J. Wiley and Sons: New York, 1988; Collect Vol VI, p 373.
12. Ratcliffe, R.; Rodehorst, R. *J. Org. Chem.* **1970**, *35*, 4000.
13. Holum, J. R. *J. Org. Chem.* **1961**, *26*, 4814.

14. Leung, M. K., personal communication, Ph.D. candidate, Iowa State University, 1990.

15. Leopold, E. J. *Organic Synthesis*, J. Wiley and Sons: New York, 1986; vol 64, 164.

16. Munzel, N.; Schweig, A. *Angew Chem. Int. Ed., Engl.* **1987**, *26*, 471.

17. Huang, Y. C. Ph.D. Dissertation, Iowa State University, Ames, Iowa, 1987.

18. Dean, F. M. *Advances in Heterocyclic Chemistry* **1982**, *31*, 237.

19. Padwa, A. in "Rearrangements in Ground and Excited States"; DeMayo, P., Ed.; Academic Press: New York, 1981; Vol. 3, p 501.

20. Braslavsky, S.; Heicklen, J. *Chemical Reviews* **1977**, 473.

21. Rendall, W. A.; Torres, M.; Lown, E. M.; Strausz, O. P. *Rev. Chemi. Intermed.* **1986**, 335.

22. Horvath G. *Spectrochim. Acta, Part A* **1967**, *23A*, 921.

23. Buemi, G.; Zuccarello, F.; Romeo, G. *J. Molec. Structure* **1983**, *94*, 115.

24. Veszpremi, T.; Nyulaszi, L.; Nagy, J. *J. Organomet. Chem.* **1987**, *331*, 175.

25. Bird, C. W.; Cheeseman, G. W. H. in "Comprehensive Heterocyclic Chemistry" Katritzky, A. R.; Rees, C. W. Eds.; Pergamon Press: New York, 1984; vol. 4, pt 3, p 14.

26. Wilzbach, K. E.; Kaplan, L. *J. Am. Chem. Soc.* **1964**, *86*, 2307.

27. Bryce-Smith, D.; Gilbert, A. *Tetrahedron* **1976**, *32*, 1309.

28. Pitt, I. G.; Russell, R. A.; Warrener, R. N. *J. Am. Chem. Soc.* **1985**, *107*, 7176.

29. Rendall, W. A.; Clement, A. ; Torres, M.; Strausz, O. P. *J. Am. Chem. Soc.* **1986**, *108*, 1691.

30. Price, D.; Ratajczak, E.; Sztuba, B.; Sarzynski, D. *J. Photochem.* **1987**, *37*, 273.

APPENDIX

Figure A-1. ^{1}H NMR spectrum of 2-methyl-3-ethenylfuran (**4**) in $CDCl_3$

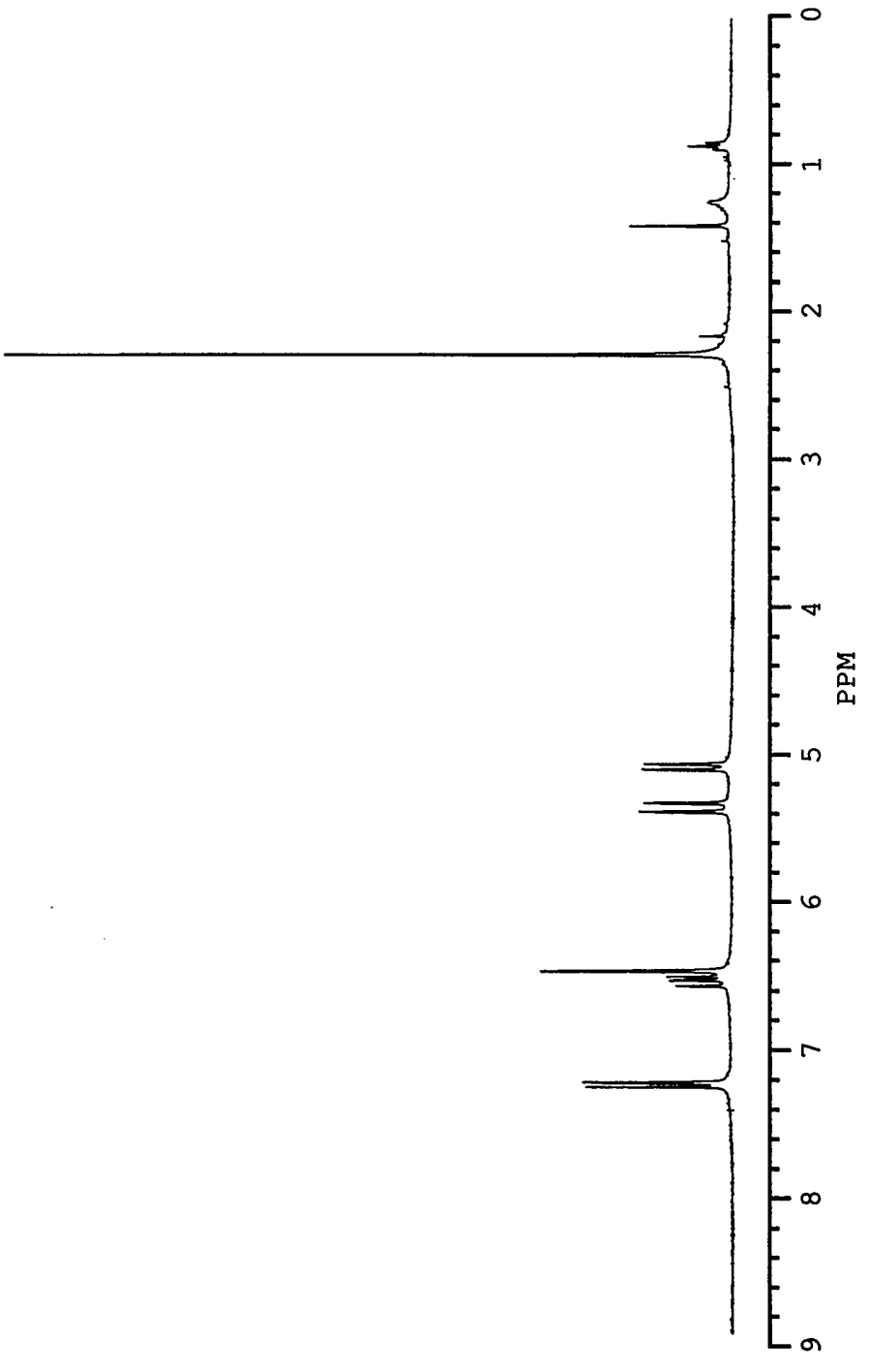
0
1
2
3
4
5
6
7
8
9
PPM

Figure A-2. ^{1}H NMR spectrum of the photodimer (9) in C_6D_6

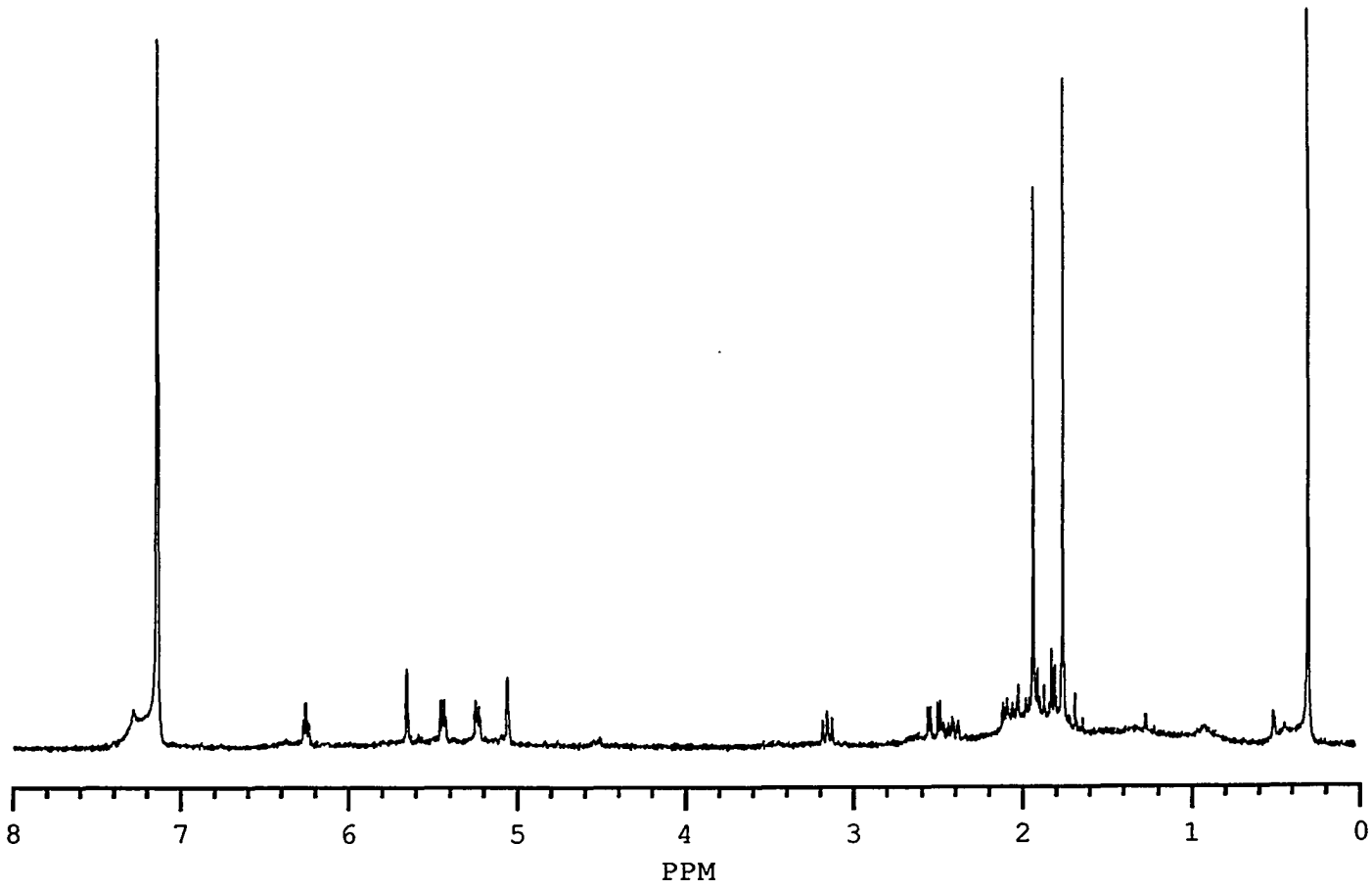
8
7
6
5
4
3
2
1
0
PPM

Figure A-3. Expanded segment of spectrum from Figure A-2 (6.3-4.9 ppm)

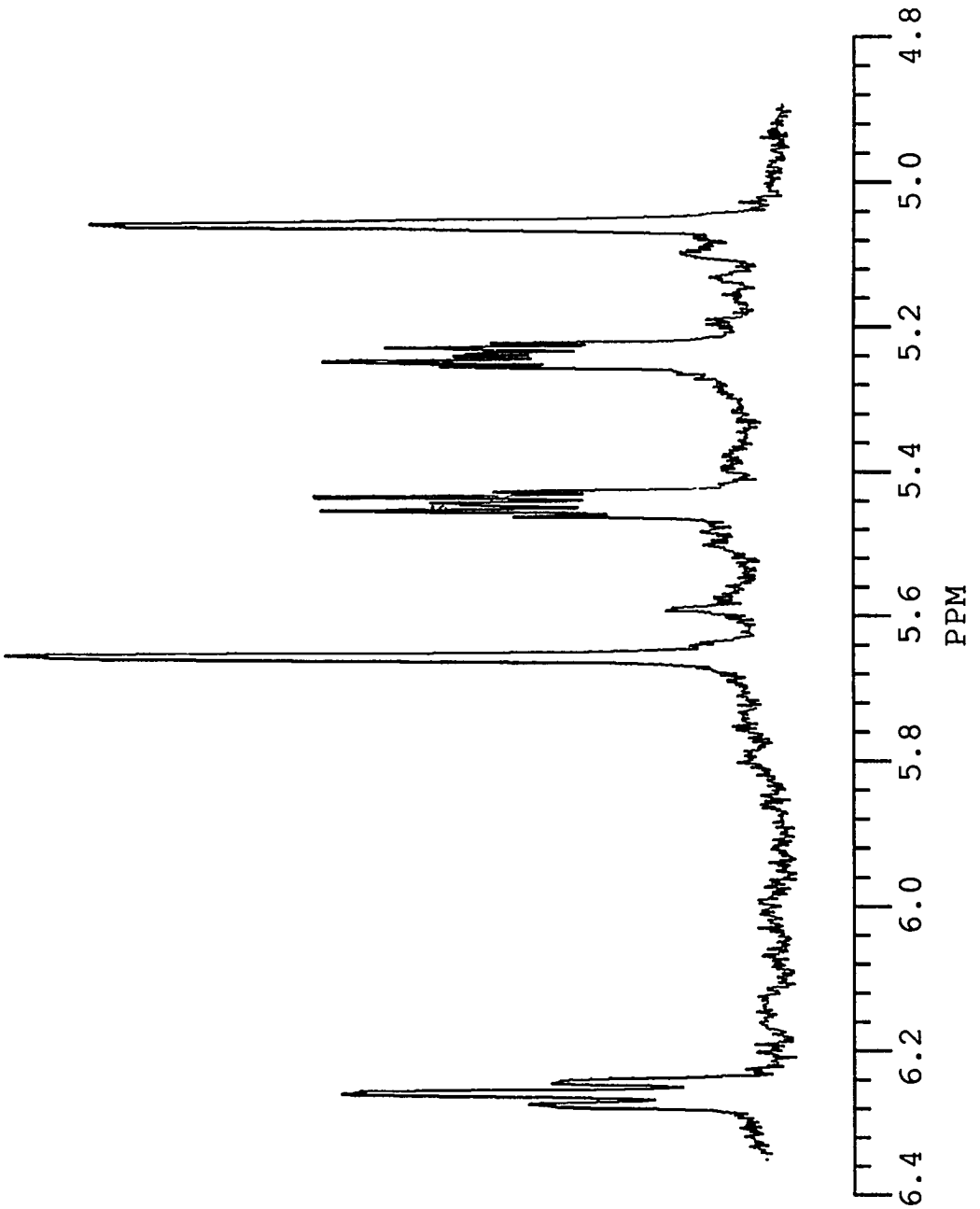
6.4
6.2
6.0
5.8
5.6
5.4
5.2
5.0
4.8
PPM

Figure A-4. Expanded segment of spectrum from Figure A-2 (3.2-2.5 ppm)

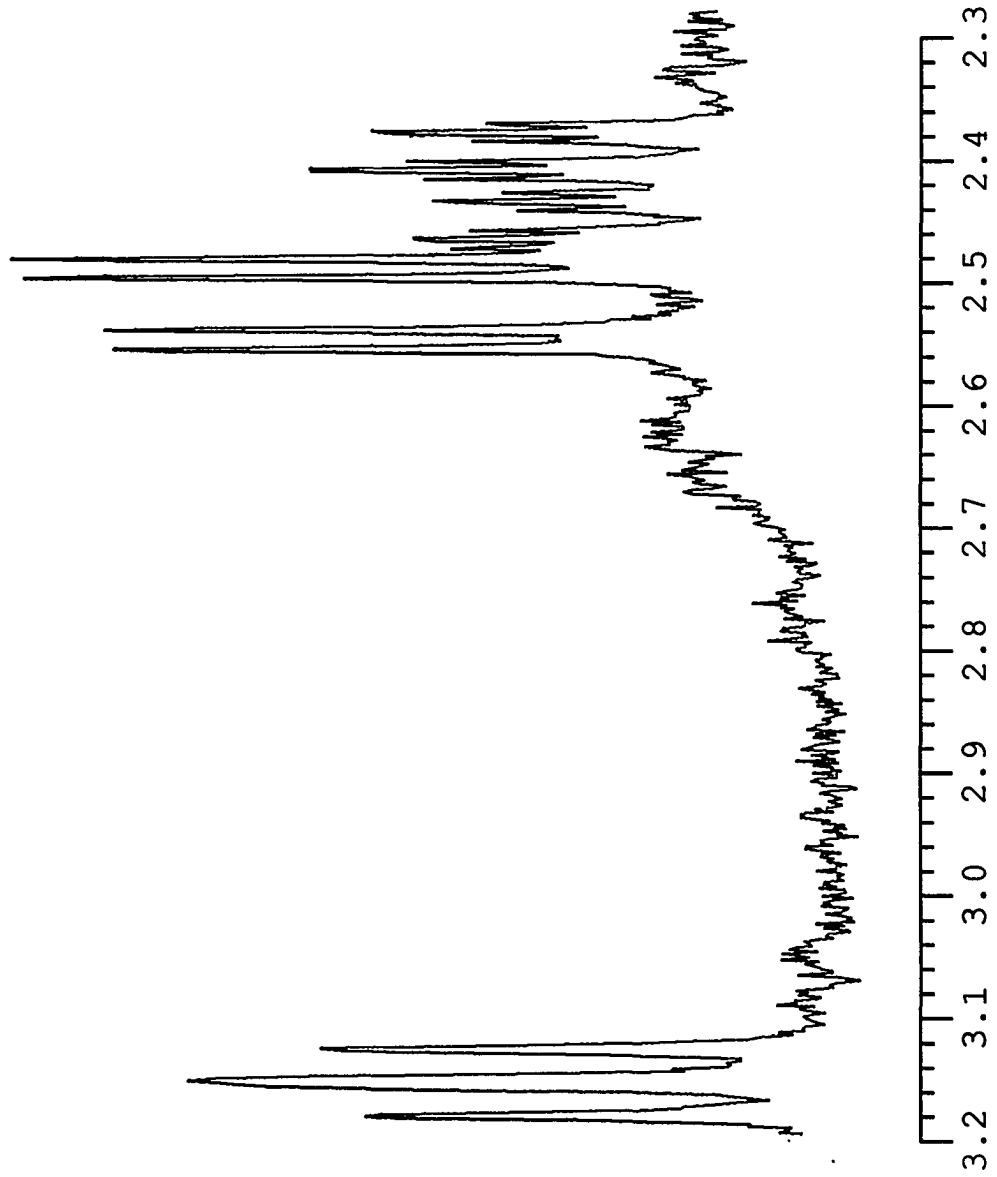
3.2
3.1
3.0
2.9
2.8
2.7
2.6
2.5
2.4
2.3
PPM

Figure A-5. Expanded segment of spectrum from Figure A-2 (2.1-1.6 ppm)

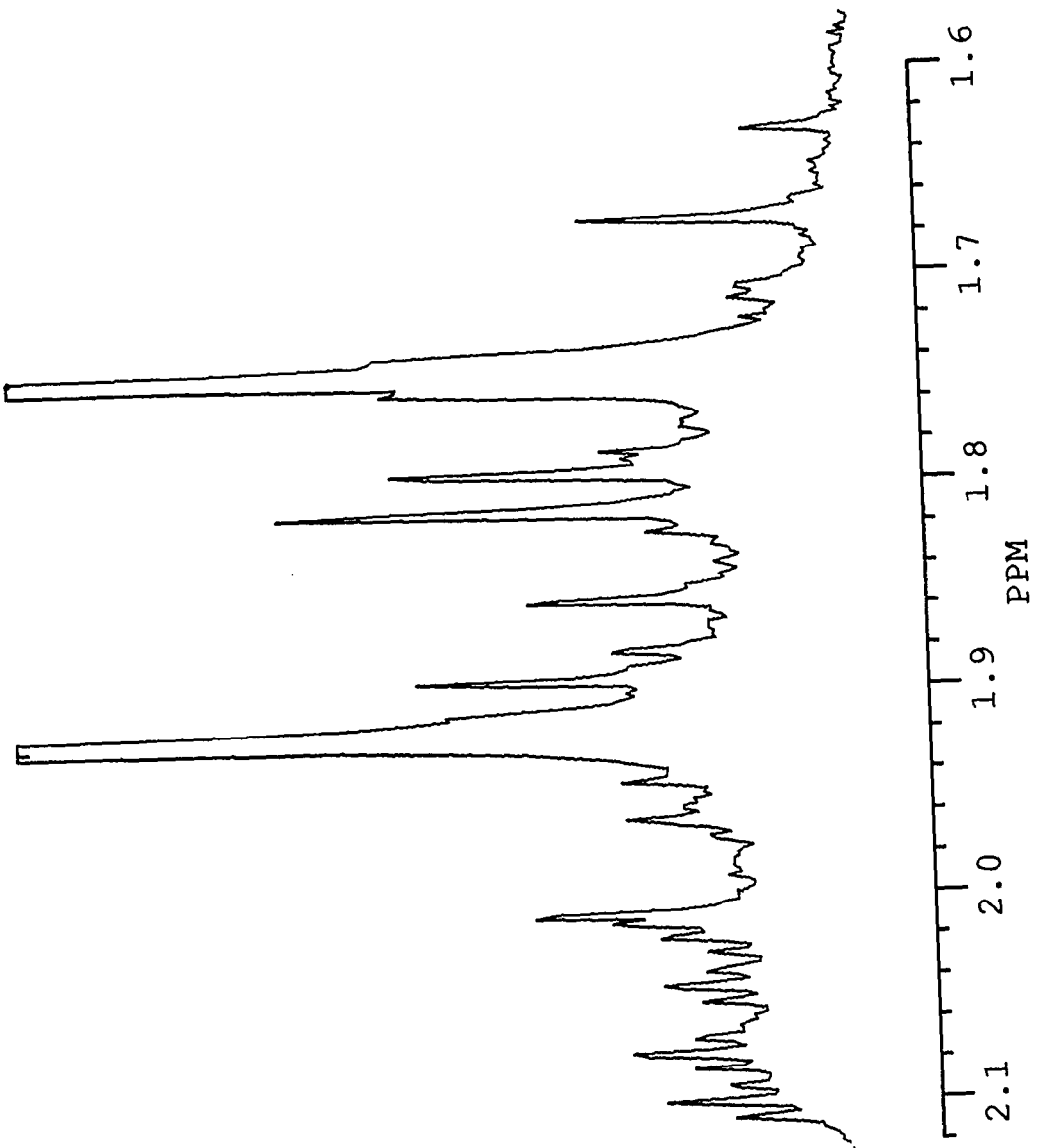
1.6
1.7
1.8
1.9
2.0
2.1
PPM

Figure A-6. COSY NMR spectrum of the photodimer (**9**) in benzene-d_6

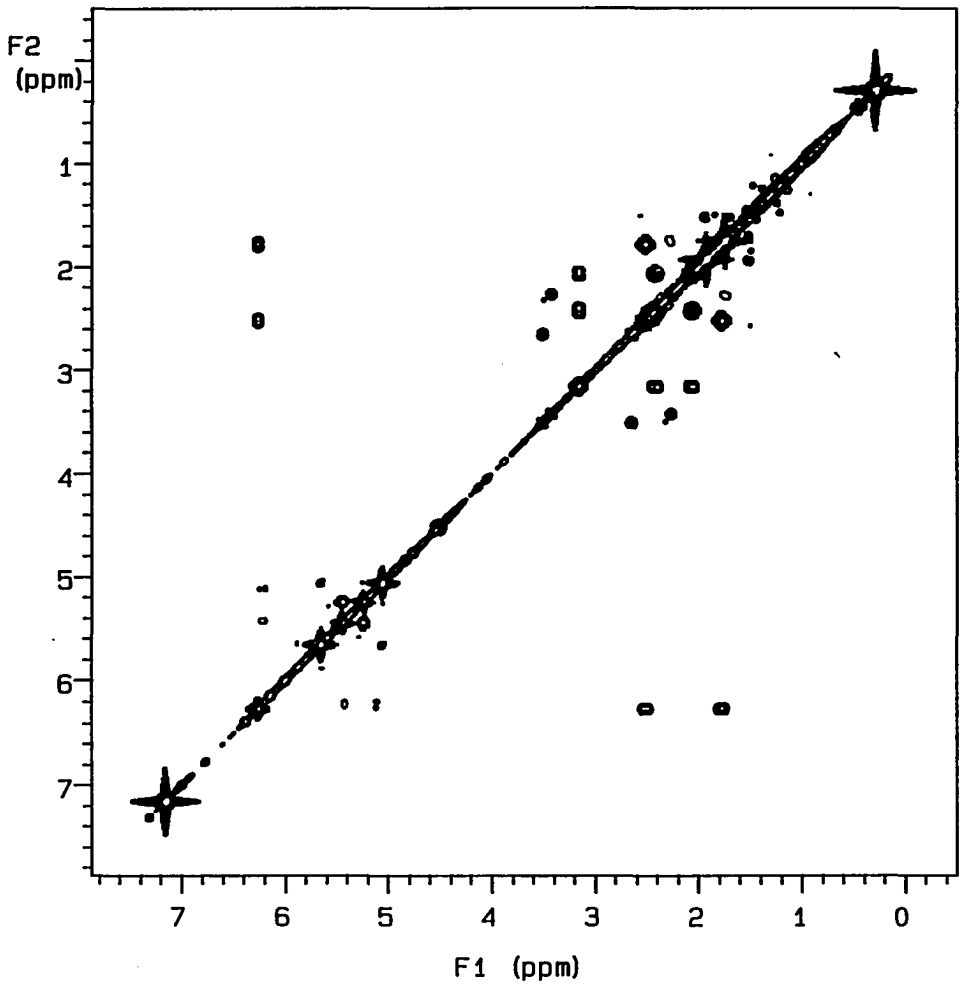
F2
(ppm)
1
2
3
4
5
6
7
7
6
5
4
3
2
1
0
F1 (ppm)

GENERAL SUMMARY

The successful photochemical electrocyclization of several *o*-quinodimethanes has been achieved as well as the kinetic analysis of the retrograde electrocyclic reaction of each compound. Furthermore, the enthalpy difference between these *o*-quinodimethanes and their cyclized isomers has been investigated.

In Section 1 the first solution phase synthesis of 4,5-dihydrocyclobuta[*b*]furan was reported, and the preparation of an alkyl substituted analogue was also described. IR data for 4,5-dihydrocyclobuta[*b*]furan matched that from the literature, and previously unpublished characterization data were collected for this compound. It was shown that the prepared dihydrocyclobuta[*b*]furans were at least 4 kcal/mol less stable than their respective *o*-quinodimethane isomers and that the presence of a *t*-butyl group on the cyclobutene moiety raised the transition state energy by 4 kcal/mol.

In Section 2 a synthesis is described which enables conversion of 9,10-dimethylene-9,10-dihydrophenanthrene to 1,2-dihydrocyclobuta[*l*]phenanthrene in considerably greater yield than previously reported. Activation parameters for the electrocyclic ring opening of 1,2-dihydrocyclobuta[*l*]-phenanthrene were determined by kinetic analysis and an approximate K_{eq} for the equilibrium between this compound and

its *o*-quinodimethane isomer at 200 °C was obtained. An energy profile for the interconversion was presented and compared with that for the *o*-xylylene - benzocyclobutene interconversion using Dewar Resonance Energies.

In Section 3 results are presented for the preliminary investigation into the photochemical preparation of a furan *o*-quinodimethane. Though no evidence has yet been collected for the *o*-quinodimethane, an intriguing dimer was obtained which has eluded initial steps to fully characterize it.

ACKNOWLEDGMENTS

I am very grateful to Dr. Trahanovsky for his patience, guidance, encouragement, and support while studying under his supervision. I am also thankful for the friendship and experimental advice generously given by members of the Trahanovsky group.

I would like to thank Nancy Qvale for her perseverance in preparing the final draft of this dissertation.

I am especially grateful to my family without whose love and support this work would not have been possible.

This work was performed at Ames Laboratory under contract no. W-7405-eng-82 with the U.S. Department of Energy. The United States government has assigned the DOE Report number IS-T 1456 to this dissertation.